EXPERIMENTAL AND THEORETICAL ROUTES TOWARDS ASSESSING THE POTENTIAL OF EMULSIFIED PALM BIODIESEL AS AN ALTERNATIVE TO DIESEL FUEL

A Thesis
Submitted in Partial Fulfillment of the Requirements for
the Award of the Degree of

DOCTOR OF PHILOSOPHY

By

BIPLAB KUMAR DEBNATH

DEPARTMENT OF MECHANICAL ENGINEERING
INDIAN INSTITUTE OF TECHNOLOGY GUWAHATI
GUWAHATI, INDIA

JUNE, 2013

Dedicated to my Parents....

Mrs. Bela Pal (Debnath)

and

Mr. Kajal Debnath

whose endless faith and blessings always
inspired me to move forward

Declaration

I hereby certify that the work compiled in this dissertation is the outcome of the research work, performed by myself, else stated, under the guidance of Professor Ujjwal K. Saha and Associate Professor Niranjan Sahoo.

Any part of this work has not earlier been submitted for the award of any degree, diploma, associate-ship, fellowship or its equivalent to any University or Institution.

Biplab Kumar Debnath
Registration No. 09610305
Department of Mechanical Engineering
Indian Institute of Technology Guwahati

Certificate

It is certified that the work contained in the thesis entitled Experimental and Theoretical Routes Towards Assessing the Potential of Emulsified Palm Biodiesel as an Alternative to Diesel Fuel, by Biplab Kumar Debnath (Registration No. 09610305), a student of the Department of Mechanical Engineering, Indian Institute of Technology Guwahati, India, for the award of the degree of Doctor of Philosophy has been carried out under our supervision and this work has not been submitted elsewhere.

Prof. Ujjwal K. Saha
Professor
Department of Mechanical Engineering
Indian Institute of Technology Guwahati
Guwahati – 781039, India

Dr. N. Sahoo
Associate Professor
Department of Mechanical Engineering
Indian Institute of Technology Guwahati
Guwahati – 781039, India

Abstract

Diesel engines, the most fuel-efficient combustion devices, are widely used in various sectors such as agriculture, transportation and industry. Diesel vehicles are counted up to 40% and 65% of the total vehicles in India and world, respectively. A higher price of petrol in India will cause these numbers to increase further. However, the public has ample disquiet about the emission released by diesel engines. The emissions from diesel engines namely, black smoke, hydrocarbon, nitrogen oxides, carbon, sulfur etc., are often converted into other lethal materials that harm both ecology and human welfare. The most effective means is to trim down the emission level right at its root.

Biodiesel, methyl or ethyl esters of biofuel, is a renewable, ecologically benign fuel and has been regarded as a promising alternative fuel for diesel engines. This is because biodiesel provides superior lubricity, bio-degradability, and low toxicity than diesel. However, oxidized biodiesels forms higher nitrogen oxide (NO_X) when burnt in diesel engines. It is seen that exhaust gas recirculation (EGR) can shrink NO_X, but rises particulate emission. Again, oxygen enrichment does the reverse. When both of these methods are employed, they raise cost, repairs and added energy supply. Further, lesser calorific value of biodiesel causes lower efficiency than diesel. The abovementioned problems can be suitably resolved by applying a method, emulsification of biodiesel.

In emulsification, two or more immiscible fluids are mixed together such as water and fuel oil. When sprayed through a nozzle, the emulsified fluid is atomized into fine liquid droplets. Owing to its lower boiling point than fuel oil, water droplets reach their boiling point first after absorbing an ample amount of heat. The vaporized water then blows up the oil layer, forms smaller oil droplets, and raises the oil's surface to volume ratio. This is known as "micro-explosion". As a result, a stronger degree of mixing amid the atomized oil droplets and the surrounding air takes place, resulting improved combustion efficiency. Hence, the fuel intake drops, which in turn, boosts the efficiency. Further, the vaporization of water absorbs heat, which reduces the maximum cylinder temperature, thereby lessening thermal NO emission.

Palm Oil Methyl Ester (POME) esterified form of palm oil is selected to study it in emulsified form. POME has the greatest oil yield per unit land on earth. Because, palm oil has the higher fossil energy balance, i.e., energy produced over energy consumed. Therefore, it possess the lower production expenses relative to other energy crops. Besides, it has higher Cetane number and decent calorific value (39.84 MJ/kg) comparable to its contenders. POME ($C_{18.07}H_{34.93}O_2$) also has a sizable amount of oxygen bonded in its molecular

structure that makes it to burn more intensely. As a result, POME presents a performance close to that of diesel.

Being a fuel of different origin, the standard design parameters of a diesel engine may not be suitable for POME. Therefore, the initial part of the present investigation targets at finding the performance characteristics of 100% POME in a 3.5 kW Variable Compression Ratio (VCR) diesel engine at various combinations of compression ratios (CR = 16, 17, 17.5 and 18) and injection timings (IT = 20°, 23°, 25°, 28ºBTDC). During this study, the engine load is varied from 'No load' (0.1 kg) to 'Full load' (12 kg) in steps of 20% for each CR-IT combination tested. This test identifies the superior combination of CR and IT for POME run VCR diesel engine compared to neat diesel performance. Later on, the water in POME (WIP) emulsion is tested in a variable compression ratio (VCR) diesel engine. For this, WIP is initially prepared in an ultrasonic bath sonicator and its stability analysis and calculation of droplet diameter is performed. Thereafter, a stable WIP is tested in the VCR engine for above mentioned CR, IT and load variation (with 10% overloading condition too). The performance parameters evaluated are brake power (BP), brake thermal efficiency (BTHE), brake specific fuel consumption (BSFC) and exhaust gas temperature (EGT). The combustion parameters studied are variation of cylinder pressure, ignition delay (ID), peak cylinder pressure (PCP) and net heat release rate (NHRR). The emission quantities recorded are carbon monoxide (CO), carbon dioxide (CO_2), nitrogen oxide (NO_X) and hydrocarbon (HC). All the measured, calculated and recorded quantities for POME and WIP at different CR-IT combinations are compared with the standard diesel performance (CR=17.5; and IT=23). The superior combinations of CR and IT for both POME and WIP are also compared in between them for qualitative and quantitative assertion.

This is followed by a thermodynamic potential study for the aforementioned test results. It includes the first and second law analysis of WIP and POME run engine for a load where maximum BTHE take place. The focus of the study is to identify the energy and exergy losses through some of the primary processes and locations of diesel engines with respect to CR-IT variations and quantify the maximum amount of energy that can be utilized from the viewpoint of second law. It is found that, the WIP employed, has lesser calorific value than diesel and even lower than POME. Still it is performed more efficiently than POME and even diesel. This is the clear sign of the presence of micro-explosion for emulsified POME. WIP have performed better at 18 CR and 20ºBTDC of IT along with drop in emission quantities.

Keywords: *Compression ignition, Variable compression ratio, Injection timing, Biodiesel, Emulsion, Surfactant, Performance, Combustion, Ignition delay, Heat release, Emission*

Acknowledgements

PhD is although a small part of life; still it teaches us how to live the life in a large scale. It is equally a magnificent and a prodigious training. Apart from acquiring some knowledge about a tiny, part of scientific fraternity, PhD also teaches one, how to talk, to work in a group, to know people and also to make one understandable to others. In this regard, I have also interacted with a number of personalities, without the support of whom, I may not come this far.

Firstly, I will take this opportunity to express my earnest gratitude to my honorific supervisors, Prof. Ujjwal K. Saha and Dr. Niranjan Sahoo, Department of Mechanical Engineering, Indian Institute of Technology Guwahati, India, for accepting me as their PhD student. They have provided me the complete freedom in my research and allowed me to work in my own way. They always have listened to my ideas with patience and constantly motivated to accomplish my goal. I have learnt from them, how to work with enthusiasm, energy, and life, yet remain composed and grounded. It is hard to express my gratitude with only a few words to these two personalities. The best way to express my thanks to them will probably be to follow the lessons I have leant from them throughout my life.

My sincere acknowledgement goes to Prof. D. Chakraborty and Prof. P. Mahanta, former and present Heads of Mechanical Engineering Department. I thank them for their encouragement, guidance, and support from the initial to the final stages of my PhD work. I am also indebted to the members of Doctoral Committee Dr. A. Verma and Dr. C. Somayaji for their precious suggestions about critical issues related to my work. I am also thankful to Dr. S. Kanagaraj, who has permitted me to work in Material Science Laboratory of Mechanical Engineering Department. I will also drive to thank Prof. A. K. Dass, Dr. P. Muthukumar and Dr. A.K. De for their immense support during the course work.

I would like to thank Scientific Officers, Mr. R. Saikia, Mr. S. Sarma, Mr. N. Borah of Department of Mechanical Engineering, Mr. P. Kalita and Mr. D. Huzuri, of Centre for Energy, for their enthusiastic support for various apparatus purchase and laboratory necessitates. Sincere thanks to Mr. D. K. Saikia and Mr. N. Das for looking into my official papers during the course of my stay.

I owe to my senior Dr. B. B. Sahoo to introduce me to the fascinating field of Diesel Engine and Alternative Fuels. Accompanying him in the laboratory and helping him during his experimental works have bestowed me with valuable knowhow and search the objectives of my work. I am also thankful to my colleagues, Mr. B. Bora and Mr. M. Dabi, who have provided me technical assistance during experimentation and helped me to gather data. I am fortunate enough to get ample support from the technicians Mr. J. Saikia, Mr. M. Sarma, Mr. D. Khaklary, Mr. D. Chetri, Mr. M.K. Baishya, and Mr. C. Banikya, directly or indirectly, to build the experimental setup.

I am also grateful to MHRD, Govt. of India, for providing me financial support through DST to attend and present a technical paper in ASME 2011 International Mechanical Engineering Congress & Exposition, held at Colorado, USA during November 11-17, 2011.

I am also thankful to Dr. M. Eswaran, Dr. R. P. Chopade, Dr. S. S. Mohapatra, Mr. R. Kumar, Mr. S. Mahto, Mr. C. Shravankumar, Mr. J. Sardar, Mr. A. Ghatak, Mrs. M.D. Ghatak, Mr. S. Anbarasu, Mr. S. Roy, Mr. R. K. Peetala and many other individuals with whom I have come into contact during my stay in IIT Guwahati. The friendship and unforgettable attachments shared with them has made my life pleasant.

I am blessed to be the son of my parents, with whom I was unable to spend at least 1 month continuous for last 10 years. Their love and support without any complaint or regret has enabled me to complete this Ph.D. My mother once did not inform me that my father had a stroke, as I was preparing for a foreign trip and took every responsibility of my father's treatment alone. I owe to both of them, whatever I achieve in life. Last but not the least; I am indebted to SRI SRI THAKUR for keeping me capable to counter the tests of life and making my life beautiful. May everyone's life be anointed and blooms with YOUR blessings.

June 2013

Guwahati, India ***Biplab Kumar Debnath***

Contents

Nomenclature

Notations

A	Availability (kW)
BP	Brake Power (kW)
C_p	Specific Heat (kJ/kg-K)
d	Diameter of the Orifice (m)
D	Engine Cylinder Diameter (m)
K	Number of Cylinder
L	Engine Stroke Length (m)
$\dot{m}$	Mass Flow Rate of Air (kg/s)
N	Revolutions per Minute (rpm)
p	Pressure (bar)
Q	Energy (kW)
r	Dynamometer Arm Radius (m)
R	Gas Constant (kJ/kg-K)
T	Temperature (K)
n	Number of Revolutions per Cycle
V	Volume (cc)
VE	Volumetric Efficiency
W	Dynamometer Load (Newton)

Greek symbols

θ	Crank Angle (degree)
η	Efficiency
ρ	Density of Fluid, kg/m^3
μ	Dynamic Viscosity, Ns/m^2
γ	Ratio of Specific Heats
λ	Stoichiometric Air Fuel Ratio

Subscripts

air	Air
amb	Ambient Condition
den	Density
eic	Exhaust Gas Inlet to Calorimeter
eoc	Exhaust Gas Outlet from Calorimeter
gf	Gaseous Fuel
IG	Fuel Ignition
in	Input
IN	Fuel Injection
lf	Liquid Fuel
plf	Pilot Liquid Fuel
we	Water Flowing through Engine Jacket
wic	Water Inlet to Calorimeter
wie	Water Inlet to Engine
woc	Water Outlet from Calorimeter
woe	Water Outlet from Engine

Abbreviations

ATDC	After Top Dead Centre (degree)
BSEC	Brake Specific Energy Consumption (kJ/kW-s)
BSFC	Brake Specific Fuel Consumption (kg/kW-h)
BTHE	Brake Thermal Efficiency
BTDC	Before Top Dead Centre (degree)
CA	Crank Angle (degree)
CI	Compression Ignition
CO	Carbon Monoxide (ppm)
CNT	Carbon Nanotube
CPO	Crude Palm Oil
CR	Compression Ratio
DI	Direct Injection
EGR	Exhaust Gas Recirculation
EGT	Exhaust Gas Temperature (ºC)
EA	Emulsion Activity
ES	Emulsion Stability
HC	Hydrocarbon (ppm)
HLB	Hydrophilic Lipophilic Balance
IC	Internal Combustion
ID	Ignition Delay (degree)
IP	Indicated Power (kW)
IT	Injection Timing (degree)
JOME	Jatropha Oil Methyl Ester
LHV	Lower Heating Value (kJ/kg)
NG	Natural Gas
NHRR	Net Heat Release Rate (J/deg.CA)
NO	Nitric Oxide (ppm)
NO_X	Oxides of Nitrogen (ppm)
O/W	Oil-in-Water
O/W/O	Oil-in-Water-in-Oil
PCP	Peak Cylinder Pressure (bar)
PM	Particulate Matter
POME	Palm Oil Methyl Ester
rpm	Revolution Per Minute
SI	Spark Ignition
SO_X	Oxides of Sulfur (ppm)
VCR	Variable Compression Ratio
WIP	Water in POME
W/O	Water-in-Oil
W/O/W	Water-in-Oil-in-Water

List of Figures

List of Tables

CHAPTER 1

Introduction

A vital segment of the growth of any civilization rests on the use of petroleum fuels, in various fields namely, industry, aviation, power production, transportation etc. However, the use of petroleum fuels needs to be reduced. This is because, they have limited potential and produce serious ecological impact. One of the feasible solutions that has got popularity during last few decades is the use of the fatty acid methyl esters, termed as biodiesels, as alternative fuels of diesel. While burnt in diesel engines, biodiesels offer drop of carbonated emissions and no sulfurized emission. However, being oxidized fuels, biodiesels emit nitrogen oxide (NO_X) emissions when burnt in diesel engine. The fuel emulsion can be a potent solution of this problem. The emulsified fuel, sprayed inside the cylinder, gets atomized and undergo "micro-explosion." If biodiesel is emulsified with water, then evaporation of water will reduce the adiabatic flame temperature and cut the thermal NO and NO_X emission. However, the study of emulsified biodiesel is rare in literature. Alongside, the emulsified biodiesel does not have the same properties to that of diesel too. Hence, the use of emulsified biodiesel at standard diesel engine setting will not offer the best performance. Therefore, it is necessary to study and optimize the performance, combustion and emission characteristics of emulsified biodiesel in a diesel engine at varied operating conditions, namely, load, compression ratio (CR) and injection timing (IT). In order to perform this, a bio-origin alternative fuel, palm oil methyl ester (POME), is selected and tested at various CR and IT settings. Moreover, the thermodynamic energy and exergy analyses are executed for both emulsified and neat POME at maximum efficiency condition. This chapter briefly describes about alternative fuels, especially, biodiesel, emulsified fuel, and various emission norms. Finally, the chapter concludes with the objectives of the present investigation and the layout of the thesis.

1.1 Preface

The world-wide increase of energy consumption is drastically increasing day by day. A report published by "The International Energy Outlook in 2011" shows that, energy consumption of the world will rise by around 53% between 2008 and 2035. This is because of the strong economic growth of the two most important developing countries in the world, namely, China and India. The day is not far, when both the countries will alone consume almost half of the projected rise of world energy use. The petroleum and other liquid fuels are the largest energy source world-wide which presently counts at almost 35% (India Energy Book, 2012). The present (2011) crude oil price is about $110 per barrel which is almost 30% higher than the level at the start of December 2010 on the New York Mercantile Exchange (Winter, 2011). This is expected to rise to $169 per barrel by 2020 and $200 per barrel by 2035. As far as India is concerned, the situation is not good since 2005. This is because the historical growth of oil production of 3% has been stagnated at that time and reduced in the following years (Figure 1.1). Since then, India has become heavily dependent on the oil import which started at $147 per barrel. Report shows that the rise of oil import, only from 2010 to 2011 has cost India almost 20.5 million US$ (25.7%) extra expenditure (India Energy Book, 2012). Presently, India is importing more than 80% of its fuel needs (Garg, 2012).

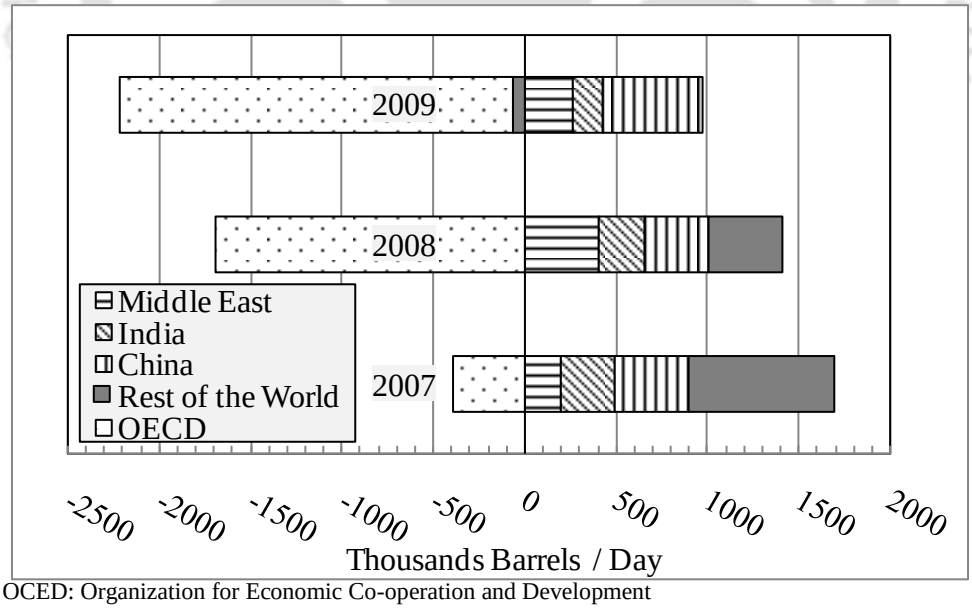

OCED: Organization for Economic Co-operation and Development

Figure 1.1 Global oil supply (India Energy Book, 2012)

The high increase of petroleum import is the result of the increase of petroleum product consumption (Figure 1.2). The market share of diesel, one of the primary products of petroleum in India was raised from 35.52% in 2006-07 to 43% in 2011-12, which is alone

11.9% in 2011-12 fiscal year (Modi, 2012). The demand of petroleum products is not going to lessen in coming years, because it's proportional to the urban development rate of nation. Hence, it is near to impossible for the government to cut down oil imports and thereby cease the huge outflow of currency. Neither petroleum companies can frequently generate new petroleum drilling sites. Therefore, the natural solution of this problem that comes into mind is to try to scratch petroleum intake by means of its suitable alternatives.

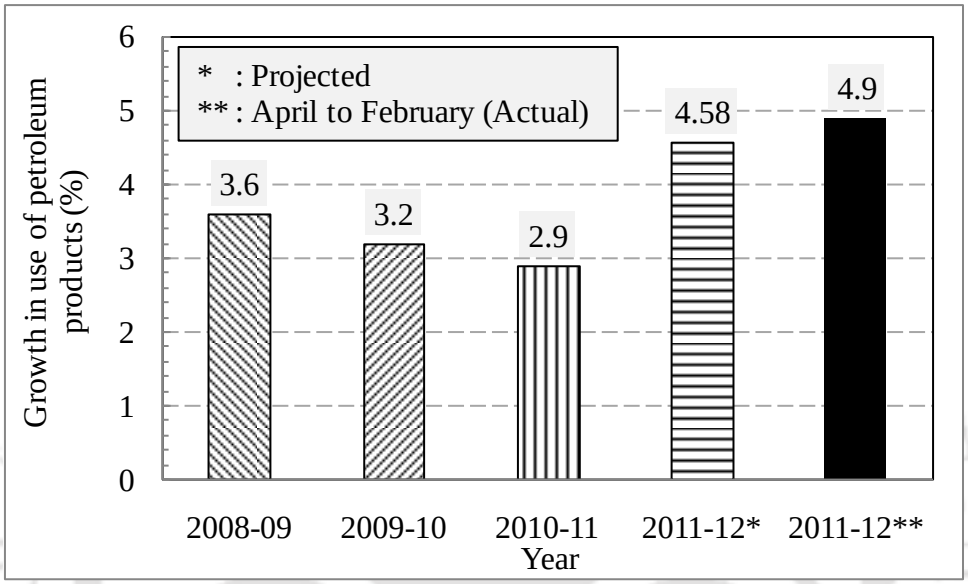

Figure 1.2 Petroleum product consumption (%) in India (Modi, 2012)

1.2 Alternative Fuels

The primary expectations from the alternative fuels are generation of power with economical fuel consumption and minor emission of pollutants. Alongside they should be safe enough to handle and store for both stationary and mobile application. An alternative fuel turns out to be pretty attractive to use, when it provides provision for local production and easy distribution through marketing networks. Finally an alternative fuel is acceptable when any combination of engine technology and fuel meets the prescribed vehicular emission norms as far as environmental prospective is concerned (Thipse, 2011).

Alternative fuel also known as non-conventional or advanced fuel can be defined as the fuel that can be utilized in the internal combustion (IC) engines with the exception of diesel or petrol. Principally, the alternative fuels are classified into three categories. The first type take account of petroleum fuels with non-petroleum additives namely ethers. The synthetic liquids that comprise properties comparable to that of traditional petroleum fuels but found

subsequent to treating of gaseous, solid or liquid fuels falls into second type. The last category non-petroleum fuels, namely alcohol, bio-fuels, biogas, hydrogen etc., are obvious choices (Lapidus *et al.*, 2005). In the midst of these the biofuels and biogas have an important role to be present-day scenario of energy crisis. This is because, biofuels, types of liquid alternative fuel, can be produced locally, from renewable sources. This helps to generate employment, thereby supporting domestic economy. This is helpful to shrink down the huge drainage of national currency in the form of petroleum import.

1.2.1 Biodiesel

The concept of using biodiesel, obtained from vegetable oil, as an alternative to diesel is not new. The "diesel engine", developed by Dr. Rudolf Diesel in 1895 was intended to run on a variety of fuels. In fact, at the World Exhibition in Paris in 1900, his engine was run by 'peanut oil' as fuel. Since then, the diesel engine has been periodically modified to run on petroleum based fuel, more specifically diesel obtained from petroleum. Historically, it was the cheapest fuel available (Clean Alternative Fuels: Biodiesel, 2012). At present, the dual crisis of modern era, the depletion of fossil fuel and its environmental constraints mandated people to interchange or alternate the use of fossil diesel.

Biodiesel is a renewable, environmental friendly fuel and has been regarded as a promising alternative fuel for stationary and mobile applications. Biodiesel, produced from animal fat, vegetable oil or waste cooking oil, can be used as the foundation for a clean substitute for fossil fuel in diesel engines, boilers or other combustion equipment. Its additional advantages consist of outstanding lubricity, superior combustion efficiency and low toxicity, among others (Lin and Lin, 2007a). It has a high flashpoint and low volatility, thus does not catch fire as easily as diesel. This increases the margin of safety in fuel handling, transport, and storage. Biodiesel, more or less contains, approximately 10% of oxygen by weight and thus can be considered as a kind of oxygenated fuel. The high oxygen content in biodiesel results in the improvement of its burning efficiency, reduction of PM, CO and other gaseous pollutants (Lin and Lin, 2007b). It can be used in two ways, either directly or blended with other liquid fuels together with diesel. Hence, it is considered as an environmentally friendly alternative fuel or its additive. Some commonly used biodiesels in diesel engines are the methyl esters of jatropha oil, honge oil, sunflower oil, soybean oil, rubber seed oil, rice bran oil, palm oil, etc. Presently a new type of alternative fuel has enticed the researchers around the globe and is called as emulsified fuel.

1.2.2 Emulsified Fuel

Diesel engine generally runs with excess air. As a result, at high combustion temperature nascent oxygen and nitrogen react together to form, NO which subsequently produces NO_X. Therefore, researchers around the globe are trying several options to reduce peak combustion temperature without deteriorating engine performance to cut NO_X emission. However, most in-cylinder methods adopted do not reduce NO_X and soot simultaneously. It has been seen that exhaust gas recirculation (EGR) can reduce NO_X emission but increases particulate emission. On the other hand, oxygen enrichment does the reverse. Further, when these two methods are employed together, they increase the cost, maintenance and added energy ingestion (Subramanian, 2011). Therefore, a modest method has to be established to reduce both of these emissions. Emulsification of fuel may be one of the methods which can solve this problem for a long term. This technique enhances fuel efficiency and reduces emission of hazardous pollutants from diesel engines (Crookes *et al.*, 1997). In emulsification, two or more immiscible fluids are mixed together such as water and diesel. This emulsified fluid (water-in-diesel) when sprayed through a nozzle gets atomized into fine liquid droplets. Since the boiling point of water is lower than that of diesel fuel, water droplets reach their boiling point first after it has absorbed sufficient reaction heat. The vaporization phenomenon of water then blows up the oil layer and thereby forms smaller oil droplets which results in an increase of the oil's surface to volume ratio. This phenomenon is called "micro-explosion" (Basha and Anand, 2011a). The mixing extent and the contact surface between air and fuel are increased due to micro-explosion, which leads to a significant increase in the burning rate and burning efficiency. The schematic diagram of mico-explosion is shown in Fig. 1.3.

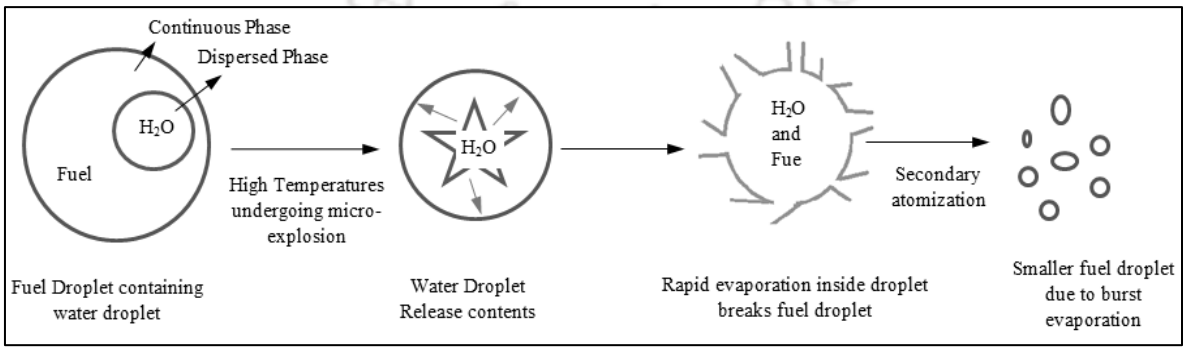

Figure 1.3 The process of micro-explosion (Basha and Anand, 2011a)

1.3 Emission Control Norms

Diesel engines are widely used in a variety of applications, namely, power generation, transportation, agriculture, marine, military, telecommunication generator sets, etc. They are more proficient and resilient than gasoline engines. However, they suffer awful nuisance due to their higher emission of wrongdoer pollutants like CO, HC, SO_X, NO_X and soot along with the traditional greenhouse gas CO_2. In order to trim down this hazardous emission, India has adopted stringent emission norms, which are also updated. The execution program of European Union emission standards in India is demonstrated in Table 1.1. Emission standards in Euro norms for Diesel Truck and Bus Engines are showed in Table 1.2.

Table 1.1 Indian emission standards for four wheelers
(Emission Standards, 2012)

Standard	**Reference**	**Date**	**Region**
India 2000	Euro 1	2000	Nation wide
Bharat stage II	Euro 2	2001	NCR*, Mumbai, Kolkata, Chennai
		April, 2003	NCR*, 11 Cities§
		April, 2005	Nation wide
Bharat stage III	Euro 3	April, 2005	NCR*, 11 Cities§
		April, 2010	Nation wide
Bharat stage IV	Euro 4	April, 2010	NCR*, 11 Cities§
* National Capital Region (Delhi) § Mumbai, Kolkata, Chennai, Bangalore, Hyderabad, Secunderabad, Ahmedabad, Pune, Surat, Kanpur and Agra			

Table 1.2 Emission standards for diesel truck and bus engines, g/kWh
(Emission Standards, 2012)

Year	**Reference**	**CO**	**HC**	**NO_X**	**PM**
2000	Euro 1	4.5	1.1	8.0	0.36*
2005§	Euro 2	4.0	1.1	7.0	0.15
2010§	Euro 3	2.1-5.45	0.66-0.78	5.0	0.10-0.16
2010§	Euro 4	1.5-4.0	0.46-0.55	3.5	0.02-0.03
* 0.612 for engines below 85 kW § Mumbai, Kolkata, Chennai, Bangalore, Hyderabad, Ahmedabad, Pune, Surat, Kanpur and Agra					

However, no matter what the emission standards implemented, the rate of increase in the vehicles both in the developed and developing nations cannot stop the rate of increase in environmental effluence single-handedly. The immediate solution of this problem may be the trim down with the substitution of diesel fuel by their alternatives.

1.4 Objectives

In the present investigation, a bio-origin alternative fuel, palm biodiesel, which is a Methyl Ester of Palm Oil (POME), is selected to study in emulsified form. This is because POME has the greatest oil yield per unit land on earth. The palm oil has the highest fossil energy balance, i.e., energy produced over energy consumed, and the lower production cost relative to other energy crops (Sumathi *et al*., 2008). POME ($C_{18.07}H_{34.93}O_2$) also has a sizable amount of oxygen bonded in its molecular structure that makes it burn more intensely. This also increases NO_X emission, which can be reduced by emulsifying it. A number of people have worked with POME in various types of diesel engines. However, work with emulsified POME as an alternative to diesel is rare. This is maybe because emulsified POME does not possesses the properties of diesel along with a lower heating value (LHV). This causes its inferior performance in standard diesel settings. Hence, there is a need to have a thorough and a systematic study on emulsified palm biodiesel in various engine settings in order to optimize its performance, combustion, and emission characteristics. These types of studies have not been reported in the literature. In view of this, the present investigation is aimed at optimizing the compression ratio (CR) and the ignition timing (IT) of an emulsified palm biodiesel (emulsified POME) run engine to achieve lower emission levels together with an improved or equivalent performance trends than a standard diesel engine. Besides, to locate and estimate the energy and exergy distribution, and destruction for the emulsified POME run diesel engine, a thermodynamic route, has also been considered. This study can play a significant role to understand the enhanced available energy management, of a diesel engine run by emulsified palm biodiesel (Caton, 2012). In summary, the following set of studies, in order, have been performed to arrive at the intended objectives:

- Experimentation with neat POME run engine at various CR and IT to optimize its performance, combustion, and emission characteristics as compared to a standard diesel run engine.
- Preparation of water-in-POME (WIP) samples and their characterization in order to select the optimum emulsion specification for the engine test.
- Experimentation with the WIP run engine at various CR and IT to optimize its performance, combustion, and emission characteristics as compared to a standard diesel run engine
- Thermodynamic analysis (energy and exergy potential) of both WIP and POME run engines.
- Exploring the potential of WIP as a pilot fuel in a biogas run dual fuel engine.

1.5 Organization of the Thesis

The thesis has been organized by focusing the concentration towards the clean and efficient power production from a diesel engine using emulsified biodiesel. **Chapter 1** offers the motivation acquired towards the use of alternative fuel especially emulsified fuel. This is followed by the objective of the dissertation. **Chapter 2** introduces the renewable biodiesels especially POME, literatures on emulsified fuels, some earlier, and recent works done in variable compression ratio (VCR) engines, the thermodynamic analysis, and the scopes of work. **Chapter 3** elaborates emulsified POME preparation and its characterization. It describe in brief about the surfactants used, hydrophilic lipophilic balance, ratio of emulsifying fluids, emulsion preparation procedure, measurement of droplet diameter and stability study of the emulsified POME. **Chapter 4** refers to the VCR engine setup and its different measurement and instrumentation devices. The experimental methods adopted for neat diesel, neat and emulsified POME are also described. **Chapter 5** shows the outcome of the experiments done by using POME in VCR diesel engine for a various compositions of load, CR, and IT. The results of the experiments help to optimize the aforementioned design parameters to achieve optimum performance, combustion and emission characteristics of neat POME in the diesel engine. **Chapter 6** represents the performance, combustion and emission analysis of emulsified POME tests in VCR mode in view of neat diesel. **Chapter 7** has a comparative study between the results obtained at optimized CR and IT combination for neat and emulsified POME test in view of neat diesel test. **Chapter 8** explains the thermodynamic analysis covering both first law and second law study of the aforementioned works at a load where maximum efficiency prevailed. **Chapter 9** portrays an attempt to check the influence of emulsified palm biodiesel as a pilot fuel in a biogas run dual fuel mode. **Chapter10** recaps the key findings of the experiments performed and the future works are proposed.

CHAPTER 2

Literature Review

The diesel engine has walked a long way from its invention, development, and run by peanut oil by Sir. Rudolf Diesel. He initially designed it to run with biofuel. Later on, the production of biofuel had become limited and expensive. Alongside, the increased supply of petroleum diesel made it economical to use. Hence, the following researchers got motivated to redesign the engine for petroleum diesel. The friendship with petroleum fuel with diesel was going good until the decade of seventies, when rise of the price of petroleum fuel and its emission was noticed seriously. Until then people are searching for suitable alternative for petroleum fuel especially diesel due to its almost exponential increase of use. It has been found that, biodiesel, produced from biofuels can be a suitable alternative. However, its detrimental issues, namely, lower calorific value and higher nitrogen oxide emission have to be resolved. In this regard, this chapter is dedicated towards the detailed review of the literature performed in the fields of biodiesel, especially POME and its blends with diesel. This is because, as mentioned in the objectives of the present investigation, POME is the carrying fluid of the emulsified fuel. This is followed by a detailed analyses of the emulsified fuels used for diesel engine run. Thereafter, an overview on the history of variable compression ratio (VCR) diesel engine is provided along with some earlier studies executed in it. Then, the recent investigations in VCR diesel engine are also revisited in view of the variation of some engine operating parameters, namely, load, compression ratio and injection timing. The chapter also includes a sincere discussion of literature on the thermodynamic potential study of various types of diesel engine. The special focus is provided on the first and second law studies performed by various researchers using various alternative fuels. Finally, the objectives drawn in the earlier chapter are justified by identifying the key scopes of works from the comprehensive review of respective literature.

2.1 Preface

This chapter describes the works performed with liquid alternative fuel. More focus is provided on methyl esters of biofuel, mainly palm oil methyl ester (POME) and its emulsion in diesel engine. Side by side, a detailed review on the performance, combustion and emission studies of variable compression ratio (VCR) diesel engine are also elaborated. The systematic investigation is executed for thermodynamic analysis of diesel engine.

2.2 Biodiesel from Palm Oil

Biodiesel is generally produced from vegetable oils through transesterification. This takes place between vegetable triglycerides and proper type of alcohol. Afterward, two products are left behind, fatty acid methyl esters and glycerin. These methyl esters are called as 'biodiesels' and are of biodegrading in nature (Duran *et al.*, 2005). Biodiesel emits less carbon monoxide (CO), particulate matter (PM), soot, unburned hydrocarbons and sulphur oxide (SO_X) than diesel (Schmidt and Van Gerpen, 1996). Some of the major works done by using biodiesels are shown in Table 2.1.

Oil palm, an oleaginous tropical plant, has the greatest oil productivity per unit of land on earth (Duarte *et al.*, 2007). Palm oil has dominated the world's vegetable oil demand because of its versatile uses ranging from food to consumer products, and now as biodiesel. Figure 2.1 shows the global vegetable oil production (Carter *et al*., 2007). The large supply of palm oil can be attributed to the superiority of palm oil in terms of oil yield (Table 2.2) requiring smaller area of land to produce oil. Besides, palm oil has the highest fossil energy balance, i.e., energy produced over energy consumed (Table 2.3), and the lowest production cost relative to other energy crops (Figure 2.2). It can be used in diesel engine in various ways, namely, crude palm oil (CPO), palm oil methyl ester (POME), and blending of CPO or POME with diesel. Some of the vital works done with palm oil are described as follows.

Assessment of the carbureting eminence of biodiesel, the physical and chemical properties, namely, calorific value, BTHE, distillation curve, viscosity, cloud point, etc., needs to be resolute. Table 2.4 compares the physical-chemical specifications of POME to that of diesel fuel. As reported by Duarte *et al.* (2007), transesterification of palm oil reduces its calorific value, density, cloud point, and carbon residue as compared petroleum diesel. However, the higher cetane level pays for this drawback. POME produces an efficient burning, making more use of its energy content.

Table 2.1 Important research findings by various researcher(s) on different types of biofuels or biodiesels

Researchers	Biodiesels	Key findings
Agarwal *et al.* (2008); Agarwal and Rajamanoharan (2009); Sinha and Agarwal (2010)	Linseed, Rice-bran, Karanja	A blend of 20% Linseed methyl ester with diesel shows higher BHTE and lower smoke emission. After 100 h of endurance test with 20% Rice-bran oil in diesel shows lower carbon deposit on in-cylinder parts, lower wear on piston rings and cylinder inner surface than diesel. Karanja oil blends with diesel (up to 50%) without as well as with preheating can provide lower emissions and improved engine performance.
Altin *et al.* (2001)	Sunflower, Soybean, Cottonseed	Diesel engine run by Cottonseed biodiesel provides higher engine power, lower CO, CO_2 and NO_X emissions than Sunflower or Soybean biodiesel run. However, smoke emission is higher for the Cottonseed biodiesel.
Buyukkaya (2010); Gokalp *et al.* (2011)	Rapeseed, Soybean	Running Rapeseed oil in diesel engine increase BSFC, NO_X emission; decrease ID, CO, HC and smoke emission as compared to neat diesel. The 5% to 50% blends of Soybean biodiesel with marine diesel produces 74% lower smoke opacity, 12% higher BSFC than diesel in diesel engine.
Banapurmath *et al.* (2008, 2009); Banapurmath and Tewari (2008, 2009);	Honge, Rice Barn, Neem	The maximum BTHE for diesel, Honge, Rice Barn and Neem oils is found to be 31%, 28%, 27% and 26% respectively. Using methyl ester of Honge oil and producer gas in dual fuel mode shows better performance without using the gas carburetor than with gas carburetor. Moreover, Smoke and NO_X emission reduces; whereas CO and HC emission increases with Honge oil as pilot fuel. Injection advancement from 19° to 27° improves performance moderately.
Devan and Mahalakshmi (2009, 2010)	Paradise, Eucalyptus, Poon	A blend of 50% Paradise biodiesel with Eucalyptus oil provides a drop of CO (37%), HC (35%) and smoke (49%) emission, along with a 2.4% rise in BTHE. In addition, a little rise in NO_X is also reported. Diesel engine run by a blend of 40% Poon biodiesel with diesel shows that smoke, HC and CO were reduced by 65%, 20% and 37%, respectively than diesel run.

Jindal *et al.* (2010a, 2010b); Panwar *et al.* (2010)	Jatropha, Karanja, Castor seed	Both Karanja and Jatropha biodiesel perform poorer than diesel, whereas former provides higher ID than the later. Both of these fuels produce lower HC, NO_X, and smoke emission than diesel. The combined increase of CR and injection pressure for Jatropha biodiesel run engine increases the BTHE, and reduces BSFC and emissions. The best combination is found at CR=18 at an injection pressure of 250 bar. The lower blends of Castor seed biodiesel increased the BTHE, reduced the BSFC and EGT.
Puhan *et al.* (2005, 2007); Vedaramana *et al.*(2012a, 2012b)	Mahua, Sal, Neem	At full load, the methyl and ethyl ester of Mahua oil produce BTHEs of 28.3% and 26.42%, respectively, as opposed to 26.36% for neat diesel. For methyl ester, the highest drops in HC, CO and NO_X emissions are obtained as 60%, 67%, and 9% as compared to 49%, 79% and 27% for ethyl ester, respectively. The use of Sal biodiesel in diesel engine cuts CO, HC and NO_X by 25%, 45% and 12%, respectively without major change in BTHE.
Raheman and Phadatare (2004); Raheman and Ghade (2008)	Karanja, Mahua	Up to 40% blend of Karanja oil with diesel is found to increase BP, BTHE and BSFC by 6%, 25% and 7.4%; whereas reduce CO, smoke density and NO_X emissions by 80%, 50% and 26%, respectively. At all CRs (18:1-20:1) and ITs (35-45°BTDC) tested in diesel engine, an increase in the proportion of Mahua oil with diesel, the BSFC and EGT are increased, whereas BTHE is decreased. The use of Ricardo diesel engine showed satisfactory performance even with neat Mohua oil at various CR-IT settings.
Rakopoulos *et al.* (2006, 2008)	Cottonseed, Sunflower,	A blend of 20% Cottonseed oil with diesel provides a similar BTHE, increased BSFC, HC and NO_X; reduced CO and soot emissions than 10% or 20% blends of Sunflower biodiesel with diesel.
Kumar *et al.* (2010, 2011)	Jatropha	The Jatropha biodiesel offers almost a similar performance with diesel mode. However, HC and smoke emissions are increased by 10%. Further, a higher ID and a lower NO_X emission are also reported.

Table 2.2 Oil production and yield of major oil crop in 2006 (Sumathi *et al.*, 2008)

Oil crop	Average oil yield (tones/ha/year)	Planted area (million ha)
Soybean	0.40	94.15
Sunflower	0.46	23.91
Rapeseed	0.68	27.22
Oil palm	3.62	3.62

Table 2.3 Estimated ranges of fossil energy balance (FAO, 2008)

Fuel	Feedstock	Fossil energy balance (ratio)*
Biodiesel	Soyabean	14–3.4
	Rapeseed	1.2–3.6
	Waste vegetable oil	4.8–4.8
	Palm oil	8.6–9.6
Diesel	Crude oil	0.8–0.9

*The fossil energy balance = [Energy contained in the fuel]/ [fossil energy used in its production]

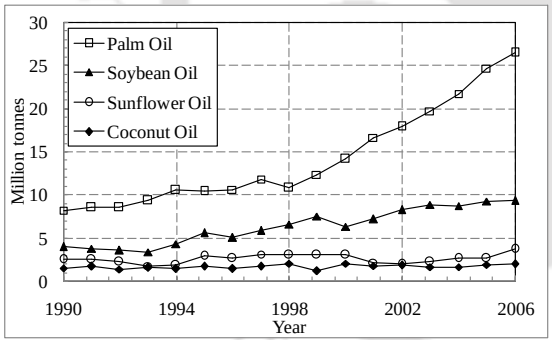

Figure 2.1 Global vegetable oil production for the duration of 1990 to 2006 (Carter *et al.*, 2007)

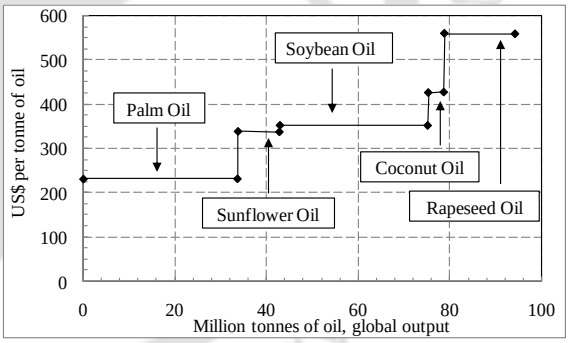

Figure 2.2 Average cost and quantity of vegetable oil production, 2004/05 (Carter *et al.*, 2007)

Rodríguez *et al.* (2011) performed an experimental study by using POME to find its ID and compared with diesel. Table 2.5 shows the comparison at different speed and torque. The ID of POME is lower than diesel engine. Further, with an increase in speed ID increases, whereas an increase in load reduces ID. This is because; at higher speeds fuel-air mixing time reduces, whereas at higher loads cylinder temperature elevates. They also proposed a new correlation to calculate the ID of biodiesels with available literature and experimental findings to predict it more accurately.

Table 2.4 Physical-chemical properties of petroleum diesel and palm biodiesel

SN	Properties	Diesel	POME (from different sources)					
1	Viscosity (cST)@ 40 °C	4.0	4.30[§]	4.73[#]	4.5*	4.5[♦]	4.58[◊]	4.7[Δ]
2	Density (kg/L)@ 40 °C	0.823-0.85	0.870[§]	0.872[#]	0.855*	0.870[♦](@ 25°C)	0.872[◊](@ 15°C)	0.87[Δ](@ 15°C)
3	Flash Point (°C)	98.0	142.0[§]		174.0*	174.0[♦]		121[Δ]
4	Pour Point (°C)	14.0	16.0[§]	12.0[#]	16.0*	16.0[♦]		
5	Cloud Point (°C)	18.0	19.0[§]	16.0[#]	16.0*	--	--	
6	Calorific Value (MJ/kg)	42-44.8		37.13[#] (Lower)	40.135*(Higher)	40.135[♦](Higher)	37.13[◊](Lower)	41.7[Δ](Higher)
7	Cetane Number (Cst)	45-53-55		62[#]	65*	50[♦]	51.1[◊]	51[Δ]
8	Chemical formula	$C_{12}H_{26}$	$C_{18.07}H_{34.93}O_2$					
9	Average molecular weight		284.2					
10	Oxygen (%wt)		11.26					
12	Carbon residue (wt. %)	0.14			0.02*	0.02[♦]		

§ Nova Oleochem Limited, ShahiwalaBldg, Zaveri Bazar, Mumbai – 400 002 (India); [#] Benjumia *et al.* (2009); * Nagi *et al.* (2008); [♦]Masjuki *et al.* (1993); [◊]Agudelo *et al.* (2009); [Δ]Husnawan *et al.* (2009)

Table 2.5 ID of POME and diesel (Rodríguez *et al.*, 2011)

Rotation (rpm)	Torque (Nm)	ID of POME (°CA)	ID of diesel (°CA)
1500	138	13	13
1900		13	16
2300		16	18
1500	277	12	14
1900		12	15
2300		14	16
1500	415	11	12
1900		11	15
2300		13	16

Benjumia *et al.* (2009) have found that with an increase of altitude, the injection of POME automatically advanced by 2°. This is attributed to the lower heating value of biodiesel that increased the supply of fuel by 12%. Usually, POME produces earlier combustion timings than diesel. This is endorsed by the higher Cetane rating of POME that reduces the premixed combustion duration. Therefore, the heat release starts before TDC. This is further justified by the curves of pressure and temperature.

Masjuki *et al.* (1996) have showed that brake power (BP) produced by the engine is affected as the temperature of the POME is increased especially for POME9535 (POME9535: POME at 95℃ and intake air at 35℃) and POME 5034. As the temperature of POME is increased, its viscosity is reduced resulting better fuel spray, atomization, and fuel evaporation. Same group of authors (Masjuki *et al.*, 1997) studied the effect of POME and diesel emulsions containing 5 and 10% of water by volume in diesel engine and compared with the 100% POME and diesel.

Blends of palm oil or POME with any other fuel alters the fuel's physicochemical properties, with viscosity, cloud point, BTHE, heat value, and boiling point. For example, BTHE of the fuel drops due to the drop in the viscosity. Therefore, the properties of blend must be kept within certain limits (Aziz *et al.*, 2005). The effect of emulsified bio-solution or POME-diesel blends on the emission of a 4 cylinder diesel engine is stated by Chen *et al.* (2010). The tested fuels are P0 (diesel), P10 (10 vol% POME + 90 vol% P0), P20, P30, E16P10 (16 vol% bio-solution + 10 vol% POME + 74% P0, extra 1 vol% of surfactant), E16P20 and E16P30. The bio-solution is made by natural organics as additives and surfactant is used to cut interfacial tension. Agudelo *et al.* (2009) revealed that with the increase in POME quantity, IT automatically gets advanced. This is because; the injection pump has to operate a little early to inject more fuel to maintain same BP and speed. As a result, the energy release starts early

and peak combustion pressure increases to about 12 bar for neat POME. This results the peak combustion temperature to shift near TDC. Although POME provides almost similar (or sometimes better) combustion than diesel, but its lesser LHV causes the BSFC to increase for the same BP, thereby reducing the BTHE marginally.

Husnawan *et al.* (2009) have studied the effect of emulsifying the bland of diesel and POME by 5%, 10% and 15% volume of water on diesel engine. According to them, with the increase in water in fuel mixture, the amount of deposition reduces. However, the least amount of carbon and hydrogen is found for the fuel mixture having 10% water (Figure 2.3). This was due to the thermal degradation process of polymeric components as well as the vaporization of highly oxidized hydrocarbons. The increase of water in the POME-diesel mixture causes bigger fuel droplets and poor fuel air mixing. As a result, the flammability of the fuel reduces; the combustion efficiency drops and hence CO rises. The emulsified fuels provide lower NO_X emissions. The water vaporization causes the local temperature to drop and thereby suppressing the thermal-NO. As a result, N_2 does not get full activation energy to react with oxygen to form NO_X (Figure 2.4). In addition, long run test (up to 500 h durability test) conducted by them provided no significant difficulties in engine operation or damage problems.

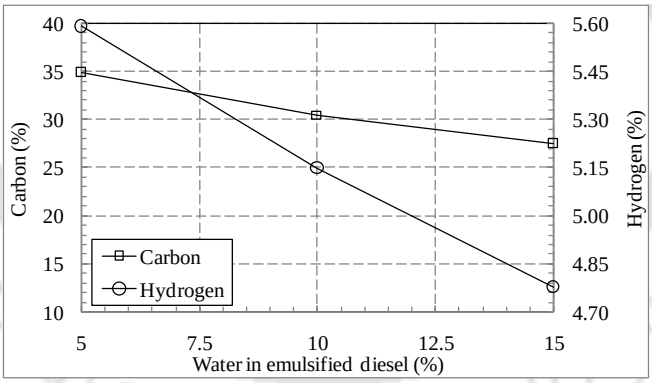

Figure 2.3 Percentage carbon and hydrogen in diesel carbon deposits derived from diesel–water fuel containing varying proportion of water (Husnawan *et al.*, 2009)

Lin *et al.* (2006) have studied the effect of POME-diesel blends (20%, 30%, 50 and 75%) on the engine PM emission and energy efficiency in a 4 cylinder, 4 stroke diesel engine. Their study have showed that blending of POME up to 30% with diesel produces lower particulate matter (PM) emission than neat diesel. However, beyond 30% blend, PM emission increases. Similar results are also reported for soluble organic fraction of (SOF) of PM (Figure 2.5). Beyond 50% blend of POME shows incomplete combustion. The energy efficiency also shows peak value within 10% to 20% blend and it deteriorates beyond 20% blend.

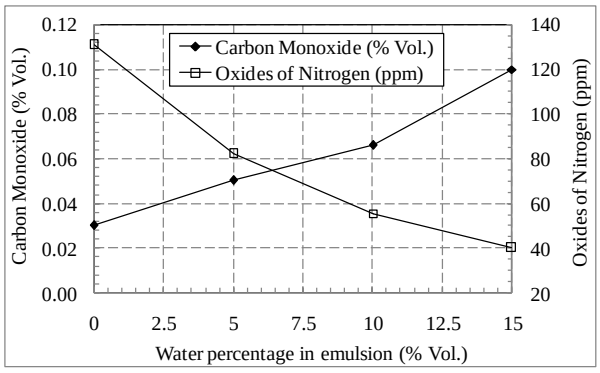

Figure 2.4 Carbon monoxide and nitric oxide emissions (Husnawan *et al.*, 2009)

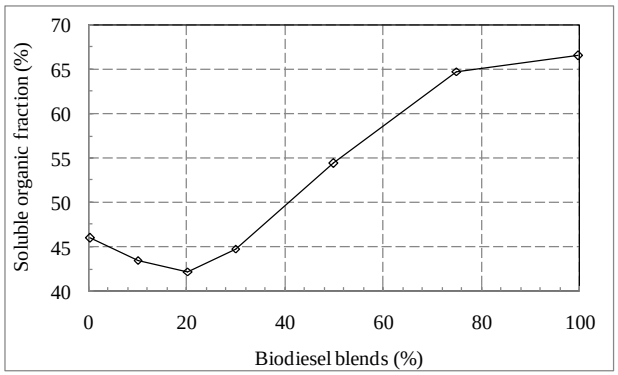

Figure 2.5 SOF (%) in the exhaust of diesel generator (Lin *et al.*, 2006)

Aziz *et al.* (2005) have showed that 3, 5 and 10% POME blends with diesel maintains almost similar BTHE, and an increased BSFC as compared to diesel. However, the ID reduces with the increase of biodiesel quantity in the blend. It is the increased quantity of O_2 in POME is responsible for this behavior. The rise of CPO substitution, all the brake specific quantities of CO, CO_2 and HC drop except NO_X (Aziz *et al.*, 2006). It means that the blend of CPO and neat diesel improves combustion rather than the petroleum diesel alone. The rise in NO_X emission depicts the presence of higher quantity of oxygen in the CPO, which ultimately boosts the rate of combustion.

Kalam and Masjuki (2002) have revealed that addition and increment of palm oil in diesel engine have increased the BP and reduced NO_X, CO and HC emission. The addition of palm oil and corrosion additives in diesel have resulted better combustion of the liquid fuel in the diesel engine. This increases BP and reduces HC emission. Side by side, fuel additive reduces the ion formation for oxidation process which cuts the heat release rate thereby maximum temperature and hence NO_X formation. Application of palm oil with corrosion additive had reduced the engine wear too, which was observed from the reduction of Fe, Cu and Pb debris found in the lubricating oil. Viscosity changes are also found to be normal for both the OD-palm oil compositions tested. Hence, finally they have concluded that the palm oil is suitable for diesel engine comparable to its competitive like soybean or rapeseed biodiesels.

2.3 Emulsified Fuel

The core review process starts with the idea of surfactants and HLB number, elementary types of emulsion. Thereafter, review process proceeds toward the study performed by various researchers on emulsion characterization and standardization.

2.3.1 Surfactants and HLB Number

Surface active agents or surfactants are substances that contain both polar and nonpolar groups in their molecules. These dual characters, called amphipathy or amphiphilicity, results in a double affinity of polar or nonpolar substances, and mix them through stable interfaces (Schwartz *et al.*, 1977). However, the surfactants may contain unequal concentration of polar or nonpolar molecules too. The surfactants, which have more affinity to polar liquids like water are called hydrophilic. On the contrary, lipophilic surfactants are more soluble to nonpolar liquids like oils. Based on their affinity to polar or non-polar liquids, each surfactant is given a particular number; called hydrophilic lipophilic number or HLB. Griffin is the first to offer the idea of HLB (Griffin, 1949). In 1954, he suggested a formula for calculating the HLB number of nonionic surfactants (Griffin, 1954):

$$\mathrm{HLB} = 20 \times \frac{M_h}{M_h + M_l} \tag{2.1}$$

where M_h and M_l are the molecular mass of the hydrophilic and lipophilic portion of the molecule. As a consequence, a scale of 0 to 20 results, where, an HLB value of 0 represents a completely hydrophobic molecule and 20 resembles to a molecule built with totally hydrophilic parts. Table 2.6 shows some of the applications of surfactants, range of HLB values and their behavior in water with examples.

Table 2.6 Some common use of surfactants, HLB ranges and conduct with water (Rosen, 2004; Guo *et al.*, 2006; DOW Surfactants, 2011)

Sl No.	Use	HLB Range	Behavior in water	Example (HLB Value)
1	Mixing unlike oils	1-3	No dispersibility	SPAN 85 (1.8), SPAN 65 (2.1)
2	Making water-in-oil emulsion	4-6	Poor dispersion	SPAN 80 (4.3), SPAN 60 (4.7)
3	Wetting powders into oils	7-9	Milky dispersion after vigorous agitation	SPAN 20 (8.6), TRITON X-35 (7.8)
4	Making self emulsifying oils	7-10	Stable milky dispersion	TWEEN 61 (9.6), TRITON X-45 (9.8)
5	Making oil-in-water emulsions	8-16	From translucent to clear	TWEEN 85 (11), TWEEN 21 (13.3)
6	Making detergent solutions	13-15	Clear solution	TWEEN 80 (15), TWEEN 60 (14.9)
7	Making oil-in-water emulsion	13-18	Clear solution	TWEEN 40 (15.6), TWEEN 20 (16.7)

2.3.2 Types of Emulsion

Emulsions, being liquids, do not exhibit a static internal structure. The droplets dispersed in the liquid matrix are usually assumed to be statistically distributed. The emulsion types vary based on their use. There exist certain classes or types of emulsions, as stated below:

2.3.2.1 Based on Droplet Size

The researchers on emulsion around the globe classify emulsions in three categories based on droplet size of the dispersed substances (Holmberg and Österberg, 1986; Rieger and Rhein, 1997; Rosen, 2004). They are listed below:

(i) Macroemulsions: These are the most known type opaque emulsions with particles having larger than 400 nm (0.4 μm). The particles can easily be observed under a microscope. In this type, the particle size of the dispersed phase is higher, and hence the interfacial surface per unit volume is lesser. Thus, they have a lesser interfacial tension. This makes the interfacial film or the surfactant layer to expand and swallow the smaller droplets causing an increase in instability of the emulsion. Producers have primarily chosen the macroemulsion path because it minimizes their costs by using a limited amount of surfactant.

(ii) Microemulsions: Microemulsion is a thermodynamically stable and a dispersion of two immiscible liquids, such as oil and water, stabilized by an interfacial film of surfactant molecules. The free energy of microemulsion formation can be considered to depend on the extent to which surfactant lowers the surface tension of the oil–water interface and the change in entropy of the system. The emulsion looks like a bluish white semi-opaque solution. The particle sizes lie between 100-400 nm (0.1-0.4 μm). These emulsions need a little more time to prepare and find their use in cosmetic and pharmaceutical industry.

(iii) Nanoemulsions (miniemulsions): They are formed by mixing its constituents gently unlike others. These emulsions are generally transparent and kinetically stable. The particle size is less than 100 nm (0.1 μm). Unlike microemulsions (which require a high surfactant amount), nano-emulsions can be prepared by reasonable surfactant concentrations (less than 10%). Because of their tiny droplet sizes and high kinetic stability, they are found in various industrial applications such as personal care and cosmetics, health care and agrochemicals. Nanoemulsions, are particularly adapted for the generation of nanomaterials.

2.3.2.2 Based on Phase

Again, based on phase, emulsions can be classified broadly into two categories. These are two- and three-phase emulsions and some of the important studies performed by using these emulsions are shown in Table 2.7.

(i) Two-phase emulsion: These emulsions are generally created by mixing two inherently immiscible fluids. The fluid which is intruded is called 'dispersed phase' and the base fluid is called the 'continuous phase'. The common types of two-phase emulsions are water-in-oil (W/O) and oil-in-water (O/W) emulsion. Since in W/O emulsion, water is the dispersed phase, it is considered as an alternative to diesel. The O/W emulsion is generally used in pharmaceutical, and such other areas (Lin and Wang, 2004b; Lin and Chen, 2006a).

(ii) Three-phase emulsion: In this type of emulsion the inner and outer phases are separated by a dispersed phase, called intermediate phase. The three-phase emulsions are also called as "multiple emulsion" or "emulsions of emulsions." This is because the droplets of the dispersed phase consist of even smaller droplets in them (Garti, 1997). Later on, researchers started preparing three-phase emulsions by three different methods, namely, (a) phase inversion, (b) mechanical agitation, (c) two-stage emulsification. However, the last technique, two-stage emulsification is frequently used. The two major types of multiple emulsions are the water-in-oil-in-water (W/O/W) and oil-in-water-in-oil (O/W/O) emulsions. The O/W/O emulsion is generally implemented as an alternative for compression ignition diesel engines (Lin and Wang, 2003). One experimental investigation performed on W/O/W and O/W/O emulsion using SPAN 80 and TWEEN 80 shows that SPAN 80 alone can provide better stabilization than TWEEN 80 with same quantity of concentration (Hou and Papadopoulos, 1997).

2.3.3 Emulsion Characteristics

The purpose of this section is to accumulate and analyze various characterizations associated to the emulsions studied by numerous researchers.

2.3.3.1 Surfactant and Hydrophilic Lipophilic Balance (HLB)

As observed earlier that, the surfactants are required to adjust the surface tension of the dispersed and the continuous phase, to prepare stable emulsions. Primarily, there are two types of surfactants necessary to increase the affinity between the continuous and dispersed phase. These are called lipophilic and hydrophilic surfactants. Although there are a variety of

surfactants available under these two categories, most of the researchers have preferred the use of SPAN 80 and TWEEN 80 as the lipophilic and hydrophilic surfactants (Table 2.8).

Table 2.7 Two and three-phase emulsions

Type	Researcher	Emulsion type	Continues phase (%vol.)	Dispersed phase (%vol.)
Two-phase	Lin and Wang (2004b)	O/W	Water: (90, 80, 70)	Diesel: (10, 20, 30)
		W/O	Diesel: (90, 80, 70)	Water: (10, 20, 30)
	Lin and Chen (2006a)	O/W	Water: (90, 85)	Diesel: (10, 15)
		W/O	Diesel: (90, 85)	Water: (10, 15)
	Samec *et al.* (2002)	W/O	Diesel: (90, 80)	Water: (10, 20)
	Abu-Zaid (2004)	W/O	Diesel: (100, 95, 90, 85, 80)	Water: (0, 5, 10, 20, 30)
	Lin and Chen (2008)	O/W	Water: (85)	Diesel: (15)
		W/O	Diesel: (85)	Water: (15)
	Kumar *et al.* (2005)	AFE	Animal fat: (88, 78, 68)	Water: (5, 10, 15) Methanol: (5, 10, 15)
	Lin and Lin (2007a)	W/O	Soybean Oil Methyl Ester: (90)	Water: (10)
	Ghannam and Selim (2009)	WO	Diesel: (90, 80, 70, 60, 50)	Water: (10, 20, 30, 40, 50)
	Ashok (2012a, 2012b)	EMF	Diesel: (50)	Ethanol: (50)
	Basha and Anand (2011a, 2011b)	W/O	Diesel: (83, 93)	Water: (15, 5)
Three-phase	Lin and Chen (2006a)	O/W/O	Diesel: (85)	Water: (15)
	Lin and Wang (2003, 2004b)	O/W/O	Diesel: (85, 70, 55)	Water: (10, 20, 30) Diesel: (5, 10, 15)
	Lin and Chen (2008)	O/W/O	Diesel: (85)	Water: (15)

It has been reported that, for two and three-phase (W/O and O/W/O) emulsions prepared by the same quantity of water and oil, the former one has the lower viscosity than the later one. This is because of the more dissimilar surface contact that leads to an increase in friction between phases of the O/W/O emulsion (Lin and Chen, 2006a). As a potential diesel engine fuel, lower the dispersed phase (e.g. water) diameter, more is the possibility of water droplets to become accommodated inside the fuel droplets when injected. This will intensify the simultaneous droplet breakup and can improve fuel-air mixing. However, while emulsifying, animal fat, SPAN 83 is reported to produce a stable emulsion (Kumar *et al.*, 2005).

Table 2.8 Various surfactants used with quantities and HLBs for emulsion preparation

Researcher	Emulsion type	Surfactants	Quantities (%)	HLB
Lin and Wang (2004b); Lin and Chen (2006a); Lin and Lin (2007a)	O/W	TWEEN 80	1	15
	W/O	SPAN 80	1	4.3
	O/W/O	SPAN 80 and TWEEN 80	1, 2, 3	6,7,8,9, 10,11,13
Abu Zaid (2004)	W/O	SPAN 80 and TWEEN 80	2, 3	-
Basha and Anand (2011a, 2011b)			2	8
Kumar *et al.* (2005)	W/O	SPAN 83	2.0	7
Ghannam and Selim (2009)	W/O	Triton X-100	0.2, 0.25, 0.5, 0.75, 1, 1.75, 2, 3, 5	-
Nadeem *et al.* (2006)	W/O	SPAN 80 and Gemini Surfactant	0.2, 0.4, 0.5, 1.0	-

2.3.3.2 Additives

The additives are used in a fuel to enhance its the physical and thermal properties, which improves the engine performance, as well as reduces emission (Sajith *et al.*, 2010). Some of the additives used to improve the emulsified fuel property are shown in Table 2.9. The application of diglyme additive, which has 35.8-wt% oxygen compound causes higher increase in viscosity for two-phase O/W emulsion than W/O emulsion. This is because of the interfacial areas between the diglyme additive, dispersed phase, and outer phase in the two-phase emulsions are significantly increased (Lin and Wang, 2004b). It is observed that the use of 10% aqueous ammonia, as a NO_X inhibitor, in three-phase O/W/O biodiesel emulsion is found to have enhanced the heating value, as compared to the O/W/O emulsion without ammonia. Alongside, it substantially reduces the kinematic viscosity, mean droplet size of the dispersed phase and weight of carbon residue. Hence, aqueous ammonia may reduce NO_X emission, but it will increase HC emission (Lin and Lin, 2007b; Lin and Lin, 2008). Applying dimethyl ether, diethyl ether and H_2O_2 as additives with diesel-ethanol emulsified (EMF) fuel have shown that, the higher Cetane number of dimethyl ether have led to a better performance, combustion and emission of a diesel engine (Ashok, 2012a; Ashok, 2012b). The alumina and carbon nanotubes are found to increase the calorific value and Cetane number of the water-diesel emulsified fuel, with the expense of emulsion stability (Basha and Anand, 2012a; Basha and Anand, 2012b).

Table 2.9 Various additives used with quantities for emulsion preparation

Researcher	Additive	Quantities
Lin and Wang (2004b)	Diglyme (%)	5, 10
Ashok (2012a, 2012b)	Dimethyl Ether, Diethyl Ether	12
	H_2O_2	12
Basha and Anand (2012a, 2012b)	Alumina (ppm)	25, 50, 100
	Carbon Nanotube (CNT) (ppm)	25, 50
Lin and Lin (2007b, 2008)	Aqueous ammonia (%)	5, 10

2.3.3.3 Mixing Parameters

As stated earlier, the emulsion is known to be the heterogeneous mixture of two immiscible fluids, mostly liquids. The mixing process, therefore, performed with the help of some external means – mechanical blending or ultrasonic agitation. In this regard, the frequently used apparatus, and the two significant parameters – the speed of revolution and the time of emulsifications are shown in Table 2.10. The mechanical homogenizing machine, the mostly used emulsifying machine, stirs up the mixture of continuous and dispersed phase with the presence of surfactant (Lin and Wang, 2003). With the increase in the revolution of homogenizer, the mean droplet diameter is found to be reduced almost linearly (Lin *et al.*, 1995; Lin and Wang, 2004b). Alongside, there has been some application of ultrasonic agitation in literature to prepare emulsified fuel. The ultrasonic waves are of mechanically vibrating types and propagate through a transmission medium causing cavitation. Side-by-side, the motion of ultrasonic wave creates an alternate positive and negative pressure waves. Both of these methods forms a strong stirring effect and mixes the two immiscible fluids (Lin and Chen, 2006a). For the two-phase water diesel emulsion, prepared by both mechanical homogenizer and ultrasonic emulsion have shown that, the later one can yield emulsion with finer distribution of water than the earlier one (Lin and Chen, 2006a; Lin and Chen, 2008).

2.3.3.4 Criteria of Effective Emulsion

It is known that, emulsions are generally the mixture of dissimilar fluids. Hence, it is necessary to study the duration of which the dispersed phase remain uniformly spread all over the continuous phase. This study is performed by two methods, namely, Emulsion Stability (ES) and Emulsion Activity (EA) (Lin and Wang, 2003).

(i) Emulsion Stability (ES): The ES represents the capability of an emulsion to conserve the emulsifying layer after being kept motionless or heated at some temperature for a preset time. The ES value is determined by calculating the ratio of the emulsifying layer volume to the total volume of the emulsion. The experimental study performed by water and diesel emulsion shows that the emulsion layer remains for 6-7 days. However, for any percentage of water used to prepare emulsion, after 1 day of keeping it motionless, the deposition reaches at least 10-15% of the solution (Lin and Wang, 2004b). The emulsification stability of the three-phase O/W/O emulsions is found to be much better than that of the two-phase W/O emulsions. Figure 2.6 illustrates that, for water in diesel emulsion, the increase of temperature from 25ºC to 50ºC, increases the sedimentation. This is again the highest for two-phase W/O emulsion (Lin and Chen, 2006a).

Table 2.10 Type of apparatus, speed and duration of emulsion preparation

Researcher	Apparatus	Speed (rpm)	Time (minute)
Lin and Wang (2003, 2004b)	Mechanical Homogenizing Machine	3000, 5000 and 8000	1
Lin and Lin (2007a)		3000 and 8000	5
Basha and Anand (2012a, 2012b)		2500	15
Kumar *et al.* (2005)	Electrical Homogenizing Machine	2000	-
Ghannam and Selim (209)	Silent Crusher M Homogenizer	15000 - 20000	2, 10, 30
Lin and Chen (2006a, 2008)	Ultrasonic Vibration Machine	-	1, 5, 10, 15, 20, 30, 60, 90, 120, 150 and 180

(ii) Emulsion Activity (EA): The EA is the ability of the emulsion to retain its emulsifying layer under the action of any centrifugal force. It has been reported that, with the increase of centrifuging time or percentage of dispersed phase in the emulsion, the deposition increases. However, for the same amount of water and oil in W/O and O/W emulsion; the deposition percentage remains same for both the cases at the same centrifugal speed (Lin and Wang, 2003). As the centrifugal speed is increased, the height of the O/W emulsion sediment layer increases. This is because the specific gravity of oil is lighter than that for water and the O/W emulsion droplets float to the top (Figure 2.7). For O/W, emulsion with 10% oil content in the emulsion has found to be stronger to resist the centrifugal force. The same amount of

water (10%) has been found to be sufficient in W/O emulsion to produce lesser sedimentation (Lin and Wang, 2004b).

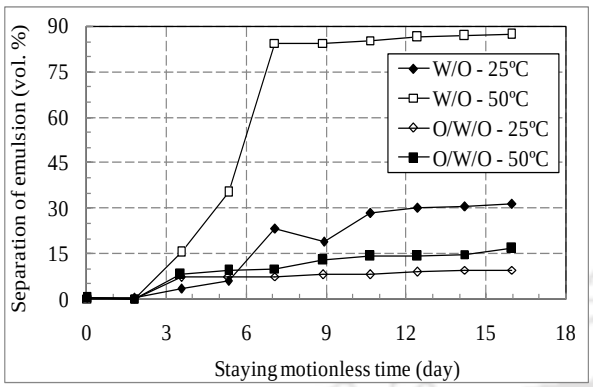

Figure 2.6 The separation of W/O and O/W/O emulsions for temperature variation after being motionless for a duration of 16 days (Lin and Chen, 2006a)

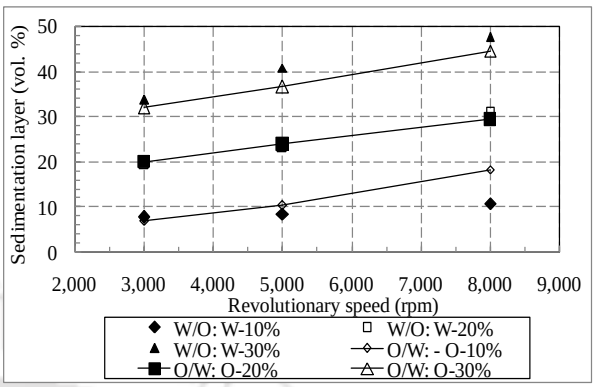

Figure 2.7 Effects of water contents and revolutionary speed on the sedimentation layers of the W/O and O/W emulsions (Lin and Wang, 2003)

2.3.4 Effect on Engine Performance

The most generalized emulsions used as fuel in a diesel engine are the emulsion prepared by water and diesel with various phase orientations. As soon as these emulsions are injected into the cylinder, the fine water droplets burst spontaneously and form a high pressure steam. This acts as an additional pressure force on the piston top that increases the torque of the engine and effects on the engine performance (Dryer, 1977; Abu-Zaid, 2004). These are discussed as follows.

2.3.4.1 Brake Power

Experimental studies show that with the increase of speed, brake power (BP) increases but upto a certain speed (Abu-Zaid, 2004; Nadeem *et al.*, 2006). This is again related to the rating of the engine and number of cylinder. The increase of water percentage in water-diesel emulsion increases the BP marginally. This is attributed to the increase of dispersed water molecules in emulsion that increase the rate of micro-explosion of the same during the combustion process. Again, the effect of emulsions prepared using gemini surfactant (1, 2-ethanebis) and conventional surfactant (SPAN 80) showed a very little alteration in BP (Nadeem *et al.*, 2006). Almost all other investigations have been performed at constant speed engines, which produce same BP at identical loads and are employed to explore its effect on other parameters (Ashok and Saravanan, 2007; Ashok, 2011a; Ashok, 2011b; Subramanian, 2011).

2.3.4.2 Brake Thermal Efficiency

An experimental work with water in diesel emulsion using SPAN 80 and TWEEN 80 as surfactant with water quantity varied from 5 to 20%. It is noted that, at various engine speeds, the increase in water percentage in the emulsion increase brake thermal efficiency (BTHE) with (Abu-Zaid, 2004). This type of trend was also observed in other studies (Sawa and Kajitani, 1992; Ganesan and Ramesh, 2002). Investigation performed on two and three-phase water-diesel emulsion with water quantity varied from 10%, 15% to 20% at speeds of 1600 and 1800 rpm. The study showed a higher BTHE is obtained for W/O emulsion with 15% of water at 1600 rpm (Lin and Wang, 2004a; Lin and Chen, 2006b). However, at high speed conditions (2000 rpm to 3000 rpm), BTHE reduces with the increase in load (Armas, 2005). A study performed by using carbon nanotubes (CNT) with 5% water emulsified diesel shows to improves engine efficiency at higher loads (Basha and Anand, 2011a). This is because at higher load condition, the CNT with its high surface area captures more heat and accelerate the 'micro-explosion' of water. As a result, the micro-explosion process takes place at a faster speed, which boosts the engine efficiency. Same group of authors reports similar results using alumina nanoparticles with 5% of water (Basha and Anand, 2011b).

Experimental study with emulsion of diesel and ethanol (or EMF), in the ratio of 50:50, 60:40, and 70:30 without surfactant showed a performance improvement with higher ethanol quantity (50%) (Ashok and Saravanan, 2007). The presence of higher oxygen quantity in ethanol is believed to enhance the BTHE. Again the variation of injection angles to 18°, 20°, 23° and 24° showed that at higher injection angles 50:50 diesel ethanol emulsion provides a better BTHE. This is because of the increase in rotational movement of fuel, which enhances air and fuel vapor mixing and improves efficiency. They extended their study to emulsified ethanol diesel fuel with 5% water and 6% H_2O_2 with the presence of hydrophilic surfactant TWEEN 80 (Ashok, 2011b). Their study shows that emulsified fuel without water shows better performance than same with water. Presence of water reduces the quantity of free oxygen in the emulsion and hence the Cetane number. The addition of dimethyl ester (DME) and diethyl ester (DEE) with 50:50 ethanol diesel emulsion have shown to increase in BTHE further than H_2O_2 (Ashok, 2011a). As observed in Fig. 2.8, at lower load condition water injection of 0.4 ratio shows efficiency improvement than emulsion of same water-diesel ratio. This is because, at lower loads, the presence of water in emulsion overcools the charge against the effect of water injection in the inlet manifold.

2.3.4.3 Brake Specific Fuel Consumption

Brake specific fuel consumption (BSFC), on the other hand, seems to improve with an increases in water quantity in water diesel emulsion (Tsukahara and Yoshimoto, 1992; Abu-Ziad, 2004; Nadeem *et al.*, 2006). As water quantity increases in emulsion, a higher amount of diesel is moved by equal amount of water. As a result a lower quantity of diesel is actually remains in emulsion. The presence of water causes finer droplet of diesel just after injection due to quick vaporization of water and results more premixed combustion. Experimental study performed by three-phase and two-phase emulsion shows that W/O emulsion always produces a lesser BSFC than O/W/O emulsion (Lin and Chen, 2006b; Lin and Chen, 2008). The water droplets in O/W/O emulsion are larger than W/O due to the presence of another inner oil phase inside water droplets. This causes to restrict the extent of micro-explosion for a while and hence combustion of O/W/O emulsion stays a bit incomplete (Chung and Kim, 1991). This fact also reduces calorific value of O/W/O emulsion than W/O ones. However, the result of BSFC is little contrary with 20% water for water-diesel emulsion at 1800 rpm (Lin and Wang, 2004a).

As reported, the presence of CNT in water diesel emulsion reduces BSFC than without CNT (Basha and Anand, 2011b). This is because it improves thermal property of the charge thereby reducing the duration of autoignition. Hence, an increase in CNT in emulsion further reduces BSFC as observed in Fig. 2.9. Similar results are also reported for implementing alumina nanoparticle in water diesel emulsion (Basha and Anand, 2011b). The lower calorific value of ethanol causes to reduce the BSFC of the ethanol blended diesel fuel (Ashok and Saravanan, 2007). With the increase of ethanol percentage the BSFC value further reduces. This is because increase in ethanol quantity reduces energy content of the emulsified fuel (Likos *et al.*, 1981). Variation of injection angle (18°, 20°, 23° and 24°) of 50:50 composition of ethanol diesel emulsion causes reduction of BSFC. The lower energy content of emulsified fuel coupled with the increase in rotational movement of fuel reduces BSFC. For the same reason, the BSFC of H_2O added ethanol diesel emulsified fuel run engine reduces as compared to a diesel run engine. Besides, lesser energy content of H_2O_2 than ethanol (Born and Peters, 1998) is also responsible of its reduced BSFC than diesel (Ashok, 2011b). Oxygen enriched DME and DEE cause lesser fuel consumption than H_2O_2 added ethanol diesel emulsion fuel as described by Ashok (2011a). It is mainly because of less energy content of the esters used than H_2O_2. However, this result is contradictory. Because, Lin and his coworker opine that, a reduction in energy content of fuel generally increases BSFC (Lin

and Lin, 2007b). As reported by them, the presence of 10% water in O/W/O water biodiesel emulsion reduces its energy content. Hence, BSFC of emulsion is bound to increase than diesel fuel. However addition of aqueous ammonia increases the energy content of the emulsion and hence BSFC reduces.

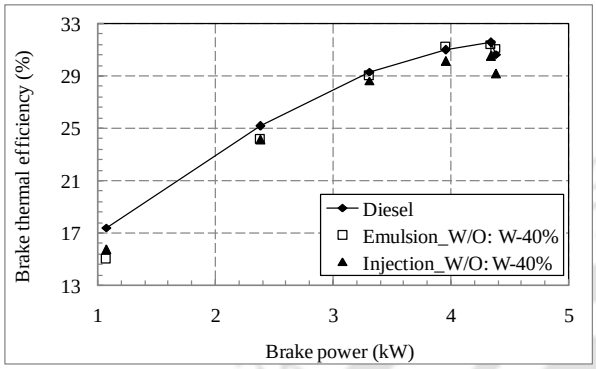

Figure 2.8: Comparison of brake thermal efficiency with application of emulsified fuel and water injection in cylinder (Subramanian, 2011)

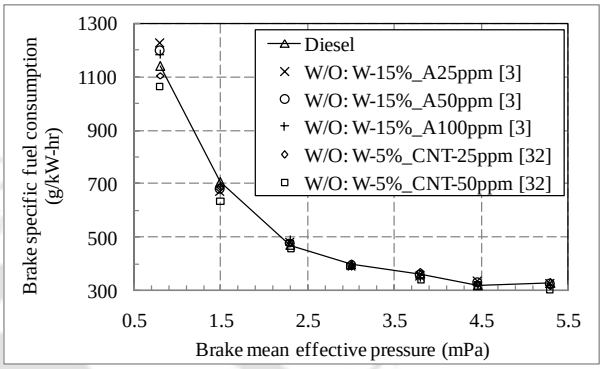

Figure 2.9: Variation of brake-specific fuel consumption for CNT and alumina blended water diesel emulsion (Basha and Anand, 2011a; Basha and Anand, 2011b)

2.3.5 Effect on Engine Combustion

One of the prime purposes of using emulsified fuel in diesel engine is to improve its combustion characteristics. A number of researchers have studied various types of emulsion by implementing a number of additives to improve burning characteristics of emulsified fuels. These are discussed in following subsections.

2.3.5.1 Ignition Delay and Combustion Duration

A number of the researchers have suggested that, ignition delay (ID) of emulsified fuel run engine is higher (Kumar *et al.*, 2005; Ganesan and Ramesh, 2002). This is because, for emulsified fuel, the physical delay period during the evaporation of dispersed phase inside the continuous phase and thereby the breakup of the continuous phase (i.e. mother fuel) becomes more. The high viscosity of emulsified fuel causes the needle to lift for a little more time. However, this is not sufficient to reduce ID, as it is compensated by the increase in delay time due to micro-explosion (Armas *et al.*, 2005). A study with water emulsion and direct water injection in diesel engine shows that, with the emulsion even though there is no change in the air temperature at the time of injection, the presence of water (having higher specific heat than diesel) along with diesel increase the specific heat of the droplets (Subramanian, 2011). The ID of an emulsified fuel is found to reduce with load, a common fact for all the fuels (Basha and Anand, 2011a; Basha and Anand, 2011b; Kannan *et al.*, 2012). Some researchers

suggest that, lower ID reflects lesser compressive power and a lesser quantity of fuel required to produce the same power. At the end, this is profitable for the concerned BTHE (Basha and Anand, 2011a). The ID is higher for animal fat emulsions with water and methanol (Table 2.11). Vaporization of water and methanol reduces the temperature of the intake air and fuel. In addition, water and methanol reduces the overall Cetane number of the emulsions. However, the combustion duration is reduced with water and methanol. Due to the longer ID, more fuel is physically prepared (evaporation, mixing, etc.) with the emulsions for chemical reaction, and rapid burning occurs in the premixed stage. The micro-explosion further accelerates diffusion combustion and decreases total combustion duration (Kumar *et al.*, 2005).

Table 2.11 Variation of ignition delay and combustion duration with neat animal fat and its emulsions (Kumar *et al.*, 2005)

Type of fuel	Ignition delay (ºCA)		Combustion duration (ºCA)
Neat Diesel	6.2		40.5
Neat animal fat	8.2		48.5
Emulsified animal fat 1 (Water-5%, Methanol-5%)	8.2		48.5
Emulsified animal fat 2 (Water-10%, Methanol-10%)	9.2		45.5
Emulsified animal fat 3 (Water-15%, Methanol-15%)	9.2		44.4

2.3.5.2 Cylinder Pressure

The use of 10% water in diesel emulsion has found to provide almost similar trend of cylinder pressure and peak pressure values to that of diesel. With the increase of speed, peak pressure increases for both diesel and its emulsion with water (Armas *et al.*, 2005). It is noticed that, the increases of water quantities from 10% to 40% by volume have found to shift the cylinder pressure curve more towards the expansion stroke. As a result, the premixed combustion phase becomes larger and the combustion occurs impulsively (Park *et al.*, 2001). While studying different ITs, namely, 10°, 15°, 20° before top dead center (BTDC), it is observed that, the peak pressure value shifts more towards the top dead center (TDC) for advanced injection of the emulsified fuels. The cylinder pressure trends in Fig. 2.10 shows that the magnitude of peak pressure drops almost 0.7-1.5 MPa as the IT is further retarded (Park *et al.*, 2000). Investigations have also been performed using neat animal fat and emulsified animal fat with 5, 10, 15% methanol and 5, 10, 15% water. The study shows that

emulsified animal fat starts burning a little late. However, at a later stage, its combustion improves and results a higher peak pressure than pure fat. Side-by-side, with the rise of water and methanol fraction in emulsions increases the peak pressure. This work says that, presence of water and methanol lowers the temperature of the cylinder and leads to added fuel increase. This causes a rapid combustion of emulsions, when its is initiated. Thereafter, the combustion rate is enhanced, and the peak pressure is increased (Kumar *et al.*, 2005).

2.3.5.3 Heat Release Rate

Water in diesel (W/O) emulsified fuel with alumina and CNT nanoparticle shows an increase in heat release rate than diesel run (Basha and Anand, 2011a; Basha and Anand, 2011b). This is because of the enhancement of the premixed combustion phase. This may be attributed to its shortened ID and improved ignition properties due to the presence of nanoparticles which probably have initiated an early combustion as compared to that of neat diesel. Investigation on the use of animal fat emulsion shows an improvement in heat release rates, as shown in Fig. 2.11. It initiates a late combustion, but provides an increase in the heat release rate at the premixed burn period when compared with neat animal fat (Kumar *et al.*, 2005). The diffusion combustion phase is somewhat less productive with the emulsion when compared with neat fat. It can be noted that the end of combustion also arrives earlier with the emulsion when compared with neat animal fat. The good atomization and vaporization of emulsions promote rapid mixing with the surrounding air. The oxygen enrichment with the presence of methanol boosts the overall combustion process and helps in further oxidation of the unburned fuel in the diffusion phase. Hence, the diffusion combustion is improved. Oxygenated additives like DME and DEE improves premixed combustion of emulsified fuel (Ashok, 2011a). It is seen that, the fuels which have oxygen in their molecules, possess a higher Cetane number. As a result, the emulsified fuels with DME and DEE start burning early but release a lesser amount of heat.

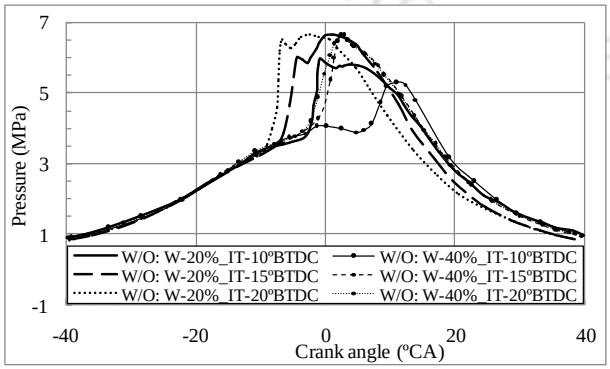

Figure 2.10 Variation of cylinder pressure for different water quantities and injection timings for W/O emulsion (Park *et al.*, 2000)

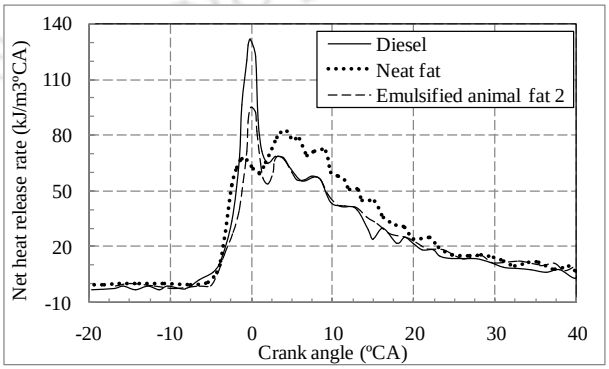

Figure 2.11 Variation of heat release rate with neat animal fat and its emulsion (Water-10%, Methanol-10%) (Kumar et al., 2005)

2.3.6 Effect on Engine Emission

The "micro-explosion" of emulsified fuel is known to create a stronger degree of mixing, which boosts reaction rate between the atomized oil droplets and air next to it. This causes a rapid rise in the premixed combustion rate, thereby improving the burning efficiency. Some of the researchers explain this as the reason for the drop of hydrocarbon by emulsified fuel (Murayama *et al.*, 1978). The water vaporization absorbs heat causing fall in the adiabatic flame temperature. This is liable for the reduced chemical reaction between N_2 with O_2 to form NO or NO_X emission (Song *et al.*, 2000). In this regard, the various emission characteristics of emulsified fuel run are diesel engines are reviewed.

2.3.6.1 Oxides of Nitrogen

The formation of NO_X emission is a very complicated process. It depends on the fuel type, engine design, and the factors related to the test cycle (Chokri *et al.*, 2012). Several orthodox and alternative techniques have been studied to trim down the diesel engine NO_X emission. Among these, the addition of water is considered as one of the effective tactics to the in-cylinder reduction of NO_X (Isihada and Chen, 1994, Sheng *et al.*, 1995). The reduction of NO_X emission for water emulsions are governed by chemical kinetics (Zeldovich mechanism) and some physical phenomena such as water vaporization (Curran *et al.*, 1995). When different amounts of water are added to the fuel, the corresponding amount of fuel is replaced by water resulting a lower combustion temperature. In a diesel engine, the combustion temperature is further reduced during the water vaporization processes. Lower combustion temperature, however, directly influences thermal NO formation during the reduction in chemical reaction rates for Zeldovich mechanism reactions (Warnatz *et al.*, 1996). Moreover, the NO concentration reduces more, due to the drop of the oxygen atoms concentration, consumed during the OH radical's formation by the dissociation of water. The simultaneous occurrence of these processes causes an effect, once called, 'heat sink', thereby limiting the formation of NO_X (Dryer, 1977). The effects of single and multi-points water addition systems on the NO_X emissions of a heavy-duty diesel engine have been studied and verified in Fig. 2.12 (Samec *et al.*, 2000; Samec *et al.*, 2002).

The application of oxidation catalyst (platinum coated on a sieve containing wastcoat) and nanomaterial (CNT, alumina) are also found to reduce NO_X emission of water diesel emulsion, significantly (Basha and Anand, 2011a; Basha and Anand, 2011b). Generally, for alcohol/diesel fuel emulsions, the Cetane-depression properties of alcohol causes higher NO_X

emission. Low Cetane number leads the fuel to increase ID and greater rates of pressure rise, which results a higher peak cylinder pressure and high peak combustion temperature. This high peak temperature increases NO_X emission (Ishida *et al.*, 1997). As a result, more the oxygen-enriched, additive, higher is the value for Cetane number of emulsified fuels, lower is the NO_X emission (Ashok, 2011a).

2.3.6.2 Oxides of Carbon

The formation carbon monoxide (CO) is due to the incomplete combustion of fuel. It has been seen that, if there are any chances of increase in combustion temperature, then the oxygenation of CO increases (Heywood, 1988). For example, Lin and his coworkers showed that, with the increase of load and with lower water quantity in water-diesel emulsion, CO emission reduces (Lin and Wang, 2004a; Lin and Chen, 2006b). It is a well-known fact that with an increase in load, an engine consumes more fuel, and its combustion increases the cylinder temperature. Alongside, for emulsions with higher water quantity, higher will be the water evaporation. This consumed considerable amount of sensible and latent heat, thereby reducing the combustion temperature and increasing CO emission (Figure 2.13) (Lin and Wang, 2004a). For high-speed diesel engines, the relative time required for a complete combustion of one cycle, reduces. In that case, the time consumed during micro-explosion becomes predominant that significantly increases CO emission, especially beyond 1800 rpm (Nadeem *et al.*, 2006). Moreover, for three-phase (O/W/O) diesel-water emulsion, the burning rate is lower than two-phase W/O emulsion. The application of ultrasonic emulsifier has been found to disperse the water droplets with smaller diameter than the mechanical homogenizer. This is found responsible for an increase of burning gas temperature and consequently a reduction of CO emission (Lin and Chen, 2008). The application of nano-particles (CNT, alumina), of 50 ppm or more, is found to reduce CO emission for water diesel emulsion in a diesel engine. However, the exothermic reaction of carbon oxidation is probably responsible for larger CO reduction, while using CNT than alumina (Basha and Anand, 2011a; Basha and Anand, 2011b). Similarly, application of H_2O_2 as a fuel additive has been found to increase the molecular oxygen, which reduces CO emission for diesel-ethanol emulsion run engine (Ravikkumar *et al.*, 2001; Ashok, 2011b).

With the increase in load, the fuel consumption is increased. This reduces the equivalence ratio, and results a fuel rich combustion. Hence, more fuel is reacted with air to increase the CO_2 emission, irrespective of the fuel type (Lin and Chen, 2006b). However, engine run with

three-phase water-biodiesel emulsion with 10% water is found to produce lower CO_2 emission than neat biodiesel (soybean) run. This is because, the water content might have soaked the partial enthalpy of reaction, which reduces the conversion rate of CO to CO_2. However, with the increase of engine speed, the mixing of the atomized fuel particles with air might have improved. This has subsequently increased the CO_2 emission of the three-phase biodiesel emulsion run engine (Lin and Lin, 2007b).

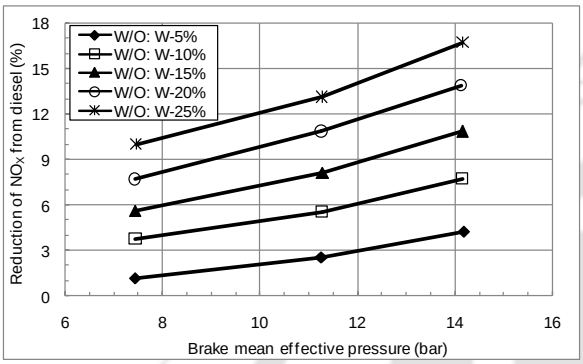

Figure 2.12 Reduction of NO_X emission with the increase in water percentage in water-diesel emulsified fuel (Samec *et al.*, 2000)

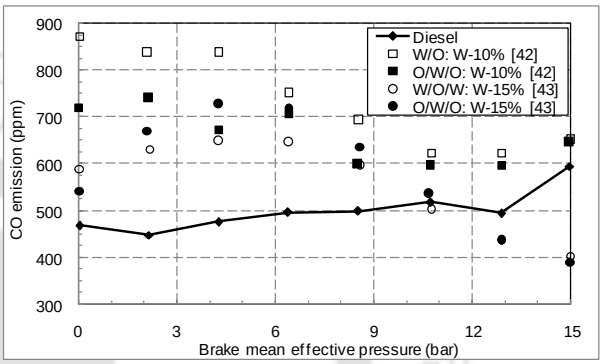

Figure 2.13 Variation of CO emission of water-diesel emulsion for various engine load and water percentage (Lin and Wang, 2004a; Lin and Chen, 2006b)

2.3.6.3 Hydrocarbon and Smoke

The hydrocarbon (HC) emission from a diesel engine depends mainly on the mixing of fuel and air. In this regard, the over-mixing or under-mixing of fuel, the penetrating force of fuel spray, the atmosphere (pressure and temperature) inside the cylinder at the instant of fuel injection are vital points (Heywood, 1988). The earlier studies on emulsified fuel in a diesel engine show that, in one side, micro-explosion improves mixing of fuel and air. On the other side, it also prompts quenching of local flames owing to a lower temperature, an inhibitory consequence of water (Tsukahara *et al.*, 1982a; Tsukahara *et al.*, 1982b; Subramanian, 2011). The effect is seen predominant in the work of Park and his coworkers (Park *et al.*, 2001), where at each load, for water diesel emulsion, the increase in water percentage from 10% to 40%, with a step of 10%, have increased the HC emission almost linearly. However, preheating emulsified waste vegetable oil with 40% water by volume has been found to produce almost diesel equivalent HC emission, when run in a diesel engine (Reding *et al.*, 2009). Alongside, to achieve a lower HC, the IT of the water emulsified diesel fuel has also to be optimized (18ºBTDC) rather than just retarding (15ºBTDC and 12ºBTDC) or advancing it (21ºBTDC and 24ºBTDC). The addition of methanol, ethanol and diesel with biodiesel

water emulsion has also found to produce a higher HC emission than neat diesel or neat biodiesel (Kannan and Anand, 2001). Further, applications of CNT or alumina with water diesel emulsion have not reduced the smoke emission significantly, either (Basha and Anand, 2011a; Basha and Anand, 2011b). The effect of these nanoparticles in the particulate emission is also not explored by the researchers in respective works. The primary importance of using water-emulsified fuel may be the reduction in NO_X. However, it can simultaneously reduce smoke emission too (Murayama *et al.*, 1978). It is reported that, neither water fumigation, nor water direct injection can reduce both NO_X and smoke emission together. This is because of the water vapor from emulsion present in the fuel rich side and destroy soot precursors. However, this is not the case for water fumigation or direct injection (Greeves *et al.*, 1976). Hence, with the increase in water in emulsion, the smoke emission reduces progressively (Park *et al.*, 2001; Subramanian, 2011). The same trends of results are reported for water-animal fat emulsion with methanol. The presence of methanol oxygenates the charge. Alongside, the micro-explosion of water vapor eliminates the formation of rich pockets and dilutes the black smoke released (Kumar *et al.*, 2005; Lin and Lin, 2007b).

2.4 The VCR Engine

In a VCR engine, the CR can be changed. This is generally done by changing the clearance volume. The basic idea of using VCR concept is to use high CR during low loads for high efficiency. Side by side at higher loads reduced CR can match knocking and internal heat transfer. The result is a small super charged engine with high specific performance leading to good fuel consumption, with performance equal to a larger engine.

2.4.1 Brief History

Sir Harry Ricardo first built VCR engine in 1920 when he was dealing the problem of knocking. This work led to him devising the octane rating system that is still in use today. However, that engine never came out from the test bench. Later on, two US patents (Kemper, 1978; Freudenstein and Maki, 1981) reported that by changing the piston stroke length or by tilting the engine block, CR could be changed. Finally, SAAB Automobiles (Ozcan and Yamin, 2008) made a SVC engine in which they were able to change CR from 8:1 to 14:1 by changing the cylinder volume at piston top dead center. Later on Nissan, MCE-5, Lotas are different companies who built different types of VCR engines. The creative skills they used came out with a variation in CR from 7:1 to 50:1 for both two and four stroke engine.

2.4.2 Earlier Work on VCR engine

- One of the primitive works done on the VCR engine was to build the AVCR 1360-2 engine of 335 brake mean effective pressure (BMEP) by Teledyne Continental Motors' (TCM) after fifteen years of VCR piston and high specific output research. The engine was adept to create adequate steady state with reduced peak transient smoke burst at suitable levels (Grundy *et al.*, 1976).

- A novel research work was performed under British Petroleum Oil Company (Sobotowaki *et al.*, 1991) by modifying a direct injection (DI) diesel engine into VCR mode. The prototype engine was having large crevice volume and equivalent fuel injection equipment. The experimental observation showed that the engine provided extremely low NO_X and HC emission; whereas light load particulate emission and high load fuel consumption were increased.

2.5 Recent Work on VCR Engine

The numerous work performed using VCR engine in research and development field throughout the globe are basically on performance enhancement by parametric optimization. Various alternative liquid and gaseous fuels are also used for this purpose. Some of these important contributions are described in the following subsections.

2.5.1 Effect of Load

The study performed in Kirloskar TV1 VCR engine (Jindal *et al.*, 2010b) showed for 100% Jatropha methyl ester that the increase in load reduces BSFC and increases BTHE. This is the result of reduction in losses and increase in power at higher loads. Laguitton and his coworkers reported that at lower loads slower rate of combustion at lower CR results reduction in maximum rate of pressure change. However, NO_X and smoke formation increases with the increase in load and fuel consumption remains unaffected (Laguitton *et al.*, 2007). Experimental works performed for Mahua biodiesel (B100) and its four blends (B20, B40, B80, and B100) with diesel in VCR engine showed the similar results as reported by earlier researcher (Raheman and Ghadge, 2008). For constant CR and speed, the surge in load in a VCR diesel engine in dual fuel mode will lead to the increase in the mass of gaseous fuel to be admitted. Hence, the BTHE of the engine will increase for constant pilot fuel supply. Later, when it auto ignites, the gaseous fuel burns with a higher rate of pressure rise (Selim, 2004).

2.5.2 Effect of Compression Ratio

The experimental works of Jindal and his coworkers (Jindal *et al.*, 2010b) show that increase in CR increases BTHE. This is because of the combination of higher power output at higher CR, better combustion and improved lubricity of biodiesel. Side by side, HC emissions tend to increase with the increase in CR from 17 to 18. At lowest CR, insufficient heat of compression delays ignition and hence HC emission reduces. However, at higher CR, CO and smoke opacity is lower. This is because; at lower CR, temperature attained inside cylinder is low resulting incomplete combustion, which reverses in higher loads. As a result higher CR increases CO_2 and exhaust gas temperature (EGT) and subsequently NO_X emission.

Raheman and Ghade, (2008) reported that, B100 provides 19.3% and 11.5% reduction in BSFC when CR is increased from 18 to 19 and 19 to 20 respectively; whereas for diesel the corresponding values are 10.7% and 8.0%. The increase in BTHE are 23.1%, 29.5%, 32.5%, 37.8%, 40.6% and 41.7% for diesel, B20, B40, B60, B80 and B100 when CR is increased from 18 to 20. That is running the engine at higher CR is more beneficial with biodiesel comparable to diesel. This is because; biodiesels provide lower volatility and better viscosity than diesel that results improved combustion characteristics at higher CR. Laguitton *et al.* (2007) varied the CR (18.4:1 and 16.0:1) by reducing the bowl pip size, while maintaining the same squish height**.** Their study showed that at lower CR the combustion starts very late even at higher load also. As a result, combustion remains incomplete; hence, temperature falls resulting drop in the NO_X. This fact also cuts smoke formation at high load and low CR.

Selim (2004) reported that LPG has most nonuniform behavior as its knock onset was observed very early (8.1 Nm torque) for a CR of 22. However, at these lower CR engine can withstand more amount of gaseous fuel. For N_2 and methane, the onset behaviors of knock and ignition failure are almost similar with a tendency to burn a little more quantity. He also reported that increasing the CR increases the combustion noise due to the higher self-ignition possibility of the gaseous fuels at higher pressures and temperatures. Selim and his coworkers reported that, pressure rise rate increases as the CR increase due to increase in temperature (Selim *et al.*, 2008). This consequently increases the susceptibility of the gaseous fuel to auto ignite. This fact also causes the increase in the maximum pressure. The increase in CR increases the expansion ratio thereby increases in power output and thus the fuel intake falls. LPG-diesel is the most effective dual fuel composition. Their study showed that increase in CR cuts HC emissions for all dual fuel compositions studied. However, dual fuel composition

with Jojoba methyl ester yields more CO and HC compared to diesel. This is because of the higher kinematic viscosity (3 to 10 times) of that particular biodiesel than diesel.

2.5.3 Effect of Injection Timing

The effect of ethanol fuels on the spray behavior, combustion and emission characteristics of a common rail four cylinder diesel engine were studied by Park *et al.*, (2011) at 1,500 rpm of engine speed and various ITs. Both the ethanol blended fuel compositions are showing unstable combustion characteristics at the lowest and highest load (0 and 60 Nm). However, at 30Nm load fuel IT of 6° and 9°BTDC provides the best combustion characteristics comparable to TDC and 3°BTDC. The ethanol-blended fuels offer larger ID than diesel due to low BTHE of the ethanol. The peak combustion pressure and heat release rate is also increased with the advance of IT because of the shift of combustion towards TDC from expansion stroke. Alternatively, IT retardation reduces the peak pressure and temperature inside cylinder, which consequently drop in NO_X formation.

As observed in Fig. 2.14 (Sayin *et al.*, 2010), both advancing (25°BTDC) and retarding (15°BTDC) the IT result rise in the BSFC, BSEC and drop in BTHE comparable to original IT (20°BTDC). This is due to the joint effect of low density, low viscosity, and lower BTHE of methanol. Therefore, more fuel consumption takes place and efficiency falls. However, all the three blending of methanol are producing affective drop in CO, HC and smoke opacity compare to diesel. Further, IT advancement causes additional drop of the above emissions. The IT advancement causes increase in the NO_X and near TDC peak cylinder pressure and hence maximum combustion temperature increases (Sayin *et al.*, 2009) and reflected in the EGT. Advancing IT surges the CO_2 and is expected to be the combined effect of high fuel intake and ample time access to complete the combustion. Same group of authors (Sayin *et al.*, 2008) reported fall of CO and HC emissions due to the IT advance. CO_2 and NO_X emissions are increased with IT advance. Raheman and Ghade (2008) have studied the effect of IT of Mahua methyl ester and its blend with diesel. The IT advancement causes BSFC to drop for almost all the fuel blends except 20CR and 45°IT. At this advanced IT, it is difficult to attain ample temperature to auto ignite the fuel. Further, IT advancement from 35° to 40° and 40° to 45°BTDC causes surge in BTHE from 12.9% to 18.1% and 2.9% to 7.5% for the fuel blends studied. Therefore, advancing IT from 35° to 40° is more useful because further advancement marks miss matching of the peak pressure growth. This is the result of partial burning of fuel due to lower temperature caused at that IT.

Papagiannakis *et al.* (2007) studied the effect of pilot fuel injection advance (4°, 6° and 8° before normal IT) on performance and emission of a NG-diesel dual fuel engine by using numerical methods. Their study showed that advancing IT reduces the BSFC and increases maximum cylinder pressure for (Figure 2.15). The advancement of IT of pilot fuel compensates its increase in ignition lag in dual fuel mode resulting maximum combustion pressure to shift towards the TDC. As a result, less amount of fuel is required to produce same amount of pressure. Side by side increase in nitric oxide and reduction in carbon monoxide and soot emission results as reported by the other researchers (Sayin *et al.*, 2008).

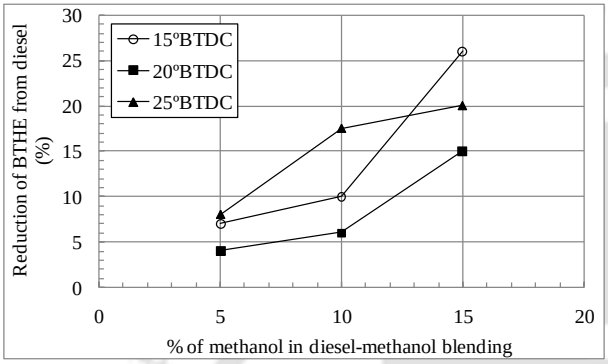

Figure 2.14 Performance variation with blends compared to diesel fuel at different ITs and ORG IP (Sayin *et al.*, 2010)

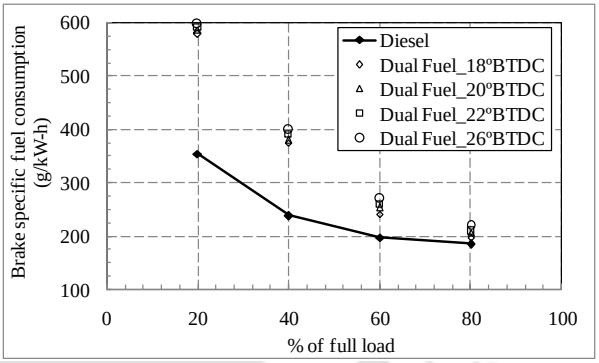

Figure 2.15 Brake specific fuel consumption versus engine load for various Its (Papagiannakis *et al.*, 2007)

2.6 Thermodynamic Analysis of Diesel Engine

The exergy or availability of a thermodynamic system is defined as the maximum useful mechanical work that can be produced when the system is brought to thermal, mechanical, and chemical equilibrium with its surroundings (Moran and Shapiro, 1995). The second law analysis locates the availability loss or destroyed in various parts of the engine system and thereby determines the maximum possible performance of a thermodynamic system (Caton, 2000). The study of calculating combustion irreversibility and working medium availability in a diesel engine cylinder have led people to find solutions to improve the performance of the engine in terms of efficiency and power output (Rakopoulos and Kyritsis, 2001; Kumar *et al.*, 2004).

The second law analysis performed on various engine parts (Cummins make, USA) as well as whole diesel plants are reported by Flynn *et al.* (1984). Van Gerpen and Shapiro (1990) performed a detailed analysis for a closed cycle, bringing into focus the belligerent term of chemical availability along with the thermo-mechanical one. Caton (2012) showed experimentally and thermodynamically that, implementation of lean operation, high exhaust

gas recirculation (EGR) levels and high CR can improve indicated thermal efficiency from 37.0% to 53.9%. Rakopoulos and Giakoumis (2004) applied the equations of second-law to all the subsystems of the diesel engine plant and quantified availability terms during transient operation. Further, Rakopoulos and Andritsakis (1993) studied the irreversibility in direct and indirect injection diesel engines combustion. They also have performed direct comparisons for various operating parameters of the two thermodynamic laws (Rakopoulos and Giakoumis, 2006). The concept was implemented in the low heat rejection (LHR) engine where the availability destruction reduces and the mechanical work does not increase but rather the potential for extra work recovery through the exhaust gas increases (Rakopoulos and Giakoumis, 2005). According to Giakoumis (2007), the availability destruction in a low heat rejection (LHR) engine is small, which does not allow the mechanical work to increase. Rather, it increases the potential for extra work recovery owing to the higher availability content of the exhaust gas. Their study uncovered a method for calculating both combustion irreversibility and working medium availability for a diesel engine (Rakopoulos and Kyritsis, 2001). They have implemented second law analysis and chemical equilibrium hypothesis to estimate combustion irreversibility as a function of fuel reaction rate. Parlak *et al.* (2003, 2005) have analyzed the exhaust energy and exergy loss in a low heat rejection diesel engine to that of a standard diesel engine. According to their investigation, it is impossible to recover all the exhaust gas energy to useful work. The maximum extractable power of both engines is less than 50% of the exhaust power. Kecebas (2012) implemented exergoeconomic analysis for combustion of fuel in boilers and indicated that excess air, stack gas temperature, and combustion chamber parameters are more vital to define the ideal insulation thickness.

As far as alternative fuel is concerned, the engine operating on 15 and 20% ethanol-diesel blends are found to provide considerably different thermal balance than 5 and 10% ethanol-diesel blends when compared to diesel (Ajav *et. al.*, 2000). In recent times, Sahoo *et al.* (2011) performed second law analysis of syngas with a mixture of hydrogen (H_2) and carbon monoxide (CO), in a 5.2 kW engine (Kirloskar make, India) for various loads. The results indicate that, compared to the 100% CO dual fuel mode, increasing the H_2 content in syngas from 50% to 100%, increased second law efficiency from 8 to 51%. This is due to better combustion process and increased work output with the presence of added H_2. They also stated that at lower loads (20% and 40%), the in-cylinder combustion temperatures have reduced for dual fuel combustion (Sahoo *et al.*, 2012a). Hence, the availability destruction is increased due to poor combustion and reduced heat transfer availability losses. At maximum

load, higher exergy efficiency is observed for higher volumetric fraction of CO syngas due to better combustion of CO at high temperature regions. The same group of authors (Sahoo *et al.*, 2009) have carried out the second law analysis of a diesel engine with variable throttle opening (TO) and loads, and optimized the engine operating conditions. The availability destruction for isooctane vapor and air mixtures at constant pressure, constant volume, and constant temperature combustion processes have been studied by Chavannavar and Caton (2006). This study reveals that the availability destruction is decreased with increasing reactant temperatures. The effect of the reactants mixture pressure on availability destruction is found insignificant. Canakci and Hosoz (2006) have performed energy and exergy analyses on a turbocharged diesel engine (John Deere make, USA). The engine is run with soybean methyl ester, yellow grease methyl ester, diesel fuel and a 20% blend of each biodiesel and diesel fuel. They have shown that around 45% of total soybean methyl ester fuel exergy has been destructed, which include loss through exhaust gases and heat. It is found that the fuels have similar energy and exergy performance, and most of the energy and exergy destruction occur during combustion. Caliskan *et al.* (2010) conducted exergy analysis on a diesel engine fueled with biodiesel from higholeic soybeans.

2.7 Scope of Work

It is seen that although POME has a superior yield of production, especially at the tropical countries and has almost similar physical, thermodynamic and chemical properties to that of diesel. Still it has not explored as a potential IC engine fuel globally. Researches by using these fuels are concentrated in Malaysia only. India has a huge potential of renewable biofuels and biodiesel production and its usable fields based on internal combustion (IC) engines, namely, transportation, industry, power production plants etc. require a massive amount of petroleum fuels. Hence there is a scope of detailed research in this field.

- A number of literature is found, in which POME is used in diesel engine with or without blending with diesel. However, the conduct of POME in diesel engine, for a variation of different engine operating parameters (namely, CR, IT, IP, etc.) is missing. Therefore, a study elaborating the consequence of load, CR, IT, IP and various possible compositions of these parameters can have uniqueness.

- There are a number of works performed with diesel emulsion as an alternative fuel. However, a very limited number of works on biodiesel emulsion restricts the knowledge

regarding its effects on engine performance. Side-by-side, from the literature, the effect of engine operating parameter (namely; CR and IT) variation is also unknown.

- Almost all of the types of emulsions prepared to be used as an alternative fuel for diesel engine, are by using mechanical homogenizer or magnetic stirrer. The application of ultrasonic waves in emulsification to prepare biofuel emulsion is very rarely used and still needs to be understood.

- The use of POME and its emulsion with water as a pilot fuel in dual fuel study is almost zilch. Hence, there are enough scope to investigate POME and its emulsion as a pilot fuel with variety of gaseous fuels. Especially, the exceptional emission quality of POME and emulsified fuel (lower carbonated emission than diesel) can be coupled with reduced NO_X formation (higher in case of POME than to diesel).

- The literature is almost silent about the thermodynamic potential study of emulsified fuel. Hence, first and second law analysis coupled with the variation of engine operating characteristics is essential to know about the maximum energy utilization of emulsified fuel run engine.

- Most of the biogas dual fuel engine shows a reduction of peak pressure and efficiency. This is because of the higher ID of dual fuel mode. Therefore, it is required to modify the engine design and operating parameters, specially CR and IT (pilot fuel), to reduce the ID as minimum as possible to shift the peak pressure towards TDC to improve the performance. The biodiesels having high Cetane number can be used in the dual fuel study, since they generate lower ID than diesel. In this regard the use of emulsified biodiesel is rare and can also be as a pilot fuel for dual fuel diesel engine.

2.8 Summary

This Chapter contains some significant work done by using different types of biodiesels (methyl esters). Some of the works done on POME and its emulsion are also discussed. Later on, inferences are drawn on the summary of the details experimental works done in VCR diesel engine. The discussions are concentrated on the effects of load, CR, and its variation on engine performance. Finally, the thermodynamic analyses performed in diesel engines with various alternative fuels.

CHAPTER 3

Characterization of Emulsified Palm Oil Methyl Ester

The emulsified fuels, being a potential alternative to diesel, are becoming popular day by day. The uses of emulsion in compression ignition (CI) diesel engines are mostly based on the emulsions prepared with diesel as a mother or carrying fluid. However, being a renewable source of energy, the emulsified biodiesels have not received proper attention as an alternative to diesel. This is possibly because of their lesser heating values than the conventional fuels. There are a number of engine operating parameters, namely, compression ratio (CR) and injection timing (IT), the changes of which may improve the performance of biodiesel emulsion. Alongside, the presence of a popular phenomenon, called 'micro-explosion', may also enhance its combustion. With an intention to realize this fact, in this work, the emulsion of water in biodiesel (palm oil methyl ester) has been explored in variable compression ratio diesel engine. In this chapter, the preparations of water emulsions of palm oil methyl ester (WIP) with various specifications are discussed elaborately. The emulsions are prepared by ultrasonication. The quantity of water and surfactants and the hydrophilic lipophilic balance of the surfactants are few parameters that are varied during WIP preparation. The measurement of mean droplet diameter and stability study provided the optimized specification of stable WIP with properly dispersed water droplets. Thereafter, the WIP with optimized specification is tested to find out its various physical, thermodynamic and petroleum properties. These properties are necessary to calculate the performance parameters and to discuss the combustion phenomena of the emulsified fuel after it is run in diesel engine.

3.1 Preface

The main purpose of this experimental study is to explore the emulsification characteristics and fuel properties of water in POME (WIP) emulsions prepared by ultrasonic wave for an option to be used as alternative fuels for diesel engines. An emulsion (WIP) that will be used as an engine fuel should have the water, evenly dispersed and stable for suitable time. However, before going to the details investigation, it is essential to know about parameters, which characterizes emulsion. These include surfactants (Becher, 1965), their hydrophilic lipophilic balance (Rosen, 2004; Guo *et al*., 2006) and ratio of emulsifying fluids (Abu-Ziad, 2004; Ghannam and Selim, 2009) which are discussed below. Most of the works in the field of emulsified alternative fuel, for diesel engine are performed with diesel as a continuous phase (Lin and Wang, 2003; 2004a; 2004b; Abu-Ziad, 2004; Basha and Anand, 2011a; 2011b). The dispersed phases are considered from water, methanol, ethanol, etc. (Kumar *et al*., 2005; Lin and Chen, 2006a; 2006b; Ashok, 2011a; 2011b). However, the application of biodiesel as an emulsified fuel is very rare and needs to be explored exclusively. Alongside most of the researchers used homogenizing machine to prepare emulsion. Conversely, Lin and Chen (2006a; 2006b) showed that, ultrasonic emulsifier also can be used efficiently to discretize dispersed phase into continuous phase for water-diesel emulsion. Further exhaustive study in this field is also yet to be done.

3.2 Characteristics of Emulsion

The emulsion prepared in this work is a two-phase WIP emulsion. The two-phase emulsion is prepared by intruding a phase, called dispersed phase into another phase, called continuous phase (Figure 3.1). The emulsion prepared in this work will be used as an alternative fuel for diesel engine. Therefore, the continuous phase with larger volume, will be POME; whereas, water will be the phase to be dispersed. The characteristics of the emulsion prepared are dependent upon some parameters, which are described in the following sections:

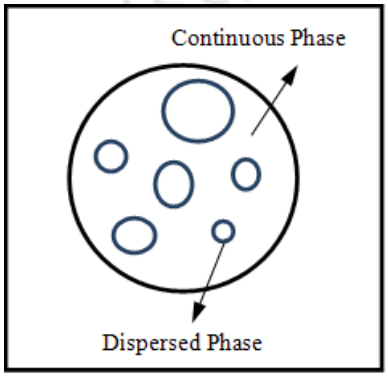

Figure 3.1 The physical structure of two phase water in oil emulsion

3.2.1 Surfactant and Hydrophilic Lipophilic Balance

POME and water are immiscible with each other. In order to form a uniform distribution of a dispersed phase into another continuous phase, suitable surfactant(s) need to be used. The surfactant reduces the surface tension between water and oil, maximizing their superficial contact area, and activating their surfaces. The measurement of this activation force is performed by a parameter called hydrophilic lipophilic balance (HLB).

HLB can be defined as the measure of the degree to which a liquid molecule is hydrophilic or lipophilic. Hydrophilic molecule are dissolved by, water and other polar substances; whereas, lipophilic molecule dissolves in fats, oils, lipids, and non-polar solvents. In 1949, Griffin defined the HLB number by a mathematical expression shown in Eq. 2.1. Based on Eq. 2.1, he has developed a 'scale' of HLB, which is ranging from '0' (zero) to '20' (non-dimensional value).The HLB number of all the hydrophilic, lipophilic surfactants or combination of both are measured within this range. In the water-oil emulsion the HLB number should lie within 4 to 6 whereas for oil in water emulsion it will be 8 to 18 (Griffin, 1949). When two surfactants (hydrophilic and lipophilic) are used to prepare emulsion, the HLB number of the solution is calculated as below:

$$HLB_{LH} = \frac{\left(H_L \times V_L + H_H \times V_H\right)}{\left(V_L + V_H\right)} \tag{3.1}$$

where HLB_{LH} is the HLB of the total emulsion prepared. The HLBs of lipophilic and hydrophilic surfactants are denoted by H_L and H_H respectively, whereas the corresponding volumetric percentages are denoted by V_L and V_H. To observe the effect of variation of HLB, its range is fixed from 4.3 to 6 as described for lipophilic dominating emulsion. The surfactants selected for the emulsification of POME with water are the commonly used Sorbitan monoleate (SPAN 80) and Polyoxyethylene sorbitan monooleate (TWEEN 80) as shown in Table 3.1. These lipophilic and hydrophilic type of surfactants (SPAN 80 and TWEEN 80) increase the POME/water affinity, reduce the POME/water interfacial tension and develop the emulsion stability (Lin and Wang, 2003). However, in order to prepare WIP emulsion of HLB 4.3, only SPAN 80 is used. The quantity of surfactant is varied from 1% to 3% of the total solution. Table 3.2 includes the matrix of the various emulsion samples prepared during this study.

.**Table 3.1** Specifications of the surfactants SPAN 80 and TWEEN 80 (Rosen, 2004)

Type	**HLB**	**Specific gravity**
SPAN 80 (Sorbitan monoleate)	4.3	0.98
TWEEN 80 (polyoxyethylene sorbitan monooleate)	15	1.08

Table 3.2 Matrix quantification of the emulsion components (for each 1000 ml emulsion prepared)

Water in the emulsion (% of total solution)	**HLB**	**Quantity of surfactant**											
		1%				**2%**				**3%**			
		POME (ml)	**W (ml)**	**L_S (ml)**	**H_S (ml)**	**POME (ml)**	**W (ml)**	**L_S (ml)**	**H_S (ml)**	**POME (ml)**	**W (ml)**	**L_S (ml)**	**H_S (ml)**
5	**4.3**	940	50	10	0	930	50	20	0	920	50	30	0
	5	940	50	9	1	930	50	18.5	1.5	920	50	28	2
	6	940	50	8.2	1.8	930	50	16.5	3.5	920	50	24.8	4.2
10	**4.3**	890	100	10	0	880	100	20	0	870	100	30	0
	5	890	100	9	1	880	100	18.5	1.5	870	100	28	2
	6	890	100	8.2	1.8	880	100	16.5	3.5	870	100	24.8	4.2

3.2.2 Ratio of Emulsifying Fluids

The ratio of fluids has a huge effect on the stabilization of the emulsion to be prepared. The proper dispersion of the water into POME, the diameters of the dispersed water bubbles and separation have major consequence with the quantity of the water used for emulsification. In a previous work, the amount of water content is fixed to 10%. However, in this work (Lin and Lin, 2007a) the volumetric quantity of water is taken as 5% and 10% of total emulsified fuel.

3.3 Emulsified POME Preparation and Stability Study

3.3.1 Ultrasonic Bath Sonication Machine

Ultrasonic waves are of such a high frequency that they are generally unable to be detected by the human ear. Sound waves with a frequency higher than 20 kHz are referred to as ultrasonic waves (Lin and Chen, 2006a). These are widely applied in the medical field, industry, food processing fields and even in household electronic appliances. An ultrasonic wave is a mechanically vibrating wave that requires a transmission medium to be propagated. Application of violent ultrasonic waves at a high frequency generates a huge extent of tiny air bubbles. The continuous production and consequent collapse of these air bubbles result a phenomenon called 'cavitation'. Side-by-side, the motion of ultrasonic wave creates an alternate positive and negative pressure waves. As soon as the hydrostatic pressure of the surrounding liquid becomes lesser than the pressure produced by the ultrasonic waves, the particles of liquid get twisted and hollowed out, causing far more cavities. As a result, twisting of liquid particles along with cavitation of bubbles creates a strong mechanical stirring effect which mixes the two immiscible fluids (Lin and Chen, 2006a). Table 3.3 shows the brief specification of the ultrasonic bath sonicator used in this work (Buehler, 1993).

Table 3.3 Specifications of the ultrasonic bath sonication machine (Buehler, 1993)

Parameter	Specification
Power capacity (W)	80
Operating voltage (V)	115
Operating frequency (Hz)	60
Transducer tank material	Stainless steel
Tank dimension (cm^3)	12.7 x 12.7 x 7.6

3.3.2 Emulsion Preparation Procedure

This study used an ultrasonic emulsification method to prepare two-phase WIP emulsions and observe their fuel properties such as emulsion stability and droplet-size distribution of the dispersed phase. The factors such as ultrasonic processing time, quantity and HLB (hydrophilic lipophilic balance) of the emulsifier mixture, as well as the diesel fuel to water proportions were considered in this study. The first step in preparing the WIP emulsion is to load the lipophilic surfactant into the base oil and stir the mixture evenly by using an electromagnetic stirring machine. For HLBs ranging from 5 and 6, the hydrophilic surfactant TWEEN 80 is added with measured quantity of distilled water and again stirred in electromagnetic stirring machine. For example, to prepare 1000 ml of 5% WIP with HLB 5 and 1% surfactant quantity, 940 ml of POME and 50 ml of water is used. The quantity of lipophilic (9 ml) and hydrophilic (1 ml) surfactant is measured by using the equation (3.2). After mixing particular surfactants with respective fluids by electromagnetic stirring machine, the continuous phase, i.e. POME with surfactant is poured into a beaker and placed in ultrasonic bath sonication machine. Now sonication is started and the surfactant mixed distilled water is slowly injected into POME surfactant mixture and sonicated for around 3 hours. For complete mixing and no deposition of sediments, WIP is checked at time intervals of 15, 30, 60, 90, 120, 150 and 180 minutes. After 180 minutes of sonication, almost no deposition is observed. A sample of the emulsion prepared with 5% water, 4.3 HLB and 1% surfactant quantity is shown in Fig. 3.2. Similar procedure is followed for other HLB, surfactant quantity and 10% by volume of water (Lin and Lin, 2007a).

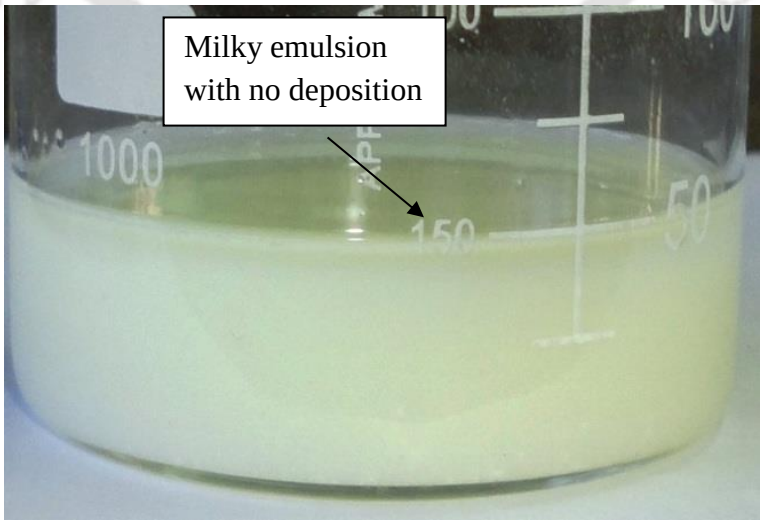

Figure 3.2 Emulsion sample after 180 minutes (5% WIP with HLB 4.3 and 1% surfactant)

3.3.3 Measurement of Droplet Diameter

The distribution of water in POME (WIP) is observed in an optical electron microscope (Axioscope: 100X magnification). The software used for measuring the mean diameter of the emulsion droplet is known as Axiovision. The digital image processing provided in this software has the ability to detect the droplet size variation, measure the diameter of the droplets and their mean value. In order to carry out this study, the drops of WIP are observed under the microscope after each 15, 30, 60, 90, 120, 150 and 180 minutes.. For each samples pictures are captured, stored into the computer, analyzed and discussed as follows.

The mean droplet diameter measured for total 12 samples (Table 3.2) are shown in Figs. 3.3(a) through 3.3(f). Each of these figures represent the variation of mean droplet diameters for 1%, 2% and 3% surfactant for each HLB of 4.3, 5 and 6 of each 5% and 10% water content. The figures show that, with longer the emulsification time, lower mean droplet diameter of the emulsion is achieved. Side-by side, for almost all the HLB numbers 3% surfactant has shown the lower value of mean droplet diameter. Becher (1965) has defined that the droplet diameter of the micro emulsions should lie at least within the range of 0.1 μm to 20 μm. In all the figures, the maximum to minimum range of mean droplet diameter lies within 4.9μm to 1.2μm, which absolutely agrees the criteria set by Becher for micro emulsions. Figure 3.4(a) shows the variation of mean droplet diameter with emulsification time and HLB variation. It is further observed that for HLB 6, after 90 minutes of emulsification, a solution of the lowest droplet diameter is achieved. Further, an interesting fact has also come out from the study. The HLB of 4.3, i.e. the emulsion produced by single surfactant SPAN 80 has produced lower droplet diameter that of emulsion produced by double surfactant (SPAN 80 and TWEEN 80) with HLB 4. However, further increase in the HLB value upto 6, i.e. increase in the quantity of hydrophilic surfactant (TWEEN 80) reduces the mean droplet diameter the most. Figure 3.4(b) shows that mean droplet diameter (by average) for HLB 6 and 5% water WIP is 1.68 μm, lower than the WIP produced with same HLB with 10% water. This is probably because of the higher water quantity encapsulated inside biodiesel that increases the chance of cohesion of water droplets scattered throughout the solution. Due to this cohesion, water droplets are forced to come closer to each other, form bigger droplet and settle down due to an increase in weight. Lin and Lin (2007a) found that the mean droplet size of the dispersed water into soybean oil biodiesel for two phase emulsion is 2.94 μm. Hence, with proper surfactant combination and proper emulsification method can disperse water with lower mean droplet diameter inside POME.

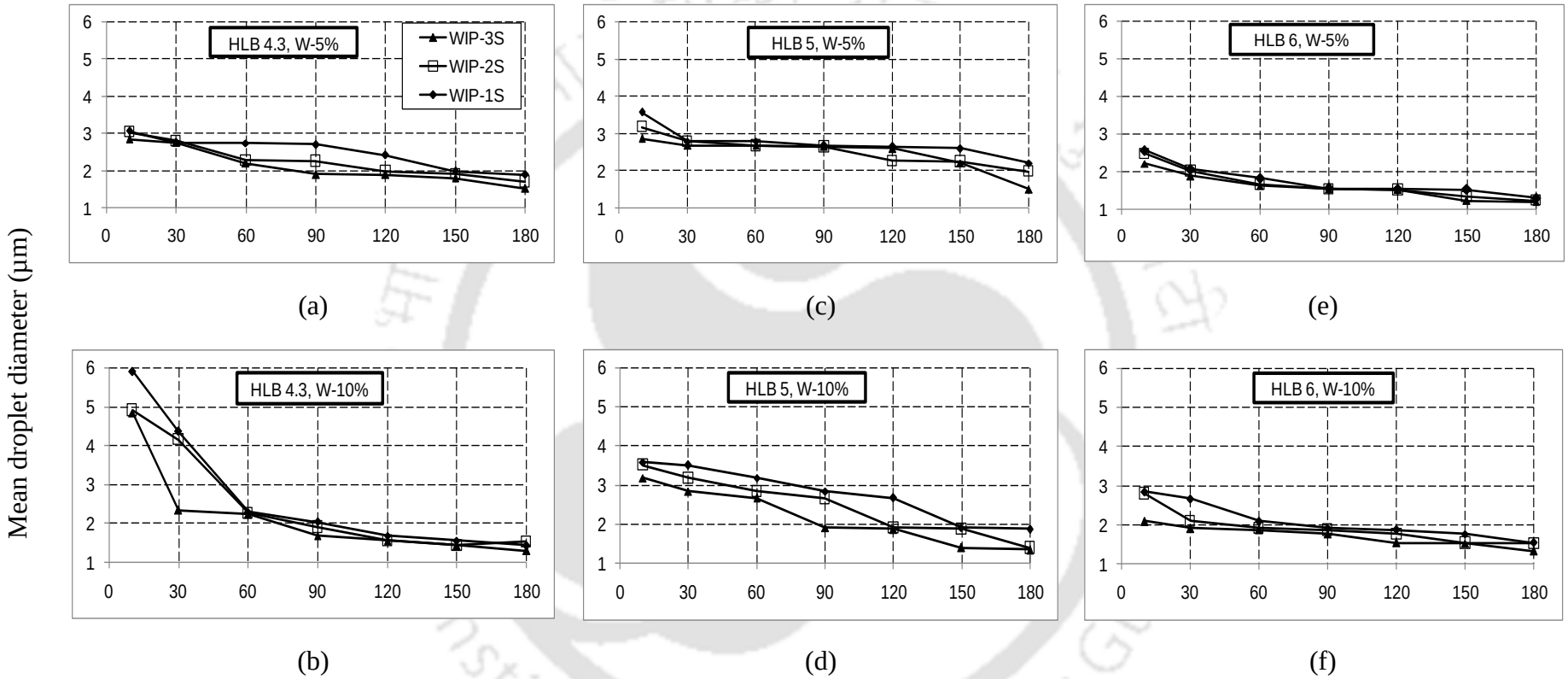

Figure 3.3 Variation of mean droplet diameter with emulsification time, surfactant quantity, HLB and water content

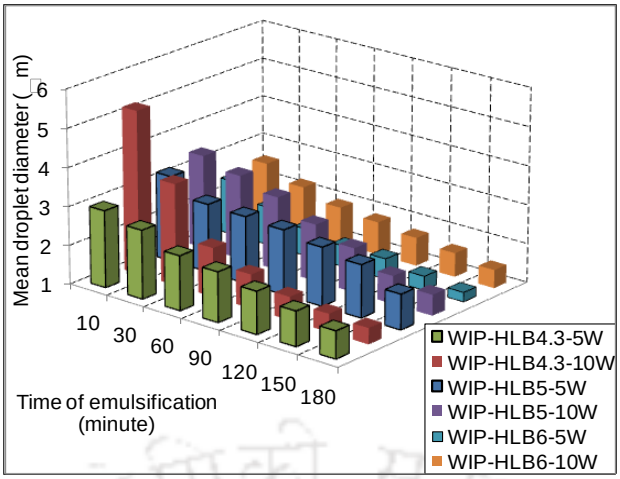

(a)

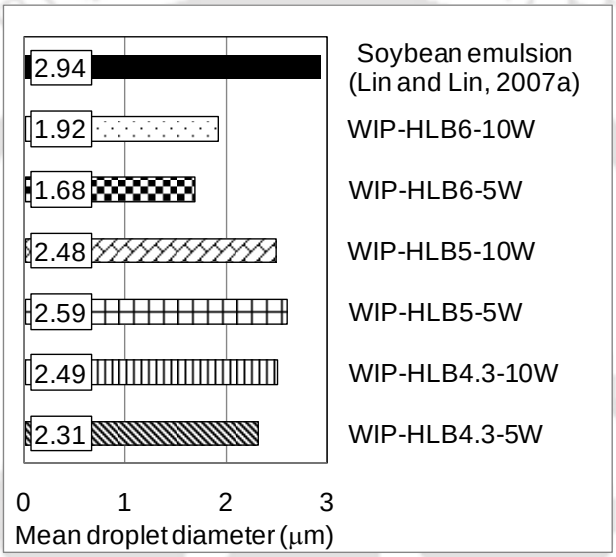

(b)

Figure 3.4 Variation of mean droplet diameter; (a) with emulsification time, HLB and water quantity; (b) with HLB and water

From the above analysis of mean droplet diameter it is found that, increase of surfactant quantity reduces mean droplet diameter. Hence, some photographs of only 3% surfactant with HLB and water content variation are shown in Figs. 3.5(a) through 3.5(f). Figures show the droplet distribution of the two phase WIP emulsion which was observed by an optical electron microscope at a magnification of 100X. Figures 3.5(a) and 3.5(b) show that although the emulsion is prepared with the presence of single surfactant, SPAN 80 (HLB 4.3), the dispersion of the water droplets are uniform. Unlike Figs. 3.5(a) and 3.5(b), the dispersed water droplets are more agglomerated for HLB 5 with the presence of both lipophilic and hydrophilic surfactants (Figures 3.5c and 3.5d). Probably this is the reason why, the mean droplet diameter of the dispersed water is a little higher for HLB 5 emulsions, than that of

HLB 4.3. However, when the HLB is further increased to 6, the increase of hydrophilic surfactant has modified the tension between water and oil interface in such a way that, the implementation of ultrasonic force downsizes the globular water pellets. This makes the emulsion more uniform than other two HLBs as shown in Figs. 3.5(e) and 3.5(f). Obviously, the presence of larger quantity of water for 10% WIP – 6 HLB sample results a little increase in the droplet size which is previously observed from Fig. 3.4(b).

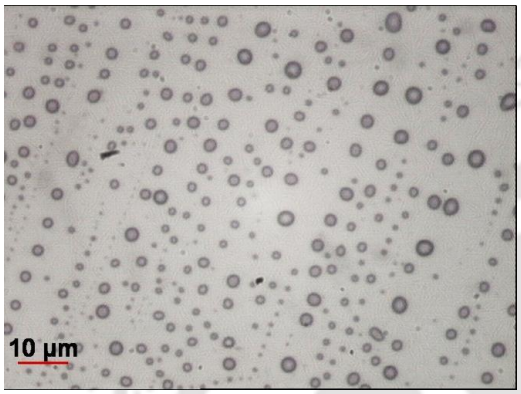

(a) 5% WIP, 4.3 HLB and 3% surfactant

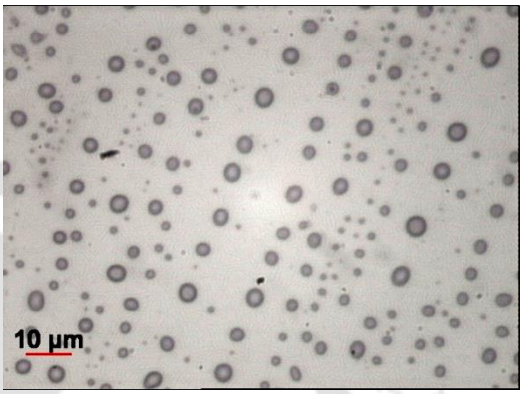

(b) 10% WIP, 4.3 HLB and 3% surfactant

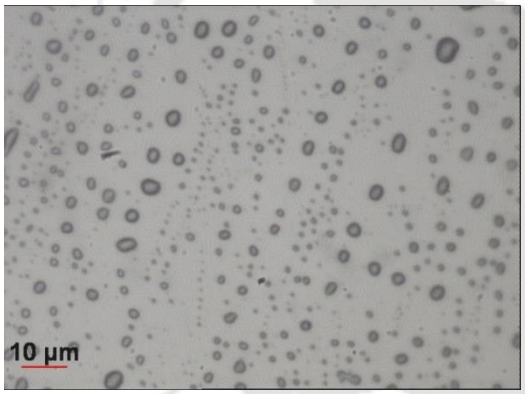

(c) 5% WIP, 5 HLB and 3% surfactant

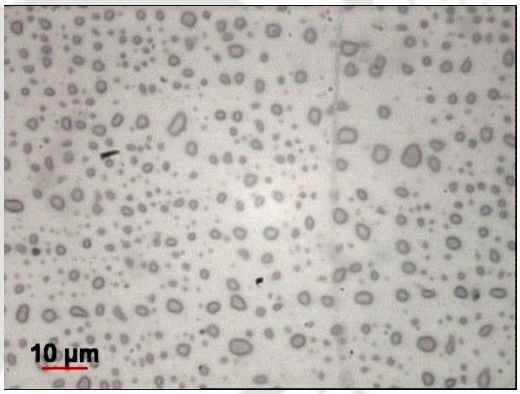

(d) 10% WIP, 5 HLB and 3% surfactant

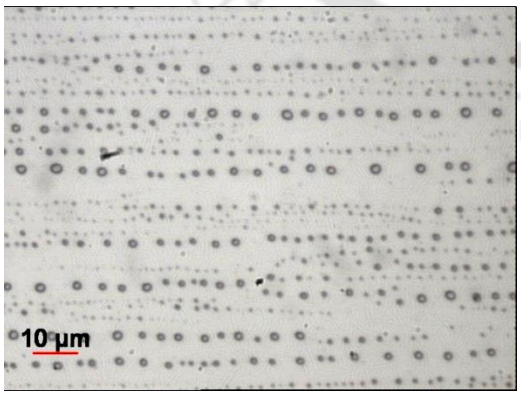

(e) 5% WIP, 6 HLB and 3% surfactant

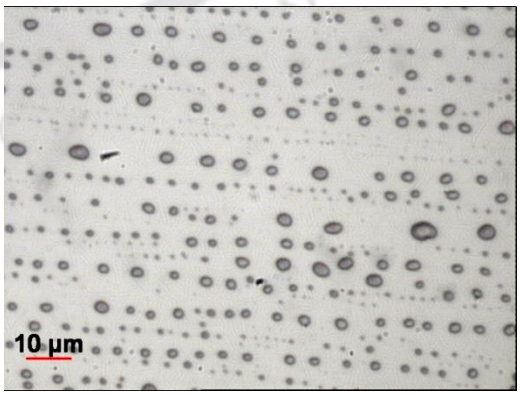

(f) 10% WIP, 6 HLB and 3% surfactant

Figure 3.5 Photograph of image obtained from optical electron microscope (100X), after 180 minutes of emulsification

3.3.4 Stability Study

The stability of emulsion represents its capability to conserve the emulsifying layer after being kept motionless or heated at a certain temperature for a specific time (Lin and Wang, 2003). In this study, the emulsion stabilities of the two-phase WIP samples are determined based on the percentage of separation of the emulsion, which is represented by the extent of the separation phenomenon of the emulsion. Once the proper WIP emulsions are prepared, the stability of the solution is checked by keeping the solutions motionless for 3 hours in measuring cylinders. At every 1 hour interval, the volumetric deposition of WIP sediment layer and water from unaffected emulsion layer is observed and recorded.

The bar graphs in Figs. 3.6(a) through 3.6(f) show the volumetric sedimentation of the WIP emulsion at the bottom of the measuring cylinders for various HLB and water content in the emulsion. It has been seen from Figs. 3.6(a) and 3.6(b) that, for the 4.3 HLB-WIP emulsions, separation including completely separated water quantity is less than 5% of the total volume for 5% water emulsion and this value is around 6.5% in case of 10 % WIP emulsion. This is probably because of the higher water quantity encapsulated inside biodiesel that increases the chance of cohesion of water droplets scattered throughout the solution. Due to this cohesion, water droplets are forced to come closer to each other, form bigger droplet and settle down due to an increase in weight. This tendency is lower in case of 5% WIP.

More interestingly, it is observed that for double surfactant emulsions (HLB 5 and 6) the separation, agglomeration and sedimentation rate is much lower than the emulsion prepared with single surfactant. Keeping in mind, the higher mean droplet diameter of emulsion with HLB value 5, than that of 4.3, it can be said that, presence of hydrophilic surfactant definitely improves the stability of two-phase WIP emulsions. Although, the dispersion of water droplets are not uniform in case of 5-HLB-WIP emulsions, but it can carry the dispersed water for longer duration as observed from Figs. 3.6(c) to 3.6(d). This is probably because of the more likely interstitial tension between water and POME and due to the presence of both lipophilic and hydrophilic surfactants. This situation is further developed for 6-HLB-WIP emulsions as seen in Figs. 3.6(e) and 3.6(f). On the other hand, with the presence of ultrasonic wave although water droplets are properly dispersed for 4.3 HLB emulsions, but it cannot carry the dispersed water droplets for long time, probably because of the presence of a little higher dissimilarity of interstitial tension between water and POME for this type of emulsion.

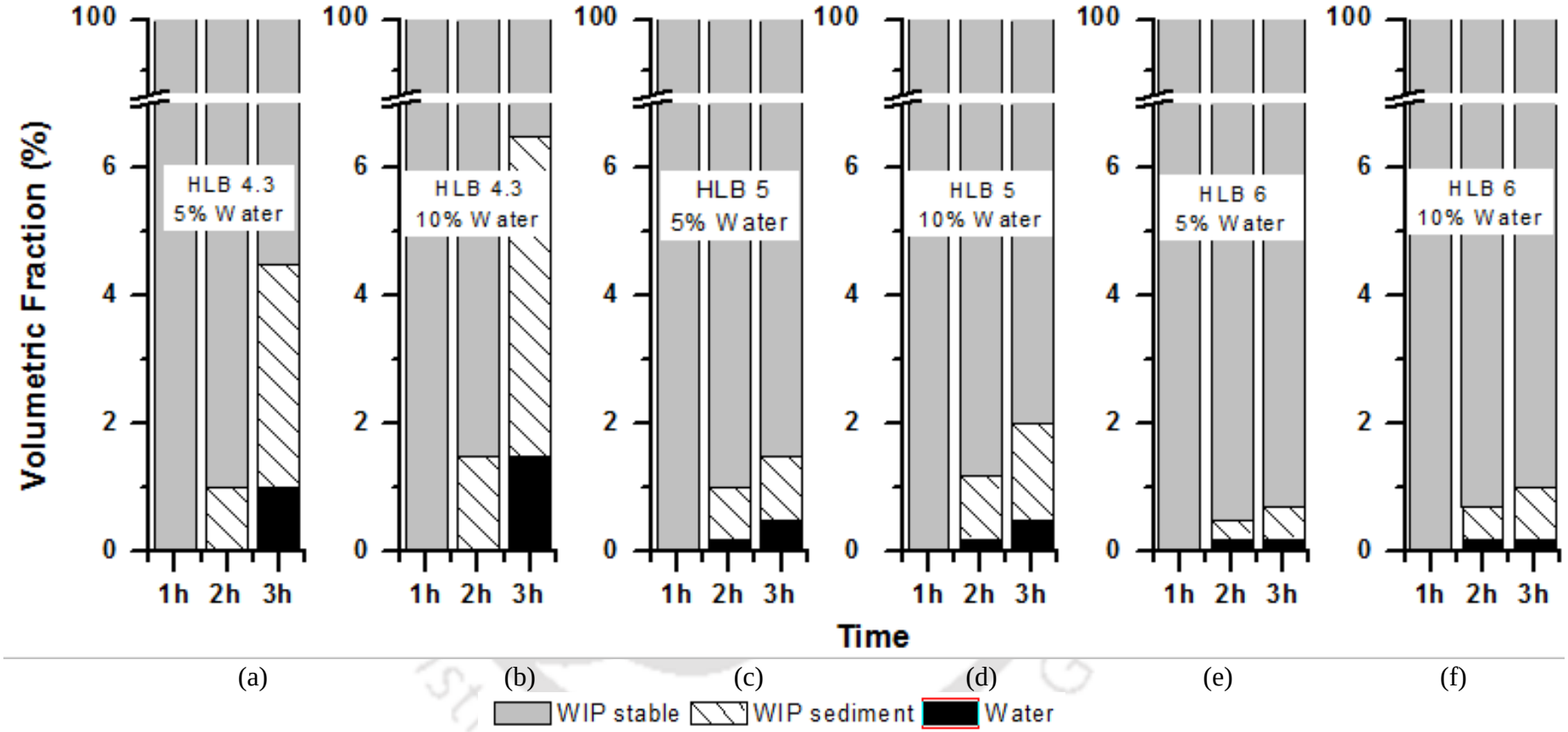

Figure 3.6 Volumetric fraction of layers with time (3% surfactant)

Finally, it is found that water in POME emulsions prepared with both lipophilic and hydrophilic surfactant has better stability. The HLB of 6 and 5% water quantity is the most stable sample prepared. The analysis of mean droplet diameter disclosed that the emulsion with higher quantity of surfactant (3%) has lower mean droplet diameter. Hence, it is decided that the 5% WIP with 3% surfactant of 6 HLB is the best among the samples prepared. This is because, smaller is the dispersed water droplet size, more will be the number of water droplets encapsulated inside the fuel droplet. This will enhance the intense of droplet breakup of the emulsified fuel and augment the surface to volume ratio. Its potential as alternative fuel will now be tested by running it in VCR diesel engine. Prior to conduct of experiments, the petroleum property of 5% water WIP is also carried out. Table 3.4 shows the data along with diesel and original POME (Masjuki *et al.*, 1993; Debnath *et al.*, 2011). Due to micro-explosion, water added through WIP is vaporized well before combustion to start and does not take part to produce heat (Langer and Daly, 2000). Hence, the calculation of the lower calorific value and stoichiometric air fuel ratio of WIP is performed with the actual fuel quantity which produces the heat and is assumed to be 92% of total emulsion. All of the stability studies are carried out within 20±2ºC.

Table 3.4 Significant properties of diesel, POME and WIP

Properties	**Diesel**	**POME**	**WIP**
Chemical composition	$C_{12}H_{26}$	$C_{18.07}H_{34.93}O_2$	5% H_2O, 2.48% SPAN, 0.52% TWEEN, 92% $C_{18.07}H_{34.93}O_2$
Density (kg/m^3) (Sahoo *et al.*, 2012b)	840	870	890
Lower calorific value (MJ/kg)	42*	39.84*	37.88*
Cetane number (Kumar *et al.*, 2003) (Masjuki *et al.*, 1993)	48	57	51
Auto-ignition temperature (K) (Swami Nathan *et al.*, 2010)	553	--	-
Stoichiometric air fuel ratio	14.92*	12.52*	12.93*
Energy density (MJ/m^3)	2.82*	3.18*	2.93*

*****calculated by using equation A9, A10 and A11

3.4 Summary

This chapter describes the preparation of WIP in the laboratory with two commercially available surfactants with their appropriate HLB values. It is observed that longer the emulsification time, lower is the mean droplet diameter. It is also seen that the highest amount of surfactant with 5% water provides lower mean droplet diameter. The presence of hydrophilic surfactant, in double surfactant emulsions, lowers the separation, agglomeration and sedimentation rates than the single surfactant ones. Finally, the thermodynamic, physical and petroleum properties of the optimized sample are measured and tabulated.

CHAPTER 4

Variable Compression Ratio Engine Test Setup

The uses of emulsion as an alternative fuel for compression ignition (CI) diesel engines are mostly diesel based. Recently, the fatty acid methyl esters, termed as biodiesels, have got popularity as alternative fuels for diesel engines. However, owing to their lesser calorific values compared to conventional diesel, emulsified biodiesels have not got proper attention. When combusted in diesel engine, the proper adjustment of some engine operating limits, namely, compression ratio (CR) and injection timing (IT), with the presence of 'micro-explosion', may amend the performance of biodiesel emulsion. Alongside, the variation of these operational parameters may lead to the optimum settings for which the performance of the diesel engine run by a biodiesel and its emulsion will be superior. In order to realize this fact, the emulsion of water in biodiesel (palm oil methyl ester) is explored in a variable compression ratio diesel engine. Prior to this study, the performance of neat POME under variable CR-IT condition is also checked to have a proper baseline comparison. In this chapter, the details of the specifications of the engine and instruments are included. Thereafter, the experimental procedures are elaborated in three sections. The complete experimental observations include the neat diesel tests, the test of neat POME and finally emulsified POME (WIP). The neat diesel is tested in the standard CR-IT setting, whereas the neat and emulsified POME are run for a set of CR-IT settings which are duly included in the experimental matrix.

4.1 Preface

Sir Harry Ricardo (1920) first built the variable compression ratio (VCR) engine for solving a knocking problem. Afterwards, various researchers tried to increase the range of compression ratios (CRs) (Kemper, 1978; Ozcan and Yamin, 2008). It has been used mostly, for automobiles to have better output and lower emission at varying load condition (Grundy *et al.*, 1976; Sobotowaki *et al.*, 1991). Now a days, with the increasing trend of the use of alternative fuels, especially biodiesels, the details about their performance, combustion and emission behavior are unknown from the recent works with VCR engine (Selim, 2004; Raheman and Ghadge, 2008; Jindal *et al.*, 2010b). This chapter describes in details the VCR engine setup installed for test of various fuels. During the tests, initially engine is run with neat diesel to have data for baseline assessment. Afterwards, the engine is run with neat and finally emulsified POME (WIP) in the engine for various compositions of load, CR and IT. The various arrangements appended with the setup for performance, combustion and emission study are also discussed elaborately. Finally, the chapter is wrapped up by addressing the procedure of the experiments performed.

4.2 The VCR Engine Setup

The experimental setup consists of single cylinder, four stroke, direct injection, water-cooled diesel engine. It is connected to an eddy current and water-cooled dynamometer for loading on crankshaft with the help of electromagnetic force. A tilting cylinder block arrangement is used for varying the CR without stopping the engine and without altering the combustion chamber geometry. The fuel injector in the engine has three circular holes having 0.3 mm diameter which spray fuel with a spray angle of 120º. The piston top of the engine is bowl type. Hence, the combustion chamber is of hemispherical type when piston reaches TDC. The liquid fuel reaches engine fuel pump from fuel tank by gravity. A regulator, fixed on the panel box, controls electric supply for load variation. The load sensor, fitted with the dynamometer, sends the load signal to the digital display in kg. Instruments for combustion pressure and crank-angle measurement are provided along with the setup. The signals are interfaced to computer through engine indicator for pressure-crank angle (P-θ) and pressure-volume (P-V) diagrams for each of 360° rotation of crank. Provisions are also made to count airflow, fuel flow, and temperatures. Rotameters are used for cooling water and calorimeter water flow extent. The cooling water flows through the jackets of the engine block and cylinder head to remove excess heat produced during combustion. The schematic diagram of

the VCR diesel engine setup is shown in Fig. 4.1. The specification of the engine is added in Table 4.1.

Table 4.1 The specifications of VCR diesel engine and accessories

System specifications	
Parameter	**Specification**
Product	Research engine test setup, Code 240
Type	Single cylinder, four stroke, DI diesel engine
Power	3.5 kW (@ 1500±50 rpm)
Type of cooling	Water cooled
CR range	12:1 – 18:1
Injection variation	0 – 25º BTDC
Combustion chamber	Hemispherical bowl in piston type
Dynamometer	Eddy current type, water cooled with loading unit
Air box	MS fabricated with orifice meter and manometer (100 - 0 - 100)
Fuel tank	Capacity 15 lit with measuring tube (0-450 ml)
Calorimeter	Pipe in pipe type
Rotameters	Engine cooling 40-400 lph, calorimeter 25-250 lph
Data acquisition Software	'Enginesoft' engine performance analysis software
Transmitters, sensors and indicators	
Fuel flow transmitter	DP transmitter, range 0-500 mm WC
Air flow transmitter	Pressure transmitter (-) 250 mm WC
Pressure sensors	Piezo type, range 5000 PSI, with low noise cable
Temperature sensors and transmitters	PT100 (RTD) type, range 0-100º C, output 4-20 mA (4 nos) K (ungrounded) type, range 0-1200º C, output 4-20 mA (2 nos)
Load sensor and indicator	Strain gauge type load cell with digital indicator, range 0-50 kg
Speed sensor and indicator	Resolution 1º, range (5500 rpm) with TDC pulse
Data acquisition device	NI USB-6210, 16-bit, 250 kS/s
Setup constants	
Pulse per revolution	360º
No. of cycles	10
Fuel measuring interval	60 s
Speed scanning intervals	2000 ms
Bore × Stroke	87.5 mm × 110 mm
Capacity	661 cc
Orifice diameter	20 mm
Dynamometer arm length	185 mm
Connecting rod length	234 mm
Theoretical constants	
Orifice coefficient of discharge	0.6
Specific heat of exhaust gas	1.00 – 1.25 kJ/kg-K
Specific heat of water	4.186 kJ/kg-K
Density of Air	1.174 kg/m^3

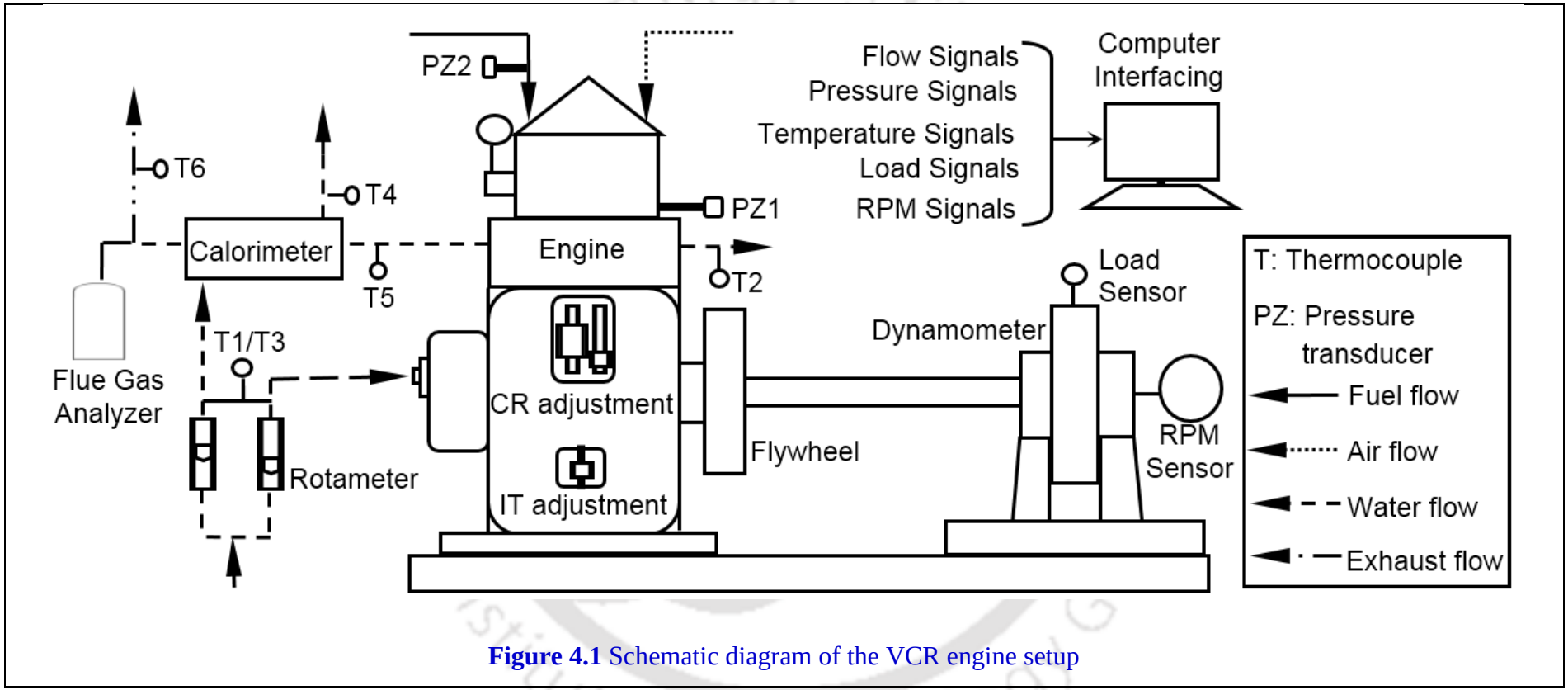

Figure 4.1 Schematic diagram of the VCR engine setup

4.3 Instrumentations for Measurements

The VCR research diesel engine setup is consists of a several sensors, transmitters and indicators. These are interfaced with the data acquisition computer (DAC), established for automatic measurement of almost all of the direct and indirect performance parameters. The CR and water flow rates to the engine and calorimeter are measured and entered manually to the software. The elementary measurement parameters are described in the following sections.

4.3.1 Performance Measurement

The measurement of the performance parameters are done automatically by collecting the data from the computerized system after setting the running engine at particular load level. The density and the calorific value of the respective fuel are included according to the requirement. The parameters evaluated are air and fuel flow rates, air fuel ratio, power, mean effective pressure, efficiencies and heat balance. The basic correlations used for estimating the above parameters are included in Appendix-A.

4.3.2 Air and Fuel Flow Measurement

Both air and fuel flow measurement can be performed manually and automatically. Manual airflow measurement is carried out by recording the difference in height of water column in the manometer. It is interconnected across the orifice meter, through which air comes into the engine panel box, before leaving towards the engine manifold. Manual measurement of fuel is executed by transferring fuel from the tank through the measuring tube for known duration. Airflow transmitter (WIKA Instruments Ltd.) and differential pressure transmitter (Yokogawa Electrical Corporation) that are lined with DAC assess the automatic air and fuel flow amount.

4.3.3 *P-θ* Measurement

The PCB Piezotronics made two dynamic pressure sensors are fitted on the cylinder head and fuel injector. Both of them has identical specification and capable of distinguish pressure of compression, combustion, explosion, pulsation, cavitations, blast, pneumatic, hydraulic, fluidic etc. An optical crank angle sensor (Kubler make) is used to measure each degree rotation of crank with TDC pulse.

4.3.4 Temperature Measurement

Four PT100 (RTD) temperature sensors measure the inlet and outlet temperatures of engine cooling water flow and calorimeter water flow. The inlet and outlet temperatures of exhaust gas to calorimeter are measured by two K type thermocouples. All of these are interfaced with computer for automatic data recording. The thermocouples used in this work, have a response time more than 0.08 seconds (for the 1500 rpm constant speed engine). Hence, they cannot show the pulsation nature of the exhaust gas in the form of temperature readings and are found almost steady after a certain time (nearly 5 minutes) at a particular load.

4.3.5 Compression Ratio Variation Control

The VCR diesel engine has provisions for eight (8) step CR variation from 12 to 18. This is done by tilting cylinder head with the help of locknut and adjuster arrangement. However, the engine starting should be done at the standard CR (17.5) and later on CR change is done online. There are six (6) socket headed vertical allen bolts fitted on two supporting blocks on the two sides of the cylinder, which needed to be loosen for CR variation. The appropriate value of CR should be entered manually in the software for data acquisition.

4.3.6 Injection Timing Variation Control

The IT of the liquid fuel can be tuned online and updated timing is learnt from the fuel pressure data at certain crank angle in the software. The fuel injection point on the plot shifts horizontally to retard or advance injection point depending on the way of rotation of the adjusting nut.

4.3.7 Emission Measurement

A Testo 350S/M/XL flue gas analyzer is used to measure the emission. The analyzer follows ASTM - D6522 emission measurement standard. The calibration of the instrument is performed automatically by measuring oxygen quantity in the air, each time it is restarted. The measurement is performed by letting the flue gas samples to surge through a probe in steady operation of the engine. A condensation trap is used next, to dry out the gas sucked. The samples are investigated inside the flue gas analyzer and return the values of CO, CO_2, NO, NO_2, NO_X and HC emissions on the display of control unit. CO and NO_X are measured through electrochemical measurement cells; whereas, CO_2 and HC are measured by Infrared and Pellistor Heat Affect Detector, respectively. The specifications of these emission parameters are shown in Table 4.2.

Table 4.2 The specifications of Testo 350 S/M/XL flue gas analyzer

Sl. No.	Measured gas	Resolution	Accuracy	Range
1	O_2	0.1%	± 0.8%	0 – 25%
2	CO	1 ppm	± 10 ppm < 200 ppm	0 – 10000 ppm
3	CO_2	0.01% vol. < 25% 0.1% vol. > 25%	± 0.3% vol. < 25% ± 0.5% vol. > 25%	0 – 50%
4	NO	1 ppm	± 5 ppm < 100 ppm	0 – 3000 ppm
5	NO_2	0.1 ppm	± 5 ppm < 100 ppm	0 – 500 ppm
6	HC	1 ppm	400 ppm < 4000 ppm	0 – 40000 ppm

4.4 Experimental Design and Procedure

The total experimental study is performed into two parts. In the first part, the VCR engine is run using diesel fuel for baseline reading. Later on, POME is tested in the VCR engine for various combination of load (0-12 kg), CR (16-18) and IT (20-28 ºBTDC). The significant properties of diesel, POME and WIP are listed in Table 3.4.

4.4.1 The Neat Diesel Test

The 'Neat Diesel Test' is performed to launch the foundation for comparison of later experimental works. The test is performed by running the engine by using neat diesel as a liquid fuel. The standard setting (CR=17.5 and IT=23°BTDC) is maintained while operating the engine with diesel at constant speed of 1500±50 revolution per minute (rpm) thorough out the load range. The variations of loads are performed from 'no load' (0.1 kg) to 100% load (12 kg) with a step of 20%. Initially, the engine is allowed to run at no-load condition for a few minutes to warm up. The water flows are adjusted to 300 and 100 liters per hour for the engine cooling and calorimeter respectively according to the engine supplier instructions. The different experimental observations including load, temperatures, air and fuel flow rate, speed, cylinder and fuel pressure variation for each crank angle rotation are automatically detected by the DAC, calculate performance parameters and are saved in the appropriate format for further analysis. The samples of flue gas are then allowed to pass through the Testo flue gas analyzer probe, which quantifies the amount of CO, CO_2, NO_X and HC emissions. Thereafter, the load level is raised as mentioned in the experimental matrix (Table 4.3) and the same processes as described above are repeated. This completes the total neat diesel test.

4.4.2 The Neat POME and Emulsified POME Tests

The VCR engine allows online modification of CR and IT variation. The various CRs set to study are 16, 17 and 18 along with the standard (17.5) one. ITs are allowed to vary from 20°to 25° and 28º BTDC along with the standard 23ºBTDC. The various combinations of CR and IT are incorporated in Table 4.3. In the table, 'Diesel' indicates neat diesel 'P' stands for neat palm oil methyl ester (POME) and WIP specifies water-in-POME emulsion. According to the company manual, the engine always has to be started at the standard CR of 17.5 and then according to the requirement, the CR has to be changed.

After the neat diesel test is performed the diesel tank of the engine is emptied and filled up with B100. Now the engine is started with B100 at standard diesel engine specifications (CR = 17.5, IT = 23º BTDC) and ran for 10 minutes to clear the entire diesel in the fuel line and to get steady at no load condition. Necessary modifications are made in the DAC software to provide the density and calorific value of the B100 (Table 3.4) for automatic calculation of the performance parameters. The experiments show that, IT advances by 0.5º to 1º from the standard one due to the change of the physical properties of POME. However, this minor change is corrected and the IT is brought back to the standard one to have a true comparison between diesel and POME run engines. Once the engine is reached at steady state condition the data is recorded in excel sheet. Emission performance is recorded by using exhaust gas analyzer. Now the load is increased slowly by rotating the load adjustment knob and set to 20% of the full load (i.e. 2.4 kg). Again, the engine is allowed some time to get steady and then data recording is completed in the same file. Similarly, the experiments are conducted for other loads as mentioned in the experimental matrix (Table 4.3). Finally, the engine load is brought back to no load condition and allowed to run for few minutes to modify the CR or IT or complete shutdown.

The same procedure described above is followed for water in POME (WIP) emulsion test in VCR engine too. However, in this case the 110% overload condition is also tested along with other loads. The experiments are performed maintaining the procedure described by Bureau of Indian Standard (BIS). The standards are described through IS 10000 (Part I to Part XIII) – 1980 (IS 10000). The performance and emission parameters are measured thrice as per experimental design for diesel, POME, and WIP modes and averaged for each operating point. The average values of the recorded experimental data are employed for analysis purpose. The equations (A1-A9, A13) used for performance and combustion analysis are

provided in Appendix A. During the analysis of heat release rate, it is necessary to use the ratio of specific heats γ. The value of γ is essentially dependent on combustion temperature, which is known to be very non-linear and ranges amid 300 K to 1700 K. Further, it is very difficult to measure the trend of actual combustion temperature. Hence, traditional practice is to use a mean value of γ for the calculation of heat release rate. As quoted by Heywood (1988) and Pundir (2010) and many other researchers, the mean value of γ lies within 1.3 to 1.35 for single cylinder, CI, diesel engine of low to mid ratings. In this study, after multiple inspection, the value of γ is considered is 1.35. The justification of this is provided in Appendix A, with the help of ideal gas law and correlations provided by Hanson (1989) and Goering (1998) spatially averaged temperature in the combustion chamber. The heat release rate measured by variable γ and constant γ of 1.35 are well matched. All the experiments are executed within 20±2ºC and atmospheric condition.

Table 4.3 The experimental matrix for studying emulsified and neat POME in VCR engine

Load	**Injection Timing (°BTDC)**			
	20	**23**	**25**	**28**
No load	CR(POME), CR(WIP): 16 CR(POME), CR(WIP):17 CR(POME), CR(WIP):17.5 CR(POME), CR(WIP):18	DIESEL (CR:17.5) CR(POME), CR(WIP):16 CR(POME), CR(WIP):17 CR(POME), CR(WIP):17.5 CR(POME), CR(WIP):18	CR(POME), CR(WIP):16 CR(POME), CR(WIP):17 CR(POME), CR(WIP):17.5 CR(POME), CR(WIP):18	CR(POME), CR(WIP):16 CR(POME), CR(WIP):17 CR(POME), CR(WIP):17.5 CR(POME), CR(WIP):18
20%				
40%				
60%				
80%				
100%				

POME-Palm Oil Methyl Ester, WIP-Water in POME (Palm Oil Methyl Ester)

4.5 Summary

This chapter includes the discussion about the engine setup, devices, and equipment required to accomplish the experiments. The brief specifications and the schematic diagram of the engine are included. Some of the important specifications of the flue gas analyzer are also tabulated. Finally, the ways adopted for diesel, neat and emulsified POME tests are elaborated corresponding to the experimental matrix. The later chapter discusses about the measured and calculated performance, combustion, and emission results of neat POME run engine.

CHAPTER 5

Results and Discussion: Neat Palm Biodiesel Run Engine

The prime objective of the thesis is to understand the behavior of the emulsified POME run diesel engine under variable CR-IT condition. However, to realize this fact, it is necessary to know the effects of original neat POME in similar combinations of CR and IT, which may be considered as the baseline knowhow from the perspective of palm oil biodiesel. This fact is vague in the available literature. Alongside, being a fuel of different origin, the standard design limits of a diesel engine is not suitable for POME. Therefore, in this chapter the experimental observation performed in a VCR diesel engine with neat palm oil methyl ester (POME) is analyzed to find out its optimum performance. The engine is run at a constant speed of 1500±50 rpm and rated power output of 3.5 kW. The overall analyses are segregated into performance, combustion and exhaust gas emission studies of the POME run engine. In each of these sections, explanations are provided based on load, CR and IT variations. The outcome of the experimental study is compared with respect to the diesel run engine performance at standard CR-IT setting for quantitative and qualitative assertion. The mechanical performances of the engine are determined on the basis of brake power, brake thermal efficiency, brake specific fuel consumption and exhaust gas temperature. The parameters for combustion analyses include cylinder pressure variation with crank angle, ignition delay, peak cylinder pressure and net heat release rate. Finally, the emission concentrations of CO, CO_2, NO_X and HC in the exhaust gas are recorded with the help of a flue gas analyzer. The purpose of this study is to understand the behavior of neat POME in a diesel engine under various combinations of CR and IT.

5.1 Preface

The applications of methyl and ethyl esters derived from vegetable oils as a substitute of diesel has been widely assessed by many researchers (Bari *et al.*, 2002; Banapurmath and Tewari, 2009). It includes the oil made from jatropha, karanja, neem etc., and their biodiesel in both diesel and dual fuel engines (Yadav and Singh 2010; Kumar *et al.*, 2011; Sahoo *et al.*, 2012b). The vegetable oil such as crude palm oil and its esterified form, the palm oil methyl ester (POME), used mostly by blending with diesel (Kalam and Masjuki, 2002; Aziz *et al.*, 2005; Lin *et al.*, 2006). The increase of POME in its blending with diesel advances the timing of fuel injection. Further, having the LHV a little lower than diesel, POME causes the BSFC to increase for the same BP, thereby reducing the BTHE (Agudelo *et al.*, 2009; Benjumea, 2009). While working with several combinations of preheated POME and intake air conditions, it has been found that a rise in POME temperature causes a reduction in viscosity, resulting a better fuel spray, atomization and fuel evaporation in diesel engine (Masjuki *et al.*, 1996). However, preheated palm oil also increases carbonated emission (Almeida *et al.*, 2002).

The review of literature on POME run diesel engines confirms that, until now, the mechanical, combustion and emission characteristics of POME run engine under variable compression ratio (CR) and injection timing (IT) are not transparent. Hence, this chapter explores on the behavior of a diesel engine, run with neat POME for a set of CR and IT. The CRs are varied from 16 to 17, 17.5, and 18, where ITs are set at 20º, 23º, 25° and 28ºBTDC. Thus, sixteen (16) combinations of CR and IT are prepared to check. The variations of load are performed from no-load to full-load (12 kg) with an increment of 2.4 kg (20%). The standard diesel specification is CR=17.5 and IT=23º BTDC and used a baseline for comparison with the findings with POME run engine. The performance analyses evaluated are brake thermal efficiency (BTHE), brake specific fuel consumption (BSFC) and exhaust gas temperature (EGT). The combustion analyses include the cylinder pressure variation, ignition delay (ID), peak cylinder pressure (PCP) and net heat release rate (NHRR). Finally, emission analysis is performed by measuring carbon monoxide (CO), carbon dioxide (CO_2), oxides of nitrogen (NO_X) and hydrocarbon (HC). All the experiments are performed within 20±3ºC and atmospheric pressure conditions. The theoretical equations, based on which performance and combustion analysis are executed, are included in Appendix-A.

5.2 Performance Analysis

The performance analysis includes the variation of BP, BTHE, BSFC and EGT. The experiments are performed at a constant speed of 1500±50 rpm. The CR variations are made for POME run for a constant IT. Therefore, the plots of each performance parameter for constant ITs are clubbed together with diesel data for comparison. The results are discussed with respect to the three design and performance parameters, namely, load, CR and IT.

5.2.1 Effect of Load

The variations of BP with respect to load for different CR and IT combinations are included in Fig. 5.1. The engine is run for constant speed for both diesel and POME at each loading condition. However, with the increase in load, BP increases. BP has a linear relationship with load (Eq. A1) which is clearly reflected from Fig. 5.1. The trends seen in Fig. 5.2 elaborate that the POME run engine provides a closer level of efficiencies to that of diesel. It has been seen that at 20 and 40% load POME provides a maximum of 7% higher BTHE than diesel. However, on and onwards 60% load, BTHE of POME is little lower than diesel. The reason is very clear from Fig. 5.3 of BSFC. The BSFCs observed at 20°and 28ºBTDC are lower than the same at 23°and 25ºBTDC. That is, lower amount of fuel is consumed for the same BP. This increases BTHE, which crosses even neat diesel range too at those particular loads. However, on and onwards 60% load the BSFCs for POMEs increased for almost all the CR-IT combinations (Raheman and Ghade, 2008) comparable to diesel. This is because; at higher loads POME has to compensate its little lesser LHV, as well as maintains same BP and speed at each particular load. Hence, a petite increase (deteriorate) of BSFC quantity is encountered. However, with the increase in load BSFCs for all the CR-IT combinations reduce. The average values of BSFC are 0.8863, 0.5475, 0.4344, 0.3788 and 0.3481 kg/kW-h for 20%, 40%, 60%, 80% and 100% loading conditions respectively. Hence, at highest load BSFC of POME is about 61% lower than 20% load. This is attributed to the increase of the mechanical efficiency with the increase in load, irrespective of the fuel type. That is why BSFC has a lowering trend, as fuel consumption per unit of power reduces. The EGT varied almost linearly with load as seen from Fig. 5.4. The average EGT has increased from 132ºC, at no load condition to 259ºC at 100% load with an average increase of 14.5% for each 20% increase of load. Almost similar trend is observed for all the CR-IT combinations studied for POME run engine. This is because, at higher loads, the absolute fuel consumption increases to encounter the increase in power necessary to adopt heavy load. The more is the fuel consumption, the more is the combustion and hence higher is the temperature of burnt gas (Heywood, 1988).

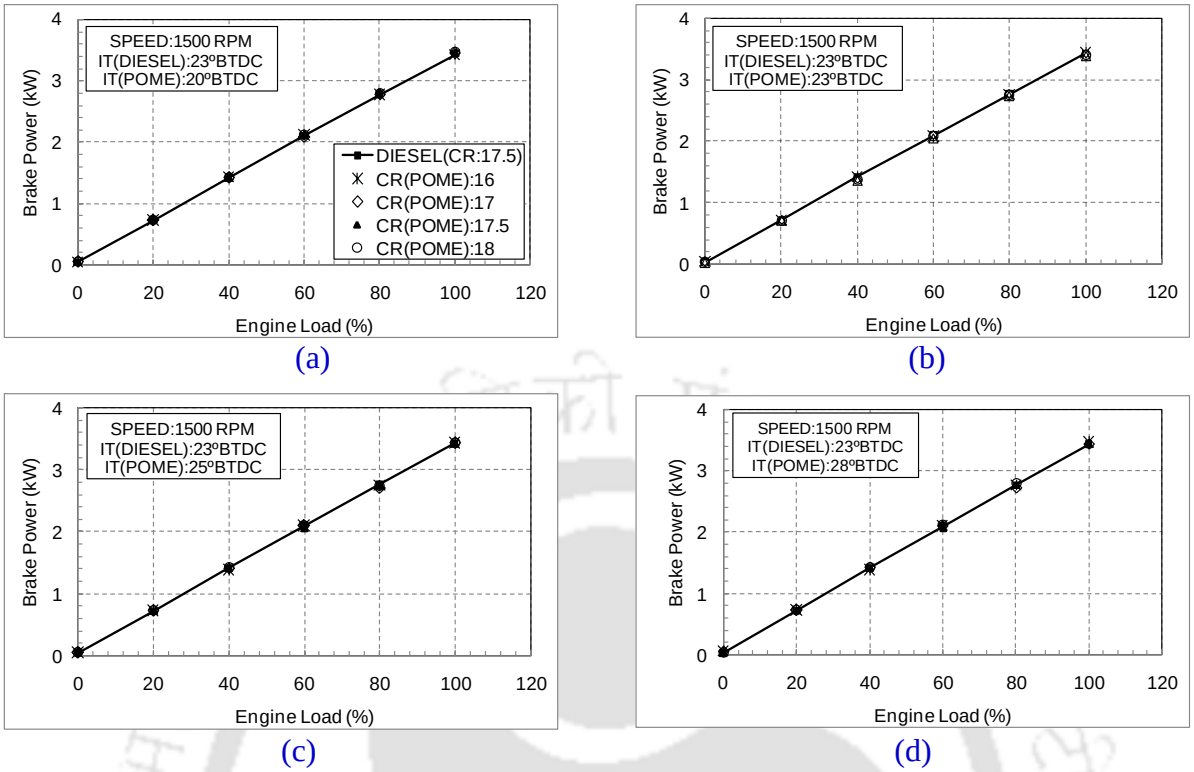

Figure 5.1 Variation of BP with engine load for different CR and IT for neat POME run engine.

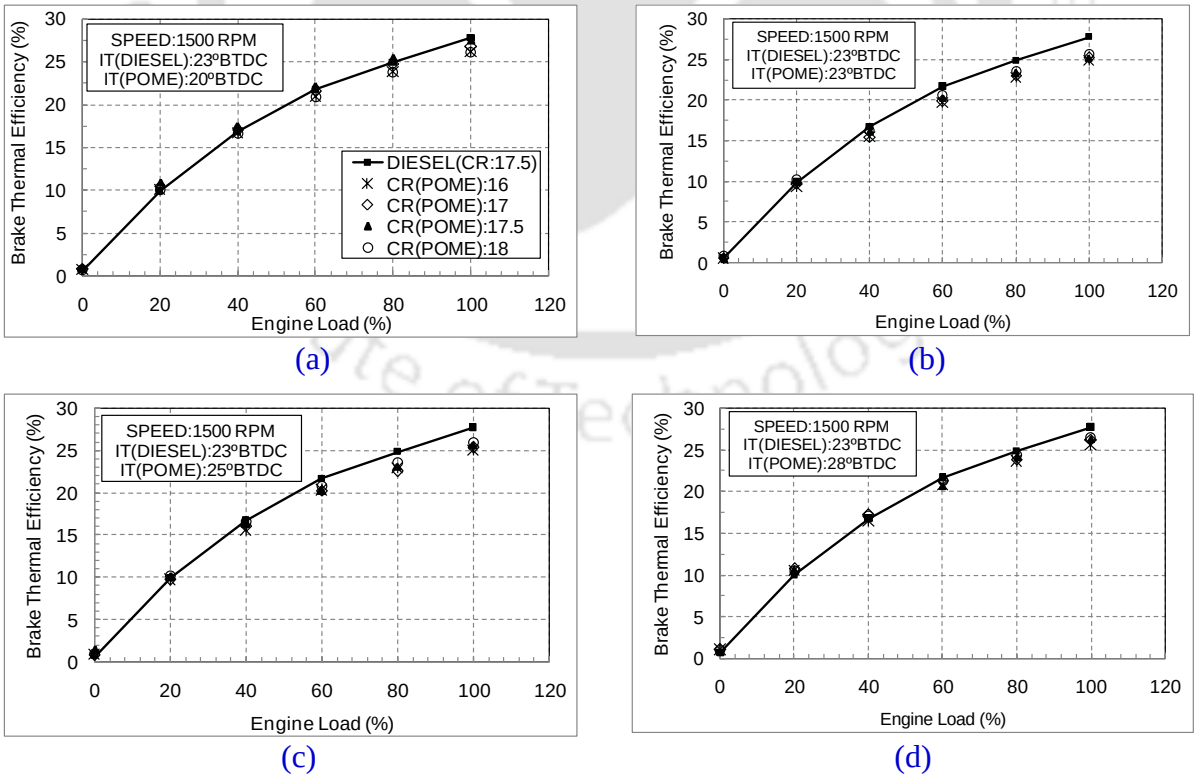

Figure 5.2 Variation of BTHE with engine load for different CR and IT for neat POME run engine

5.2.2 Effect of Compression Ratio

The effect of CR on BP is negligible. Because the engine has a constant speed, which means, it runs at almost same speed, at each CR. Therefore, BP is a function of load only. The comparisons of maximum BTHEs (at 100% load) of POME for various CR at standard IT of 23ºBTDC with typical diesel operation are shown at Fig. 5.5. The increase in CR generally tends to increase in BP (Jindal *et al.*, 2010b). However, in this study speed and BP is maintained constant. Hence, the increase in CR reduces the BSFC. The result is obtained in the form of increased BTHEs for CR enhancement at standard IT of 23ºBTDC. For each of the four IT studied, the increase of CR from 16 to 18 increases BTHE by 7%, 5%, 5% and 3% (by average), respectively. This is because POME has some molecular oxygen bonded in its chemical composition (Table 3.3). According to literature, these oxygen molecules present in biodiesel promote combustion (Puhan *et al.*, 2005). At higher CR, a hot environment is expected to increase their reactivity. The consequence is the increase in rate of heat release and hence the efficiency (Aziz *et al.*, 2005). Although use of POME results higher intake of fuel than base diesel (Figure 5.3), the increase in CR from 16 to 18 have shown drop of BSFC. The average drops of BSFCs are 11%, 12%, 4% and 1% respectively with the rise of CR from 16 to 18 for all the IT combinations studied. This is because, being a little higher dense than diesel, POME performs more frugally at higher CRs (Bhatt, 1987).

The EGT is reduced with the increase in CR for POME (Figure 5.4). An increase in CR shows a drop of the average EGT by 2% whereas 3% and 4% drop in EGT take place with the increase in CR from 17 to 17.5 and 17.5 to 18, respectively. This is because, higher CR raises the air temperature inside the cylinder. This ultimately reduces ignition lag and resulting combustion that is more complete. At no-load condition, the mean temperatures are 135ºC, 133ºC, 132ºC and 129ºC at CRs of 16, 17, 17.5 and 18, respectively. On the other hand, at full-load, these values are 274ºC, 264ºC, 256ºC and 244ºC for the CRs of 16, 17, 17.5 and 18 respectively. Based on EGT, the CR of 18 looks attractive as far as POME run diesel engine is concerned.

5.2.3 Effect of Injection Timing

The POME used in this study gave almost same power output for all CR and IT combinations as it is found in neat diesel mode (CR = 17.5 and IT = 23ºBTDC). This is because of the higher BTHE and almost equivalent LHV of POME (Table 3.3) as compared to diesel that makes POME to burn with almost equal intensity.

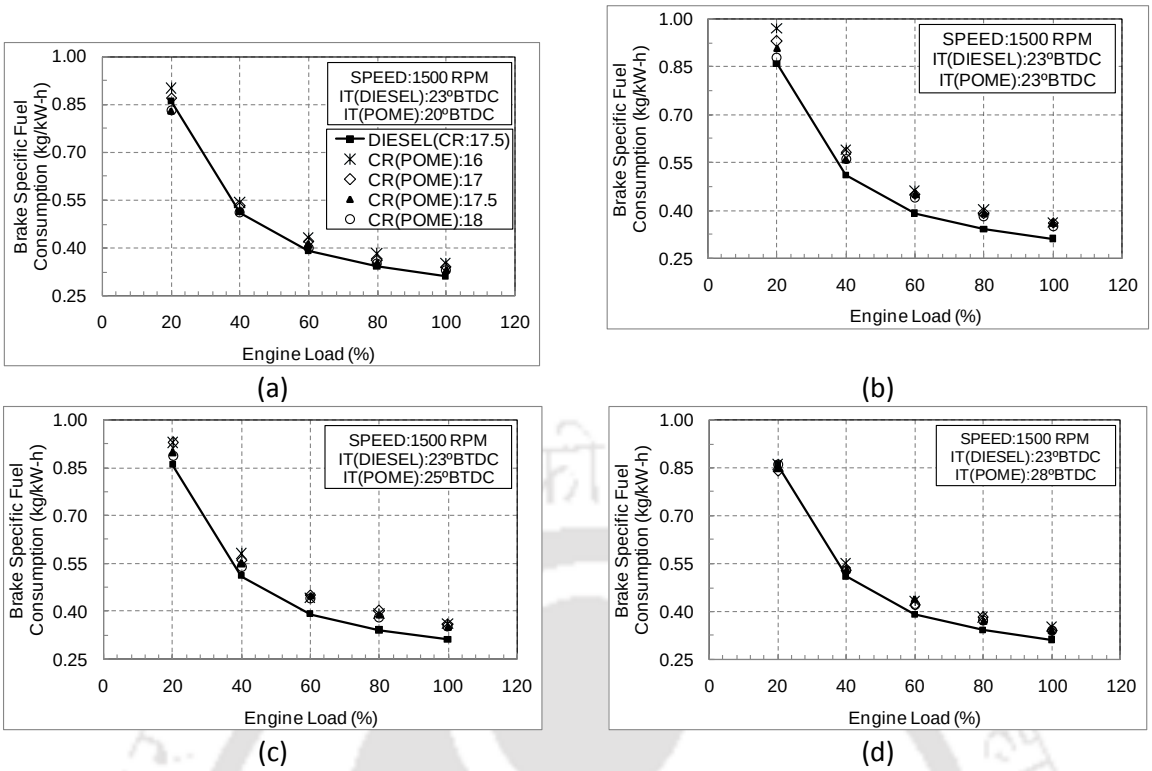

Figure 5.3 Variation of BSFC with engine load for different CR and IT for neat POME run engine

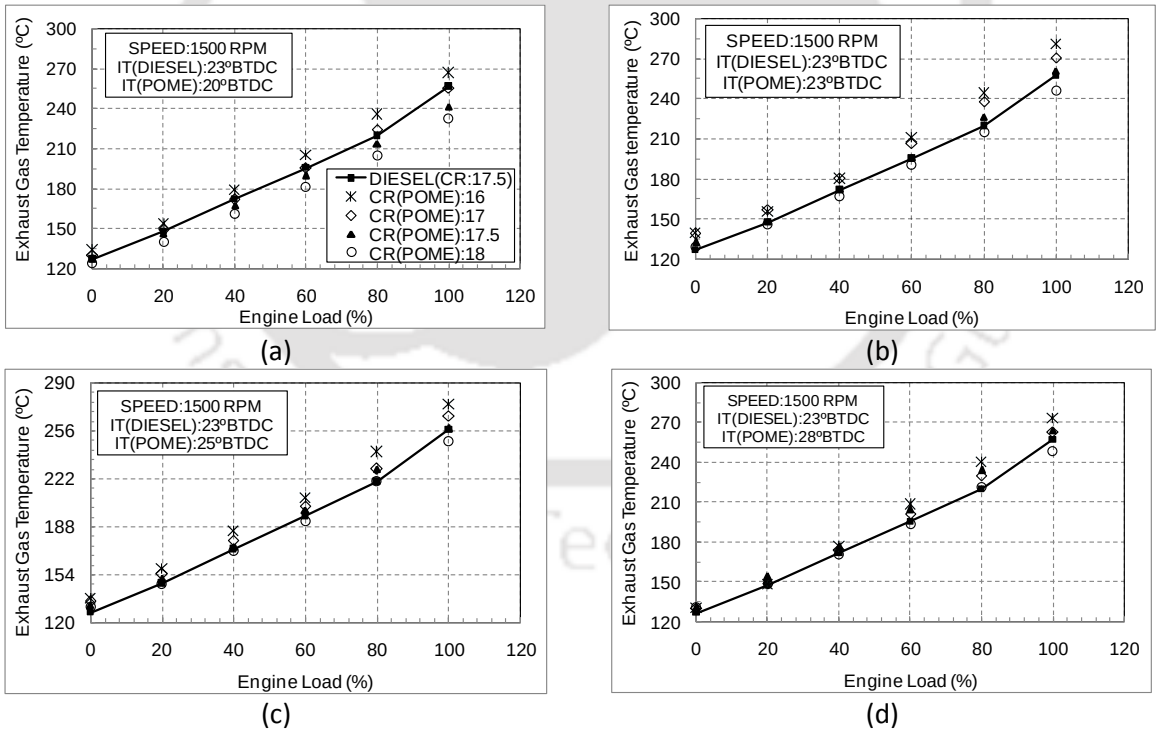

Figure 5.4 Variation of EGT with engine load for different CR and IT for neat POME run engine

The plots of BTHEs (Figure 5.2) show that, 3º retardation (from 23ºBTDC to 20ºBTDC) and 5º advancement (from 23ºBTDC to 28ºBTDC) of POME injection results higher part load efficiency than diesel. Figure 5.6 compares the peak values of BTHEs for the POME run

engine at full-load for two higher CRs (17.5 and 18) and three ITs (20°, 23°and 28ºBTDC) with base diesel. IT advancement increases the peak BTHEs around 2% each and 3% and 2% for the CRs 17.5 and 18, respectively. However, retarding the IT has a major effect on maximum BTHEs, which increase by about 9 and 7%, respectively. The average BTHEs at 20°, 23°, 25° and 28ºBTDC are 17%, 15.79%, 16% and 16.6%, respectively. Thus, retarding the IT improves BTHE by 8%, which is comparable to an increase of 4% while advancing. This is because of the incorrect matching of the peak cylinder pressure (PCP) and maximum heat release rate (MHRR) point for 25° and 28ºBTDC which is resolved by retarding the IT. Hence, 20ºBTDC provides most efficient combustion for POME run engine.

The average drops of BSFCs are obtained as 2% and 5% for IT advancement of 2º and 5º, whereas, retarding the IT (3º) causes an average drop of BSFC by 8%. This is analogous and justifies the effect of IT variation on the BTHE as discussed earlier. As per Raheman and Ghade (2008), advancing the IT meant that the combustion occurred earlier in the cycle, where the pressure and the temperature in the cylinder might be too low to cause auto ignition. Hence, more fuel is burnt before TDC and the peak pressure moved closer to TDC. Hence, advancing the IT elevates the fuel consumption and hence the BSFC. Further injection retardation (20ºBTDC) of POME might have properly matched its expected reduction in ignition delay, owing to its higher Cetane number than diesel, resulting an efficient performance.

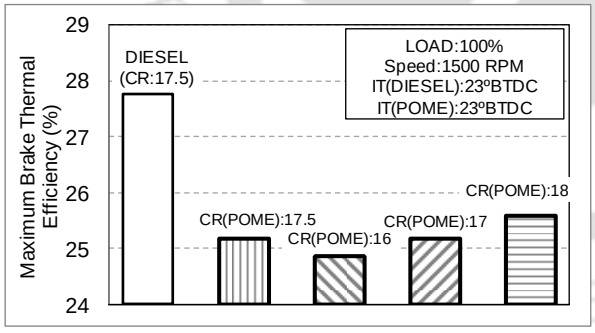

Figure 5.5 Comparison of maximum BTHE with CR (IT=23ºBTDC) for neat POME run engine

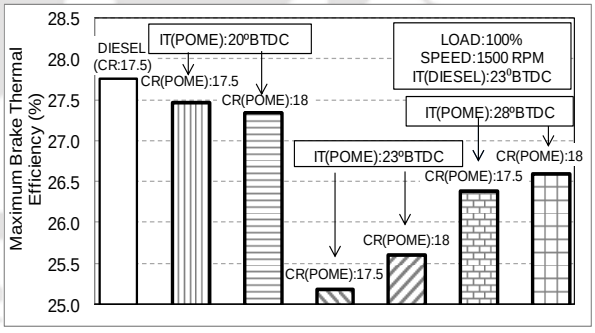

Figure 5.6 Comparison of maximum BTHE with CR and IT for neat POME run engine

The average EGTs at 20°, 23°, 25° and 28ºBTDC IT are 184º, 193º, 192.5º and 192ºC, i.e., advancing IT is found as around 1% reduction of EGT, comparable to a countable 5% for IT retardation while running the engine using POME. This is because at 20ºBTDC, combustion occurs very near to TDC as comparable to other ITs. This is favorable position for best heat release to drops in BSFC and to increases BTHE. All these facts in combination caused best

engine performance using biodiesel and thereby utilizing amount of heat produced in advanced manner. At 20°, 23°, 25° and 28ºBTDC, the mean temperatures at no load conditions are 128.6ºC, 131ºC, 135 ºC and 134ºC whereas 249ºC, 264ºC, 262ºC and 262ºC at full load conditions.

5.3 Combustion Analysis

The combustion analysis has been carried out in the form of variation of cylinder pressure, ID, peak cylinder pressure (PCP) and net heat release rate (NHRR). Similar to the performance study, the parametric variation of CRs for particular ITs are clubbed together. The effects of load, CR and IT on combustion are investigated in following sections.

5.3.1 Effect of Load

The effects of CR variations on cylinder pressure at 100% load for the all of the ITs are shown in Fig. 5.7. At this load, the maximum BTHE is observed irrespective of the CR or IT. The average maximum pressure rise rate (MPRR) for POME test is around 6 bar per crank angle as opposed to 9 bar per crank angle for diesel. This means, POME provides a relatively quieter and smoother operation as compared to diesel and observed similarly at other loads too. Thus, POME not only starts burning a little earlier than diesel, but also burns for a longer duration to give a smoother output. Figure 5.8 indicate the linear rise of PCP with the rise in load. For both POME and diesel, the average increase in PCP is found to be about 5%. The maximum value of PCP is found at full load with CR=18 for all the IT combinations. These values are 76.1, 76.3, 77.3 and 84.4 bar, respectively. For all the CR and IT, IDs vary inversely with respect to load, which are shown in Fig. 5.9. From no load to full load, the average IDs for POME are 18, 17, 17, 16, 15 and 15; whereas for diesel, they are 21, 20, 19, 19, 18 and 17. This is due to the higher BTHE of POME than diesel. The lower ID of POME is also clear from Fig. 5.7. POME starts releasing heat much prior than base diesel, which is again justified by the ID curves (Figure 5.10). The higher BTHE, and hence lower ID, is a key fuel property that determines the premixed combustion duration as observed by Benjumia *et al.* (2009). However, the peak NHRR point for POME is lower than diesel. This is due to a little lower LHV of POME than diesel. Similar kinds of trends have also been observed in a work with honge oil methyl ester (Banapurmath and Tewari, 2008).

5.3.2 Effect of Compression Ratio

Figure 5.7 show that with the increase in CR, the cylinder pressure at each crank angle rises gradually. As a result, the cylinder pressure curves spread more as seen from these plots. This

is due to the drop of cylinder volume with the increase in CR. Side-by-side, with the rise of CR, the air inside the cylinder gains more heat during compression stroke and injected fuel starts burning instantly but uniformly. As a result, at higher CR, smoother combustion is obtained for POME than diesel. However, at CR of 16, the clearance volume expands, which lowers the heat of compression, thereby causing local and irregular combustion for POME.

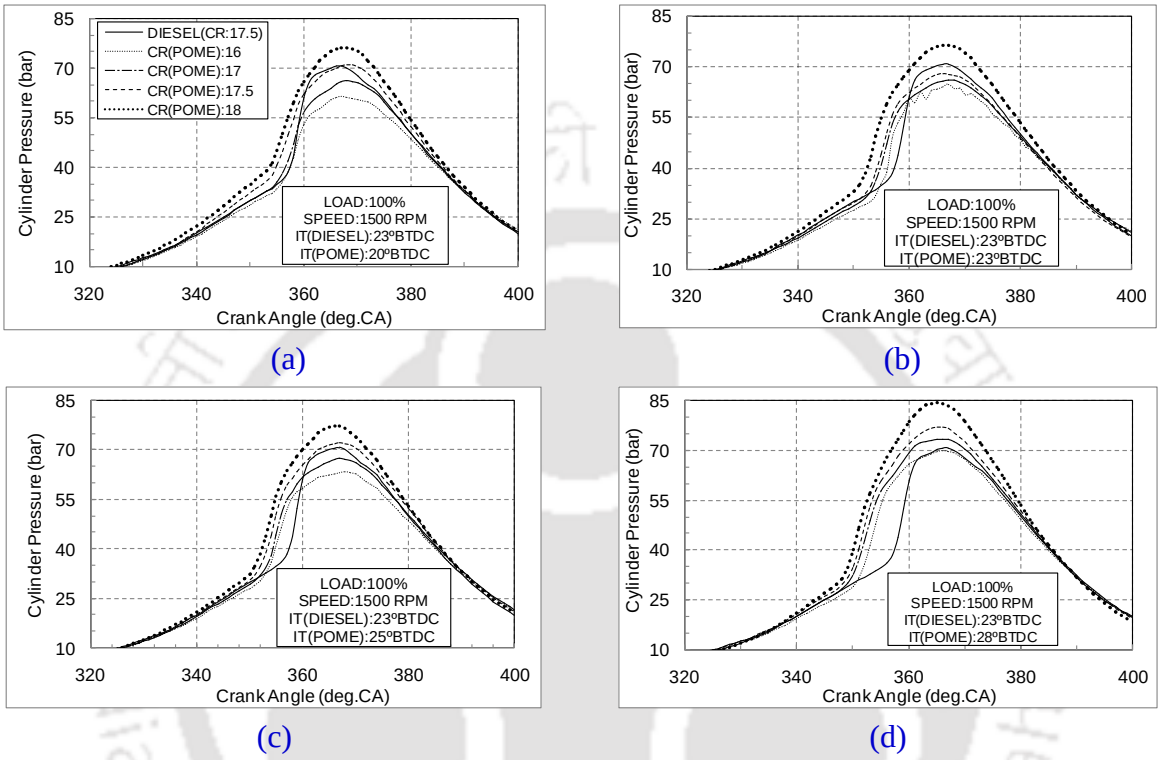

Figure 5.7 Variation of cylinder pressure with crank angle at 100% load for different CR and IT for neat POME run engine

It is seen from Fig. 5.8, that the average peak cylinder pressures obtained at CR = 16 are 55, 58, 58 and 61 bar; whereas PCPs observed at CR = 18 are 67, 68, 68 and 75 bar for the four ITs for POME run engine. The average increase in PCP for POME with the increase in CR from 16 to17, 17 to 17.5 and 17.5 to 18 are 5, 6 and 8% respectively. With the rise in CR, the cylinder volume gets reduced, and this increases temperature and pressure in compression stroke. As a result, the fuel burns with far more intensity and elevates the pressure further at TDC. This is also the reason behind the drop of ID for POME with the raise of CR (Figure 5.9). At higher CR, the warmer environment inside cylinder speeds up the commencement of combustion thereby reducing the ID. The average IDs for POME at CR=16 are 15.33, 17.67, 17.67 and 18.33º crank angle (CA) whereas 13.17, 14.67, 15.50 and 16.33ºCA of IDs obtained at CR=18. The average cut of IDs with the rise in CR from 16 to17, 17 to 17.5 and 17.5 to 18 are 4, 3 and 7% respectively.

The CR variation, from 16 to 18 affects NHRR of POME (Figure 5.10). The effects of reduced IDs are more prominent here especially from Fig. 5.10(c) where the comparison with base diesel data is performed by testing POME at 23ºBTDC. The increase in CR results an early start of ignition for POME, which later reduced the premixed combustion phase. The effect is further prominent at full load condition where the NHRR is high because of warmer environment. The reduction of the premixed combustion phase and the increase in the diffused combustion is similarly observed in literature for various blending of waste cooking oil with diesel as compared to neat diesel (Muralidharan *et al*., 2011).

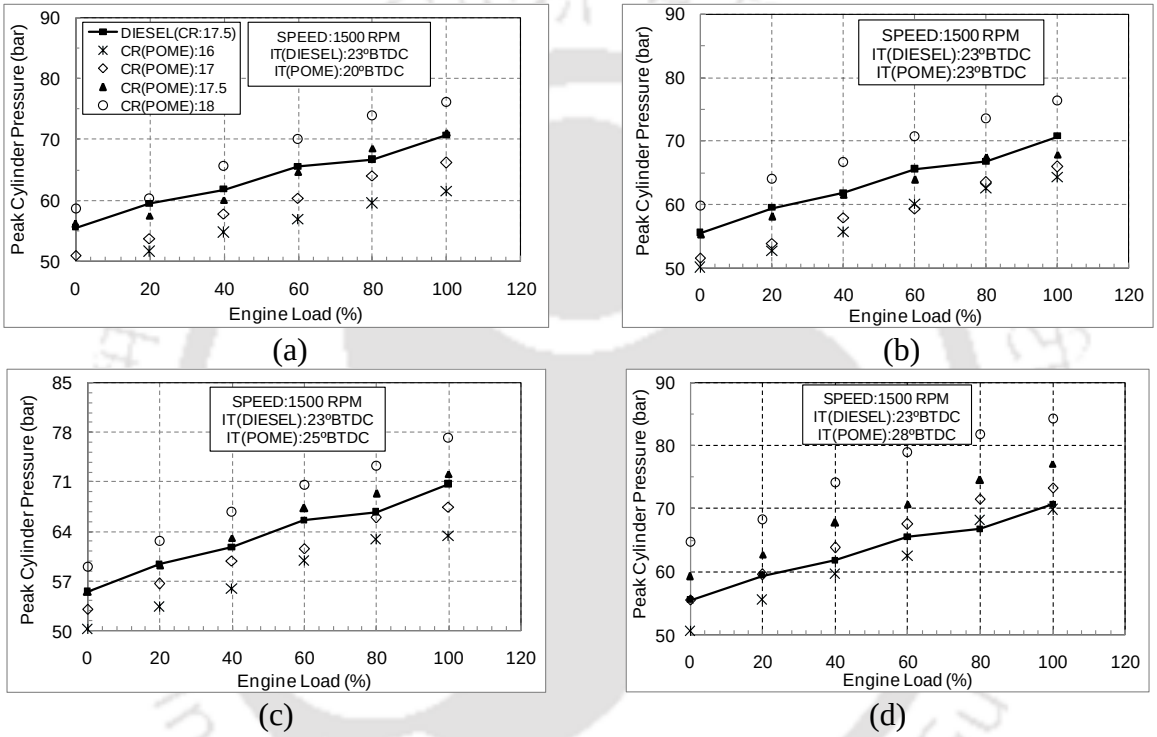

Figure 5.8 Variation of PCP with engine load for different CR and IT for neat POME run engine

5.3.3 Effect of Injection Timing

Figure 5.7 shows that IT advancement causes the fuel to start burning early and gets more time to burn completely. As a result, at higher IT, the *P-θ* curve spreads more and boosts further by the lower ID of POME. The similar trends are observed at other loads also. This phenomenon has a noticeable effect on the PCP curves too (Figure 5.8). For the four CRs studied, the average PCPs varied from 55, 59, 63 and 67 bar to 61, 65, 69 and 75 bar for 20ºBTDC and 28ºBTDC, respectively. The IT retardation shows a 1% reduction in the PCP whereas advancement causes 2% and 9% increase in PCP. During advancement, the larger combustion period allows the fuel to burn for a longer duration to give higher PCP. The IT

advancement causes increase in ID for POME and vice versa (Figure 5.9). For the CR studied, the average IDs obtained for IT of 20ºBTDC are 15.33, 14.67, 14.33 and 13.17, whereas at 28ºBTDC, these value are 18.33, 17.67, 16.83 and 16.33. The IT advancement causes an average rise of ID by about 2% and 6% whereas retardation results an average drop of ID by about 12%.

At retarded IT, POME spray takes place at a crank angle closest to the TDC. At that instant, the atmosphere in the cylinder is more pressurized and heated comparable to other ITs. This makes the burn prone POME to ignite faster, locally as well as globally inside the cylinder. Therefore, the retardation has more effect than advancement. Figure 5.10 show that advancing the IT provide a rise in the peak NHRR points. It is also clear that the curves are shifted towards the compression stroke as the IT advances. Though at an advance IT, the fuel burns for a longer duration and releases more heat, but it does not seem to increase BTHE as obtained at retardation as discussed in Section 5.2.3. This is due to the higher BSFC at advancement as opposed to retardation. The fact is also ascertained from the findings of Devan and Mahalakshmi (2009). The combustion analysis, therefore, reveals the setting of CR=18 and IT=20ºBTDC to be the optimum among all the combinations.

5.4 Emission Analysis

The components of exhaust gas are measured by using Testo flue gas analyzer. The measured quantities are carbon monoxide (CO), carbon dioxide (CO_2), nitrogen oxide (NO_X) and hydrocarbon (HC). The effect of load, CR and IT variations on these emission parameters are discussed in following sections.

5.4.1 Effect of Load

Figure 5.11 shows that, with respect to load change, almost all the CR and IT variation shows the similar effect on the CO emission. From no load to full load, the average variations of the CO emissions for POME are 62, 46, 34, 27, 35 and 48 ppm whereas for diesel, they are found as 120, 70, 56, 48, 58 and 95 ppm. An insufficient temperature at lower load region and a richer mixture at higher loads cause incomplete combustion and elevate CO emissions (Mahanta *et al.*, 2006). The average drop of CO emission based on load variation from diesel is 42%. This shows that the use POME creates lesser CO emission than diesel. Figure 5.12 illustrates the average CO_2 variations with respect to load are found as 1.56, 2.03, 2.50, 3.07, 3.82 and 4.84 % for POME whereas these variations for diesel are 2.47, 3.14, 3.33, 3.55, 4.00

and 4.39%. At low to mid load regions, the CO_2 emissions generated by POME are far lower than diesel emissions. However, at higher loads, high combustion temperatures cause additional oxidization of carbons to produce higher CO_2 emissions. POME produces overall 17% lower CO_2 emission than that of diesel.

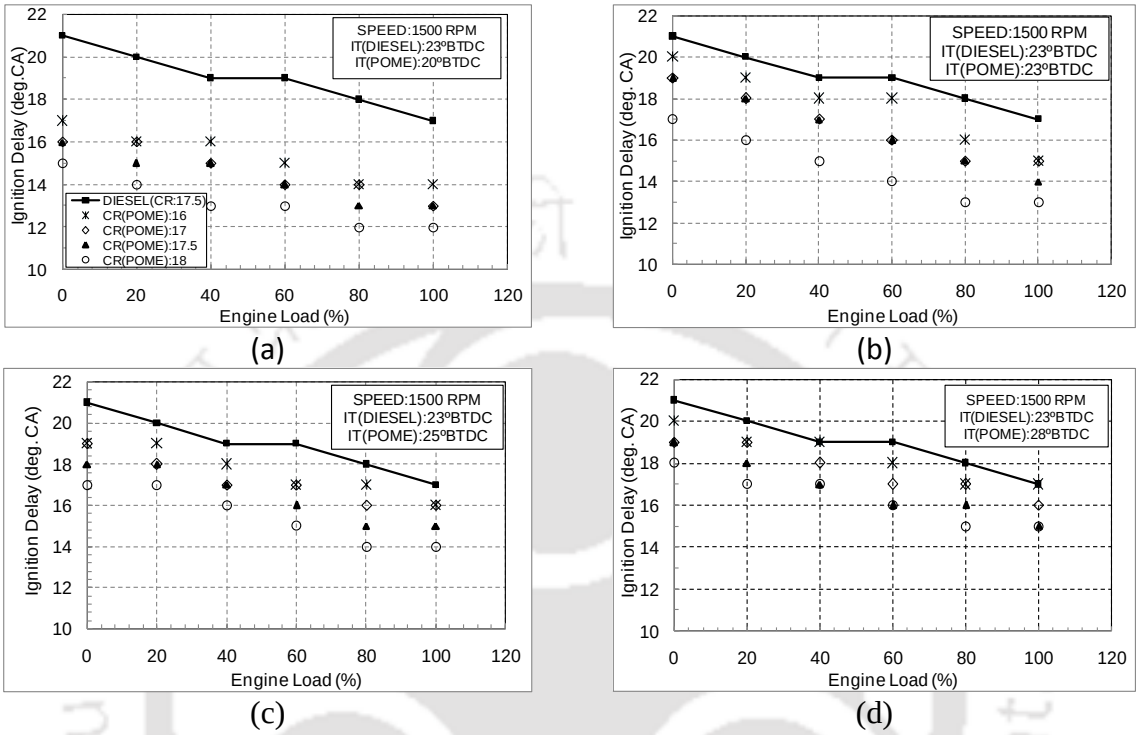

Figure 5.9 Variation of ID with engine load for different CR and IT for neat POME run engine

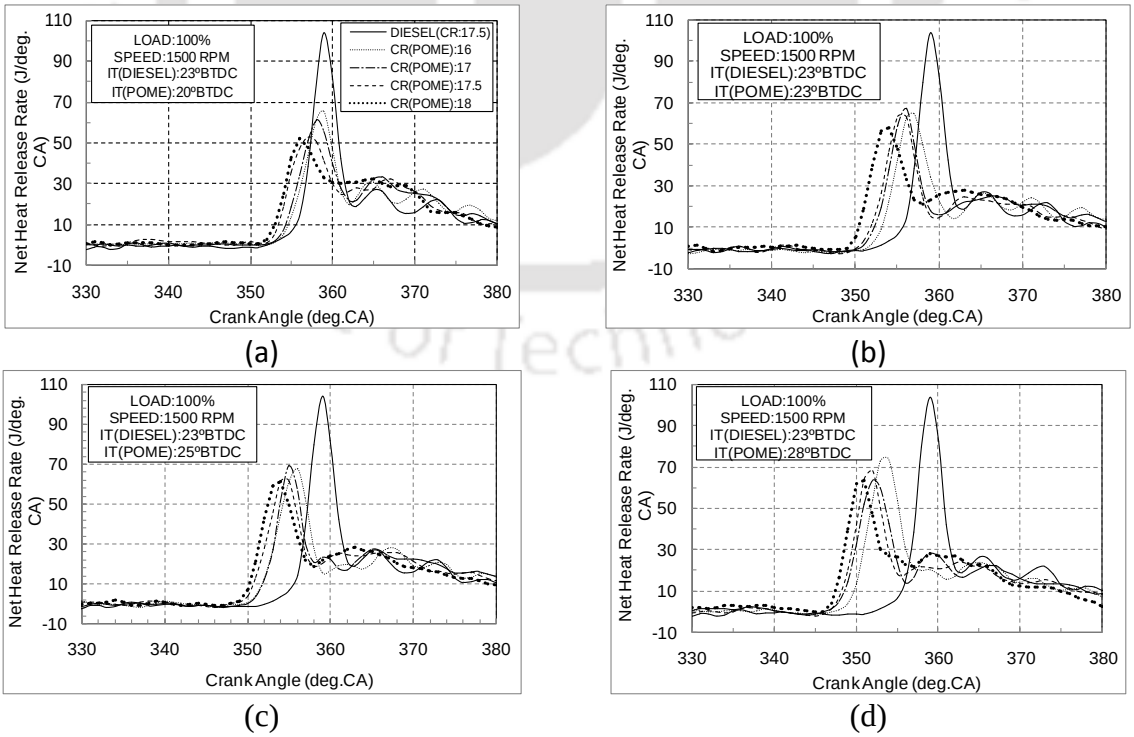

Figure 5.10 Variation of NHRR with crank angle at 100% load for different CR and IT for neat POME run engine

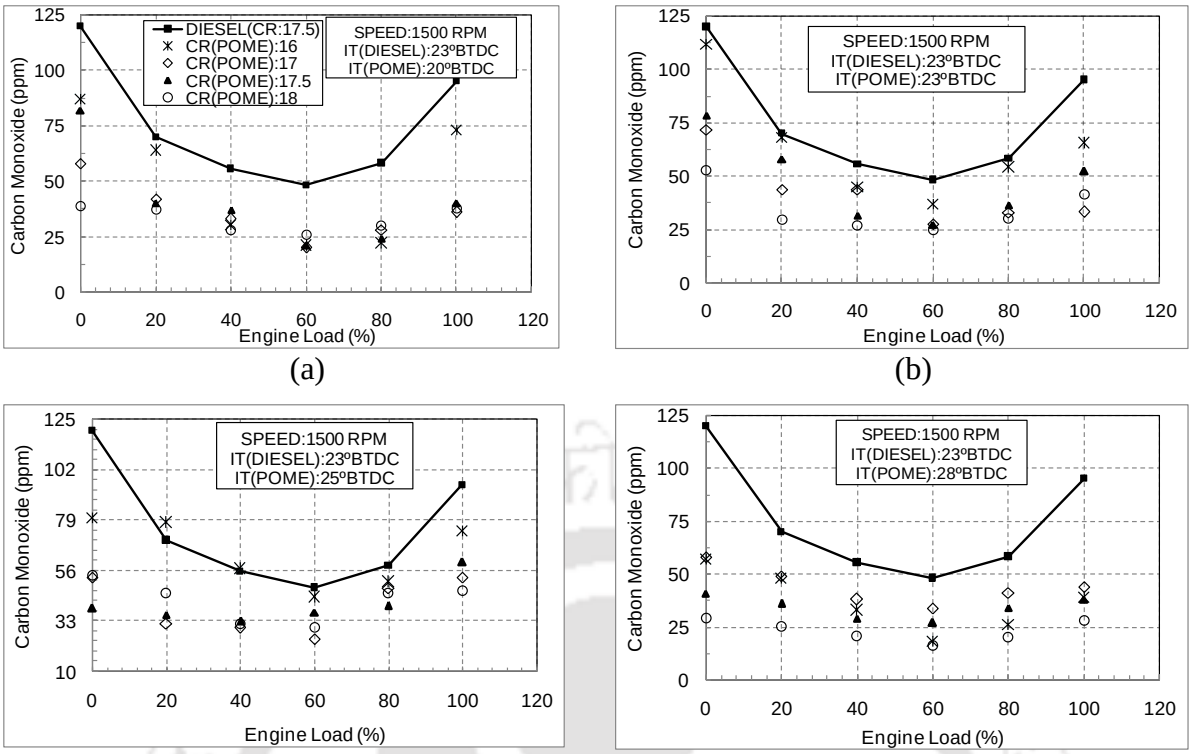

Figure 5.11 Variation of CO with engine load for different CR and IT for neat POME run engine

Figure 5.13 describe the variations of NO_X emissions with respect to load. From no-load to full-load conditions, the average NO_X emissions obtained for POME are 24, 32, 44, 59, 79 and 97 ppm, as opposed to 24, 40, 49, 61, 76 and 92 ppm for the diesel engine. This increasing tendency of NO_X emission with respect to load is dependent on combustion temperature that is supported by EGT curves (Figure 5.4). At high load region, the increases in temperature speed up the thermal NO_X formation (Heywood, 1988). That is the reason behind the higher NO_X emission for POME at higher load region. However, NO_X emission for POME is 4% higher than diesel emission in average. Figure 5.14 show that, at lower and higher load regions, HC emissions change with descending and ascending orders. For the POME run engine, the average HC emissions at no-load to full-load regions are 18, 14, 10, 8, 13, 18 ppm, whereas, for the diesel engine, the corresponding values are 30, 22, 17, 14, 15 and 19 ppm. At lower load regions, the combustion temperatures accomplish to a reasonably lower value to enable complete combustion. However, at higher load regions, the quantity of fuel supply increases to produce additional power to take up high load. These facts together are responsible for unburnt HC release (Aziz *et al.*, 2006).

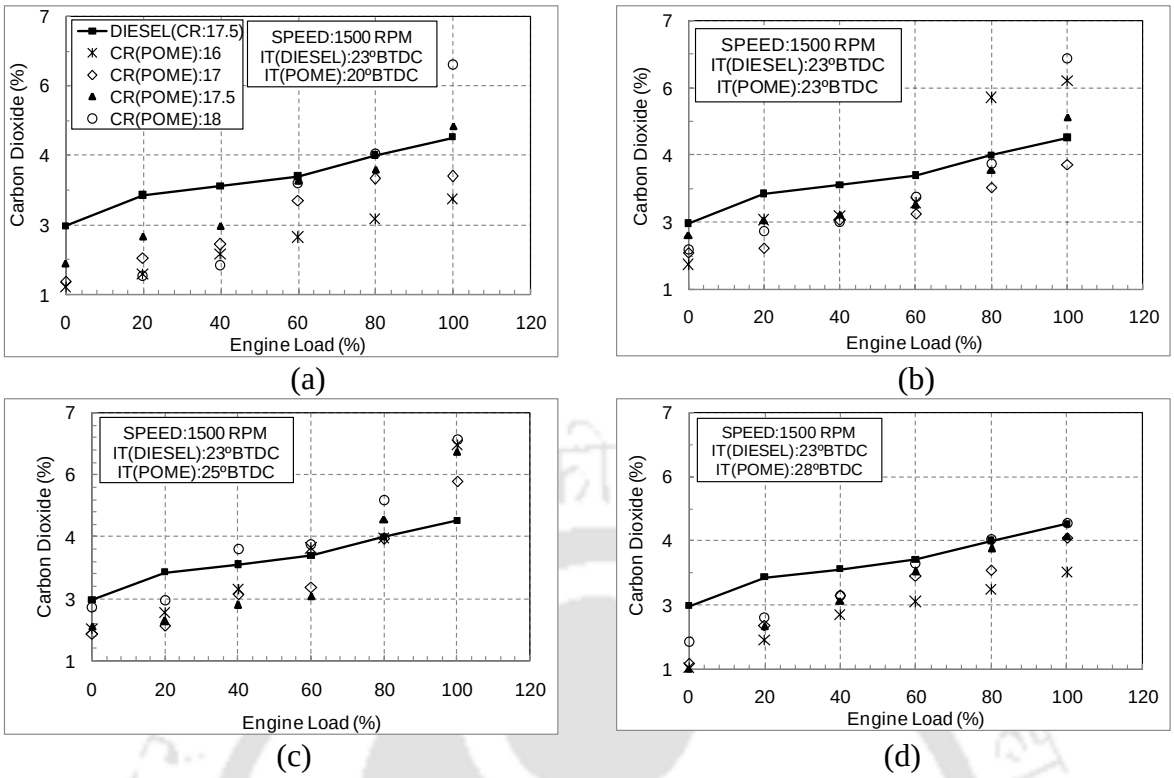

Figure 5.12 Variation of CO_2 emission with engine load for different CR and IT for neat POME run engine

5.4.2 Effect of Compression Ratio

The average values of CO emissions for POME at CRs of 16, 17, 17.5 and 18 are 53, 41, 41 and 33 ppm (Figure 5.11). The increase in CR reduces the cylinder volume, which in turn, increases the combustion temperature. This fact along with oxygenated biodiesel (POME), reduced the chances of forming fuel-rich zone, which is responsible for 38% reduction of CO emission, for an increase of CR from 16 to 18 (Rakopoulos *et al.*, 2004). The same cause attributes the increase in the CO_2 emission with the increase in CR (Figure 5.12). The average CO_2 emissions recorded are 2.8, 2.7, 3.0 and 3.3% (by volume) for CR for all four CRs. The overall increase in CO_2 emission is 18% with the increase of CR from 16 to 18. As seen in Fig. 5.13, the average NO_X emission obtained for the CR of 16, 17, 17.5 and 18 are 73, 57, 51 and 42 ppm. Hence, for the POME run engine, the rise in CR causes an overall reduction of NO_X emission by 43%. At high CR, the pressure and temperature during the compression stroke and at the primary stages of combustion increases. In addition, the lower ID of POME causes the combustion to complete a little earlier. As it is evident from Fig. 5.10, the majority of heat release of POME is performed near or before TDC. As a result the combustible products remained comparatively cooler atmosphere comparable to diesel throughout the expansion stroke. This fact slows down the NO_X formation. The variations of HC emissions are shown in Fig. 5.14. The average HC emissions obtained are 16, 14, 13 and 10 ppm for POME. Therefore, HC emission drops by 37% via increasing CR from 16 to 18. The high

pressure and temperature in the compression stroke together with lower ID cause rapid burning of oxygenated POME and reduces HC, as reported in the literature too (Schmidt and Van Gerpen, 1996).

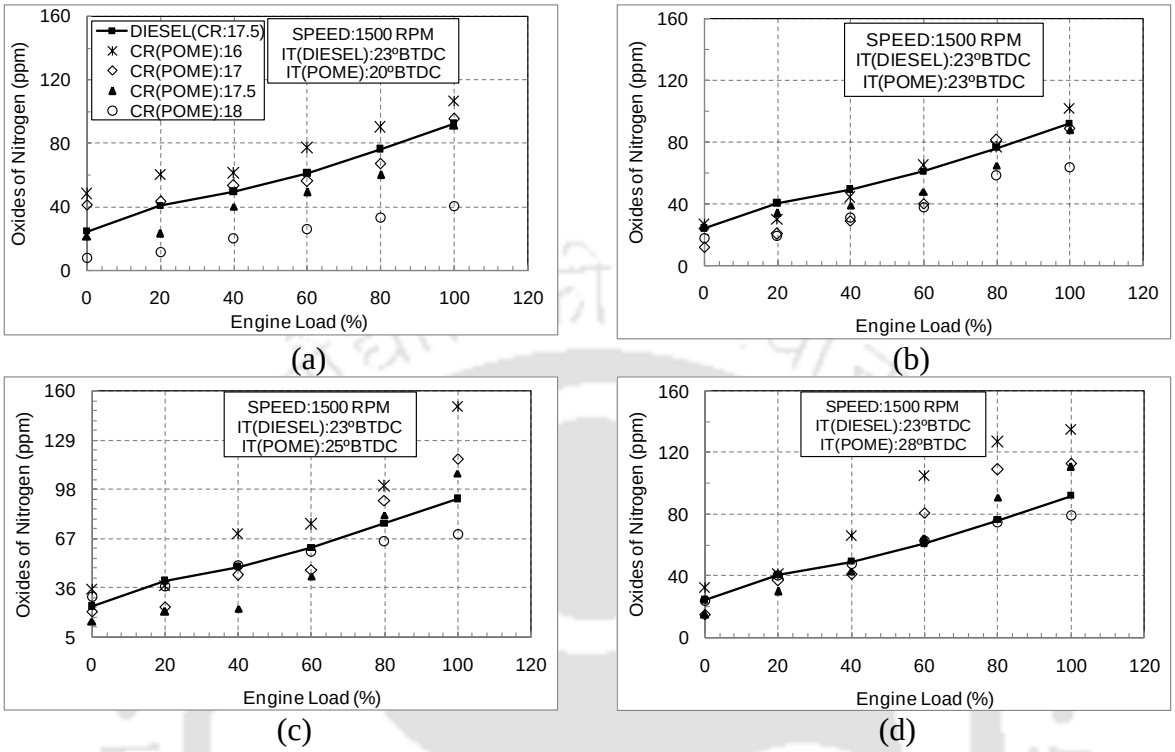

Figure 5.13 Variation of NO_X emission with engine load for different CR and IT for neat POME run engine

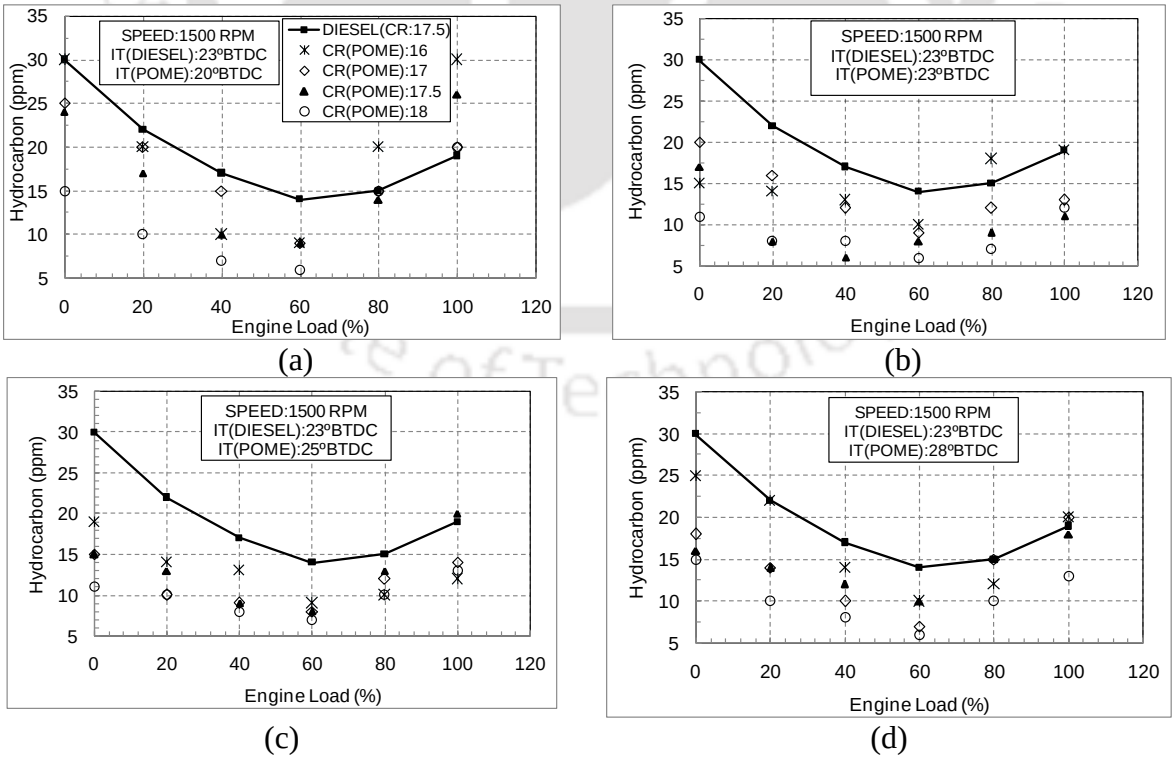

Figure 5.14 Variation of HC with engine load for different CR and IT for neat POME run engine

5.4.3 Effect of Injection Timing

The CO emission is the outcome of incomplete combustion of fuels, and hence, it is influenced by BSFC. For POME run engine, retarding (by 3º) and advancing (by 5º) the IT indicates a descent of CO emission by 15% and 26%, respectively (Figure 5.11). The results are clear from the BSFC values obtained at different ITs as particularized in Section 5.2.3 (Sayin *et al.*, 2008). Lower is the BSFC, lesser will be the quantity of unburnt fuel particles and hence lesser will be the probabilities of CO emission. The results illustrate that advancement and retardation of IT cut the CO_2 emission by 13% and 16%, respectively (Figure 5.12). The NO_X emission study demonstrates that IT advancement causes an enlargement in NO_X emission by 17% and 32% than IT retardation (Figure 5.13). As explained in the section 5.3.3, IT advancement increases PCP, which in the end rises peak temperature (Heywood, 1988). This is the reason of increase in NO_X concentration through IT advancement.

The HC emission in the exhaust gas is the consequence of the incompletely burnt fuel particles (Figure 5.14). The advancements of IT cause average reductions of HC emissions by 5% and 3% than retardation. The advancement allows an early start of combustion, and the charge being compressed as the piston moves to TDC, has relatively higher temperatures. Analyzed data show that, IT advancement increases average temperature by around 5%. This causes a reduction in the flame quenching layer thickness, leading to a lower HC emission (AbdAlla *et al.*, 2002).

5.5 Uncertainty Analysis

Any experiment is not free from error. Error may occur due to the instrument's inaccuracy, inappropriate calibration, human inadequacy etc. Therefore, uncertainty analysis is mandatory for any experimental work. The sequential perturbation technique (Kline and McClintock, 1953; Moffat, 1982) is followed to acquire the uncertainties of independent and performance parameters (Appendix - B). Some of these are air flow rate (1.1%), liquid fuel flow rate (0.1 %), engine load (0.1%), engine speed (1.3%), LHV of liquid fuel (1.0%) etc. Because of these facts, the calculated accuracy of the performance and combustion study for both POME and diesel run engine are found within ±3.6%. However, the accuracy of the emissions is found within ±2.3%.

5.6 Summary

- At higher loads BTHEs of POME is little lower than diesel. For constant IT, increase in CR increases BTHE to a maximum of 7%. However, combined variation of CR and IT shows retarding the IT to 20ºBTDC provides higher BTHE. The maximum values of 27% BTHEs are found at both CR=17.5 and 18 with 3º IT advancement. The IT retardation (20ºBTDC) causes an average 8% reduction in BSFC than injection advancement.
- However, increasing CR from 17.5 to 18 causes almost 9% reduction in BSFC at IT=20ºBTDC. EGT increases linearly with the increase of load. However, increase in CR to 18 causes a maximum reduction of EGT of 4%. Besides, IT reduction to 20ºBTDC also causes a maximum reduction of 5% for EGT.
- POME runs more smoothly than diesel in diesel engine at higher CR. Increase in CR causes a maximum of 8% increase in the PCP. Alongside, increase in IT also causes increase in PCP in the form of 9% at 28ºBTDC. The most significant finding in this study is the reduction of ID for POME run engine with respect to diesel. It is seen that a maximum of 31% drop of ID was obtained while running the engine at CR=18 and IT= 20ºBTDC of using POME. This is because; POME burn very fast near TDC (IT=20ºBTDC) causing the MHRR curve to approach near to TDC. This results increase in heat release, which ends up with maximum BTHE.
- The POME causes an average CO reduction of 42% than diesel based on load variation. The increase in CR from 16 to 18 causes 38% drop in CO and 18% increase in CO_2 emission by average. This is because of the high initial combustion pressure and temperature causes the POME to burn efficiently at CR=18. However, IT retardation causes reduction of both CO and CO_2 by 15% and 16%, respectively.
- The increase in CR from 16 to 18 causes an overall drop of NO_X emission by 43% for POME. The rise in CR although increases combustion pressure and temperature at the initial stages of combustion; but lower BTHE of POME. Thus, it causes the combustion to start and finish early, which results, the exhaust gas to cool down and then reduce NO_X emission. The increase in CR causes a reduction of HC emission by 37%. The reason is similar to that of results obtained in case of CO emission. However, the effect of IT is negligible on HC emission.

Therefore, from the above discussion of emission analysis also it is concluded that a combination of CR=18 and IT=20ºBTDC offers decent performance for POME in diesel engine.

CHAPTER 6

Results And Discussion: Emulsified Palm Biodiesel Run Engine

The emulsification is a potential technique for reducing the pollutant emissions from a combustion equipment. This is because of the occurrence of a basic mechanism, called micro-explosion, which is expected to enhance the combustion, unlike diesel. Hence, the method of emulsification can be implemented to improve the diesel engine performance by renewable fuels, namely, biodiesel that generally contains lower energy content. In order to understand this fact, an ultrasonic emulsification method has been incorporated in this study, to prepare two-phase water in POME (WIP) emulsions. In Chapter 3, the details of WIP characterization performed are discussed for various water quantity, surfactant quantity and hydrophilic lipophilic balance (HLB) of the WIP samples. It is found that, the WIP prepared with 5% water, 3% surfactants of HLB 6 is the superior among all the samples. Thereafter, the optimized WIP is tested for its physical, thermodynamic and petroleum properties. The sample is then run in a diesel engine for the selected combinations of CR (17, 17.5 and 18) and IT (20°, 23°, 25° and 28ºBTDC). Moreover, along with other loads, experiments are also performed at an overload condition (110% of full load) for the WIP run engine, as shown in experimental matrix (Table 4.3). Finally, the results of the WIP run engine are compared with those of neat diesel test to understand the performance, combustion and emission characteristics. This is followed by the presentation of the uncertainty analysis results.

6.1 Preface

In emulsification, two or more immiscible fluids are mixed together such as water and fuel oil. When sprayed through a nozzle, the emulsified fluid is atomized into fine liquid droplets. Owing to its lower boiling point than fuel oil, water droplets reach their boiling point first after absorbing an ample amount of heat (Subramanian, 2011). The vaporized water then blows up the oil layer, forms smaller oil droplets, and raises the oil's surface to volume ratio. This is called "micro-explosion" (Crookes *et al.*, 1997; Basha and Anand, 2011a). The spontaneous burst of the fine water droplets form high pressure steam and acts as an added pressure force on the piston top, which enhances the engine torque (Abu-Zaid, 2004). It is found that, the BP of a water in diesel emulsion run engine, rises with the increase of speed, and remains independent on water percentage (Sawa and Kajitani, 1992; Nadeem *et al.*, 2006). At lower loads, water injection in the inlet manifold shows better BTHE than emulsion (Subramanian, 2011). It is reported that, the vaporization of water reduces local temperature and do not allow nitrogen to get enough activation energy to react with oxygen. Thus, the formation of NO_X get reduced (Song *et al.*, 2000; Husnawan *et al.*, 2009). An experimental study using emulsified soybean oil methyl ester has showed a sizable drop in CO_2 and exhaust gas temperature (Lin and Lin, 2007b).

A number of researchers have worked with various types of emulsified fuels in diesel engine. However, the work in the area of emulsified biodiesel as an alternative to diesel is rare. This is because emulsified biodiesel has dissimilar properties than diesel. This leads to inferior performance of emulsified biodiesel in standard diesel settings. Therefore, it is needed to explore the emulsified biodiesel in a various engine settings and optimize its performance, combustion, and emission characteristics. Hence, a bio-origin alternative fuel, palm oil methyl ester (POME), is selected for the study. This is due to the highest fossil energy balance and its lowest production cost than other energy crops (FAO, 2008). The water in POME emulsions (WIPs) are prepared for various HLB, surfactants and water quantities. The emulsion with superior specification is found to have 5% water and 3% surfactant of total emulsion quantity with HLB 6 (Chapter 3). To study the effect of engine operating parameter variations on WIP run engine, the specified WIP is tested in a VCR engine to obtain the performance, combustion and emission characteristics at CR=17, 17.5 and 18 and IT of 20°, 23° and 28ºBTDC. The engine tests are performed from 'no load' (0.1 kg) to full load (12 kg) condition with 20% of increment and 10% overload (13.2 kg). Finally, the data WIP run engine are compared with the standard diesel run (CR = 17.5 and IT = 23ºBTDC).

6.2 Performance Analysis

The performance analyses discussed in following sections contain the variation of BP, BTHE, BSFC and EGT. The experiments are performed for constant speed of 1500±50 rpm. During the experiment the CR variations are executed for WIP at constant IT and plotted accordingly. The results obtained are discussed with respect to the three design and performance parameters, namely, load, CR and IT.

6.2.1 Effect of Load

It is known that BP has a liner relation with load, if speed is maintained constant. The trend is maintained linear (Fig. 6.1). Figure 6.2 shows the comparisons of BTHEs between neat diesel and WIP. The results shown in these figures are calculated by ignoring the water quantity contained in the emulsion. BTHE is defined as the ratio of BP and the product of fuel consumption and calorific value (Heywood, 1988). The rise in load increases BTHE for both neat diesel and 5% WIP for the tested CRs. For 5% WIP, the BTHEs at 100% load for CR of 16, 17, 17.5 and 18 are 27.4%, 27.7%, 27.9% and 28.7% as opposed to 28.9% for neat diesel. At overload conditions (110% of full load) efficiency is found maximum for both, WIP and diesel irrespective of CR-IT combinations. For 5% WIP, the average BTHEs at the entire load range are 1.6%, 12.4%, 19.4%, 24.0%, 27.1%, 29.4% and 30.2%, whereas, for neat diesel, these values are 1.2%, 11.6%, 18.5%, 23.2%, 26.5%, 28.9% and 29.4%, respectively. The increase in BTHE based on load for WIP compared to diesel is 7%. The BSFCs obtained for WIP are 5.66, 0.70, 0.45, 0.36, 0.32, 0.30 and 0.29 kg/kW-h, respectively (Figure 6.3). By average, these values are 4.6% lower than diesel and look interesting. Table 3.4 shows that 5% WIP emulsion has a calorific value, around 11% inferior than that of diesel. Still, it has not only covered up this shortage of LHV, but also produced same BP at lower fuel consumption compared to neat diesel. It clearly reveals that, 'micro-explosion' is present in the combustion, which promotes fuel-air mixing prior to combustion (Lin and Chen, 2008).

The variations of EGTs for various CR and IT combinations are shown in Fig. 6.4. The EGTs for load variations are 138ºC, 159ºC, 187ºC, 248ºC, 283ºC, 387ºC and 403ºC for 5% WIP tested whereas for diesel these are 132ºC, 149ºC, 178ºC, 226ºC, 306ºC, 425ºC and 498ºC. It means, the average EGT produced by WIP run engine at low-to-mid load range (0-60%) is higher than diesel. However, at higher loads (80%-110%) it is the reverse. This is because, at the lower load region, the cooler atmosphere inside the cylinder causes slow evaporation of water droplets in WIP and hence delays the combustion. This increases the exhaust gas temperature. However, at higher loads the engine consumes more fuel (which also contains more water droplets), resulting the cylinder to have ample heat and raises the rate of water

bubble explosion, consequently. As a result, more water vapor formation takes place, which have higher capacity of soaking heat, in the later phases of combustion as discussed by Abu-Zaid 2004. This causes more heat to be carried away from exhaust and notably cuts the EGT.

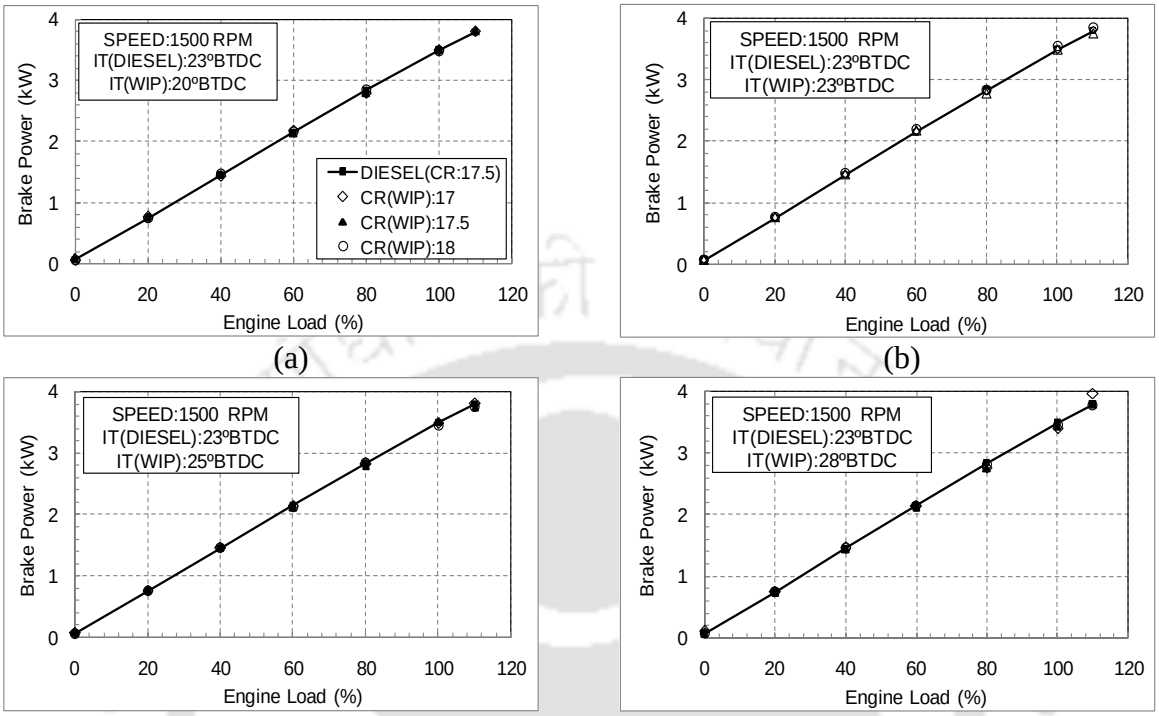

Figure 6.1 Variation of BP with engine load for different CR and IT for emulsified POME run engine

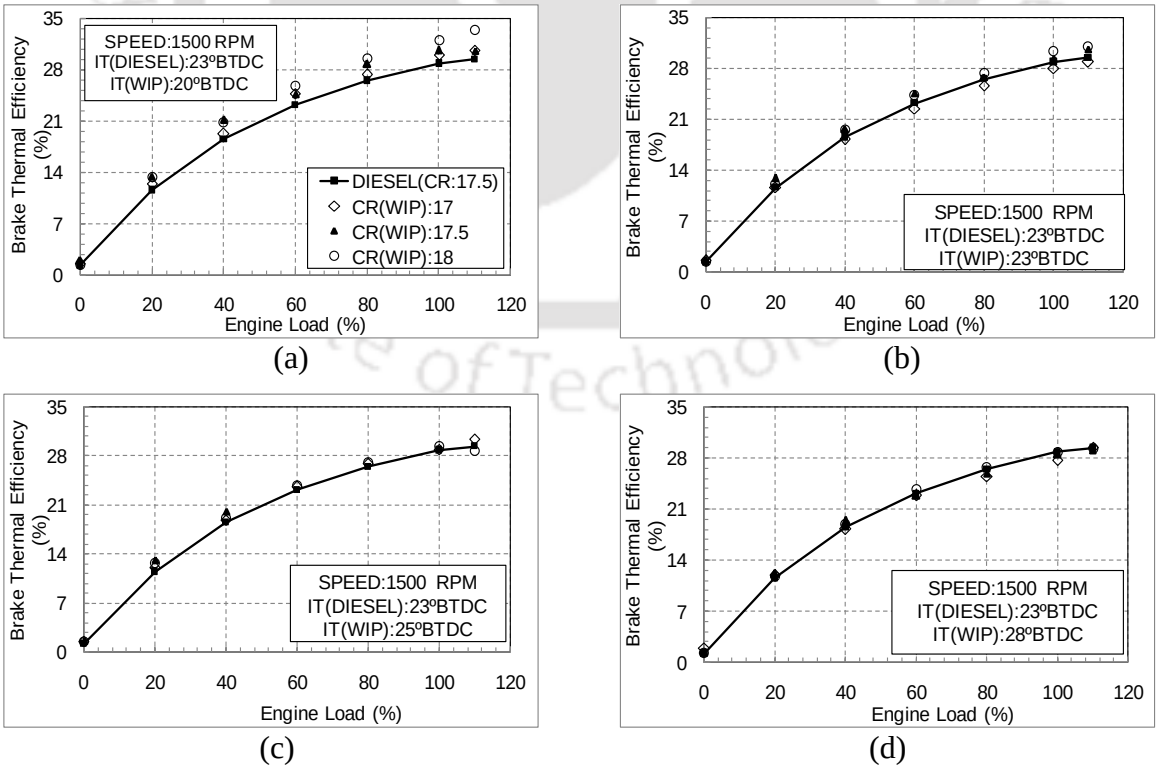

Figure 6.2 Variation of BTHE with engine load for different CR and IT for neat POME run engine

6.2.2 Effect of Compression Ratio

The BP of the engine is a function of torque and speed. In the experiment, WIP emulsion is tested in VCR diesel engine at particular loads where speed remains constant. Hence, for each CR and IT combinations, BPs at those specific loads are constant. The comparisons of BTHEs of WIP at 100% load for various CRs at standard IT of 23ºBTDC with neat diesel operation are shown at Fig. 6.5.The increase in CR generally tends to increase BP (Jindal *et al.*, 2010b). However, in this study, since the speed (hence the BP) is kept constant, the increase in CR reduces the BSFC. The result is obtained in the form of increased BTHEs for CR enhancement at 23ºBTDC. For 5% WIP, at 100% load, the BTHEs are 28.0%, 29.3% and 30.3% for CR=17, 17.5 and 18 as compared to 28.9% for diesel. That means both at standard CR of 17.5 and higher CR of 18, WIP performed more efficiently than diesel at the highest load. Similar behavior is observed at 110% load too, where maximum BTHEs of 5% WIP are obtained as 28.8%, 30.6% and 31.0% for CR of 17, 17.5 and 18 compared to 29.4% for neat diesel. Although WIP has a calorific value, lesser than diesel, still the WIP intake is almost close to diesel or even lesser than that. Till now, literature confirms this point for the emulsions made by ultrasonication with diesel as a continuous phase (Lin and Chen, 2006b). Now it is also proved for biodiesel. Since ultrasonic emulsification produces emulsion with smaller water droplet in the dispersed phase (Lin and Chen, 2008).

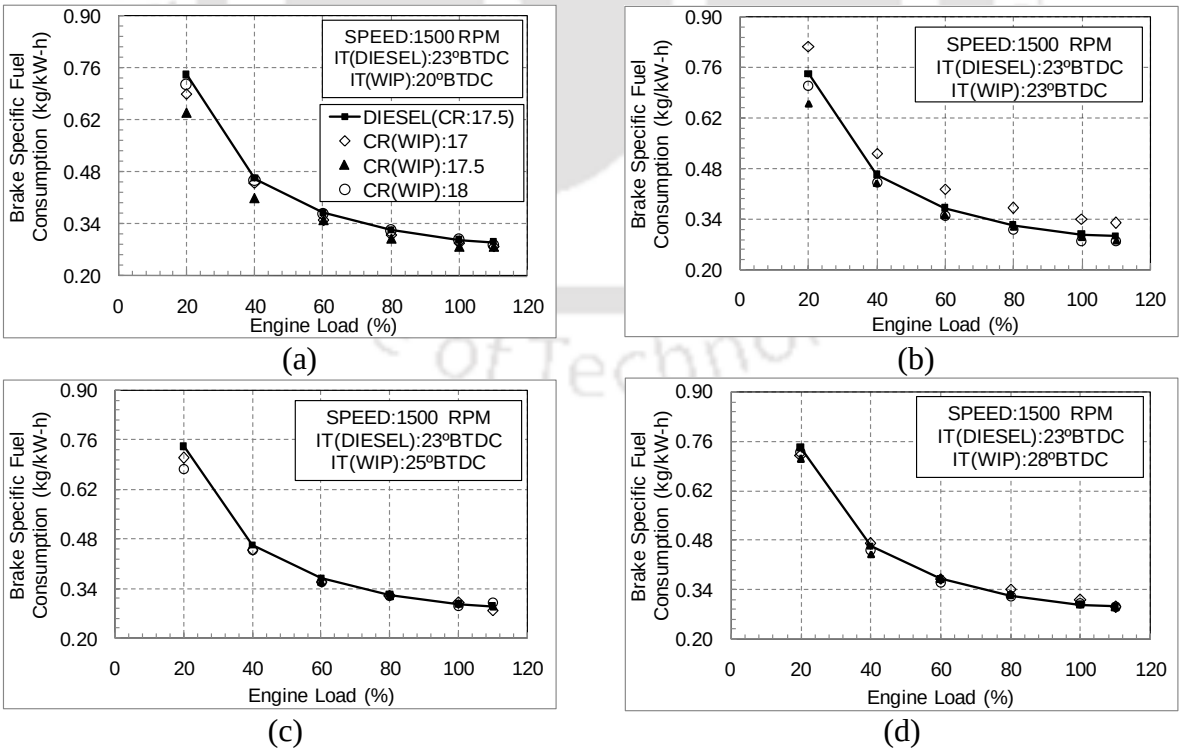

Figure 6.3 Variation of BSFC with engine load for different CR and IT for emulsified POME run engine

The increase in CR reduced the EGT of the 5% WIP, except for the case of 28ºBTDC (Figure 6.4). The average temperatures at CR of 18, 17.5 and 17 are 238ºC, 242ºC and 251ºC. Hence, reduction of CR increased EGT from 1.6% to 3.5%. This is because, as CR increases the rate of micro-explosion increases. This produces heat sink effect by consuming heat and reduces the burning time during premixed combustion phase (Lin and Lin, 2007b).

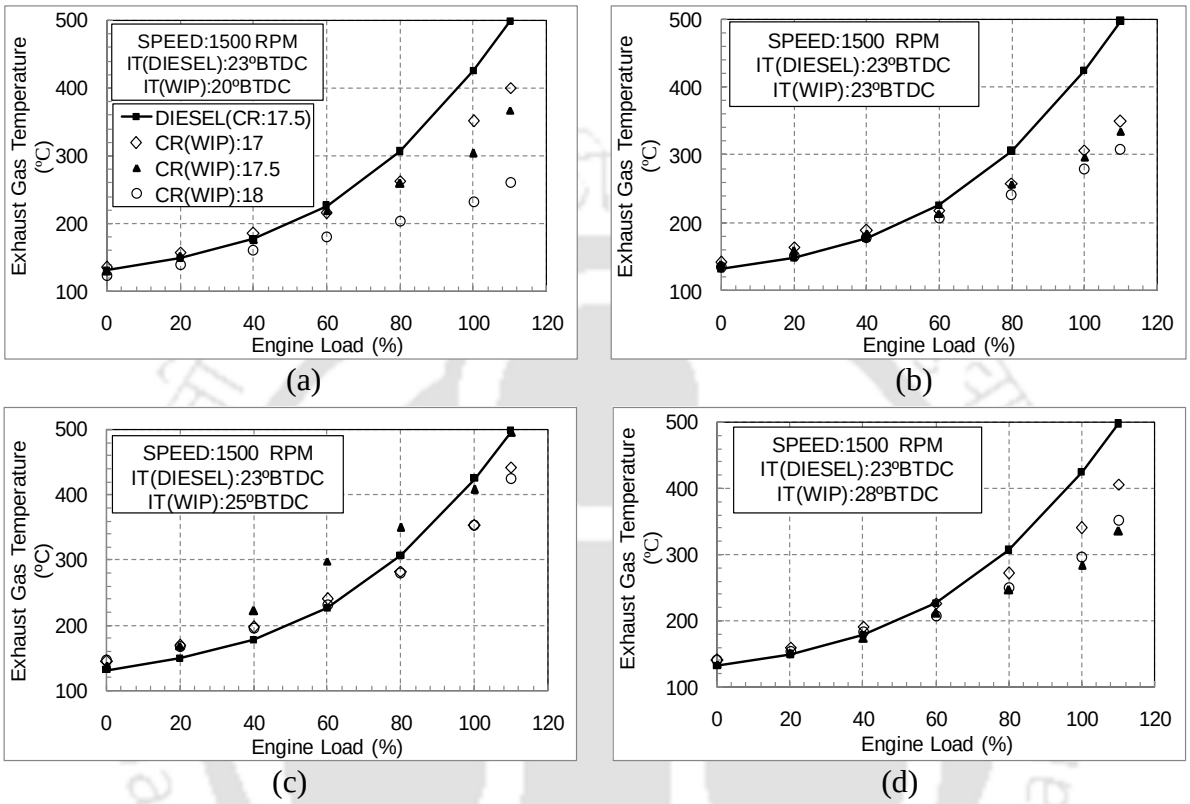

Figure 6.4 Variation of EGT with engine load for different CR and IT for emulsified POME run engine

6.2.3 Effect of Injection Timing

The variation of IT has no consequence on the BP of the engine. This is because, the change of IT may modify the combustion phenomena, but then again it has to produce the equivalent power to adjust for the specific load. Side by side at each load, speed is also constant. Hence, BP also remains unchanged with IT variation. The variations of BTHEs with respect to IT modifications are seen in Fig. 6.2, where 20ºBTDC shows the superior performance among other ITs. The overall increase in BTHEs by IT retardation is around 6.1%, whereas, IT advancement of 5º reduces overall BTHE by 2.1%. Figure 6.6 shows that at 20ºBTDC, 18 CR provides 11% higher BTHE than neat diesel. Higher CR with retarded IT creates a very hot and pressurized environment inside the cylinder, which accelerates the mico-explosion, resulting faster burning and higher rate of flame propagation (Park *et al.*, 2000). As a result, the fuel consumption is also reduced. Figure 6.3 reveals that the retardation of IT cuts the

average WIP intake by 6.2%. This reduction in fuel supply demonstrates the fact of increase of BTHE for IT reduction. Except 28ºBTDC, the injection advancements (20, 23 and 25ºBTDC) show a uniform trend of increase in EGT. This is because, advancing the injection results the spray of fuel at relatively cooler temperature, as the piston stays comparatively faraway than TDC, which is an adverse condition of mico-explosion and water vaporization. Hence, more retarded injection of fuel, better is the combustion and lower is the EGT.

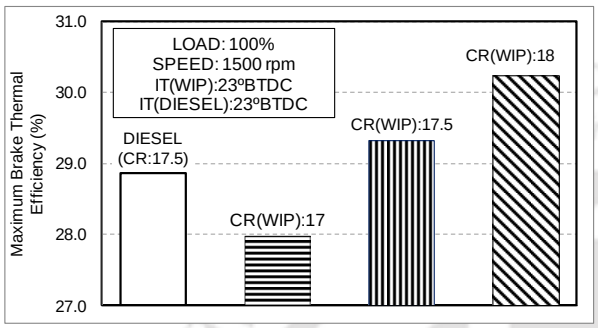

Figure 6.5 Comparison of maximum BTHE with CR (IT=23ºBTDC) for emulsified POME run engine

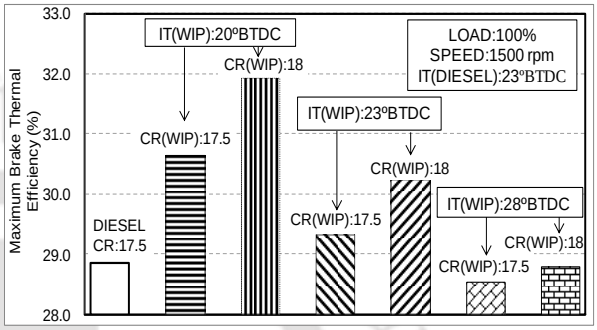

Figure 6.6 Comparison of maximum BTHE with CR and IT for emulsified POME run engine

6.3 Combustion Analysis

The combustion analyses are carried out in the form of variation of cylinder pressure, ignition delay (ID), peak cylinder pressure (PCP) and net heat release rate (NHRR). Similar to the performance study, the parameters for variation of CRs at particular ITs are clubbed together. The effects of load, CR and IT on combustion are investigated in following sections.

6.3.1 Effect of Load

The combustion of WIP in diesel engine has shown a maximum efficiency at 100% load within the loading range, irrespective of CR or IT. Figure 6.7 describes the cylinder pressure variation with respect of crank angle at full load condition. The mean value of maximum pressure rise rate (MPRR) for WIP is 4.83 bar per crank angle whereas for neat diesel it is 7.5 bar per crank angle. Therefore, WIP run engine provided a much smoother operation than diesel run. It is also observed that the premixed combustion phase of WIP is found to be little lower than the diesel. The reason here is again the secondary combustion, which enables finer fuel droplets that mixes well with air at the early periods of the premixed combustion. Hence, more amount of the fuel is burnt out during the premixed combustion (Park *et al.*, 2001). Figure 6.8 shows the PCP results for CR and IT changes. The PCP increases almost linearly with the increase in load. Maximum values of PCPs occur at 100% and 110% load within and outside the loading ranges, respectively. This is obvious because of the fact that as the load

increases, engine has to consume more fuel to adjust the power to be produced. Hence, more is the burning of fuel, higher is the production of heat and finally more is the increase of pressure inside the cylinder (Heywood, 1988). For the ITs from 20º to 28ºBTDC, the peak values of PCPs obtained at CR=18 are 68.45 bar, 71.41 bar, 71.25 bar and 76.16 bar at 100% load and 69.13 bar, 72.22 bar, 74.59 bar and 76.46 bar at 110% load.

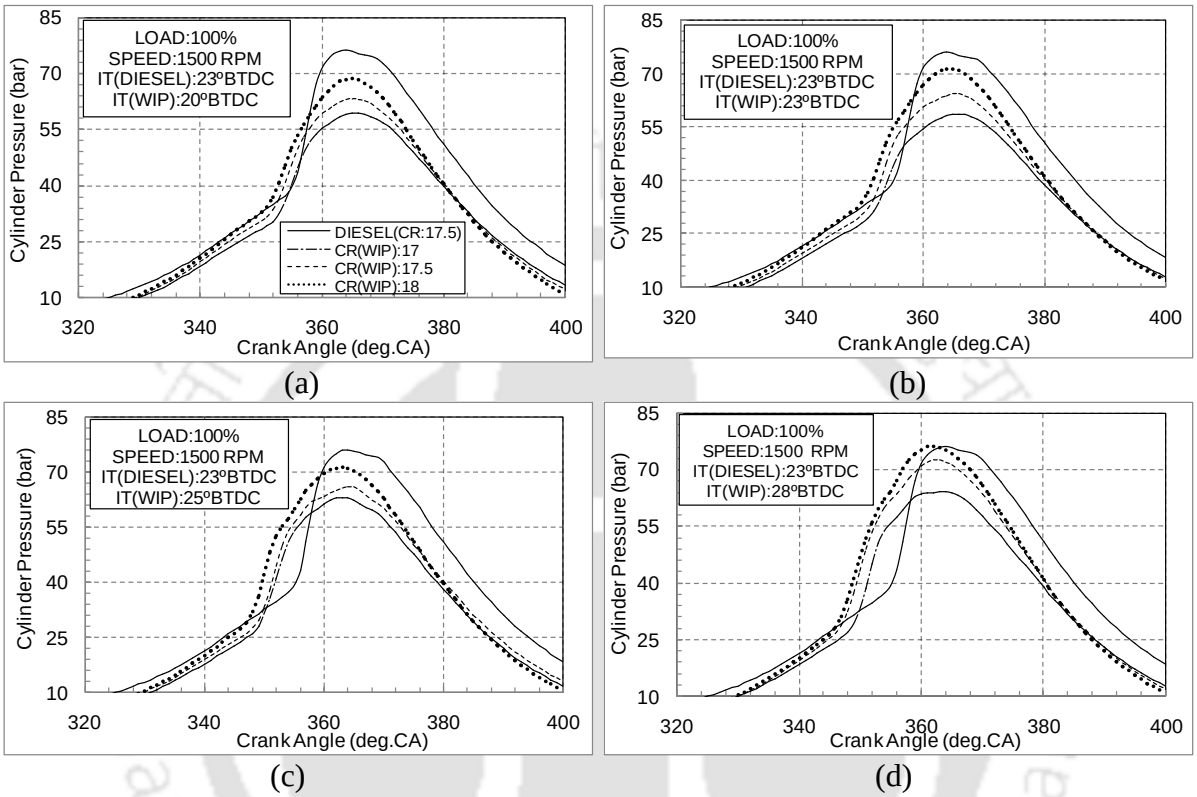

Figure 6.7 Variation of cylinder pressure with crank angle at 100% load for different CR and IT for emulsified POME run engine

The variations of IDs are illustrated in Fig. 6.9. The average values of IDs for WIP are 18, 17, 17, 16, 15, 14 and 14ºCA whereas for diesel the values are 21, 20, 19, 19, 18, 17 and 16ºCA as the load varies. The reduction in ID with the increase in load signifies the fact of the increase of cylinder temperature with load. Some researchers have indicated that emulsion prepared with diesel increases the ID (Basha and Anand, 2011a). In this study, however, the use of biodiesel (POME) in the emulsion enables a lower ID than diesel. This is probably due to the higher oxygen quantity in POME, which even in the emulsified form (WIP) provides a higher Cetane number than diesel (Table 3.4), which covers up the increase in the time required to initiate the combustion because of the time consumed during water droplet vaporization and micro-explosion. Figure 6.10 explains the variations of NHRRs at full load. It can be seen that WIP starts releasing heat much earlier than base diesel, which is justified by the ID curves, as said in the earlier paragraph. The higher BTHE and hence lower ID is a

key fuel property that decides the premixed combustion stage (Benjumia *et al.*, 2009). However, the peak NHRR point is lower than to that of diesel. This is due to a little lesser LHV of POME than diesel.

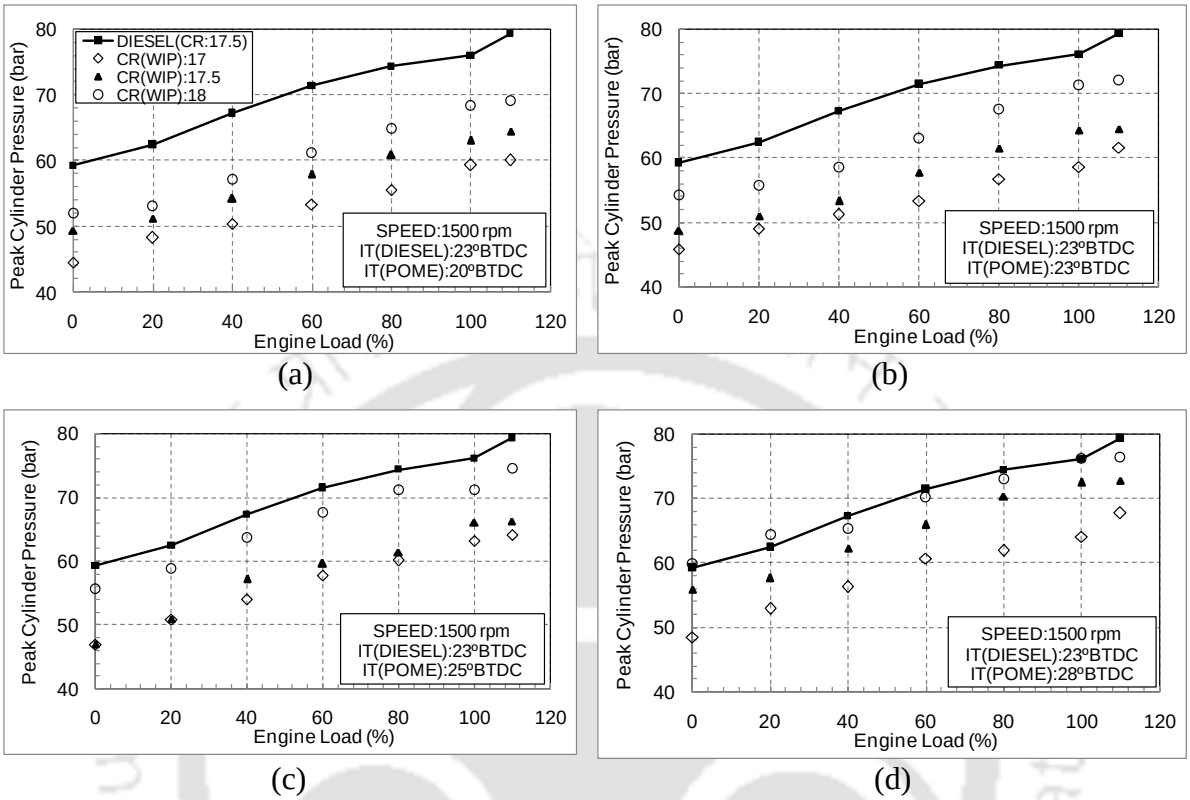

Figure 6.8 Variation of peak cylinder pressure with engine load for different CR and IT for emulsified POME run engine

6.3.2 Effect of Compression Ratio

The effect of CR variation on cylinder pressure curves at 100% load (Figure 6.7) show that for almost all CR and IT combination, the *p-θ* curves have dipping trends than diesel. The water in WIP and simultaneously production of water due to POME burning create heat sink effect by consuming a portion of heat (Lin and Lin, 2007b). As a result, a drop of the peak combustion temperature and hence, peak combustion pressure take place. Figure 6.8 expresses the average PCPs for CR=17, 17.5 and 18 are 55.61 bar, 59.60 bar and 64.92 bar respectively for WIP run, as compared to 70.06 bar for diesel. Hence, there have been 7.2% and 8.9% increase (by average) in PCPs taken place with the increase in CR from 17 to 17.5 and 17.5 to 18. The reason is the same heat sink effect as described earlier. The average IDs for CR=17, 17.5 and 18 are 16.43º, 15.79º and 15.50ºCA, respectively (Figure 6.9). Hence, the rise of CRs from 17 to 17.5 and 17.5 to 18 reduce ID by 4.1% and 1.8%, respectively. This is a very interesting finding. The reason behind is the lower evaporation temperature of water. Now, as the CR increased from 17 to 17.5, water bubbles enclosed inside POME start

evaporating, blasting the fuel droplets, and hence ignition starts a little early. Further increase of CR evaporates the water bubbles so early that, the water vapor now have additional time with higher specific heat to consume a definite quantity of heat, thereby elongating the ignition, a little.

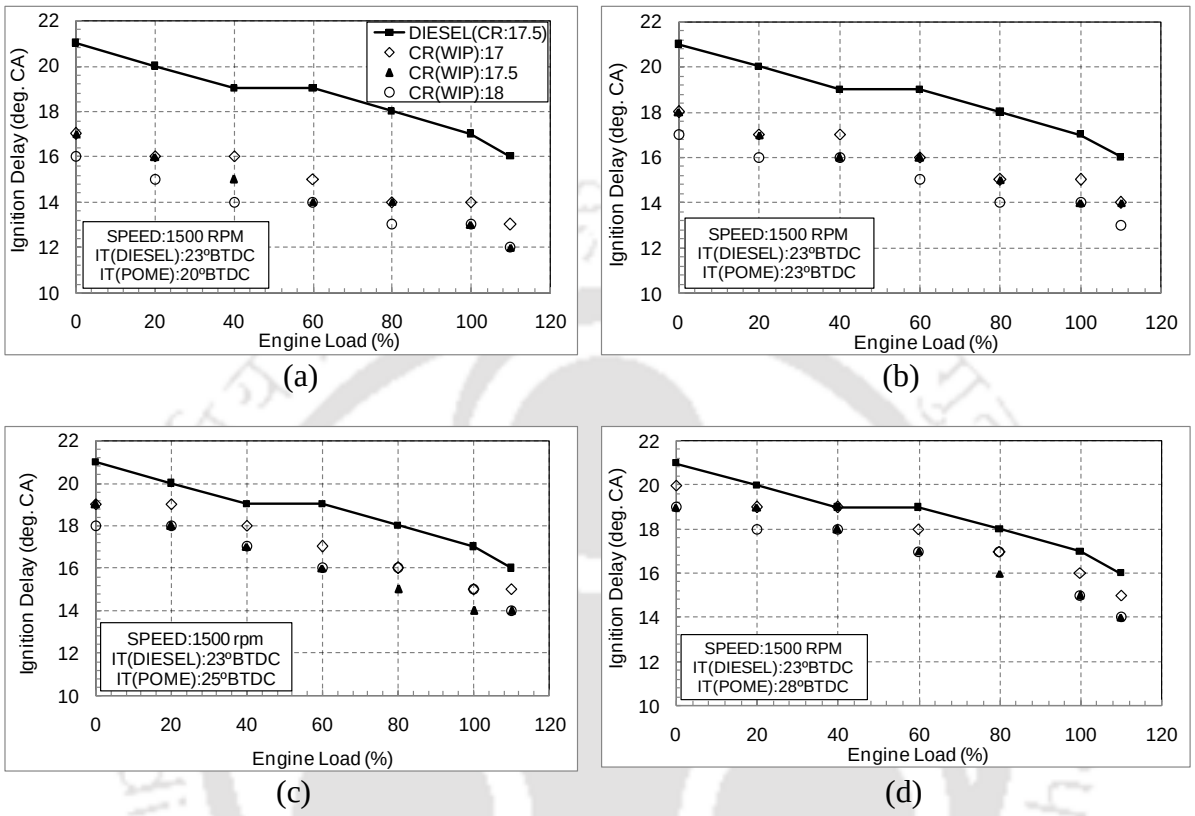

Figure 6.9 Variation of ID with engine load for different CR and IT for emulsified POME run engine

The NHRR curves (Figure 6.10) show that the heat release starts almost from same place for all the CR. However, as the CR increases, the heat release curves get much steeper than the lower CR. At higher CRs, the warmer atmosphere inside cylinder boosts flame propagation. Though the peak NHRR value is much less than diesel, the better combustion due to secondary atomization and subsequent drop in the fuel supply (sec. 6.2.1) cause the rise in the BTHE at higher CR (Figure 6.6).

6.3.3 Effect of Injection Timing

The IT variations on the cylinder pressure are shown in Fig. 6.7. It is obvious that the injection advancement will cause early burning of fuel. As a result, the fuel gets more time to burn completely and the p-θ curves spread more. The vaporization of encapsulated water in WIP has a tendency to delay the initiation of combustion. However, the micro-explosion and the presence of high oxygen content allow POME to burn rapidly. As a result, it recovers the

time lost during the water droplet evaporation process. The average PCP for WIP run diesel engine for variation of IT from 20ºBTDC to 28ºBTDC are 57.12 bar, 58.14 bar, 60.38 bar and 64.53 bar, respectively. The reduction of PCP (Figure 6.8) at retarded IT is due to the spray of WIP, when the piston reaches closer to TDC. At this condition, the environment will be quite favorable for faster micro-explosion. Further, the increase in bulk gas temperature for advanced IT increases PCP, which relates well with the results from literature (Roy, 2009). Figure 6.8 illustrates the drop of PCP as IT retards. The mean IDs at ITs from 20ºBTDCto 28ºBTDC are 14.4, 15.6, 16.5 and17.1ºCA. The effect is reasonable, as BSFC drops even for diesel at 20ºBTDC. This circumstance finally direct towards the upwelling in the BTHE as mentioned in the sec. 6.2.1.

The plots of NHRR (Figure 6.10) portray the fact that the start of heat release is more near to TDC for 20ºBTDC. Nevertheless, it is found that, WIP begins heat release a little earlier than diesel. The curves are also shifted towards the compression stroke as the IT advances. This results in the, increase of ID of the fuel a little and thus takes more time to burn completely. However, this fact does not seem to increase the BTHE as it is augmented during IT retardation. In other words, IT advancement does not encourage the BSFC to reduce to an amount as obtained during IT retardation.

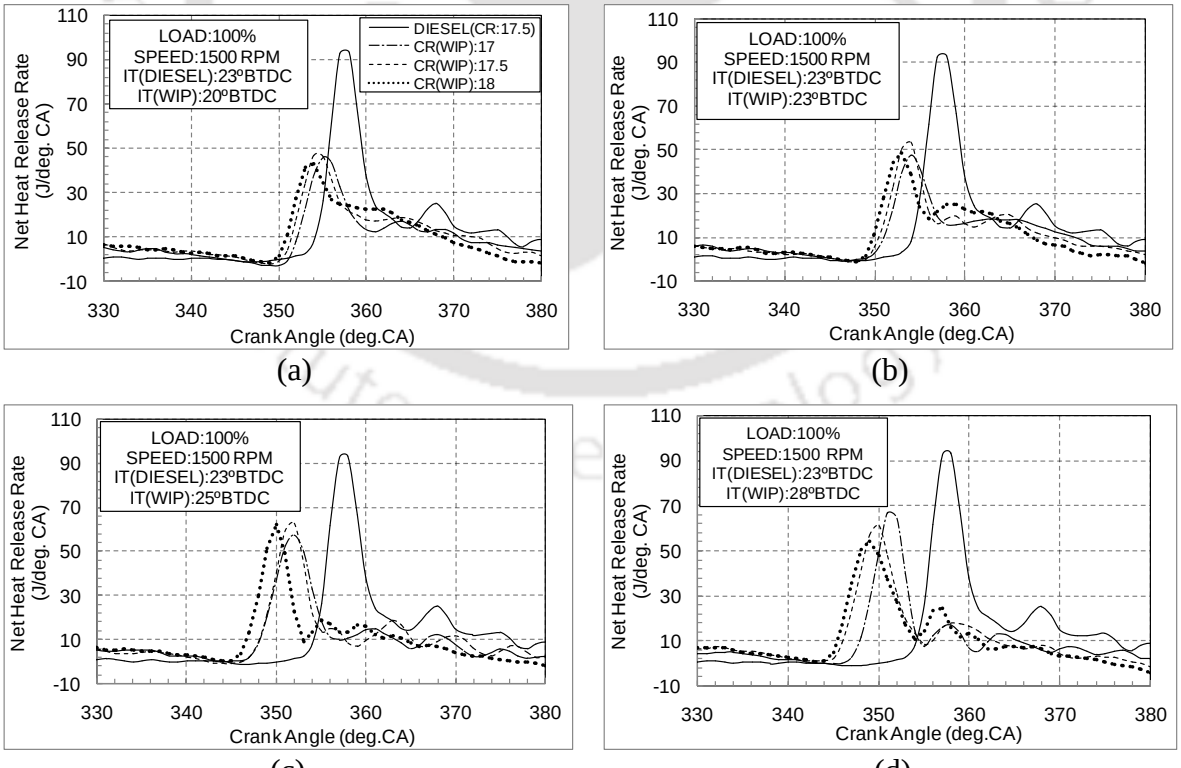

Figure 6.10 Variation of NHRR with crank angle at 100% load for different CR and IT for emulsified POME run engine

6.4 Emission Analysis

Testo 350S/M/XL flue gas analyzer is implemented to perform the emission measurements. The samples are investigated inside the flue gas analyzer and visualize the respective concentrations of carbon monoxide (CO), carbon dioxide (CO_2), oxides of nitrogen (NO_X), sum of nitric oxide (NO) and nitrogen dioxide (NO_2) and hydrocarbon (HC) emissions on the display of control unit.

6.4.1 Effect of Load

Figure 6.11 represent the variation of CO emission with respect to load, CR and IT. It is found that, in the present study, the engine operating conditions are extremely lean and air fuel ratio is about 3.6 times stoichiometric. Therefore, all the values of CO emissions are within 100 ppm and equally observed in an earlier work (Masjuki *et al.*, 1997). Further, at lower and higher loads insufficient temperature and richer fuel-air mixture cause incomplete combustion and increase CO emission. Whereas, at medium loads sufficient combustion temperature and almost stoichiometric air fuel ratio enable more complete combustion and truncate CO emission. The average reduction of CO emission with WIP as compared to neat diesel is 53.7% based on load variation. The results clearly explain the fact that WIP emulsification, with oxygenated POME causes better fuel air mixture due to micro-explosion, which properly burns fuel. Hence, CO emission, the product of incomplete combustion drops. The results of CO_2 emission with load (% by volume) for WIP are included in Fig. 6.12. For WIP, the average CO_2 variations with respect to load are found to be 1.4, 1.8, 2.2, 2.8, 3.1, 3.6 and 3.9 % by volume, whereas for diesel, these are 2.1, 2.1, 2.3, 3.5, 4.1, 4.3 and 4.6% by volume, respectively. The CO_2 reduction is the result of BSFC (Figure 6.3) results 4.6% drop of BSFC of WIP is found than diesel run.

Figure 6.13 describe the NO_X emissions obtained from no load to full load conditions for both WIP and diesel. For WIP, the average values are 11.0, 16.6, 24.7, 38.7, 49.7, 62.3 and 69.1 ppm. For diesel, these values are 22, 27.4, 38.8, 52.7, 94.6, 107.8 and 112.5 ppm. This swelling tendency of NO_X emission with respect to load is yet dependent on combustion temperature, which is validated by EGT curves (Figure 6.4). This is because; temperature increase accelerates the thermal NO formation (Heywood, 1988). However, the overall comparison shows a 43% reduction of NO_X emission with respect to diesel. The water available in the WIP reduces the overall temperature of burnt gas. The obvious result is the drop of thermal NO formation (Park *et al.*, 2001). It is justified from the EGT curve (Figure 6.4), where the temperature of burnt gas is found to be lower especially at the higher load and more NO_X prone region.

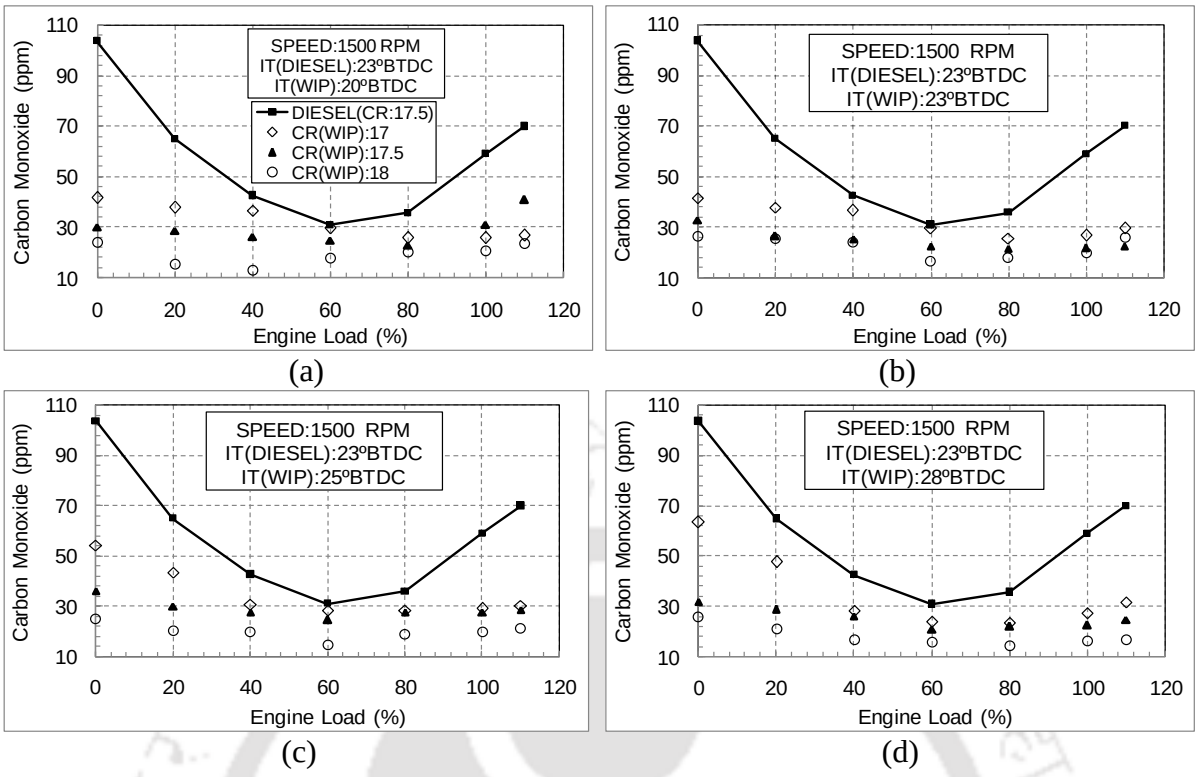

Figure 6.11 Variation CO with engine load for different CR and IT for emulsified POME run engine

Figure 6.14 show that the trends of HC emissions for WIP run diesel engine with neat diesel data. The average HC emissions at no load to 110% load regions for WIP are 28.7, 25.2, 21.5, 19.3, 22.7, 26.2 and 28.5 ppm; whereas, for diesel the corresponding values are 60, 35, 19, 15, 20, 40 and 70 ppm. There is a direct connection between HC emission and load variation. At lower load condition, the temperature becomes insufficient to burn all the fuel quantity supplied. With increase in loads, the amounts of air become insufficient to burn the increased fuel supply to cope up high load (Aziz *et al.*, 2006). Both these facts raise HC emissions at low and high load regions. However, based on load variation, a drop of 33.6% of HC emission is attained for WIP as opposed to baseline diesel. This is due to the shortage of hydrogen ion to form stable HC, as oxygen present in POME carries away hydrogen in the form of OH radicals Owen and Coley (1995).

6.4.2 Effect of Compression Ratio

The increase in CR has a definite relationship with CO emissions as found from the experimental observations (Figure 6.11). For almost all the cases of ITs rise in CR reduce CO emission. The average CO emissions at 18 to 17 CRs are 20.0, 27.1 and 33.7 ppm respectively. Hence increase in CR from 17 to 17.5 and then 17.5 to 18 reduce CO emission by 24% and 36%. This is due to the fact that rise in CR reduces cylinder volume, resulting

growth in the combustion temperature. This is further attributed to the presence of oxygen in POME (Masjuki *et al.*, 1997). This fact is also liable for the growth of the CO_2 emission with the increase in CRs as observed in the plots (Figure 6.12). The average CO_2 emissions recorded are 2.80, 2.64, 2.59% (by volume) for the CRs of 18, 17.5 and17. Hence, the increase in CR from 17 to 17.5 and then 17.5 to 18 raise the CO_2 emission by 6% and 2%, respectively. The surge of CO_2 emission and drop of CO emission at higher CR have also been observed by Owen and Coley (1995). It is emphasized that the water vapor, came out from emulsion, forms OH radicals during combustion process. These radical concentrations promote carbon oxidation to CO and CO_2 at higher temperature. As the CR increases, the cylinder becomes warmer, form more OH radicals, and convert CO to CO_2.

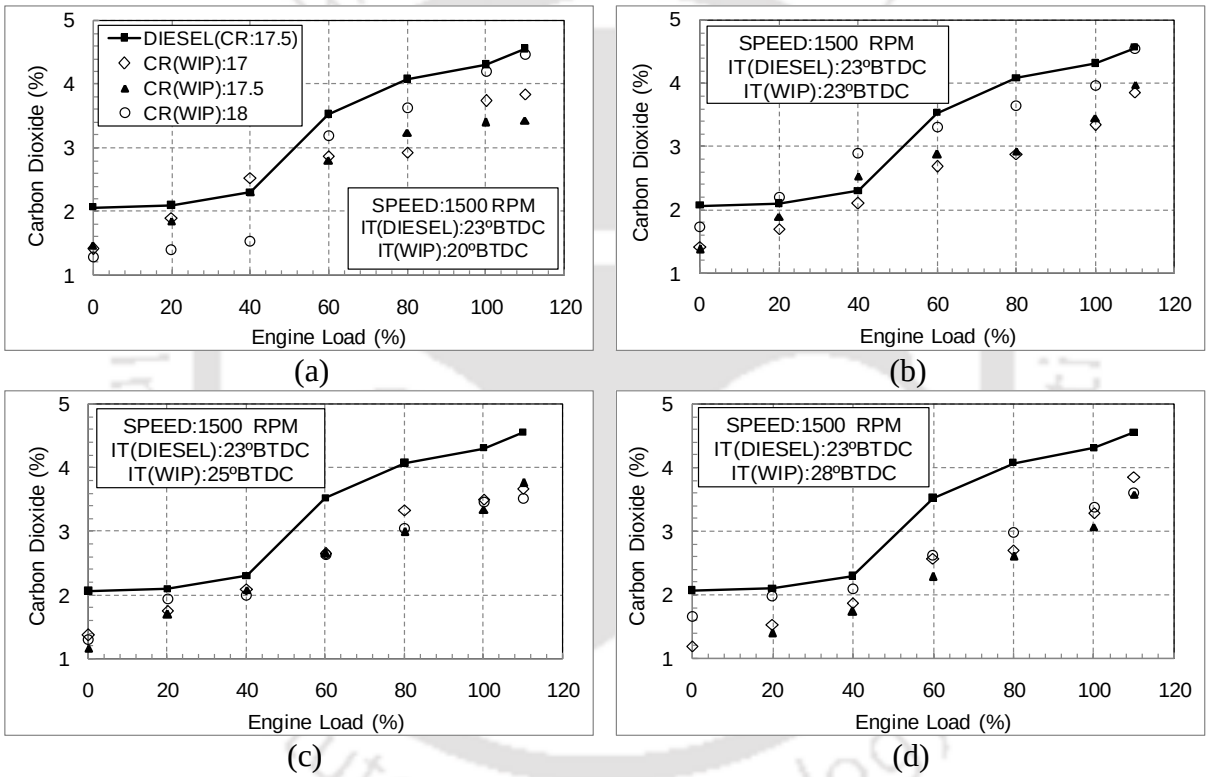

Figure 6.12 Variation of CO_2 emission with engine load for different CR and IT for emulsified POME run engine

The trends of NO_X emissions (Figure. 6.13) show that increase in CR cuts NO_X emission. The average NO_X emission obtained for the CR of 17, 17.5 and 18 are 43.3, 37.8 and 35.5 ppm. The increase in CR from 17 to 17.5 and from 17.5 to 18 causes an overall reduction of 15% and 6% for NO_X emission for WIP. At high CR (say, 18), the pressure and temperature increases during the compression stroke and at the primary stages of combustion. This improves fuel vaporization and reduces physical ignition delay. Therefore, combustion is faster near TDC, and diffusion combustion stage is shortened. Further, at higher CR, BSFC is also found to be lower. As a result, the mass of combustible products reduces for the

production of same power. This means, at higher CR, the lower quantity of combustion products reaches at cooler temperature at the end of combustion, which reverses in case of lower CR (say, 17). That is why, the NO_X emission is lower at higher CR and vice versa. Figure 6.14 shows the trend of HC emissions. The average HC emissions obtained for CR=17, 17.5 and 18 are 30.9, 23.6 and 19.2 ppm for WIP. Therefore, HC emission reduces by 31% and 23% as CR increase from 17 to 17.5 and 17.5 to 18. The micro-explosion phenomenon in the emulsified fuel is attributable to the volatility differences between water and diesel fuel. This violent collapse break up the fine droplets and augments the fuel–air mixing in the combustion chamber. That is why the HC formation decreases, as described in the literature (Kadota and Yamasaki, 2002).

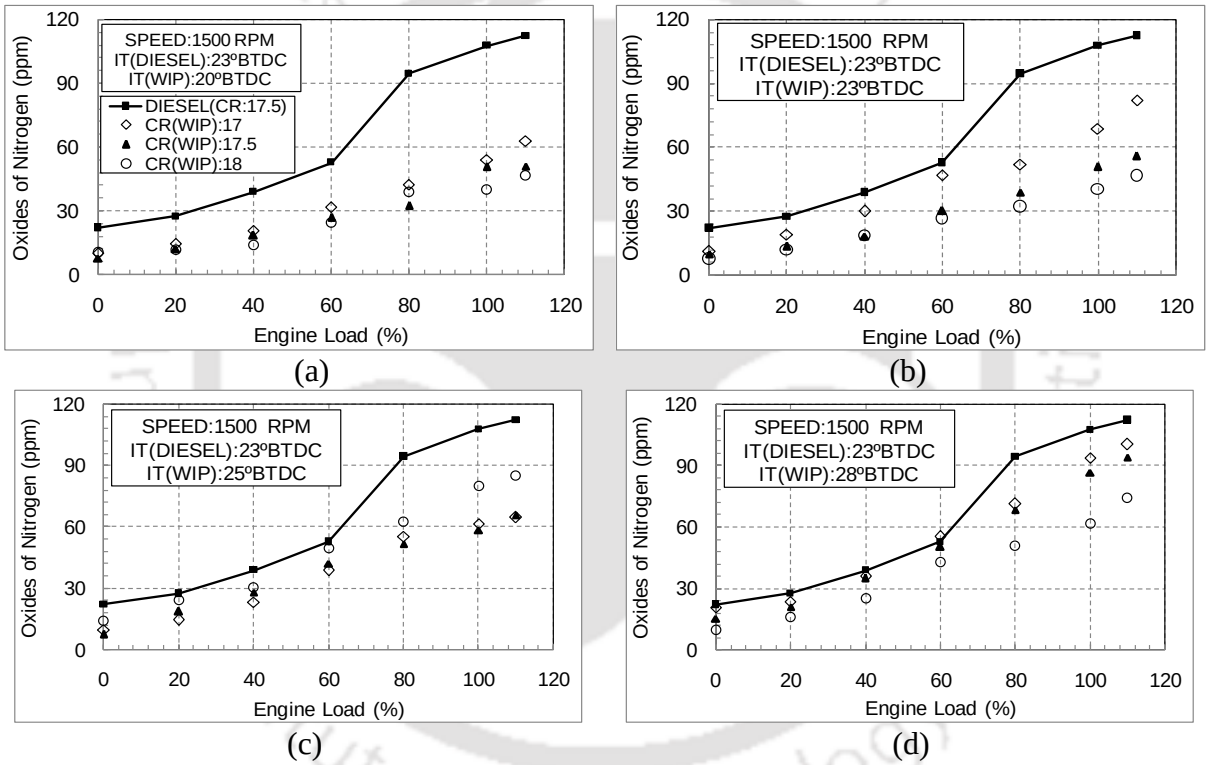

Figure 6.13 Variation of NO_X emission with engine load for different CR and IT for emulsified POME run engine

6.4.3 Effect of Injection Timing

The variations of CO emission with IT changes are shown in Fig. 6.11. For WIP, the IT retardation of 3º and IT advancements of 2º and 5º reduce CO emission by 1.0 % and increase of 4.9% and 1.5%, respectively. This is because at retarded IT of 20ºBTDC (fuel injection with piston reaches close to TDC) the cylinder environment becomes warmer and pressurized than other ITs, resulting faster combustion. The reverse phenomenon takes place at advanced IT. The trends of these results are identical to that of the works performed with canola methyl ester and its blend with diesel (Sequera *et al.*, 2011). It is seen from Fig. 6.12 that retarding

IT reduces CO_2 emission by 3.1%, whereas IT advancements decrease 9.7% and 9.9%. The drops of CO_2 emissions by both advancing and retarding IT is ascertained from the analogous effect on BSFC by performing similar IT changes. However, minor drop of CO_2 by advancing IT implies that a bit more CO_2 is formed at this IT, and lower CO is formed as discussed earlier.

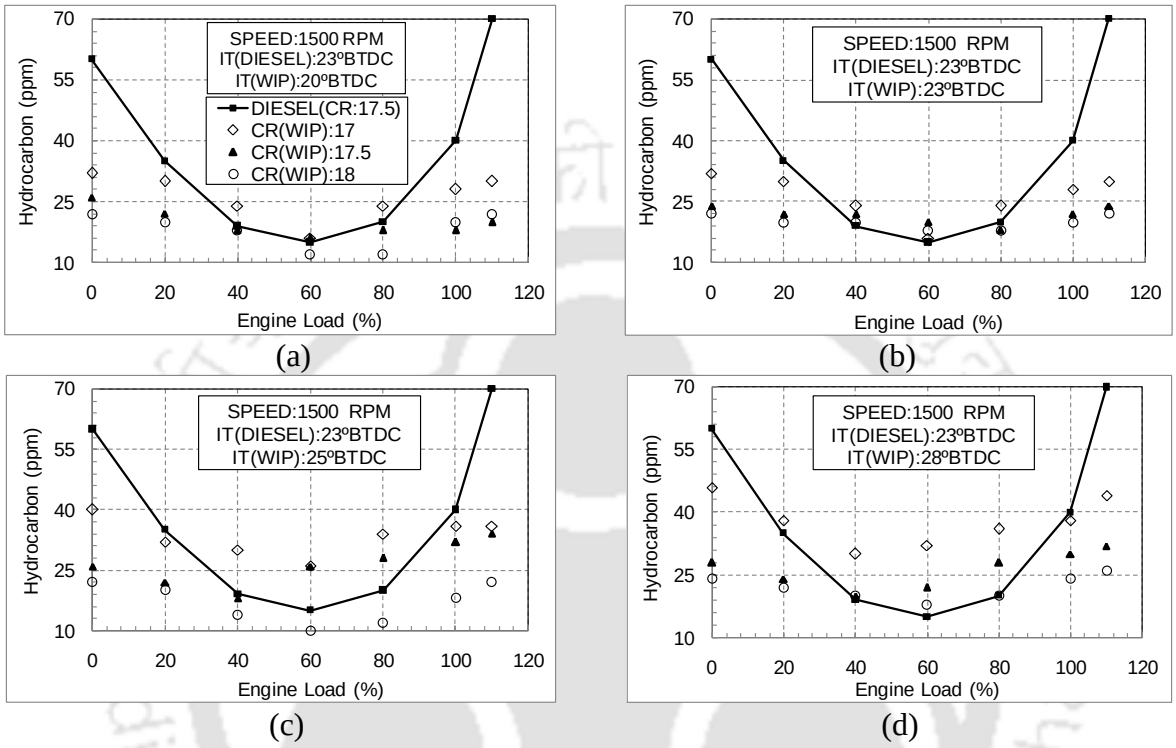

Figure 6.14 Variation of HC with engine load for different CR and IT for emulsified POME run engine

The NO_X variation of WIP run diesel engine reveals that IT retardation causes 14.6% reduction whereas, advancements cause 24.7% and 48.1% increase in NO_X emission (Figure 6.13). The discussions in the section 6.3.3 show that IT advancements increase PCPs, which ultimately increases peak temperature (Heywood, 1988). This is the reason for which NO_X concentrations increase by means of IT advancement. These trends are within close agreement with literature (Sequera *et al.*, 2011). The retardation of IT reduces HC by 6.3% and advancements increase 13.0% and 26.5%, respectively (Figure 6.14). Advancing the IT causes earlier initiation of combustion relative to the TDC. Because of this reason, the cylinder charge, being compressed as the piston moves to the TDC, had fairly higher temperatures. Data analyses demonstrate that the mean temperatures augment by 5% for all the IT modifications. This assists to cut the thickness of the flame-quenching layer. This is responsible for lesser HC emission (AbdAlla *et al.*, 2002).

6.5 Uncertainty Analysis

In experiments, uncertainty analysis has to be performed due to error caused by instrument's inaccuracy, in-apt calibration, human inadequacy etc. The sequential perturbation technique (Kline and McClintock, 1953; Moffat, 1982) is used to compute the uncertainties of the parameters (Appendix - B). Some of these are air flow rate (1.1%), liquid fuel flow rate (0.1 %), engine load (0.1%), engine speed (1.3%), LHV of liquid fuel (1.0%) etc. Based on these the calculated accuracy of the performance and combustion study of the engine is found to be within ±4.4%. However, the accuracy of the emission study is found as ± 3.3%.

6.6 Summary

In this chapter, thorough and systematic investigations have been carried out in a variable compression ratio diesel engine to optimize the performance, combustion, and emission characteristics of emulsified biodiesel. The analysis is summarized as follows.

- The rise in load increases BTHE for both 5% WIP and neat diesel for the tested CRs. The BTHEs at 100% and 110% of full load for 5% WIP, is found maximum for all the CRs. The rise in BTHE based on load compared to diesel is 7%. At all the CRs, WIP performed more efficiently than diesel. The overall increase in BTHEs by IT retardation is around 6.1%, whereas, IT advancement of 5º reduces overall BTHE by 2.1%. At 20ºBTDC, the CR of 18 produces almost 11% higher BTHE than diesel. Having 11% lower LHV than neat diesel, the WIP produces around 4.6% lower BSFC (by average) than neat diesel. It justifies the presence of 'micro-explosion' in the combustion. The retardation of IT cuts the average WIP intake by 6.2%. At lower loads the cooler environment inside cylinder slows down the rate of water droplet evaporation. However, at higher loads cylinder is suitably hot and the rate of bubble blast rises causing more heat drift by both the sensible and latent heat of water. Hence, it reduces the EGT quite a bit. The reduction of CR increased EGT from 1.6% to 3.5%.

- The mean value of maximum pressure rise rate (MPRR) for 5% WIP is 4.83 bar per crank angle compared to 7.5 bar per crank angle for diesel. The micro-explosion lowers the premixed combustion phase of WIP than diesel. For almost all the CR and IT combination, the p-θ curve has a dipping trend than diesel. The PCP increased linearly with the increase in load. Maximum values of PCPs are observed at 100% and 110% load within and outside load ranges, respectively. As load increases, engine has to burn more fuel, produce more heat, and finally more increase of pressure inside cylinder. There has

been a 7.2% and 8.9% rise in PCP occurred with the increase in CR from 17 to 17.5 and 17.5 to 18. The PCP reduces at IT retardation because of emulsion spray when the piston reaches near to TDC. The ID cuts with the increase in load. In this study, ID of POME is found to be lower than diesel. Raise of CR from 17 to 17.5 and 17.5 to 18 reduced ID by 4.1% and 1.8%. The higher oxygen quantity in POME covers up somewhat the delay of time of combustion due to the time consumed during micro-explosion. WIP starts releasing heat much earlier than diesel, which is justified for ID curves. However, the scale of maximum NHRR point is lower than diesel. This is the consequence of a little lower LHV of POME than diesel. With the increase of CR the NHRR curve gets much steeper. The NHRR curves are shifted towards the compression stroke as the IT advances.

- The values of CO emission are within 100 ppm. Since, the operating conditions are very lean, with an air fuel ratio of around 3.6 times stoichiometric. Based on load variation, the average drop of CO with 5% WIP compared to neat diesel is 53.7 %. Rise of CR from 17 to 17.5 and then 17.5 to 18 cut CO by 24% and 36%.This is due to the fact that rise in CR reduces cylinder volume, resulting growth in the combustion temperature. Therefore, the formation of nascent oxygen is accelerated and reacts with CO. IT variation of POME shows an average drop of 1.0 % and rise of 4.9% and 1.5% in CO for retarding the IT by 3^{o} and advancing by 2^{o} and 5^{o}, respectively. The drop of CO_2 for WIP compared to diesel can be answered from the 4.6% reduction of BSFC of WIP with respect to diesel. The increase in CR from 17 to 17.5 and then 17.5 to 18 increases CO_2 emission by 6% and 2% respectively. The swelling trend of NO_X emission with respect to load is dependent on combustion temperature. This is because; as temperature increases, the formation of thermal NO is accelerated. However, the overall comparison shows a 43% drop of NO_X with respect to diesel. The making of water from POME combustion and the water available in the emulsion cuts the overall temperature of burnt gas Based on load variation, WIP reduces 33.6% HC as opposed to neat diesel. At lower load, the poor temperature curbs to burn all the fuel extent supplied. At higher load, the amount of air becomes insufficient to burn the increased fuel quantity to cope up high load. Hence, there is a raise in HC emission at low and high load regions. The fall in HC emission is achieved around 31% and 23% by increasing CR from 17 to 17.5 and 17.5 to 18. The IT retardation causes 6.3% drop of HC and advancement causes 13.0% and 26.5% increase.

CHAPTER 7

Analysis at Optimized Operating Condition

It is a known fact that biodiesel and its emulsion have lesser heating value than neat diesel. That is why, at the standard diesel settings (CR=17.5 and IT=23ºBTDC), the emulsified biodiesel produce inferior engine performance. However, if looked carefully, it can be noticed that, the fundamentals of diesel engine itself provides the desired solution. The CR and IT are the two very important parameters as far as proficient diesel engine combustion is concerned. The CR can be increased just by reducing the clearance volume of the cylinder. Again, at the retarded injection of fuel, the piston is actually reached closer to the TDC and thereby the swept volume of the cylinder is reduced. Applying both of these modifications reduces the total volume available inside the cylinder at the instant of fuel injection. In other words, the temperature and the pressure at the end of compression stroke is raised by mechanical means, which is a healthier situation for combustion. In the chapters described earlier (Chapters 5 and 6), these combined alterations of CR and IT (CR=18 and IT=20ºBTDC) are performed, along with other combinations, while running both emulsified and neat POME exclusively in the diesel engine. Therefore, the target of this chapter is to bring and compare the performance, combustion and emission results of emulsified and neat POME run engines for the specific combinations at higher CR and retarded IT under a single umbrella.

7.1 Preface

This section discusses and compares the results obtained at the optimized operating condition (CR=18 and IT=20ºBTDC) of the engine run on emulsified and neat POME with respect to the neat diesel data at standard settings (CR=17.5 and IT=23ºBTDC). The comparison has been segregated into performance, combustion and emission analysis as given below.

7.2 Performance Analysis

The variations of BP for water in POME (WIP), POME and neat diesel are shown in Fig. 7.1(a). The figure clearly depicts that there is no effect in BP due to the variation of fuel types. This is because the engine is running at constant speed, which provides specific BP at each load, which is independent of CR and IT. The governor fitted with it controls the fuel supply to the engine. Hence, BP is only a linear function of load.

The more important comparison of BTHE, BSFC and fuel consumption rates of WIP and POME compared to neat diesel are portrayed in Figs. 7.1(b) and (c). WIP is prepared by emulsifying water with POME. This water is evaporated much earlier than the combustion to start and hence does not contributes any heat during combustion (Langer and Daly, 2000). Table 3.4 shows that, the LHV of WIP and POME are 11% and 5% lower as compared to neat diesel, respectively. Still, WIP not only compensated this, yet it provided an overall 11% higher BTHE than neat diesel. In case of POME, the average BTHE was 3% lower than neat diesel. At 100% load, the maximum BTHEs for WIP, POME and neat diesel are 31.9%, 27.4%, and 28.9%; whereas at 110% load, these values are 33.4%, 30.2% and 29.4% respectively. The above-mentioned values clearly identify the improvement of performance of WIP over neat POME and neat diesel. The results show nothing but a clear presence of the occurrence of "micro-explosion." The instantaneous and intense vaporization of the water droplets within POME droplets break the large POME droplets into several smaller droplets. This is attributing to a further comprehensive vaporization and turbulent mixing of the fuel and air as described by Yang and his coworkers (Yang *et al.*, 2013). Side by side, retarded injection (20ºBTDC) of emulsified biofuel at higher CR (18) has actually enhanced the rate of micro-explosion. The increase of CR from 17.5 to 18 results a reduction in the clearance volume. On the other hand, retardation of IT from 23ºBTDC to 20ºBTDC actually pushes the piston towards the TDC and thereby reduces the swept volume of cylinder at the instant of fuel injection. Hence, in a nutshell, these adjustments of engine operating parameters (CR=18, IT=20ºBTDC) have enforced WIP to be injected nearer to TDC and in a total

cylinder volume, which is lower than that of neat diesel settings (CR=17.5, IT=23ºBTDC). As a result, the environment inside the cylinder at the start of fuel injection has mechanically got warmer. This prevalence assists micro-explosion to attain boost, increases the burning rate and enhances combustion. Further, the BSFC of WIP has not only reduced from POME by 11% but also found to be lower than neat diesel by 2% as observed from Fig. 7.1(c). The values of Fuel Consumption Rates (Figure 7.1c) show an increasing trend with the increase of load for all the three types of fuel. This is because, at each step of increased load, the engine needs more energy form fuel to produce more power in order to keep the engine running at that load (Lin and Wang, 2004a). The figure also shows that the consumption of WIP is nearly similar to that of neat diesel and almost 8.4% lower than POME. Although, the consumption of WIP is almost similar to neat diesel, it produces constant BP (discussed above) similar to diesel with a lower calorific value. As a consequence, mathematically its BTHE has to increase.

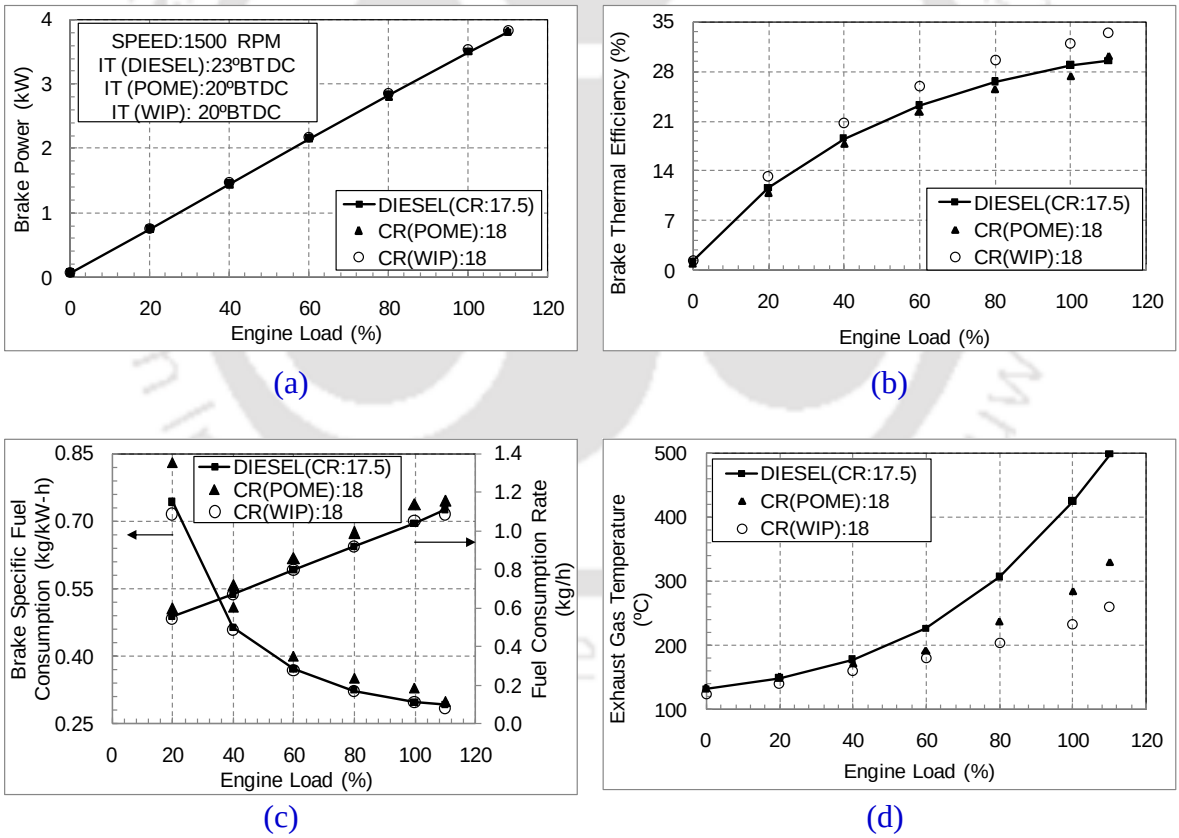

Figure 7.1 Variation of performance parameters with load for the WIP run engine

The plot of exhaust gas temperature (EGT) has shown in Fig. 7.1(d) that, both POME and WIP reduces the EGT to a substantial amount. The overall reduction of EGT for WIP is 47%, whereas for POME it is 19% as compared to neat diesel. The latent heat of vaporization

causes the water to be evaporated and thereby cooled the charge. This fact caused the overall temperature of the gas to drop. This is called as the heat sink effect created by the emulsified fuel (Yang *et al.*, 2013). Further, the reduction of lower BSFC of WIP than POME and neat diesel at higher CR and retarded IT also reduces the amount of fuel to be burnt for same power. Lower the chances of fuel to burn, lesser would be the rise of temperature of combustion products. This is also a point for the drop of exhaust gas temperature, reported in the literature as well (Parlak, 2005).

7.3 Combustion Analysis

The comparison of cylinder gas pressure for WIP, POME and neat diesel are shown in Fig. 7.2(a) at 100% load. The cylinder pressure trends are found to be smooth and are comparable to neat diesel. For POME, the peak point of the cylinder pressure curve is shifted a little towards the expansion stroke. However, for WIP, the peak pressure point occurs almost at the same crank angle as that of neat diesel showing a little drop as against the findings in the literature (Yang *et al.*, 2013). This is perhaps because, no sooner the micro-explosion starts, it escalates the rate of combustion which causes the peak pressure to occur a little early than POME. However, unlike POME, drop in the peak pressure of WIP seems to be due their double heat sink effect. Before the onset of combustion, emulsion releases water droplets in vapor form, which consumes substantial amount of heat. This phenomenon is again boosted by the water produced by the oxygen present in the chemical structure of POME ($C_{18.07}H_{34.93}O_2$). Both of these cause a substantial reduction of EGT and peak cylinder pressure for WIP as shown in Fig. 7.1(d) and 7.2(b). It is seen that with the rise in load, the peak cylinder pressure increases for all three types of fuel studied. While working with ethanol-biodiesel emulsion, similar trends are also reported (Zhu *et al.*, 2011). This is due to the increase of fuel consumption, and hence further rise of temperature with the increase of load to sustain the BP. As compared to neat diesel, the average drop in peak pressures for WIP and POME are 15.1% and 1.5%. Huang *et al.* (2012), while using emulsions of corn stalk bio-oil in neat diesel, reported a similar fall in peak cylinder pressure.

The net heat release rate (NHRR) derived from pressure crank angle and volume data histories of WIP and POME at 100% load are shown in Fig. 7.2(c). It can be seen that there is a difference in the peak value of heat release rate between WIP, POME and neat diesel. The micro-explosion and release of water due to POME combustion are responsible for this and results a heat sink effect. Side by side, in the course of diffusion combustion, this water

release phenomena of POME causes negative heat release. Hence, the heat absorption is relatively higher for WIP as compared to other tested fuels. This is also the cause for a fall of EGT for WIP as seen in Fig. 7.1(d).

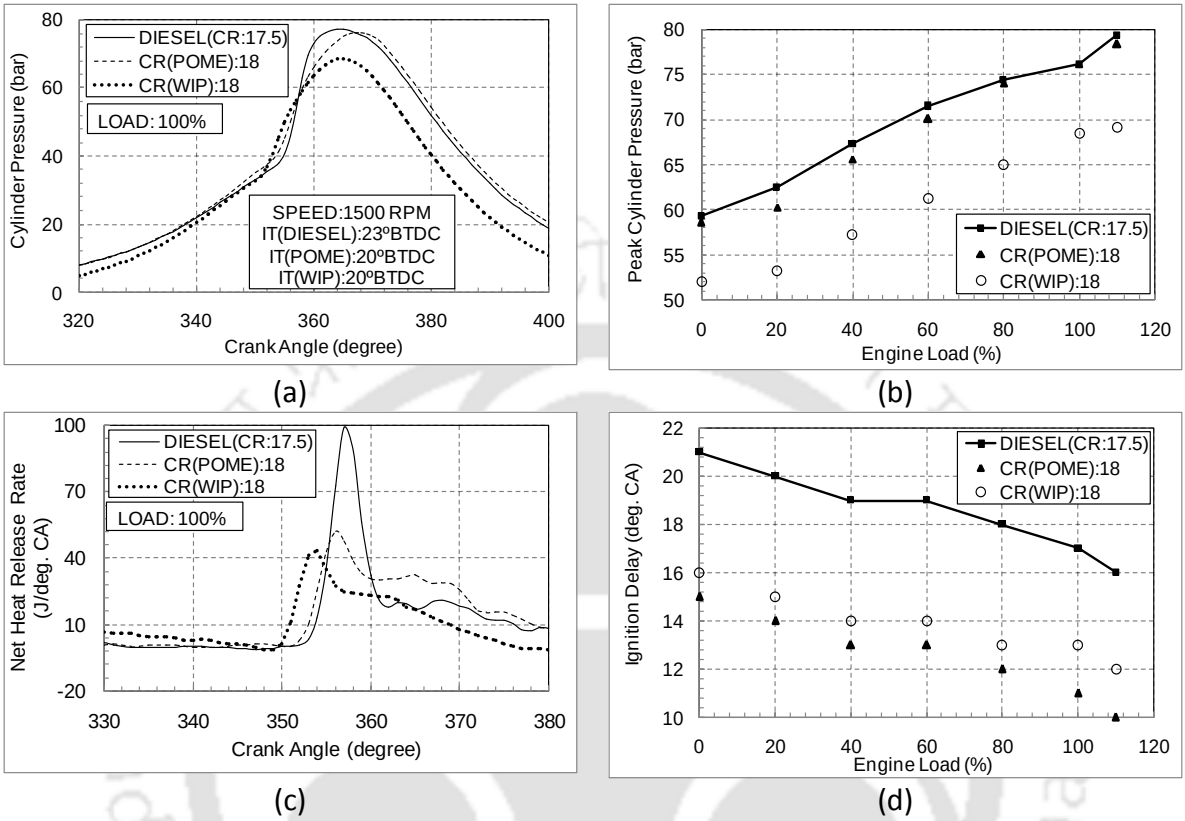

Figure 7.2 Variation of combustion parameters for the WIP run engine

The variation of ID for WIP, POME and neat diesel for load variation are shown in Fig. 7.2(d). The reduction in ID with the increase in load manifests the increase of cylinder temperature with load. Other researchers (Basha and Anand, 2011b; Kannan *et al.*, 2012) also record the similar trends of reductions of ID with load for biofuels. Researchers have indicated that emulsion produces higher ID when neat diesel is used as a carrying fuel (Basha and Anand, 2011a). However, the present study with a biodiesel POME and its emulsion with water show a lower ID than neat diesel. The increase in the pressure and temperature at the end of compression stroke at higher CR and retarded IT also help to reduce the ID (Wu *et al.*, 2011). It is observed that WIP ignition occurs at a 10% later time as compared to POME. As a result, WIP needed lesser compressive power than POME and a lesser quantity of fuel is required to produce the same power. This is lucrative for the concerned BTHE (Basha and Anand, 2011a). A little higher ID of WIP than POME is probably because of the time consumed by WIP during the micro-explosion. Moreover, both WIP and POME are injected at 20ºBTDC, whereas diesel is injected at standard injection timing of 23ºBTDC. Clearly,

WIP and POME are injected very near to TDC at a pressurized and warmer environment. Hence, it is expected that WIP and POME would produce an ID of around 34% and 48% lower than neat diesel.

7.4 Emission Analysis

The variations of CO emission for WIP, POME and neat diesel are shown in Fig. 7.3(a). In all the cases, CO emissions are within 100 ppm. This is attributed to the extremely lean operating conditions, for all the three fuels tested in the diesel engine. The average air fuel ratio has been around 3.6 times stoichiometric and is analogous to the work reported earlier (Masjuki *et al.*, 1997). As compared to neat diesel, the overall reductions of CO emissions for WIP and POME are 67% and 42%, respectively. The reason behind this outcome is the higher oxygen content of POME, present in WIP as well. This accelerates the combustion at the earlier stage, thereby allowing more time in the diffusion phase. As a result, the chances of forming CO_2 to CO increase. (Zhu *et al.*, 2011). However, it is observed that WIP causes a reduction of CO emission by 43% as compared to POME. Due to micro-explosion, the proper air-fuel mixing during the longer ID, together with the higher CR enhances the combustion and causes the trimming down of CO emission. The CO_2 emission (Figure 7.3b) has shown that at low to mid load range, POME emits 23% lower than neat diesel; whereas at 100% and 110% load, CO_2 emission is 28% higher than neat diesel. Overall, POME emits 2% higher CO_2 emission than neat diesel. On the other hand, WIP emits 17% and 16% lower CO_2 than POME and neat diesel. The above discussion shows that WIP reduces CO emission and still cuts CO_2 emission. This reveals that the total carbon quantity supplied must be less than POME. This is transparent from the BSFC data as obtained from Fig. 7.1(c). The consumption of WIP is found to be 11% lower than POME by average.

It has been reported that the oxygenated biofuel substantially trim down carbonated emissions with a small forfeit on NO_X emission, particularly at high loads (Guo *et al.*, 2011). In other words, the drops of carbonated emissions are complemented by slight rise in NO_X emissions for biodiesel with higher oxygen content. Figure 7.3(c) indicates that WIP and POME reduce NO_X emission by 63% and 53%, respectively as compared to that of neat diesel. With the use of WIP, the average reduction of NO_X is found to be 20% as compared to POME. The water brought in by the emulsified fuel changes the relative quantities of fuel oxygen. The presence of water in the emulsion lowers peak combustion temperature of the burnt gas because of its higher latent heat of vaporization. The obvious result is the reduction of thermal NO

formation (Park *et al.*, 2001). This is further justified from the EGT curve (Figure 7.1d), which shows a reduction in the temperature of the burnt gas for the WIP as compared to the POME and the neat diesel run engine. This is predominant particularly at the higher loads, where there is a trend of more NO_X formation.

As seen from Fig. 7.3(d), WIP and POME reduce HC by 51% and 62%, respectively, as compared to neat diesel. Although, hydrogen to carbon ratio in both diesel and POME are near to 2, however, the extra oxygen present in POME and WIP carries away a significant amount of hydrogen with it to form H_2O. Hence, the remaining carbon ions has no option to react with oxygen of incoming air to form CO or CO_2. That is why, POME and WIP cause significant HC reduction. WIP is found to produce 22% higher HC emission than POME. This is due to the water supplied by WIP and water produced during combustion of POME. This water depresses the temperature of the combustion products of emulsified fuel as described in the literature (Yang *et al.*, 2013). On the other hand, at higher loads (80%, 100% and 110% of full load), the WIP run engine produces 6.7% lower HC emission as compared to POME. The high temperature environment at high loads increases the micro-explosion of WIP. This enhances its combustion and thereby reduces HC emission (Song *et al.*, 2000). In conjunction with the reduction of BSFC as compared to neat diesel run, the WIP run engine also responsible for the reduction HC emission, as deliberated by some researchers (Ozsezen and Canakci, 2010).

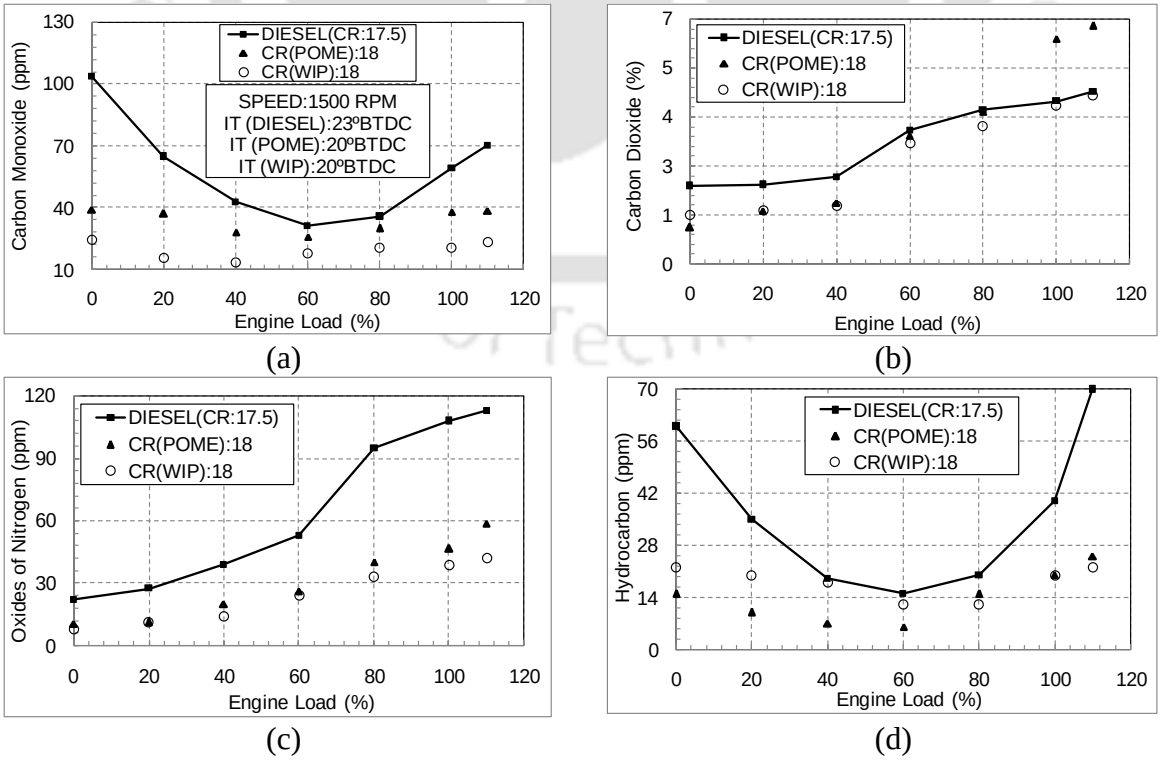

Figure 7.3 Variation of emission parameters with load for the WIP run engine

7.5 Summary

This chapter describes the results of emulsified and neat POME run engine (at CR=18 and IT=20ºBTDC) with neat diesel data. The application of emulsified POME in a diesel engine produces micro-explosion that increases the fuel burning rate. As a result, the probable consequences of emulsified POME with the viewpoint of neat POME and neat diesel run engine are summarized in following points.

* The engine used in this study is a constant speed one and provides specific BP at each load. Hence, BP is only a linear function of load. The lower calorific value of WIP and POME are 11% and 5% lower than diesel. Still WIP not only compensated this, but also provided an overall 11% higher BTHE than diesel.
* For POME, the average BTHE is 3% lower than diesel. The peak BTHEs at 100% and 110% loads for WIP, POME, and diesel are 33.4%, 31.9%, 27.4%, 30.2%, 28.9%, and 29.4%, respectively. The plot of EGT shows that, both WIP and POME cuts the EGT to 47% and 19%, than diesel.
* The average drop of peak pressures for WIP and POME than diesel 15.1% and 1.5%. There is a difference in peak value of heat release rate between WIP, POME, and diesel. This is due to the release of water through POME combustion and micro-explosion, which create heat sink effect.
* The WIP and POME both are injected at 20ºBTDC, whereas diesel is injected at 23ºBTDC. Hence, it is expected that POME and WIP will create ID, 34% and 48% lower than diesel. However, WIP has been ignited at almost 10% timing late than POME.
* The overall reductions of CO for WIP and POME than diesel are 42% and 67%. However, the use of WIP causes 43% drop of CO than POME at 18 CR and 20ºBTDC.
* The CO_2 has shown that at low to mid load range POME emits 23% lower than diesel; whereas at 100 and 110% load, CO_2 is 28% more than diesel. Overall, POME emits 2% higher CO_2 than diesel. WIP emits 17% and 16% lower CO_2 than POME and diesel.
* Further, WIP and POME cuts NO_X by 63% and 53% compared to diesel. The drop of NO_X by using WIP than POME is 20% by average. The water brought in by the emulsified fuel changes the relative quantities of fuel oxygen. WIP and POME reduces 51% and 62% HC than diesel. It is observed that, WIP produces 22% higher HC than POME.

CHAPTER 8

Thermodynamic Potential Study

The theoretical route towards the effective distribution of energy at various components of thermal energy system is done by coupling the first and the second laws of thermodynamics. The thermodynamic analysis (first and second law) as a technique, is getting attracted day by day to understand and control the thermodynamic energy distribution and maximum possible performance of the thermal energy system especially IC engines from a small scale range to robust entity. Meanwhile, this type of analysis locates and estimates the energy and exergy distribution, destruction and directs people to find strategies for better available energy management. However, the thermodynamic analysis of a diesel engine run on biodiesel emulsion is rare in open literature. In order to establish the emulsified biodiesel as an alternative to diesel, it is essential to reveal its effects on thermo mechanical energy–exergy distribution, while run in a diesel engine. It is observed that, an emulsified biodiesel has dissimilar properties than both biodiesel and diesel. Hence, the energy and availability distribution of an emulsified biodiesel run engine will not be identical to that of a diesel engine run at standard settings. To enlighten this ambiguous fact of literature, this chapter provides the first and second law analysis of a single cylinder, constant speed, and direct injection diesel engine running in variable CR-IT and full load condition with both, neat palm oil methyl ester (POME) water emulsified POME (WIP). The energy analysis is performed applying the first law of thermodynamics. It includes the effect on energy distribution (shaft, cooling water, and exhaust gas), destruction, BTHE, peak pressure, peak heat release rate and EGT for a set of CR and IT. The exergy analysis covers the results studied in view of second law. The effect of variation of CR and IT on the availability distribution (shaft, cooling water, and exhaust gas), destruction, second law efficiency and entropy generation are discussed, sequentially.

8.1 Preface

One of the earlier works on various engine parts as well as whole diesel plants through second law analysis was performed and reported by Flynn *et al.* (1984). Van Gerpen and Shapiro (1990) performed a detailed analysis for a closed cycle, bringing into focus the popular term, chemical availability along with the thermo-mechanical analysis. Further, Rakopoulos and Andritsakis (1993) studied the irreversibility's in direct and indirect injection diesel engines combustion. Rakopoulos and Kyritsis (2001) uncovered a method for calculating both combustion irreversibility and working medium availability for a diesel engine. They have implemented second law analysis and chemical equilibrium hypothesis to estimate combustion irreversibility as a function of fuel reaction rate.

According to Giakoumis (2007) the availability destruction in a low heat rejection (LHR) engine is small, which does not allow the mechanical work to increase. Canakci and Hosoz (2006) have performed energy and exergy analyses on a turbocharged diesel engine run with soybean methyl ester. It is seen that around 45% of total fuel exergy has been destructed, which include loss through exhaust gases and heat. Caliskan *et al.* (2010) conducted exergy analysis on a diesel engine fueled with biodiesel from high oleic soybeans. Caton (2012) showed experimentally and thermodynamically that, implementation of lean operation and high CR could improve indicated thermal efficiency from 37.0% to 53.9%. Kecebas (2012) implemented exergo-economic analysis for combustion of fuel in boilers and indicated that excess air, stack gas temperature, and combustion chamber parameters are more vital to define the ideal insulation thickness.

According to the literature, the energy and availability distribution along with their losses for a diesel engine, run on emulsified biodiesel for various CR and IT combinations are not clear. Therefore, the objective of the present work includes the combined first and second low analyses of a VCR diesel engine running with emulsified POME and neat POME. The analysis of data for neat (Chapter 5) and emulsified (Chapter 6) POME run engine shows that, IT advancement of 25ºBTDC provide both higher fuel consumption and higher carbonated emission than 28ºBTDC. Therefore, in the thermodynamic potential study this IT is neglected. Side by side, inside loading range the maximum efficiency is found at 100% load (12 kg). Hence, only the thermodynamic analysis at maximum load is performed and discussed in the following sections.

8.2 Thermodynamic Potential of Neat POME

The thermodynamic potential of the neat POME run diesel engine for the variation of CR and IT is discussed in this section. The equations for this study are included in Appendix-C.

8.2.1 Energy Analysis

The distributions of energy per unit time through different process calculated are included in Table 8.1. The standard deviation among the fuel energy input values lies within 0.00 to 0.06. Hence, the average value of standard deviation falls under a very negligible range (<0.03). The mean fuel energy input per unit time for entire CR and IT combinations is 13.15 kW. A portion of this input energy in the form of chemical energy of fuel has been converted into mechanical shaft work (3.43 kW). Some amount of energy is flown through engine cooling water (4.28 kW) and exhaust gas (2.47 kW). The rest amount of energy (2.97 kW) has been lost due to friction, radiation, heat transfer to surroundings. Therefore, approximately 26% of input energy is converted into mechanical work and 74% of input energy is lost in various ways from the system. Table 3.4 shows that the POME has a lower calorific value which is merely 5% lesser than diesel. The lower BTHE for the POME run engine is due to the increase in fuel energy input. Since the engine runs at a constant speed, it has to produce a constant power at a particular load. In order to achieve this, it has to consume a little more POME to cover up its lower energy content. Thus, it is seen that, at CR = 17.5 and IT = 23ºBTDC, the POME run engine produces around 9% lower BTHE than diesel. However, altering the engine design and operating parameters (CR and IT), the BTHE is found to improve for the POME run engine showing a decrease of 6% as opposed to a decrease of 9% as observed earlier. Hence, it is justified that POME with a little lower LHV can supply proportionately a substantial amount of energy to run the engine.

The effects of CR and IT on energy per unit time-sharing are included in Figs. 8.1 and 8.2. The values are obtained by using the Eqs. (C1) through (C6). To study the effect of CR on various energy distributions, the values of three ITs are averaged and included in Fig. 8.1. The engine is operated at constant speed and constant BP for all the CR and IT combinations. However, the rise in CR causes surge in the temperature during the compression stroke (Aziz *et al.*, 2005). The fact is also clear from Fig. 8.3. This is because the high temperature environment at higher CR causes the pressure to elevate to a higher value. That is why, about 21.17% of overall increase in peak pressure is observed as CR is increased from 16 to 18. Consequently, with an increase in CR due to higher heat release, there has been a 20.66% rise

in peak heat release rate too. Side-by-side, it is also observed that, advancing the IT increases peak pressure and peak heat release rate. Advancement of IT means that fuel is applied at cooler environment to that of retardation. Hence, fuel consumption becomes more for the same BP (Table 8.1). However, as the piston reaches close to TDC, the remaining high fuel quantity attains a favorable environment for combustion. This increases the rate of combustion, rises the peak pressure, and hence, the peak heat release rate. The input fuel energy is reduced with CR increase (Table 8.1). This causes an increase in shaft power (*Qs*) (% of fuel input) as seen in Fig. 8.1 as well. It is also attributed to the rise in the BTHE with the increase in CR for POME run diesel engine (Figure 8.4). The values of shaft energies are 25.5%, 26.1%, 26.4% and 26.5% of relevant fuel input for CRs studied.

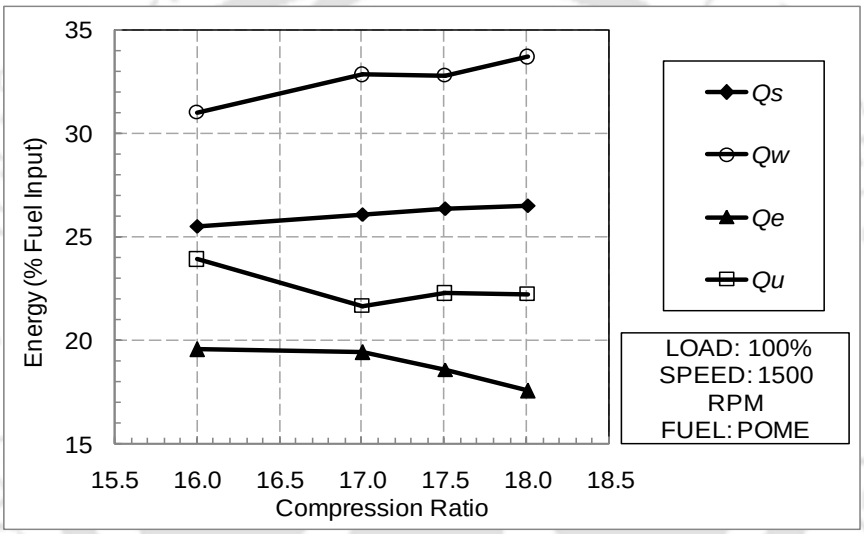

Figure 8.1 Effect of compression ratio on energy distribution for neat POME run engine

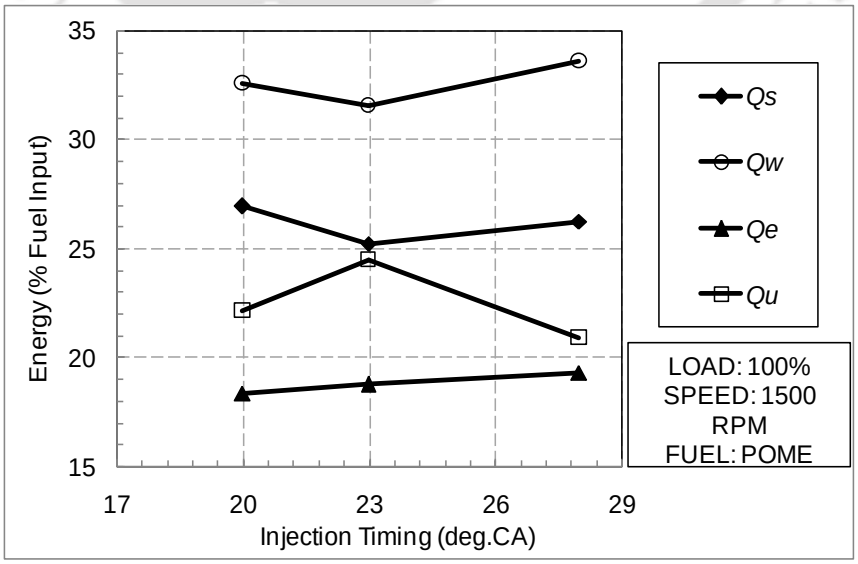

Figure 8.2 Effect of injection timing on energy distribution for neat POME run engine

Table 8.1 Results of energy analysis for neat POME run engine

Fuel	CR	IT	Q_{in} (kW)	Q_s (kW)	Q_w (kW)	Q_e (kW)	Q_u (kW)
Diesel	17.5	23	12.36 ±(0.06)	3.43 ±(0.00)	4.08 ±(0.04)	2.24 ±(0.09)	2.61 ±(0.13)
P O M E	16	20	13.06 ±(0.01)	3.41 ±(0.01)	3.98 ±(0.08)	2.46 ±(0.00)	3.21 ±(0.07)
	17	20	12.84 ±(0.02)	3.44 ±(0.00)	4.16 ±(0.03)	2.38 ±(0.04)	2.85 ±(0.04)
	17.5	20	12.50 ±(0.05)	3.43 ±(0.00)	4.20 ±(0.02)	2.38 ±(0.04)	2.49 ±(0.19)
	18	20	12.61 ±(0.04)	3.45 ±(0.01)	4.27 ±(0.00)	2.13 ±(0.16)	2.77 ±(0.07)
	16	23	13.83 ±(0.05)	3.44 ±(0.00)	4.29 ±(0.00)	2.89 ±(0.15)	3.21 ±(0.07)
	17	23	13.61 ±(0.03)	3.43 ±(0.00)	4.23 ±(0.01)	2.73 ±(0.10)	3.21 ±(0.08)
	17.5	23	13.50 ±(0.03)	3.40 ±(0.01)	4.14 ±(0.04)	2.29 ±(0.08)	3.67 ±(0.19)
	18	23	13.28 ±(0.01)	3.40 ±(0.01)	4.44 ±(0.04)	2.25 ±(0.10)	3.19 ±(0.07)
	16	28	13.50 ±(0.03)	3.45 ±(0.01)	4.26 ±(0.00)	2.55 ±(0.03)	3.24 ±(0.08)
	17	28	13.06 ±(0.01)	3.43 ±(0.00)	4.56 ±(0.06)	2.56 ±(0.04)	2.50 ±(0.19)
	17.5	28	13.06 ±(0.01)	3.45 ±(0.00)	4.46 ±(0.04)	2.58 ±(0.04)	2.57 ±(0.15)
	18	28	12.95 ±(0.02)	3.44 ±(0.00)	4.38 ±(0.02)	2.43 ±(0.02)	2.69 ±(0.10)

(± standard deviation)

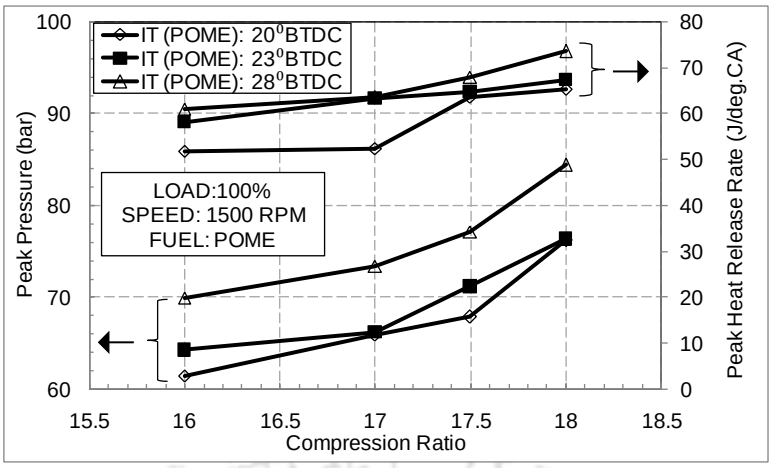

Figure 8.3 Effect of injection timing and compression ratio on peak pressure and peak heat release rate for neat POME run engine

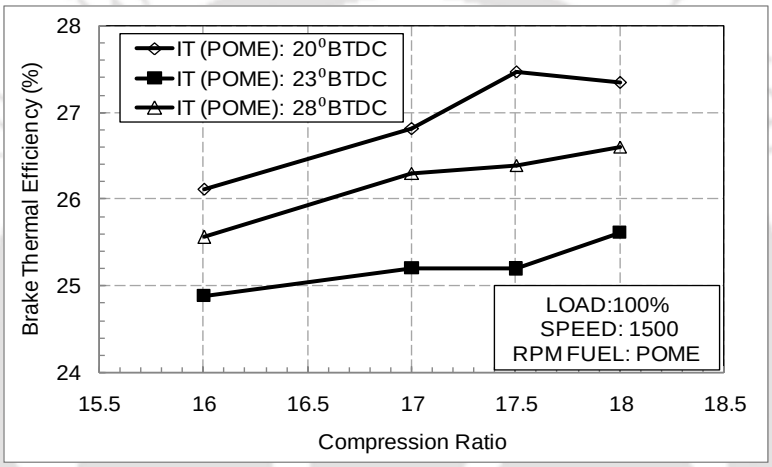

Figure 8.4 Effect of injection timing and compression ratio on brake thermal efficiency for neat POME run engine

The heat release increase with the increase s in CR during the combustion stroke at 20ºBTDC. This result an increase for heat carried away by the cooling water (Figure 8.1). Therefore, the heat loss through the exhaust gas is also reduced. The matter is further confirmed from the EGT analysis (Figure 8.5). With the increase in CR, the reduction in the heat loss through the exhaust gas also reduces the temperature of the exhaust gas. ITs, other than 20ºBTDC have similar effect at low and at high CR settings. However, in the intermediate range of CR (17 and 17.5), the combustion can be described as fully premixed and partially premixed combustion (Laguitton *et al.*, 2007). This is because, at 28ºBTDC, the POME is injected slightly earlier than other ITs and well before the piston reaches the TDC. This allows POME to have more time to mix with air, which in other words, can be called partially premixed charge. The burning of this charge releases a higher amount of heat upon combustion thereby increasing more cooling water heat loss unlike 23ºBTDC. However, the uncounted energies are unaffected at higher CRs.

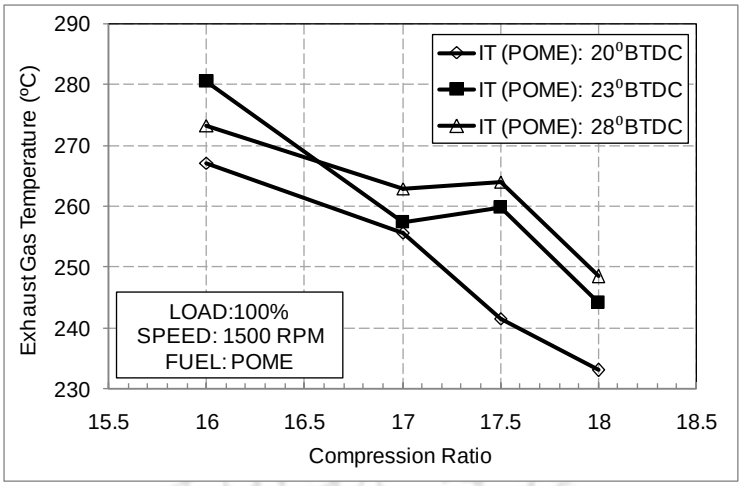

Figure 8.5 Effect of injection timing and compression ratio on exhaust gas temperature for neat POME run engine

Fuel injection advancement and retardation have a significant effect on the energy distribution (Figure 8.2). Advancing (28ºBTDC) and retarding (20ºBTDC), the IT has increased the shaft power (% of fuel input) and hence BTHE (Figure 8.4). This is because of the reduction of fuel supply during IT advancement or retardation than the standard IT. The mean values of fuel energy supplied per unit time during 20ºBTDC and 28ºBTDC are 12.75 kW and 13.14 kW which, in turn, are 6.3% and 3.2% lower than the rate of energy supplied during standard IT, respectively. There is a fluctuation of uncounted heat loss, considering CR and IT variation. However, if considered, the average values of rate of exhaust heat loss for all the CRs are 2.34 kW, 2.54 kW and 2.53 kW for 20ºBTDC to 28ºBTDC. This is because of the rise of EGT with IT advancement and increase in average cooling heat loss per unit time. These values are 4.15 kW, 4.27 kW and 4.41 kW for 20ºBTDC to 28ºBTDC. All these facts coupled with higher rate of fuel energy input at 23ºBTDC causes reduction in uncounted heat loss for IT retardation and advancement.

8.2.2 Exergy Analysis

The findings of exergy (the second law) analysis are included in Table 8.2. It represents the availability values and standard deviations of various terms including fuel availability, shaft availability, availability associated with engine cooling water and exhaust gas. The values of these parameters are calculated by using Eqs. (C7) through (C15). The standard deviation among the fuel exergy input values lies between 0.01 and 0.05. Hence, the average value of standard deviation falls below a very negligible range (<0.03). The mean fuel exergy for entire CR and IT combinations studied is 14.13 kW. This can also be termed as total input exergy; since input exergy through air for combustion is neglected. A portion of this input has

been converted into mechanical shaft work (3.43 kW). Some amount of exergy is flown through engine cooling water and exhaust gas. The rest amount of exergy has been lost due to friction, radiation, heat transfer to surroundings. However, with respect to cumulative availability, the exergy associated with the cooling water and exhaust gas come under consideration (Sahoo *et al.*, 2011). Therefore, approximately 30% of input exergy is found which can be called as available energy from the thermodynamic viewpoint. As a result, 70% of input exergy is destroyed from the system.

Figures 8.6 and 8.7 describe the variation of availability associated with shaft, cooling water, exhaust gas and availability destruction with respect to CR and IT separately. The trend of shaft availability for CR variation (Figure 8.6) is almost same to that of shaft power as described in Fig. 8.1. The shaft availabilities for the CRs of 16, 17, 17.5 and 18 are 23.8%, 24.3%, 24.5% and 24.7% of fuel input, respectively. The average input fuel availabilities are 14.47 kW, 14.15 kW, 13.99 kW and 13.91 kW for CRs of 16, 17, 17.5 and 18. This reduction of absolute value of fuel availability is responsible for the increase in shaft availability although it is considered as the shaft work or BP, which is maintained constant throughout. The cooling water availabilities for all the CRs studied are very low. Only a maximum of around 0.5% of fuel availability is found to be associated with the cooling water. This is probably as a consequence of the lesser increase of engine cooling water temperature in the course of POME test. The variation of exergy flow through the exhaust gas also has a little effect on CR variation. On the other hand, the availability destruction trend has shown a lowering trend. The increasing trend of shaft availability coupled with diminishing of fuel availability are probably be the reason of the reduction of availability destruction at the circumstances of almost unchanged cooling water and exhaust gas availabilities for CR variation.

The effect of IT on availability balance demonstrates (Figure 8.7) that the shaft availability increases with IT advance and retardation. The mean shaft availabilities at 20ºBTDC and 28ºBTDC are 7% and 4% higher than 23ºBTDC. POME having a higher Cetane number than diesel delivers lower ignition delay (Aziz *et al.*, 2005). As a result, the peak heat release rate point has a match with the top dead center point (TDC) for the IT retardation rather than advancement or the standard diesel IT. This is the reason of higher shaft availability at IT of 20ºBTDC. However, no significant variation is accomplished from cooling water availability because; the maximum cooling water availability is found as 0.5% of fuel input. The reason is discussed in the earlier paragraph. There is an insignificant increase in exhaust gas

availability encountered with the increase in IT. This is probably because of the increase in the EGT as observed from Fig. 8.5. The tendencies of availability destruction for IT retardation and advancement are found to be lower than the standard 23ºBTDC. The countable increase in shaft availability is attributable to the IT advancement and retardation comparable to other forms of exergy (cooling water and exhaust flow) is the reason of around 1.5% and 1% fall of exergy destruction.

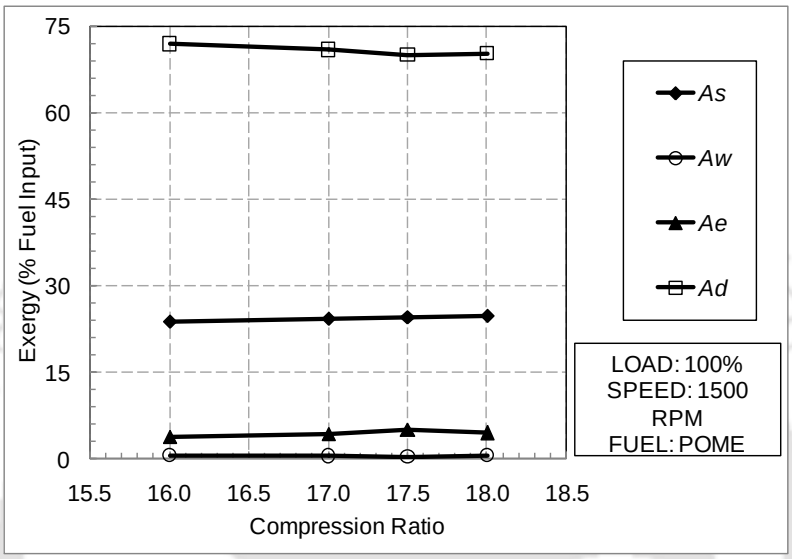

Figure 8.6 Effect of compression ratio on exergy distribution for neat POME run engine

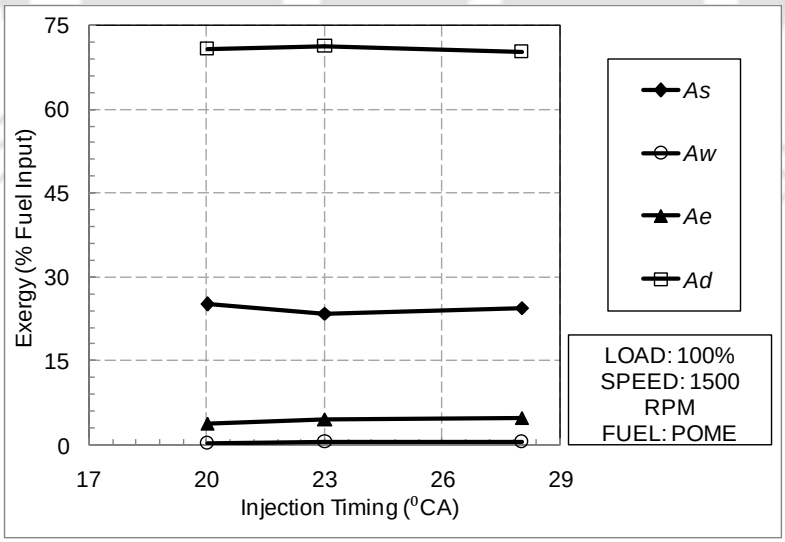

Figure 8.7 Effect of injection timing on exergy distribution for neat POME run engine

The variations of exergy efficiency with respect to CR and IT are included in Fig. 8.8. It is clear that POME provides a better second law (exergy) efficiency with advancement (28ºBTDC) and retardation (20ºBTDC) of IT rather than 23ºBTDC of IT at higher CR range.

Comparing the mean values, it is seen that POME run engine offers around 31% of maximum exergy efficiency for CR of 17%, 17.5% and 29% for CR of 16. While IT advancement and retardation allow 31% of exergy efficiency, the standard IT of 23ºBTDC gives 29% of the same. That means a lower compression ratio with standard diesel IT is not much efficient while running POME in diesel engine as far as the paramount deployment of the rate of available energy of fuel is concerned.

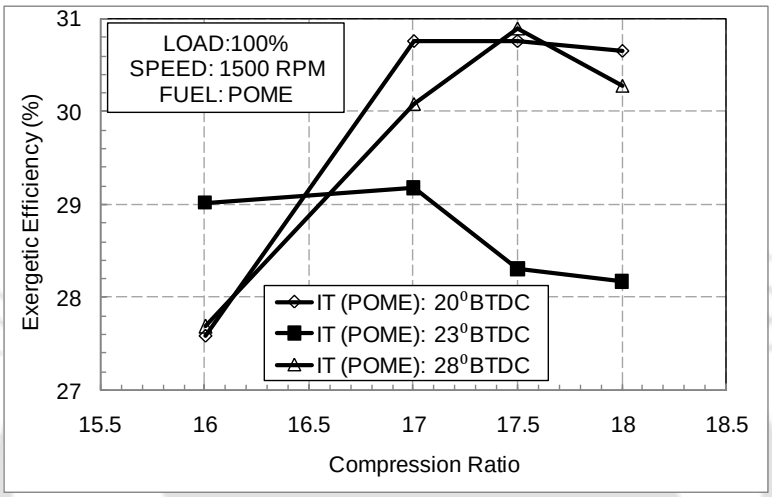

Figure 8.8 Effect of injection timing and compression ratio on exergy efficiency for neat POME run engine

The variation of entropy generation with respect to CR and IT are shown in Fig. 8.9. The trend of entropy generation is found almost reciprocal of exergy efficiency as expected. The trend suggests that a decrease in the CR increases the entropy generation. Side-by side, 23ºBTDC is bestowed with higher entropy generation than 20ºBTDC and 28ºBTDC of IT. The mean values of exergy destruction and entropy generation are 10.0 kW and 0.033 kW/K, respectively. Therefore, the exergy analysis shows that, for enhanced utilization of the available energy supplied by POME, every time the engine has to be run at higher CR with IT retardation.

8.3 Thermodynamic Potential of Emulsified POME

The experimentation of emulsified POME, described in Chapter 6, have excluded the CR=16. This is because, the study of neat POME in Chapter 5, shows that CR=16, generate the inferior performance while run in diesel engine. The circumstance is also proved from the thermodynamic point of view described in section 8.2. Hence, in the following sections, the thermodynamic analysis of emulsified POME is also illustrated, apart from the CR=16.

Table 8.2 Results of exergy analysis for neat POME run engine

Fuel	CR	IT	A_{in} (kW)	A_s (kW)	A_w (kW)	A_e (kW)	A_d (kW)	η_{II}
Diesel	17.5	23	13.64 ±(0.03)	3.43 ±(0.00)	0.03 ±(0.11)	0.73 ±(0.19)	9.45 ±(0.07)	30.74 ±(0.04)
P O M E	16	20	14.03 ±(0.01)	3.42 ±(0.00)	0.06 ±(0.11)	0.40 ±(0.43)	10.16 ±(0.01)	27.59 ±(0.07)
	17	20	13.79 ±(0.02)	3.44 ±(0.00)	0.02 ±(2.03)	0.38 ±(0.49)	9.95 ±(0.01)	30.77 ±(0.04)
	17.5	20	13.44 ±(0.05)	3.45 ±(0.00)	0.02 ±(1.67)	0.66 ±(0.15)	9.30 ±(0.08)	30.77 ±(0.04)
	18	20	13.55 ±(0.04)	3.46 ±(0.01)	0.08 ±(0.21)	0.62 ±(0.09)	9.40 ±(0.07)	30.66 ±(0.04)
	16	23	14.86 ±(0.05)	3.44 ±(0.00)	0.09 ±(0.33)	0.78 ±(0.28)	10.55 ±(0.05)	29.02 ±(0.01)
	17	23	14.62 ±(0.03)	3.43 ±(0.00)	0.10 ±(0.39)	0.74 ±(0.23)	10.36 ±(0.03)	29.18 ±(0.01)
	17.5	23	14.51 ±(0.03)	3.39 ±(0.01)	0.05 ±(0.17)	0.67 ±(0.15)	10.40 ±(0.03)	28.30 ±(0.04)
	18	23	14.27 ±(0.01)	3.41 ±(0.01)	0.08 ±(0.22)	0.53 ±(0.06)	10.25 ±(0.02)	28.17 ±(0.05)
	16	28	14.51 ±(0.03)	3.47 ±(0.01)	0.08 ±(0.20)	0.47 ±(0.20)	10.49 ±(0.04)	27.69 ±(0.06)
	17	28	14.03 ±(0.01)	3.44 ±(0.00)	0.06 ±(0.04)	0.72 ±(0.21)	9.81 ±(0.03)	30.08 ±(0.02)
	17.5	28	14.03 ±(0.01)	3.44 ±(0.00)	0.08 ±(0.24)	0.81 ±(0.31)	9.69 ±(0.04)	30.90 ±(0.05)
	18	28	13.91 ±(0.02)	3.45 ±(0.00)	0.07 ±(0.07)	0.70 ±(0.19)	9.70 ±(0.04)	30.28 ±(0.03)

(± standard deviation)

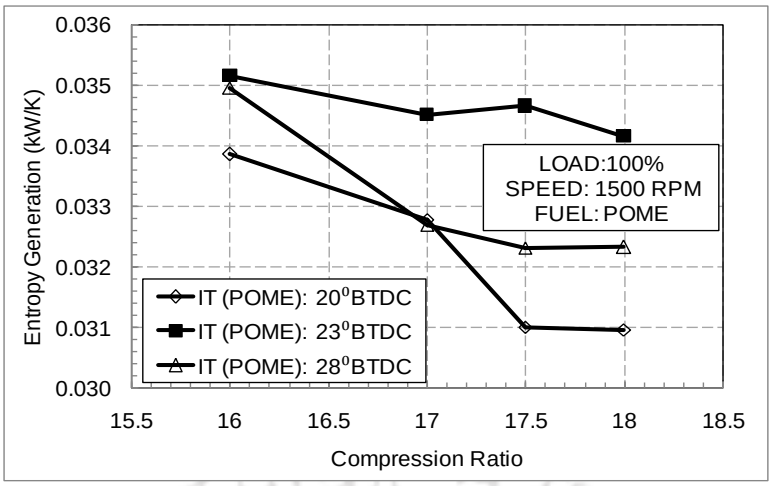

Figure 8.9 Effect of injection timing and compression ratio on entropy generation for neat POME run engine

8.3.1 Energy Analysis

The segments of energy flows per unit time at various locations of the engine systems are expressed in Table 8.3. The average value of standard deviation is found as ±0.04. The average energy input per unit time for all the combinations of CR and IT for WIP run diesel engine is 10.95 kW. The expenditure of energy per unit time are found to be 3.22 kW, 3.50 kW, and 2.55 kW for shaft work, energy flown out through engine cooling water and exhaust gas per unit time. Finally, the uncounted energy that has been lost per unit time in the form of friction, radiation, heat transfer to surrounding etc., is recorded as 1.68 kW. Therefore, the diesel engine runs on WIP, can recover almost 30% of the fuel energy supplied in the form of shaft power. Being wasted away by various means, rest 70% of the input energy still remains unused. However, this result is certainly an improvement towards the application of emulsified POME. This is because the ratio of utilized and unutilized energy of the base fuel of WIP (POME) is found to be 26% and 74%. Table 3.4 shows that, the LHV of WIP is inferior to diesel. Nevertheless, WIP provided a higher recovery of shaft work than diesel at full load condition. The vaporization of the encapsulated water, disintegrate the POME droplets into a number of small parts. As a result, the surface area of the atomized fuel increases, which allows additional air to meet it. This leads to an enhanced fuel evaporation and turbulent mixing (Yang *et al.*, 2013). In order to perform energy analysis, the values of various associated parameters are calculated by using the Eqs. (C1) through (C6). The variations of engine operating parameters (CR and IT) have a number of significant effect on the energy distributions (Figs. 8.10 and 8.11). The effect of CR change on the distributions has been considered by averaging the values of the three ITs, plotting and vice versa.

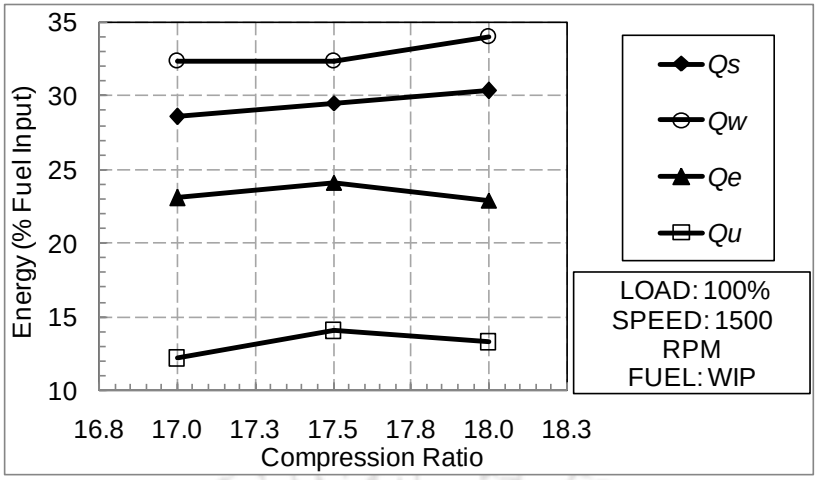

Figure 8.10 Influence of compression ratio on energy distribution for emulsified POME run engine

The percentage values of shaft works for averaged IT with respect to the fuel energy input for CRs of 17, 17.5 and 18 are 28.6%, 29.5% and 30.3%, with IT averaged. However, with averaged CR, these values are 30.86%, 29.19% and 28.36% for the ITs of 20°, 23° and 28ºBTDC. Except 18-20º (CR=18 and IT=20ºBTDC), for all other ITs, the increase in CR reduces the fuel energy input. However, unlike all other CR-IT combinations, at 18-20º WIP produces a complete 3.5 kW of rated power with a lower intake than diesel, as evident from the fuel energy input values (Table 8.3). A few researchers suggest that, the method of emulsion preparation has a significant effect on its engine performance (Lin and Chen, 2006b). The preparation of emulsion by means of ultrasonic waves, results smaller water droplets trapped inside the continuous phase (Lin and Chen, 2008). This increases the number of individual water droplets inside the fuel droplet during the high pressure atomization process of fuel injection. As the number of water droplet increases, the chances of simultaneous water bubble evaporation and more rigorous micro-explosion enhances. Finally, the mixing of fuel air improves and leads to a better combustion performance. This is the main reason for WIP to perform better than diesel. Figure 8.12 shows the effect on BTHE for the WIP run engine as consequence with CR-IT variation. It is seen that higher the CR and more the retarded IT, higher is the BTHE. The BTHEs at 17, 17.5 and 18 CR and at retarded IT of 20ºBTDC are 26.81%, 27.47% and 27.35%, respectively. The injection of WIP at higher CR and retarded IT have allowed WIP to be injected closer to TDC, in a cylinder volume which is relatively lower than other CR-IT specifications. As a result, at the start of fuel injection, the atmosphere inside the cylinder is heated up. This enhances faster breakup of fuel droplets as water inside it will evaporate quickly. Consequently, the burning ratio is

increased and the combustion is improved. This causes an increase in the percentage of shaft work with respect to fuel input at higher CR and retarded IT (Figures 8.10 and 8.11).

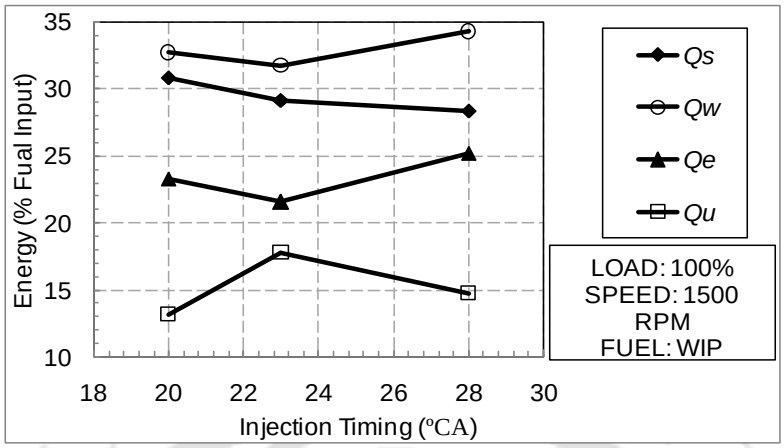

Figure 8.11 Influence of injection timing on energy distribution for emulsified POME run engine

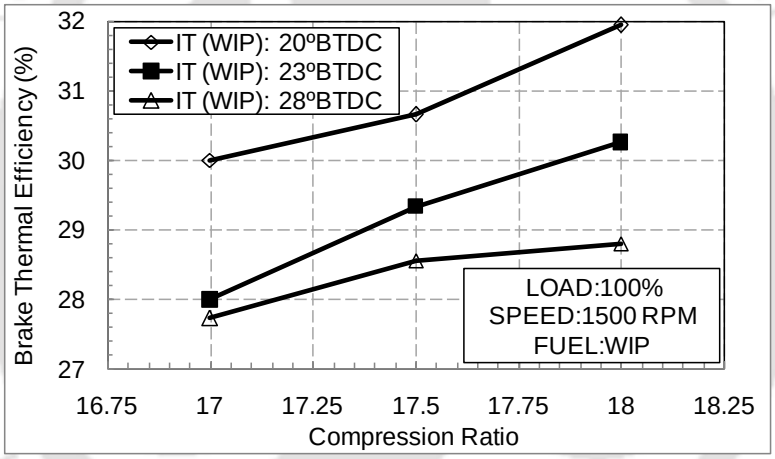

Figure 8.12 Influence of compression ratio and injection timing on brake thermal efficiency for emulsified POME run engine

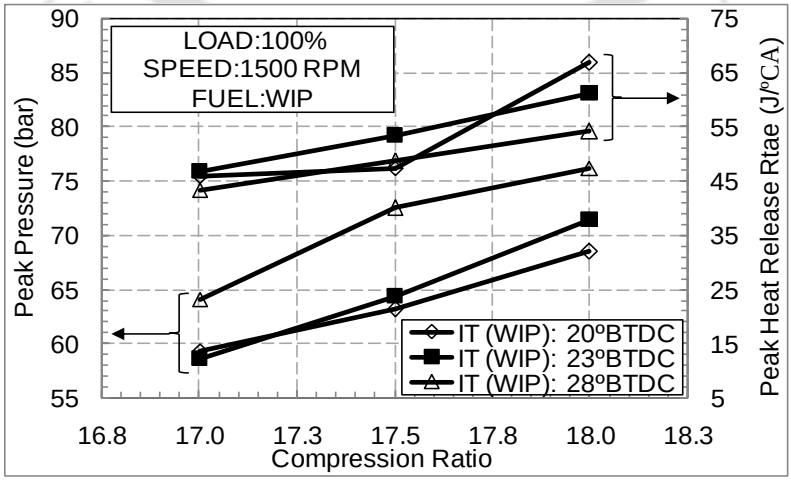

Figure 8.13 Influence of compression ratio and injection timing variation on peak pressure and peak heat release rate for emulsified POME run engine

Table 8.3 Results of energy analysis for emulsified POME run engine

Fuel	CR	IT	Q_{in} (kW)	Q_s (kW)	Q_w (kW)	Q_e (kW)	Q_u (kW)
Diesel	17.5	23	12.11 ±(0.09)	3.49 ±(0.07)	4.00 ±(0.11)	2.55 ±(0.08)	2.06 ±(0.17)
WIP	17	20	10.52 ±(0.05)	3.16 ±(0.03)	3.26 ±(0.09)	2.83 ±(0.10)	1.28 ±(0.34)
	17.5	20	10.31 ±(0.07)	3.16 ±(0.03)	3.34 ±(0.06)	2.36 ±(0.08)	1.45 ±(0.19)
	18	20	11.05 ±(0.00)	3.53 ±(0.08)	3.84 ±(0.08)	2.22 ±(0.15)	1.46 ±(0.17)
	17	23	12.45 ±(0.11)	3.48 ±(0.07)	3.88 ±(0.09)	2.29 ±(0.11)	2.80 ±(0.39)
	17.5	23	10.73 ±(0.03)	3.15 ±(0.03)	3.31 ±(0.07)	2.59 ±(0.02)	1.69 ±(0.02)
	18	23	10.63 ±(0.04)	3.21 ±(0.01)	3.45 ±(0.03)	2.35 ±(0.08)	1.61 ±(0.06)
	17	28	11.05 ±(0.00)	3.06 ±(0.06)	3.32 ±(0.07)	2.64 ±(0.04)	2.02 ±(0.15)
	17.5	28	10.94 ±(0.01)	3.12 ±(0.04)	3.51 ±(0.01)	2.77 ±(0.08)	1.54 ±(0.12)
	18	28	10.84 ±(0.02)	3.12 ±(0.04)	3.58 ±(0.01)	2.86 ±(0.11)	1.28 ±(0.34)

(± standard deviation)

The performance of WIP at higher CR can be analyzed with respect to the peak pressure and peak heat release rate curve (Figure 8.13). The CR rise from 17 to 18 increases the average value of peak pressure by 18.66% for the WIP run engine. It is reported that a rise in CR increases temperature at the end of compression stroke (Aziz *et al.*, 2005). Both of these facts cause 34.04% rise of peak heat release rate near to TDC for WIP. However, for neat POME, the rise of peak pressure and peak heat release rate, both were approximately of 15%. This high increase of peak heat release rate shows that WIP emulsion burns with almost double intensity than neat POME near to TDC. For a constant speed engine, the presence of "micro-explosion" of emulsified POME is probably the better way to explain this fact, since at each load relative air fuel ratio should be fixed to produce same power. Alongside, it is seen that, IT advancement elevations peak pressure. Advancement of IT means that fuel is supplied at cooler atmosphere to that of retardation. Hence, fuel consumption becomes more for the same BP. It is also observed from Fig. 8.11, that the increase in CR decreases exhaust heat loss. This is also proved from the curves of EGT (Figure 8.14). The increase of CR from 17 to 18 has reduced EGT around 15% by average. It is realized that, a fall of uncounted heat loss takes place for WIP run engine. The loss of energy per unit time (% of fuel input) which cannot be trapped are 17.6%, 14.6% and 13.4% for CR of 17, 17.5 and 18 and 13.14%, 17.80% and 14.72% for ITs of 20°,23°and 28ºBTDC. This is a reasonably definite drop, which can be achieved with the increase of exhaust energy loss per unit time.

8.3.2 Exergy Analysis

Table 5 elaborates the availability distribution values of fuel, shaft, cooling water, exhaust gas availability destruction, second law efficiency and their standard deviations. The average standard deviation is within ±0.4. The average value of fuel availability or input availability of the WIP run engine is 11.75 kW neglecting the availability of air intake. Therefore, by average, the shaft availability is calculated as 3.24 kW through. Remaining is lost through cooling water (0.05 kW), flowed away by exhaust gas (1.46 kW) and available energy destroyed in the form of friction, radiation, heat transfer to surroundings (7.13 kW). On the other hand, for calculating the cumulative availability, i.e., the total availability that can be harnessed, the cooling water and exhaust availability have to be taken under consideration (Sahoo *et al.*, 2011). In this respect, from the perspective of thermodynamics around 40% of the fuel or input availability is found to be trappable. Remaining 60% of the input availability is destroyed by various ways for the WIP run engine studied. The corresponding ratio was 30:70 for the POME run engine. To perform exergy analyses, the availability terms allied

with it are calculated by using Eqs. (C7) through (C13). The variation of availability parameters as a function of CR and IT are elaborated in Figs. 8.15 and 8.16.

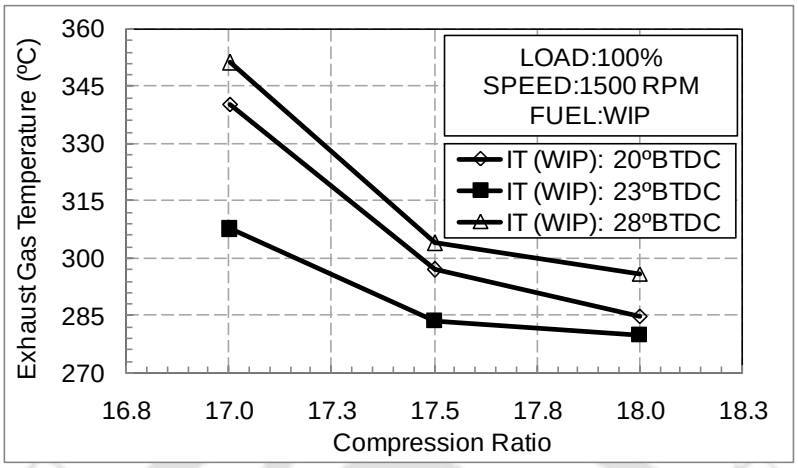

Figure 8.14 Influence of compression ratio and injection timing on exhaust gas temperature for emulsified POME run engine

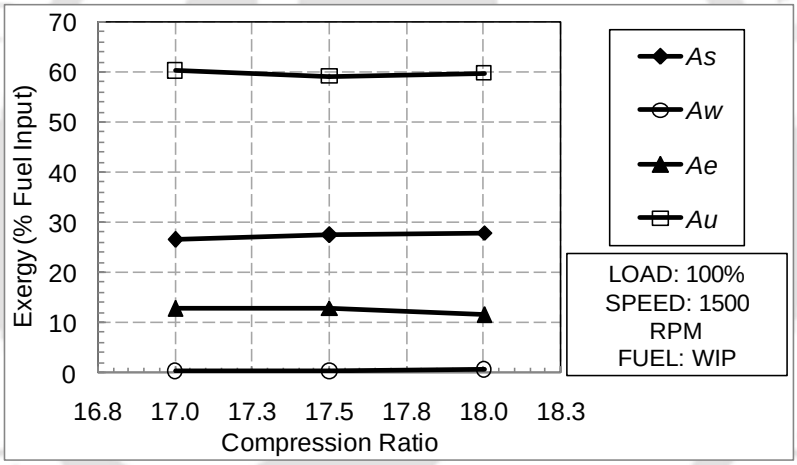

Figure 8.15 Influence of compression ratio on exergy distribution for emulsified POME run engine

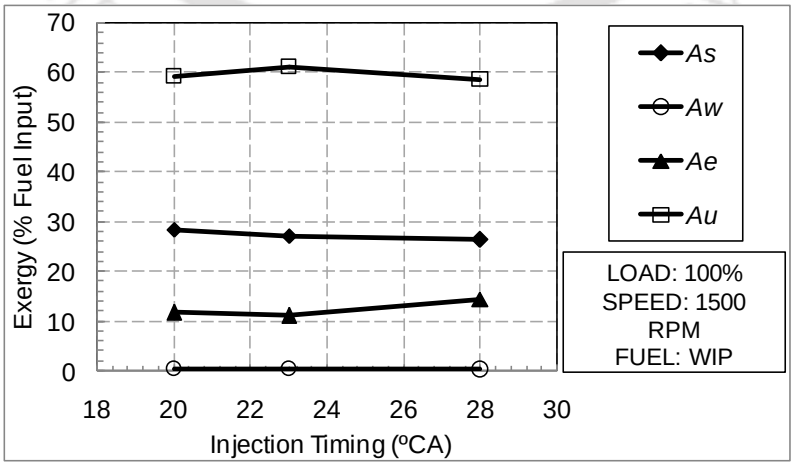

Figure 8.16 Influence of injection timing on exergy distribution for emulsified POME run engine

The fuel energy inputs for WIP run engine for the CRs of 17, 17.5 and 18 are 12.19 kW, 11.46 kW, and 11.65 kW respectively. With increase of CR, the shaft availabilities are found to be 26.59%, 27.46% and 28.07% of fuel energy input, respectively. During the engine operation, as the CR increases, the cylinder volume reduces. This increases the temperature and hence the peak pressure (verified from Fig. 8.13) of combustion. This intensifies the combustion and improves the shaft availability. It is also found that an increase in CR from 17 to 18 reduces the exhaust availability by around 11%. This is the consequence of the reduction of EGT as discussed in the earlier section (Figure 8.14). It has a significant effect on the cooling water availability that got increased by around 50%. However, the availability destruction has hardly a variation (1% drop) with the increase of CR. For the ITs of 20°,23°and 28ºBTDC, the fuel availability values are 11.42 kW, 12.11 kW and 11.76 kW. Definitely, the fuel input value for the WIP run engine is the lowest for retarded IT. It is also found that the retardation of IT provides higher shaft availability. The values of shaft availabilities are 28.56%, 27.16% and 26.39% of fuel input. As IT is retarded from 23ºBTDC (standard IT for diesel) to 20ºBTDC, the piston is actually pushed towards the TDC and thereby the swept volume of the cylinder is reduced at the instant of fuel injection. This causes the WIP to be injected at a crank angle nearest possible from TDC. As a result, at the start of fuel injection, the environment inside the cylinder gets mechanically warmer. This probably increases the shaft availability percentage. The change in cooling water availability is almost negligible. However, the exhaust availability is increased by 23% with the advancement of IT (at 28ºBTDC). This is because, at 28ºBTDC, the EGT is highest among all the other ITs (Figure 8.14). As a result, at 28ºBTDC uncounted availability is reduced. This has finally increased the exergetic efficiency as seen from Fig. 8.17.

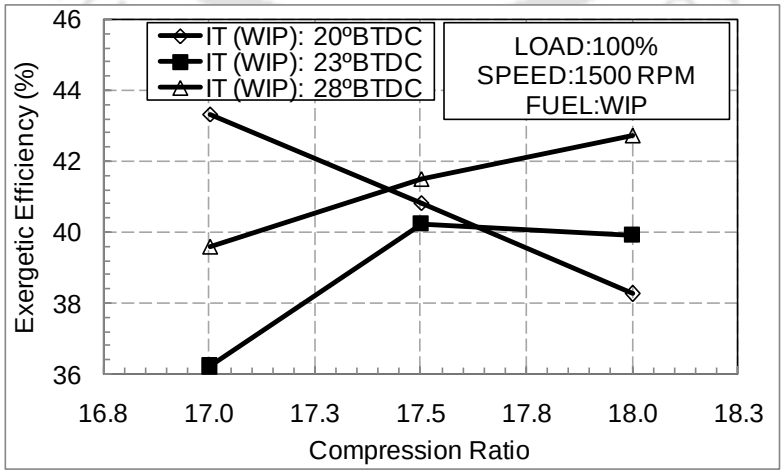

Figure 8.17 Effect of injection timing and compression ratio on exergy efficiency for emulsified POME run engine

Table 8.4 Results of exergy analysis for emulsified POME run engine

Fuel	CR	IT	A_{in} (kW)	A_s (kW)	A_w (kW)	A_e (kW)	A_d (kW)	η_{II}
Diesel	17.5	23	13.01 ±(0.09)	3.49 ±(0.07)	0.08 ±(0.34)	1.45 ±(0.01)	7.99 ±(0.11)	38.62±(0.04)
WIP	17	20	11.31 ±(0.05)	3.16 ±(0.03)	0.05 ±(0.02)	1.69 ±(0.13)	7.33 ±(0.03)	43.34±(0.02)
	17.5	20	11.08 ±(0.07)	3.16 ±(0.03)	0.03 ±(0.96)	1.34 ±(0.09)	6.56 ±(0.09)	40.83±(0.05)
	18	20	11.87 ±(0.00)	3.47 ±(0.07)	0.08 ±(0.34)	0.99 ±(0.48)	6.41 ±(0.11)	38.26±(0.11)
	17	23	13.38 ±(0.11)	3.48 ±(0.07)	0.03 ±(0.76)	1.33 ±(0.10)	8.53 ±(0.16)	36.21±(0.00)
	17.5	23	11.53 ±(0.03)	3.15 ±(0.03)	0.05 ±(0.04)	1.44 ±(0.01)	6.89 ±(0.03)	40.24±(0.01)
	18	23	11.42 ±(0.04)	3.21 ±(0.01)	0.08 ±(0.38)	1.26 ±(0.16)	6.86 ±(0.04)	39.90±(0.01)
	17	28	11.87 ±(0.00)	3.06 ±(0.06)	0.03 ±(0.70)	1.61 ±(0.09)	7.17 ± (0.01)	39.61±(0.03)
	17.5	28	11.76 ±(0.01)	3.12 ±(0.04)	0.03 ±(0.56)	1.72 ±(0.15)	6.88 ±(0.04)	41.51±(0.06)
	18	28	11.65 ±(0.02)	3.12 ±(0.04)	0.06 ±(0.07)	1.80 ±(0.19)	6.67 ±(0.07)	42.72±(0.07)

(± standard deviation)

It is also observed that, the trend of exergy efficiency for the IT of 20ºBTDC is different from the other two cases. The reason is the surge of uncounted availability at this IT. It is jointly responsible for a 4% and 50% drop of shaft and cooling water availability at CR=17.5 and a 36% drop of exhaust availability at CR=18 (at 20ºBTDC). These facts are responsible for a drop of almost 3% and 5% of second law efficiency by value. The variations of entropy generations for various CR-IT combinations are shown in Fig. 8.18. The plots of entropy generation suggest that at a lower CR, the entropy generation increases. The mean value of availability destruction and entropy generation for WIP run engine are 7.03 kW and 0.024 kW/K. The trends of entropy generations reduce with the increase of CR and retardation of IT. Therefore, from thermodynamic point of view, the emulsified fuel has to be run in a diesel engine at a higher CR and at a retarded IT.

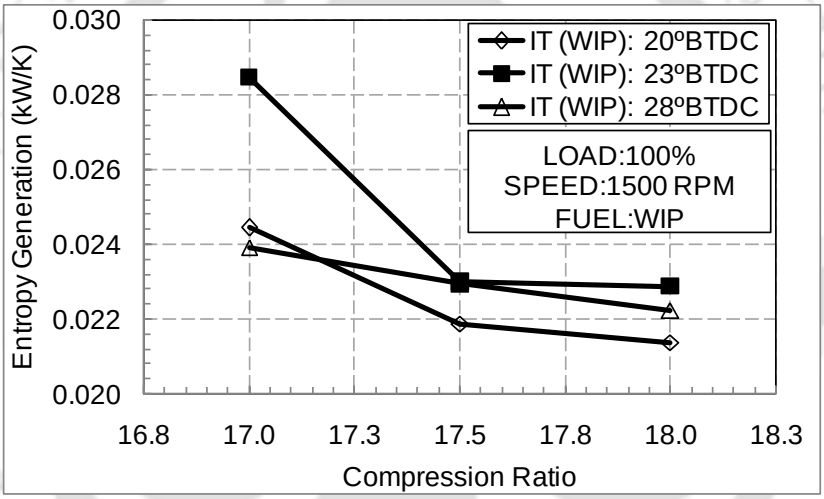

Figure 8.18 Effect of injection timing and compression ratio on entropy generation for emulsified POME run engine

8.4 Summary

The details of energy and exergy analysis of neat and emulsified POME run in VCR diesel engine for a set of CR and IT at full load condition summarizes following key points.

- The analysis demonstrates that POME can recover around 26% of the energy supplied by the fuel. Rest of the energy is flown through the cooling water, exhaust gas and other uncounted losses. The increase in CR cause decrease in fuel supply for same BP or shaft power. Therefore, shaft power per unit fuel supply is increased.

- The exergy analysis has shown that around 30% of the fuel exergy input can be converted in useful means of energy or exergy. The shaft availability is increased with the increase

of CR, IT retardation and advancement. However, cooling water and exhaust gas availability is found to be very low for both CR and IT variation.

- The exergy destruction is reduced with the rise in CR and retardation and advancement of IT. The plot of entropy generation confirms that CR rise and IT retardation causes minor entropy generation and are found to give better thermodynamic performance for POME.

- The diesel engine run by WIP can recover almost 30% of the fuel energy supplied. Rest of the energy is flown through the cooling water, exhaust gas and other uncounted losses. The rise in CR reduces the fuel energy input. At CR=18 and IT=20ºBTDC, a complete 3.5 kW of rated power is produced by WIP run engine with a lower intake than diesel.

- Higher the CR and more retarded the IT, higher is the BTHE. The results of peak heat release rate of WIP run engine shows that, it burns with almost twice intensity than neat POME. This is due to the presence of micro-explosion of emulsified POME. The uncounted heat loss of WIP run engine is lower than neat POME.

- The second law analysis of the WIP run engine shows that, around 40% of the fuel availability is trappable. Further, with the rise of CR, the percentage of shaft availability with respect to the fuel energy input increases for WIP run engine. This is because, at higher CR, the reduced cylinder volume raises the temperature and peak pressure. This actually reduces absolute fuel consumption and increases the mechanical efficiency.

IT retardation offers higher shaft availability. Because, at retarded IT, WIP is injected at a crank angle nearer to TDC. At 20ºBTDC, a drop of shaft and cooling water availability at CR=17.5, and a drop of exhaust heat loss at CR=18 are jointly liable for a rise of uncounted availability. These facts are liable for a drop of second law efficiency at these CRs. Finally, the entropy generation plots show that a diesel engine performance can be improved with emulsified fuel by increasing its CR and retarding IT.

CHAPTER 9

Influence of Emulsified Palm Biodiesel in Dual Fuel Mode

In the earlier chapters, efforts have been made to explore the potential of emulsified palm biodiesel (WIP) as an alternative to diesel. It has been seen that WIP can provide almost equivalent or even better performance than diesel engine, with a slight modification of the engine operating parameters. However, there is a combustion method available, which can further reduce the use of liquid alternative fuel without affecting the engine performance and still enjoying full independence from fossil fuel. This is nothing but the application of dual fuel with biogas. During dual fuel mode, gaseous fuel and air are mixed and inducted to the engine through the inlet manifold and is usually compressed. The lower Cetane number and higher auto ignition temperature of gaseous fuel does not allow it to auto-ignite. Hence, a liquid fuel spray (also known as pilot fuel) of low auto ignition temperature is used to initiate the combustion. The ignition centers formed by the pilot spray lead to the flame propagation through the inducted homogeneous air-gas mixture. In this study, WIP is considered as the pilot fuel, whereas, biogas is considered as the primary gaseous fuel. The engine performance analysis is executed based on brake thermal efficiency, brake specific energy consumption, pilot fuel replacement, biogas flow rate, exhaust gas temperature, and volumetric efficiency. Further, combustion analysis is performed for various parameters namely, pressure–crank angle diagrams, peak cylinder pressure, ignition delay and net heat release rate. Besides, the engine emission quantities recorded are CO, HC, NO_X, and CO_2. This work is aimed to understand and quantify the behavior of emulsified biodiesel (WIP) as a pilot fuel with biogas in dual fuel operation. The results of the study is compared with the standard diesel run and the results of an earlier work performed with neat biodiesel (Jatropha biodiesel) as pilot fuel at biogas dual fuel mode for a similar diesel engine settings and configuration.

9.1 Preface

Diesel engines have got a wide range of applications including transportation, locomotives in offshore drilling, military, marine, telecommunication generator sets, and elsewhere (Inventions and Innovations, 2001). Alongside, they are also being found to be used in countryside construction works, paddy mills, pump sets, small rural transportations (Ehsan and Bhuiyan, 2010). As a whole diesel engines can be called as the building block of the economy of the present civilization. However, the dual concerns over fossil fuels, namely, the depletion and environmental degradation have directed researchers around the world to search for suitable alternatives for combustion devices, especially for diesel engines. A number of researchers around the world have attempted to work with emulsified fuel as an alternative to diesel fuel (Abu-Zaid, 2004; Lin and Chen, 2006b; Nadeem *et al.*, 2006; Lin and Lin, 2007b; Basha and Anand, 2011a). This is possibly due to their ability to reduce NO_X emission, without declining the mechanical performance of diesel engine (Subramanian, 2011). The types of emulsified fuel that have been explored critically in diesel engines are the emulsions prepared with water and diesel (Abu-Zaid, 2004; Lin and Lin, 2007b; Basha and Anand, 2011a). It is found that, for a normal engine operation, water-in-fuel emulsion lowers NO_X and HC emissions compared to neat fuels. This stems from a phenomenon called ‘‘micro-explosions” (Crookes *et al.*, 1992; Kiannejad, 1993). Owing to its complex structure with carbon atoms, the complete combustion of emulsified fuel is hard to achieve. Therefore, scopes of achieving a competitive performance and emission characteristics of a diesel engine run by emulsified fuel with reduced quantity, yet enjoying full independence from fossil fuel are always evident.

There is a combustion method available, which can be attempted to accomplish the above goal – the application of biogas in dual fuel engine run. Biogas, acquired from plants and animal resources, is said to be one of the most environment friendly, renewable, gaseous alternative fuel used for power generation (Von-Mitzlaff, 1988). However, raw biogas contains a substantial amount of carbon dioxide (CO_2), which reduces its flammability limit. This along with the low energy density, low Cetane number and higher auto ignition temperature restricts to auto-ignite the mixture of biogas and air in the diesel engine. As a result, the direct use of biogas in a diesel engine is difficult (Sahoo *et al.*, 2011). In dual fuel mode, the biogas and air is premixed in the inlet manifold and adducted to the engine. Thereafter it is compressed similar to that of a spark ignition engine. A liquid fuel of higher Cetane number and lower auto-ignition temperature (also known as pilot fuel) is then sprayed to trigger the combustion. The ignition centers formed by the pilot spray lead to the flame

propagation through the inducted homogeneous air-gas mixture (Kumar *et al.*, 2003). As soon as the combustion is initiated, the most of the energy is then supplied by the biogas, also termed as primary fuel. In short, a biogas dual fuel engine is modified to operate simultaneously on two fuels. A conventional diesel engine can easily be converted in to a dual fuel engine, without much change in the engine compression ratio, cylinder head or basic operation of a diesel cycle (Dual Fuel (Natural Gas/Diesel) Engines: Operation, Applications and Contribution, 2001). Only an air-gas mixing device is needed to be added at the inlet manifold (Sahoo, 2010; Bora *et al.*, 2013).

The use of biogas in dual fuel diesel engine is found to be advantageous. The application of simulated biogas in diesel engine provides a 60% of maximum diesel substitution without any sign of knocking (Henham and Makkar, 1998). However, it is also reported that, a natural biogas (low-pressure biogas) run diesel engine can reduce energy consumption and chances of knock in comparison to a simulated high-pressure biogas (Jiang *et al.*, 1989). As far as biogas run engine is concerned, homogeneous charge compression ignition (HCCI) diesel engine seems to provide diesel like engine efficiency (Swami Nathan *et al.*, 2010). In a couple of earlier investigations using water emulsion of rapeseed biodiesel with non-renewable gaseous fuels, namely, natural gas (NG) and hydrogen, have increased the efficiency and reduced NO_X emission. However, HC and CO emissions are not reduced (Korakianitis *et al.*, 2010; Namasivayam *et al.*, 2010). Till date, no study seems to have been reported on the application of emulsified fuel as a pilot fuel to ignite biogas. Biogas, the primary fuel in dual fuel mode, consists of methane (CH_4), which is the lightest carbonated combustible product. Hence, if emulsion is used as a pilot fuel for biogas run dual-fuel engine, it may lead to produce a higher burning rate with the aid of micro-explosion. Further, emulsified biodiesel with oxygen molecules bonded in its chemical structure can be helpful to accelerate the combustion in biogas run dual fuel engine (Aziz *et al.*, 2005).

The objective of this study is to explore the influence of water-biodiesel emulsion as a pilot fuel in the presence of biogas in a dual fuel diesel engine. The intention is to achieve diesel like engine performance characteristics, with equivalent or reduced tailpipe emission. Two-phase water in POME (WIP) is considered as the pilot fuel, whereas biogas is considered as the primary gaseous fuel. The engine performance analysis is executed based on brake thermal efficiency (BTHE), brake specific energy consumption (BSEC), pilot fuel replacement, biogas flow rate, exhaust gas temperature (EGT), and volumetric efficiency (*VE*). Further, combustion analysis is performed for various parameters namely, pressure–

crank angle diagrams, peak cylinder pressure (PCP), ignition delay (ID) and net heat release rate (NHRR). Besides, the dry concentrations of engine emissions such as CO, HC, NO_X, and CO_2 are recorded. The results obtained are compared with that of a neat biodiesel (Jatropha)-biogas dual fuel engine run at similar engine settings (Sahoo *et al.*, 2011). Further, the results are also compared with a standard diesel run engine data.

9.2 Setup Modification and Approach

The basic experimental setup consists of a direct injection, water-cooled variable compression ratio (VCR) diesel engine used in this study is the same described in the Section 4.2. The details specification of the engine and the schematic diagram of the VCR diesel engine are already shown in Table 4.1 and Fig. 4.1. However, in order to perform the dual fuel study, the experimental setup is modified as shown in Fig. 9.1. Here, the supply circuit of biogas is attached with the inlet manifold. The circuit consists of biogas balloon, manual control valves, biogas flow meter, and an indigenously built ventury type gas mixer (Bora *et al.*, 2013). The ventury type gas mixer comprises of two biogas inlets, one air inlet, one mixture outlet and is housed in series with the inlet manifold, well upstream the engine intake. Biogas is allowed to move into the gas mixer through the two biogas inlets and mixed with air at the throat zone of the mixture as shown in Fig. 9.1. This is done for utilizing the minimum pressure and maximum velocity at this zone, which is found to improve the mixing of biogas and air. The biogas is considered to be composed of about 48% CH_4 and 42% CO_2 by volume (Sahoo *et al.*, 2011). Some of the important properties of WIP and biogas are shown in Table 9.1.

Table 9.1 Significant properties of WIP and biogas

Properties	**WIP**	**Biogas** (Sahoo *et al.*, 2012b)
Chemical composition	5% H_2O, 2.48% SPAN, 0.52% TWEEN, 92% $C_{18.07}H_{34.93}O_2$	48% CH_4; 42% CO_2 by volume
Density (kg/m^3)	890	1.27
Lower calorific value (MJ/kg)	37.88*	15.74
Cetane number	51	-
Auto-ignition temperature (K)	-	923
Stoichiometric A/F (kg/ kg)	12.93*	5.36
Energy density (MJ/Nm^3)	2.93*	2.87

*****calculated by using equation A9, A10 and A11

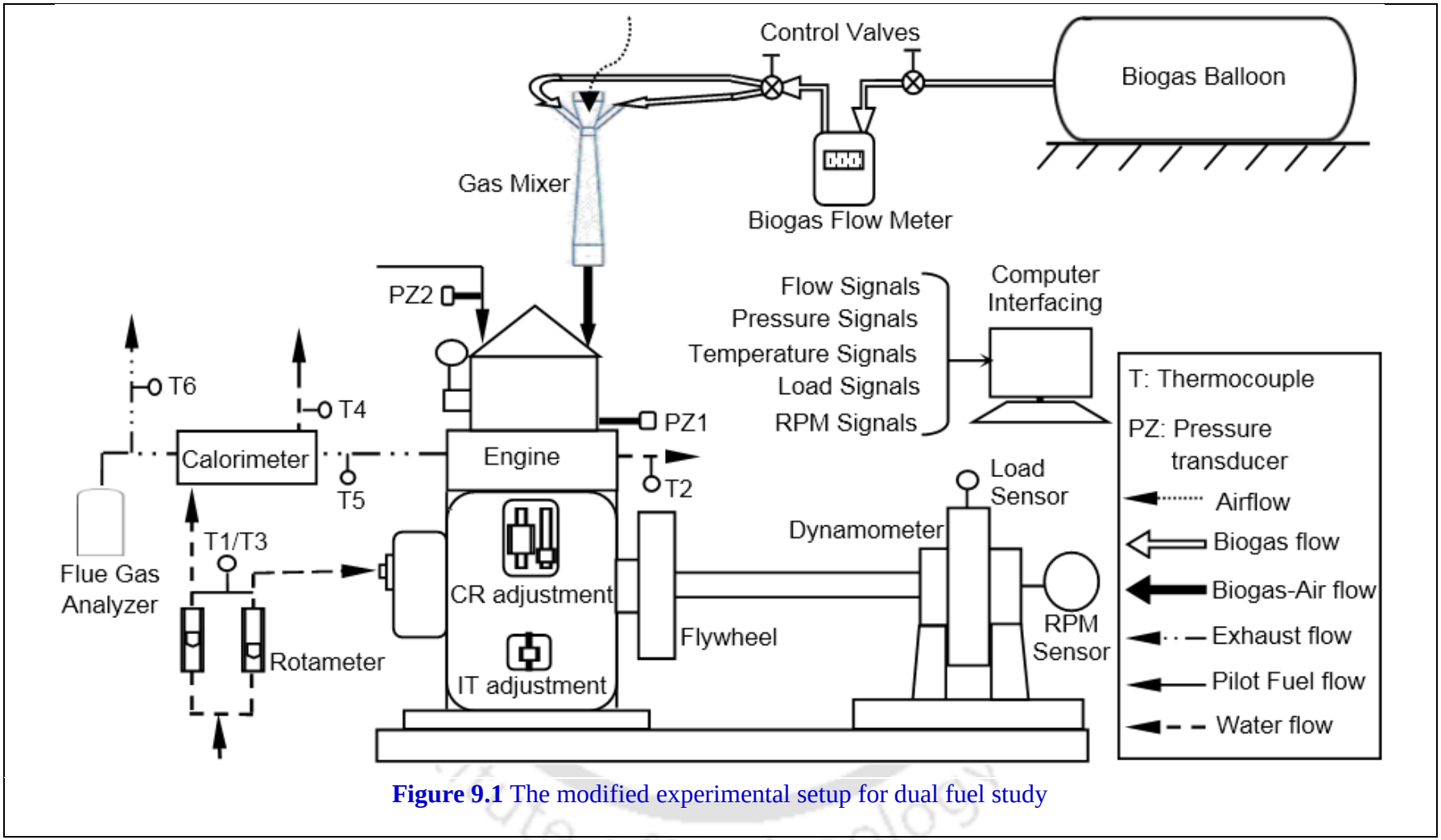

Figure 9.1 The modified experimental setup for dual fuel study

The earlier experimental work performed with a similar type of engine (Kirloskar TV1 and 5.2 kW rated power at 1500 ± 50 rpm) with biogas as primary fuel and Jatropha biodiesel as the pilot liquid fuel (Sahoo *et al.*, 2012b). That engine has the same cylinder specification (bore=87.5 mm, stroke=110 mm, clearance volume = 40.09 cc) with same dynamometer arm radius (185 mm) with the present VCR engine (3.5 kW rated power at 1500±50 rpm). Hence, at CR=17.5 and IT=23ºBTDC, the combustion phenomenon is expected to be symmetrical for each identical loading condition for both of the engines. This is to be noted that, owing to its ability to handle higher loads without much vibration, the earlier engine had a higher rated power than the VCR engine. Therefore, the designed experimental matrix of the work is shown in Table 9.2.

Table 9.2 The experimental matrix

Mode		**Diesel**	**WIP-Biogas**
Fuel		Diesel	WIP and biogas
Compression ratio		17.5	17.5
Injection timing (ºBTDC of CA)		23	23
Engine operation	Speed (rpm)	1500 ± 50	
	BP, kW (Load, kg)	0.20 (No load), 0.91 (3.2), 1.82 (6.4), 2.74 (9.6) and 3.65 (12.8)	

Initially, the engine is allowed to run on diesel with standard setting (CR=17.5, IT=23ºBTDC) for the baseline comparison. The engine is run at no load for a few minutes to attain a steady state. The cooling water supplies for the engine and calorimeter are set to 300 and 100 liters per hour, as per the engine provider instructions. Once the engine is reached the steady-state, the fuel flow rate is recorded to acquire the performance and combustion data. The engine emissions are recorded manually from the flue gas analyzer for the given sample. The method of experimentation is followed in a similar manner as discussed in section 4.4.1. Thereafter, the load is gradually increased to the levels as mentioned in Table 9.2 and data are recorded. This completes the baseline diesel test.

Prior to the start of dual fuel mode, the diesel is replaced by water-in-POME (WIP) emulsion in the fuel tank. The engine is started again and run at no load for few minutes to clear all the diesel remained in the fuel line. At this moment, the biogas flow is started gently from gas balloon to the gas mixer. The homogeneous air-gas mixture from the gas mixer is then drawn into the cylinder for the dual fuel combustion. The biogas supply into the engine cylinder is increased manually until the signal of misfire. This is the limit of the maximum gas, the

engine can combust in the dual fuel mode. Thus, the engine speed is increased due to the added extra chemical energy from biogas. In order to retain a constant power and speed level from both fuel modes, the WIP supply is reduced by pressing the liquid fuel cut-off valve. This assures the minimum pilot fuel consumption at the given engine operating condition. Thereafter, the engine performance parameters for the steady-state dual fuel operation, are measured similarly to diesel test. Further experimentations are completed as discussed above for other loading conditions (Table 9.2). At each load of diesel and dual fuel study, the data are recorded thrice and averaged before further analysis.

9.3 Performance Analysis

The equations used to calculate various performance parameters for dual fuel mode are provided in Appendix – A. The variations of the performance parameters namely, BTHE, BSEC, EGT, volumetric efficiency (*VE*), fuel replacement and biogas flow rate with respect to BP are shown in Fig. 9.2. It is observed that, the percentage of energy supplied by biogas in dual fuel mode with the increase of load are 60%, 66%, 63%, 65% and 66% . The analysis shows that, WIP-Biogas dual fuel mode provides a 25% overall drop of BTHE than neat diesel mode (Figure 9.2a). This is because of the LHV of the biogas is considerably lesser than that of diesel. However, the WIP-Biogas mode with emulsified biodiesel (emulsified POME) as pilot fuel has shown a significant improvement (41%) in BTHE than the dual fuel analysis with neat biodiesel, jatropha oil methyl ester (JOME) as pilot fuel (Sahoo *et al*, 2012b). The reason of this trend is understood from the findings of the BSEC. Although, the WIP-Biogas dual fuel mode delivers a 25% higher BSEC than diesel, but it provides almost 38% lower BSEC than JOME-Biogas mode. Some of the researchers describe this manifestation to be the consequence of the increase in the mixing rate of the emulsified biodiesel (rapeseed) as pilot fuel and air (Korakianitis *et al.*, 2010). This facilitates the combustion of pilot liquid fuel and air to be more homogeneous. Further, it is found that, the pilot fuel-air mixing rate of emulsified biodiesel is significantly higher than neat biodiesel studied earlier (Sahoo, 2010), while all the engine geometrical (bore, stroke, clearance volume, dynamometer arm radius) and operating (speed, load range, CR, IT) parameters are kept constant. Only the micro-explosion of emulsified pilot fuel can substantiate this finding. This work also unfolds one more striving point of the literature. As shown in Fig. 9.2(b), at lower load region (0.20 kW, 0.91 kW, and 1.82 kW of BP), the pilot fuel replacements (32%, 39%, and 48%) are higher for the WIP-biogas mode to that of the JOME-biogas mode (22%, 35%, and 44%), even for a significantly lower biogas flow. This means that, at lower load region the amount of emulsified biodiesel essential to initiate the combustion as a pilot fuel is

lower than that of neat biodiesel. It is known that, pilot fuel replacement is the ratio of reduction of pilot fuel in dual fuel mode to that of same fuel consumption, when used in neat mode. The temperature at the end of compression stroke is sufficient to initiate the evaporation of water droplets impinged inside WIP. This results multiple fuel droplet breakups causing more increase in the surface areas surrounding fuel droplets, which improves pilot fuel-air mixture. However, in case of neat biodiesel, the fuel droplets remained as bigger as they were injected, which takes considerably longer time to start burning and hence the combustion performance of JOME-Biogas mode is deteriorated. This is attributed to a 44% reduction in the EGT for the dual fuel mode with emulsified biodiesel than that of neat biodiesel as pilot fuel (Figure 9.2c). The lower exhaust temperature is known to reduce the thermal stress in the cylinder head, exhaust valve, piston and rings, which is expected to enhance the usual service life of the engine (Pirouzpanah and Mohammadi, 1996). It is seen in Fig. 9(d) that the application of neat biodiesel as pilot fuel and with the increase in load reduces *VE*. The reduction of *VE* has got two primary reasons. Firstly, the higher temperature of the accumulated residual gas prior to suction stroke, preheats the incoming fresh air (Abu-Zaid, 2004). Secondly, with the increase in load, the engine at dual fuel mode requires more energy to be supplied by its primary fuel to develop more power, which subsequently increases the flow rate of biogas (Figure 9.2b). Now, if the biogas supplied through the inlet manifold becomes higher, it will replace more air in the inlet manifold causing a further reduction in the *VE*. This trend has been observed in the earlier study, where fuel has been fumigated through inlet manifold (Karthikeyan and Mahalakshmi, 2007). The average *VE*s for WIP-biogas run dual fuel engine is recorded as 81% compared to 79% for JOME-biogas run (86% for neat diesel run). The reduction in biogas supply for the emulsified biodiesel (Figure 2b) can be attributed for this rise in *VE*.

9.4 Combustion Analysis

The combustion analysis results of the WIP-Biogas, JOME-Biogas, and neat diesel are shown in Fig. 9.3. The variation of cylinder pressure at loading condition for maximum BTHE (Load=12.8 kg and BP=3.65 kW) is shown in Fig. 9.3a. It is noticed that, as a pilot fuel in dual fuel engine, the emulsified biodiesel has produced the peak pressure, at an advanced crank angle, as opposed to the neat biodiesel. This is because, for WIP-Biogas run, the peak pressure is obtained at 8ºATDC, whereas for JOME-Biogas it is found at 14ºATDC. This is a significant finding for the dual fuel operation of renewable fuels and using emulsified biodiesel as pilot fuel. This is because, as the piston moves away from TDC, the increase of the cylinder volume is more. Therefore, if the peak pressure shifts more towards the

expansion stroke, the larger volume available is likely to reduce the effective thrust on the cylinder top. This consequently reduces the magnitude of peak pressure too, as observed in JOME-biogas dual fuel mode. As compared to diesel, the reduction of peak pressure at higher loads in the presence of renewable fuel (diethyl ether/diesel blend) is also observed in current literature (Rakopoulos *et al*., 2013a). Side-by-side, for producing constant power, the engine consumes more energy, thereby reducing efficiency of the device. However, in the present study with WIP-biogas dual fuel mode, the peak pressure point is successfully brought back (closer) to TDC (Figure 9.3b). It is also observed that, with the increase of load PCP of the engine increases, irrespective to the type of fuel used (Rakopoulos *et al*., 2010 Rakopoulos *et al*., 2013b). The average peak pressure for WIP-Biogas and JOME-Biogas dual fuel mode are 51.8 bar and 38.7 bar, comparatively 60.3 bar for neat diesel. Again, from another point of view, the shifting of peak pressure point far away from TDC and towards the expansion stroke reduces the expansion ratio.

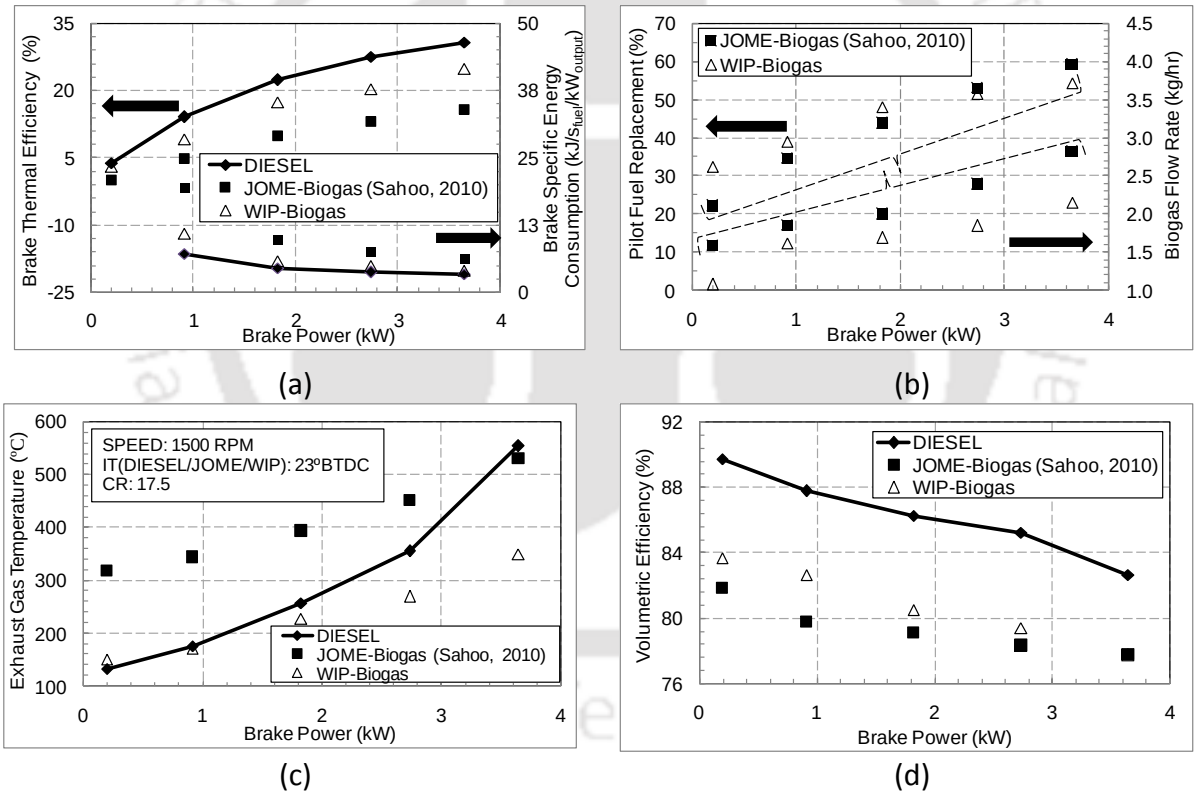

Figure 9.2 Performance analysis of WIP-Biogas dual fuel mode

This is also responsible for lower efficiency of dual fuel mode, as observed in the earlier work by Sahoo (2010) and is shown in Fig. 9.2(a). However, in case of WIP-Biogas run dual fuel mode, a little higher ignition delay (Figure 9.3c) due to micro-explosion (Basha and Anand, 2011b) is compensated by the later increase in the rate of combustion, due to the better mixing of pilot fuel and air. This has probably been further boosted up by the release of

added oxygen bonded in the chemical structure of POME (Aziz *et al.*, 2005). It is found that, as compared to neat diesel mode, the emulsified biodiesel as a pilot fuel has retarded the initiation of combustion by 8%, which is actually 11% for neat biodiesel. Owing to the use of emulsified biodiesel as pilot fuel, the CO_2 present in the biogas (Sahoo, 2010) cannot reduce the flame propagation rate, and hence, the peak pressure and peak heat release rate points remain near to TDC (Figure 9.3d). That is why an improved BTHE, with a lower BSEC is obtained for the dual fuel mode with emulsified biodiesel than neat biodiesel, as a pilot fuel. An lower peak heat release rate and a relatively more after-combustion of WIP-biogas mode is responsible for lower BTHE than neat diesel mode.

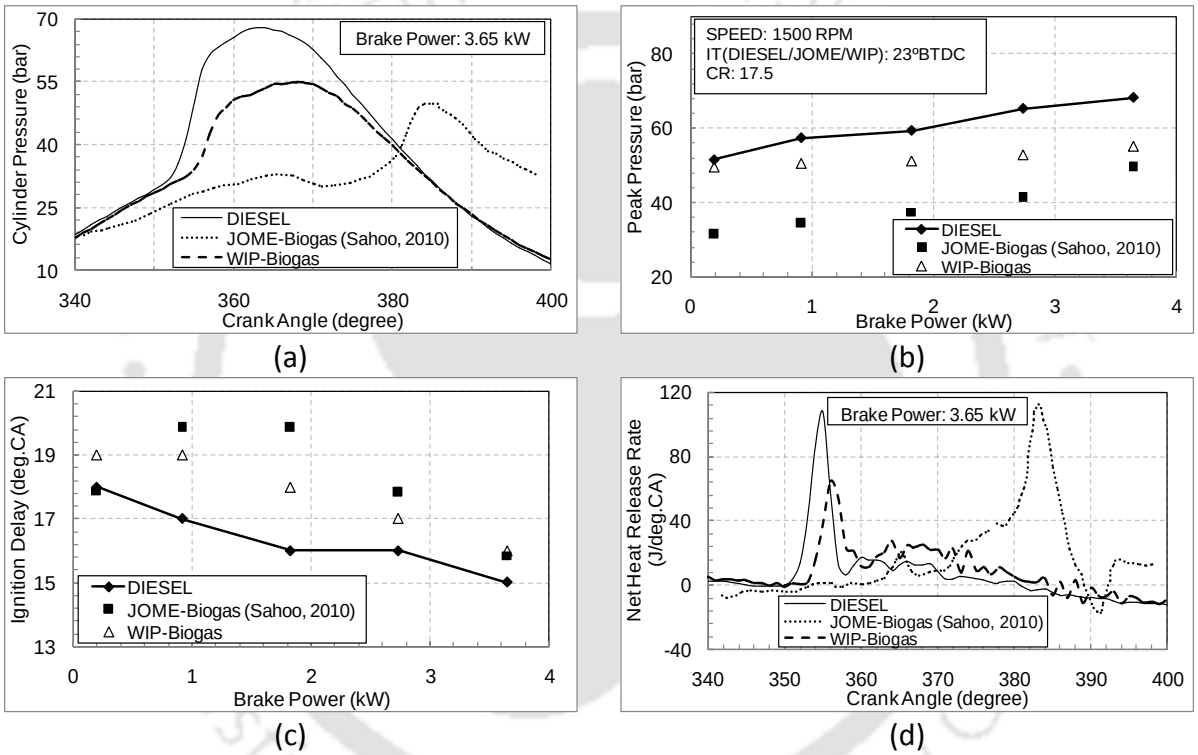

Figure 9.3 Combustion analysis of WIP-Biogas dual fuel mode

9.5 Emission Analysis

The various emission quantities, namely, CO, CO_2, NO_X and HC, measured during the WIP-Biogas dual fuel study are shown in Fig. 9.4 along with the results of JOME-Biogas and neat diesel run. Since, biogas contains 42% (by volume) of CO_2, and has a lower flame speed (0.25 m/s) than diesel (0.30 m/s), the flame front cannot move faster or far enough to consume the entire cylinder volume within the accessible combustion time. That is why; at lower load, the CO and HC emissions are higher as observed in Figs. 9.4(a) and 9.4(b). Again at higher load condition, the higher amount of biogas flow reduce air (or O_2) supply through the inlet manifold for both the dual fuel studies. This causes an increase in the CO and HC emission. However, at higher loads (1.82 kW, 2.74 kW, and 3.65 kW of BP) the WIP-biogas

dual fuel mode have provided significantly lower HC emission than JOME-biogas run. This is because, at these loads the supply of biogas has been reduced considerably (Fig. 9.2b). In other words, the fresh air-biogas charge has become leaner, as observed by some researchers while working with biogas in dual fuel mode (Swami Nathan *et al.*, 2010). This causes the heat sink effect of gaseous fuel to reduce which lessened the chances of formation of unburned charge. It is further assured to mention that, the levels of CO emissions are well below the USA- Environmental Protection Agency (EPA) non-road regulation limits. However, the NO_X emission results are not encouraging as observed in Fig. 9.4(c). They are much higher than JOME-Biogas dual fuel mode and almost equivalent to diesel emission. This is because of the higher peak cylinder pressure for WIP-Biogas dual fuel run, than JOME-Biogas dual fuel run, might have increased the peak temperature, which is a favorable condition for thermal NO formation (Zhu *et al.*, 2011; Giakoumis *et al.*, 2013). With the increase of load, combustion temperature increase (Heywood, 1988). As a result, the oxygen available in the intake air easily oxidizes the carbon components in the fuel to produce higher CO_2, which is witnessed in Fig. 9.4(d). Further, an improved air fuel mixing due to micro-explosion of WIP brings more fuel into combustion, thereby increasing CO_2 emission. However, the CO_2 emission obtained from renewable fuel (WIP-biogas) run dual fuel engine contains carbon, which is part of global carbon cycle. Hence, it has a lesser impact in global warming as discussed in an earlier work (Singh *et al.*, 2007).

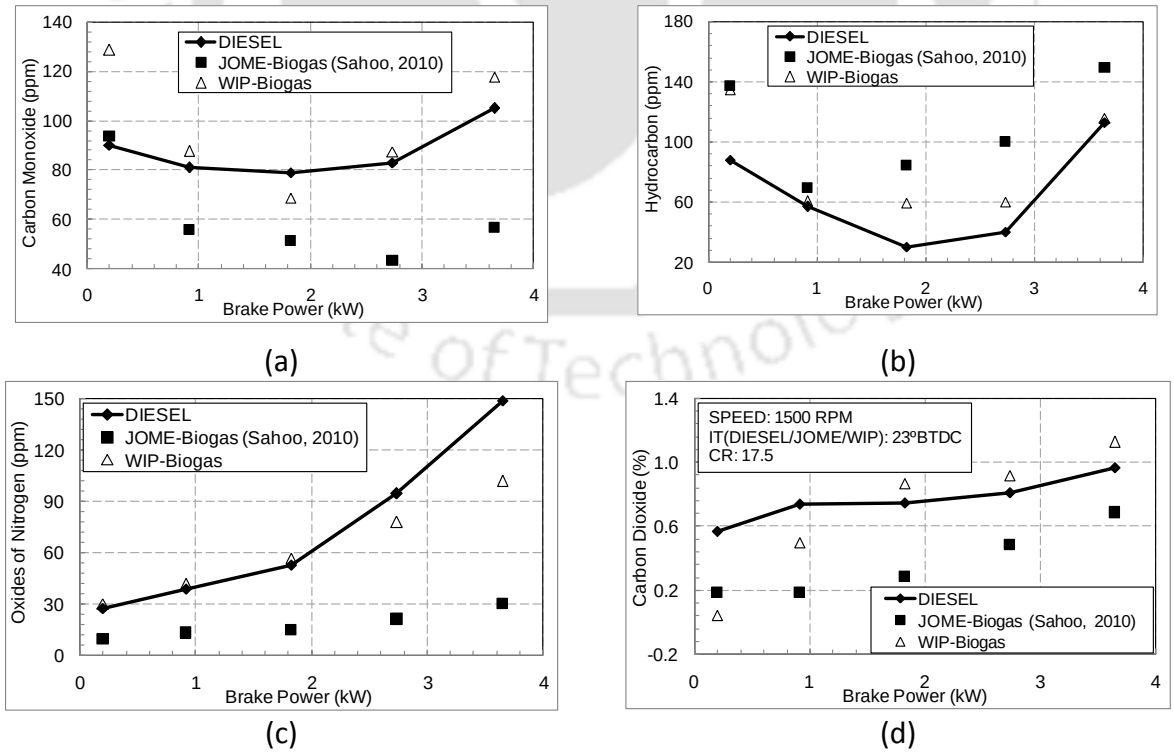

Figure 9.4 Emission analysis of WIP-Biogas dual fuel mode

9.6 Summary

This Chapter attempts to find the possibility of using water emulsified POME (WIP) as a pilot fuel in a biogas run dual fuel engine. The goal is to achieve a diesel like dual fuel engine performance with the presence of biogas, which contains lightest carbonated igneous gaseous material CH_4. This study is performed keeping in line with an earlier work with jatropha biodiesel (JOME)-biogas dual fuel engine. The study unfolds following facts.

- With the presence of biogas, emulsified biodiesel, as a pilot fuel, can present better dual fuel efficiency (41%) and lower energy consumption (38%) as opposed to the neat biodiesel piloted study.
- The presence of 'micro-explosion' of emulsified biodiesel has found to reduce the pilot fuel consumption with the presence of biogas, especially at lower loads where the burning rate of biogas is slowed down by the lean gas-air mixture and cooler charge temperature.
- To produce the same power, the intake of biogas is considerably lower in the presence of emulsified biodiesel than pure biodiesel.
- As a pilot fuel in dual fuel engine, the emulsified biodiesel has produced the peak pressure, at an advanced crank angle, as opposed to the neat biodiesel. This is because, for WIP-Biogas run, the peak pressure is obtained at 8^{o}ATDC, whereas for JOME-Biogas it is found at 14^{o}ATDC.
- The earlier and faster combustion of emulsified biodiesel (POME) has increased the thrust on the piston of the cylinder, which is responsible for the increase of expansion ratio and hence validates the increase of BTHE.
- The emission quantities are almost equivalent to the neat biodiesel (JOME)-biogas dual fuel and neat diesel data recorded.

The dissimilar properties of alternative fuels will never allow it to offer performances equivalent or better than diesel at standard diesel engine settings. Therefore, considering the present study as a baseline work, there is enough scope for further research to optimize the operating characteristics (namely, CR, IT, etc.) of emulsified palm biodiesel and biogas dual fuel study.

CHAPTER 10

Conclusions and Future Scopes

The compression ignition diesel engines are the integral part of the modern civilization. They have a diverse range of applications starting from transport sector to power generation. Run by petroleum based diesel fuel, these engines provide efficiency, durability, and reliability. The steep increase of the prices of petroleum fuels, the scare of its source degeneration and ever-growing environmental concerns, however, made the use of petroleum diesel in CI diesel engine becomes a serious issue day-by-day. Nevertheless, the vast scale of the applications of this prime mover has made it almost impossible for complete replacement, at least for the next few decades. As a result, the search of a suitable alternatives becomes essential to tackle most of these problems effectively and instantly. Around the globe, the most practiced alternative fuel for diesel engine is the methyl ester of vegetable oil or 'biodiesel'. However, present diesel engines, tailor made for fossil diesel, cannot replicate diesel like performance run by 'biodiesel', because of its diesel alien properties. There are two possible methods, by which, diesel like performance or better than that may be achieved; firstly, by modifying the fundamental operating characteristics of the engine, namely, compression ratio (CR), injection timing (IT), etc.; secondly, by modifying the fuel itself. In this regard, the concept of the present work is set to combine both of these methods in diesel engine. The perception is executed by running an optimized water emulsified biodiesel in a variable compression ratio (VCR) diesel engine. The biodiesel selected for this study is the palm oil methyl ester (POME), because of its exceptional combustion characteristics. To achieve the baseline comparison, POME is also run in VCR conditions. The results from the above studies are compared with neat diesel data, experimented at standard diesel specifications. This is followed by the systematic thermodynamic studies that are performed at loads where maximum efficiencies are obtained and mutually compared. Finally, an attempt has been made to check the potential of emulsified biodiesel in dual fuel engine with biogas.

10.1 Preface

The applications of emulsification of an alternative fuel for compression ignition (CI) diesel engines are mostly dedicated towards the emulsions prepared with diesel as a base fluid. One of the alternative fuels is the biodiesel which is a renewable source of energy for diesel engines. However, they have not received proper attention to be combusted in emulsified form, probably because of lesser calorific values compared to conventional fuels. When combusted in diesel engine, the proper tuning of some engine operating limits, namely, CR, IT, and the presence of 'micro-explosion' will amend the performance of biodiesel emulsion.

10.2 Contribution of the Present Work

To perform the work mentioned above, palm oil methyl ester (POME), an esterified biofuel is selected for the study. It has an excellent cetane number and a reasonable calorific value. Besides, POME ($C_{18.07}H_{34.93}O_2$) has around 11.25% of oxygen bonded in its molecular structure, which increases its burning intensely. However, being a fuel of different origin, the standard design limits of a diesel engine is not suitable for POME. Hence, in this work, a set of design and operational parameters are studied to find out the optimum performance of a POME run diesel engine. The parameters varied are the compression ratio (CR) and injection timing (IT) along with load in a VCR diesel engine. The POME run engine is investigated in the form of performance, combustion and emission characteristics. The result of this study will also act as a baseline data for the emulsified POME study, to be followed.

10.2.1 Neat POME

This chapter represents the results of neat POME run diesel engine for combinations of load, CR and IT. The results are evaluated and compared based on diesel run at standard CR and IT combinations.

- At higher loads, BTHEs of POME is a little lower than diesel. For a constant IT, an increase in CR increases the BTHE and lowers the BSFC. However, the collective variation of CR and IT shows that the maximum values of BTHEs occur at CR of 17.5 and 18 at 20ºBTDC.
- EGT increases linearly with the increase of load. However, increase in CR to 18 causes a maximum reduction of EGT of 4%. Side by side, IT reduction to 20ºBTDC also causes a maximum reduction of 5% for EGT.

- POME runs more smoothly than diesel in diesel engine at higher CR. Increase in CR causes a maximum of 8% increase in the PCP. Side by side, increase in IT also causes increase in PCP in the form of 9% at 28ºBTDC.
- The most significant finding of this study is the decrease of ID for POME with respect to diesel. At higher CR, the high pressure and temperature at the primary phases of combustion causes the POME to burn more proficiently.
- Further, retardation of IT cuts both CO and CO_2 emission owing to the fall of BSFC. Although a rise of CR increases pressure and temperature at the primary stages of combustion, yet, combustion starts and completes early. This causes the exhaust gas to cool down and thereby reducing the NO_X emission.
- In addition, the increase in CR from 16 to 18 causes an average reduction of HC emission by 37%. The reason is similar to that of results obtained in case of CO emission. However, the effect of IT is negligible on HC emission.

10.2.2 Emulsified POME

The WIP prepared in the laboratory using commercially available surfactants with appropriate HLB values is characterized by means of droplet diameter measurement and stability study. The results of this study is summarized as follows.

- The longer the emulsification time, lower is the mean droplet diameter.
- Higher the surfactant quantity, lower is the mean droplet diameter.
- The values of mean droplet diameter (1.68 μm for 5% water WIP) fall within the acceptable range of maximum (20 μm) and minimum (0.1 μm) values.
- For HLB=6, after 90 minutes of emulsification, the lowest droplet diameter is achieved.
- The HLB=4.3 (SPAN 80) produces lower droplet diameter than that of HLB=5 emulsion.
- At HLB=6, the increase of hydrophilic surfactant (TWEEN 80) reduces the mean droplet diameter the most.
- Increase in water quantity increases droplet size.
- Larger water quantity increases separation and sedimentation.
- Presence of double surfactant and increase of their quantity cuts separation and sedimentation.

The fuel emulsification is a proven technique for reducing pollutant emissions and improving performance and combustion characteristics of diesel fuel in particular. However, because of

its dissimilar properties to that of diesel, an emulsified fuel is unable to offer its optimum performance when run at a standard diesel engine setting. Hence, the results of the study carried out in a variable compression ratio diesel engine running by emulsified biodiesel to optimize the performance, combustion and emission characteristics are summarized as follows.

- ⊕ WIP emulsion of 5% water has a calorific value around 11% lower than that of diesel. Still it offers a BSFC, 4.6% lower than diesel by average. This emphasizes the presence of 'micro-explosion' in the combustion. At lower load condition, the cooler environment inside the cylinder slows down the rate of water droplet evaporation.
- ⊕ However, at higher load, cylinder is suitably hot and the rate of water bubble explosion rises, causing more heat drift by both the sensible and latent heat of water. As a result, at 100% and 110% of full load, 5% WIP provide highest BTHE for all the CRs of WIP studied.
- ⊕ For all the CRs, WIP performed more efficiently than diesel. At 20ºBTDC and 18 CR, WIP produces almost 11% higher BTHE than diesel. The micro-explosion pulls down the premixed combustion phase of WIP than diesel. As the load increases, engine has to burn more fuel, produce more heat and finally more increase of pressure inside cylinder.
- ⊕ By rising CR from 17 to 17.5 and 17.5 to 18, ID is reduced by 3.6% and 2.8%, respectively. The higher oxygen extent in POME and higher CR fairly covers up the delay of time consumed during secondary atomization. Alongside, a little lower LHV of POME than diesel causes the peak NHRR point to drop lower than diesel.
- ⊕ The raise in CR reduces cylinder volume resulting growth in the combustion temperature. Thus, the nascent oxygen formation is accelerated and reacts with CO. This causes the increase of CO by 24% and 36% as CR rises from 17 to 17.5 and then from 17.5 to 18.
- ⊕ The drop of CO_2 emission of WIP compared to diesel is because of the 4.6% fall of BSFC of WIP than diesel. The presence of oxygen in the chemical structure of POME in emulsion produces water at the end of combustion. This water along with the available water in the emulsion cuts the temperature of burnt gas. As a result, a 43% drop of NO_X emission is obtained for WIP than diesel. The drop of IT cuts HC emission by 6.3% and IT advancement causes 26.5% increase in HC.

There are further scopes of working with POME emulsions, as it can also be prepared with mechanical homogenizer to investigate the stability of the same. The emulsified POME can also boost the efficiency of dual fuel engines, well known for their cleaner emissions.

10.2.3 Analysis at Optimized Operating Characteristics

The application of emulsified POME in a diesel engine produces micro-explosion that increases the fuel burning rate. This causes a lesser fuel intake, a better efficiency and a reduction of carbonated emission. Side by side, the evaporation of water, used in emulsification, consumes heat. This fact reduces NO_X formation and the hazardous emissions created by oxygenated biodiesels.

- WIP provides an overall 11% higher BTHE than diesel. POME delivers a BTHE, 3% lower than diesel. The maximum BTHEs for WIP, POME and diesel at 4.14 bar of BMEP are 31.9%, 27.4%, and 28.9%; whereas at 4.55 bar of BMEP, these values are 33.4%, 30.2% and 29.4%, respectively.
- As compared to diesel, the average reduction in peak pressures for WIP and POME are 15.1% and 1.5%. There is a difference in peak value of heat release rate between WIP, POME and diesel. The 'micro-explosion' and release of water due to the combustion of POME cause heat sink affect. WIP and POME produce an ID of around 48% and 34% lower than diesel.
- WIP causes 43% reduction of CO emission than POME. Overall, WIP emits 17% and 16% lower CO_2 than POME and diesel, respectively, whereas, POME emits 2% higher CO_2 than diesel. As compared to POME, WIP reduces NO_X by 20% (by average). The water brought in by the emulsified fuel changes the relative quantities of fuel oxygen. It is observed that the WIP produces 22% higher HC emission than POME.

10.2.4 Thermodynamic Potential Study

This chapter describes the energy and exergy potential of neat and emulsified POME run diesel engine under variable CR-IT and full load condition. The details of energy and exergy analysis of POME run VCR diesel engine for a set of CR and IT at full load condition summarizes following key points.

- The analysis demonstrates that POME can recover around 26% of the energy supplied by the fuel. Rest of the energy is flown through the cooling water, exhaust gas and other uncounted losses. The increase in CR cause decrease in fuel supply for same BP or shaft power. Therefore, shaft power per unit fuel supply is increased.
- Increase in CR also causes rise in cooling water energy flow rate and drop of exhaust energy flow rate. However, IT retardation and advancement causes increase in shaft energy. This fact causes rise in BTHE too for IT retardation and advancement.

- The exergy analysis has shown that around 30% of the fuel exergy input can be converted in useful means of energy or exergy. The shaft availability is increased with the increase of CR, IT retardation and advancement. However, cooling water and exhaust gas availability is found to be very low for both CR and IT variation.
- The exergy destruction is reduced with the rise in CR and retardation and advancement of IT. Finally, the plot of entropy generation confirms that with the increase in CR and IT retardation offers, minor entropy generation and found to give better thermodynamic performance for POME.

The concluding remarks of the energy and exergy analysis of a diesel engine running in variable CR-IT condition with water emulsified palm oil methyl ester (WIP) are as follows.

* The diesel engine run by WIP can recover almost 30% of the fuel energy supplied in the form of shaft power. Rest is flown through the cooling water, exhaust gas and other uncounted losses. The rise in CR cuts the fuel energy input. At CR=18 and IT=20ºBTDC, a complete rated power is produced by WIP run engine with a lower intake than diesel.
* At higher CR and retarded IT, there is a rise in BTHE. The results of peak heat release rate of WIP run engine shows that, it burns with almost twice intensity than neat POME. This is due to the presence of micro-explosion of emulsified POME. The uncounted heat loss of WIP run engine is lower than neat POME.
* The second law analysis of WIP run engine shows around 40% of the fuel availability is actually trappable. With the increase of CR, the shaft availability rises for WIP run engine. This is because, at higher CR, the reduced cylinder volume raises the temperature and peak pressure. This swells the combustion intensity and the shaft availability too.
* The availability destruction remains unaffected with the increase of CR. IT retardation offers higher shaft availability. Because, at retarded IT, WIP is injected at a crank angle nearer to TDC. At 20ºBTDC, a drop of shaft and cooling water availability at CR=17.5, and a drop of exhaust heat loss at CR=18 are jointly liable for a rise of uncounted availability. These facts are responsible for a drop of second law efficiency at these CRs. Finally, the entropy generation plots show that the performance of a diesel engine can be improved with an emulsified fuel by increasing its CR and by retarding its IT.

10.2.5 Influence of Emulsified Palm Biodiesel in Dual Fuel Mode

- In WIP-Biogas dual fuel mode, the pilot liquid fuel and air mixture is found to be more homogeneous.

- The temperature at the end of compression stroke is ample to initiate the evaporation of water droplets inside WIP.
- For WIP-Biogas run, the peak pressure is obtained at 8ºATDC, whereas for JOME-Biogas it is found at 14ºATDC. This increases the expansion ratio and hence the a efficiency for WIP-Biogas dual fuel run.
- At higher load conditions, more amount of biogas flow reduces the air (or oxygen) supply through the inlet manifold for both the dual fuel studies. This causes an increase in the CO and HC emission.
- Because of higher peak cylinder pressure, for the WIP-biogas dual fuel run produce higher peak temperature and hence the higher NO_X emission than JOME-biogas run.
- An improved air fuel mixing due to micro-explosion of WIP brings more fuel into combustion, thereby increasing CO_2 emission.

However, further exploration of emulsified biodiesel-biogas dual fuel mode is necessary for various CR-IT settings to have further improved emission performance.

10.3 Application Probabilities

Water is traditionally known as a good fire extinguisher. However, intellectual use of water may enhance fire too. In this work, this technique is utilized to have a probable replacement of diesel in the form of alternative fuel. To make the study more interesting, the primary fluid of the emulsion is considered as biodiesel (POME). Now, emulsifying POME with water by ultrasonic waves, will disperse the water in micron level which is also confirmed. Finally, the emulsified POME (WIP) is run in diesel engine with modified specifications. The probable applications of this work are discussed as follows:

- In Chapter 6, it is found that WIP can run in diesel engine with lower intake than POME and even lower from diesel. Hence, this type of fuel is suitable for various stationary engine rigs, usually involved in power generation, back-up power production, farm engines, etc., with a little modification in engine operating conditions.

- Water emulsified biodiesel emulsion, has certain quantity of water in it. Still, it provides higher efficiency diesel with a complete independence from fissile diesel. The application of this fuel in diesel engines used in heavy transports (railways, marine engine, etc.), can save millions of currency, which is flowed away in the form of crude petroleum import.

Using this currency in the engine research and development and biodiesel production may enrich the field of alternative fuel.

- A major bottleneck of using neat biodiesel in road transport is the production of higher NO_X. Water in biodiesel emulsion can also solve this problem as observed in the discussions of Chapter 7. Presence of water vapor is expected to reduce the peak combustion temperature, the proof of which is observed in the reduction of NO_X emission of WIP from neat POME and even from neat diesel.

10.4 Future Scopes

The present investigation focuses the prospect of emulsified biodiesel in a variable compression ratio diesel engine. In order to examine the performance of emulsified biodiesel, the original biodiesel is also tested in similar operating specifications. Thereafter, the first and second law analyses are performed at full load condition for both type of fuels and discussed subsequently, in the sections above. However, there are also several scopes for future study, related to this field, which can further enrich the area of alternative fuel. These are listed below.

∇ The gaseous fuels generally used in dual fuel engine have higher auto ignition temperature and hence high ID. The ID of liquid pilot fuel is again affected. As a result, a much higher ID in dual fuel mode causes the PCP to reduce by shifting it towards the expansion stroke. This cuts the BTHE of the dual fuel engine than diesel engine. However, the study performed here showed that, WIP (water emulsion of POME) produces almost equivalent power with lower consumption then diesel. Further, it results lower ID and moderate emission values. The use of WIP provided far more improved engine performance than POME as a fuel. Therefore, this work can further be extended by using WIP as a pilot liquid fuel, along with various other gaseous fuels (CNG, LPG, etc.) in dual fuel diesel engine.

∇ In this work, only one biodiesel type (palm oil origin) is used for the possible application as an emulsified alternative fuel in diesel engine. However, various locally available biodiesel types can be emulsified and checked by running in diesel engine along with detailed life cycle analysis (LCA). These may include biodiesel produced from rice husk oil, jatropha oil, sunflower oil, rubber seed oil, peanut oil, coconut oil, karanja oil, honge oil etc. Further improvement in engine performance and emission by using biodiesel

produced from any of these oils can open huge scopes for government and related organizations in rural employment, which will boost the economy of the nation itself.

∇ Now a days, applications of nano-fuels are becoming popular. This is nothing but the addition of nanoparticles (namely, griffin, carbon nanotube, etc.) in normal liquid fuel. Addition of these nano particles increases surface area of heat dissipations. This increases the quicker heat transfers, even at the most remote locations of heterogeneous fuel air mixture in diesel engine. Consequently, combustion become faster with reduced ignition delay and lower fuel intake. However, till date almost all of the nano-fuels used to run diesel engine are diesel based. The technology can also be implemented for renewable fuels, such as, biodiesel.

∇ In this study, ultrasonic bath emulsifier is used to prepare the emulsion. This produces ultrasonic wave from the surrounding walls. However, the production of biodiesel emulsion has not been explored with tip sonicator, which produces ultrasonic waves from a tip placed at the centre of the solution. The stability study performed in this work for emulsified POME can be extended further. The emulsified biodiesel can be checked for longer duration, say, several days or weeks to check the volumetric deposition, on the basis of its use. Although the volumetric depositions are checked minutely, however, the concentration of water droplets in emulsified fuels can be checked by ultraviolet spectrometer. This may offer more precise results of water deposition, with the change of time. Further, emulsion activity analysis can also be performed for biodiesel-based emulsion. This is done by centrifuging the emulsion at various speeds to check the droplet agglomeration due to the action of centrifugal force. This study is a key for the mobile use of emulsified fuel.

∇ Preparation of emulsification needs the implementation of some extra energy in the form of ultrasonication. Needless to say that, an economic assessment of emulsified fuel run engine is necessary from the social viewpoint. A detailed cost analysis of the energy ingestion in the form of ultrasonication, cost of fuel, running cost, power generation, environmental aspects and other costs can be executed to see the profitability of the use of emulsified fuel. However, for the viewpoint of large-scale applications with implementation of renewable biodiesel as the carrying fluid of fuel emulsion that may cut the cost associated with its preparation. The alternative methods of emulsifications,

namely, gas in liquid emulsification or effervescent atomization can be tried to curb the cost associated with its preparation.

∇ Thermodynamic modeling of emulsified fuel combustion is also lacking in the literature. The micro-explosion of emulsified fuel and subsequently its combustion are two completely different phenomena. These two methods are occurring simultaneously during the combustion of water-emulsified biodiesel in diesel engine. There is no indigenous model available to replicate the combined phenomenon of micro-explosion and combustion. The assistance of zero, two or three-dimensional modeling can be implemented in varying load conditions, to know the effect of micro-explosion in the combustion temperature, ignition delay, heat release rate, combustion duration, etc. This will allow to optimize the rigorous experimentation, and will save a lot of time, effort and money.

References

AbdAlla GH, Soliman HA, Badr OA, and **AbdRabbo MF**, (2002), Effect of injection timing on the performance of a dual fuel engine, *Energy Conversion and Management*, Vol. 43, No. 2, pp. 269-277.

Abu-Zaid M, (2004), Performance of single cylinder, direct injection diesel engine using water fuel emulsions, *Energy Conversion and Management*, Vol. 45, No. 5, pp. 697–705.

Agarwal D, Kumar L, and **Agarwal AK**, (2008), Performance evaluation of a vegetable oil fuelled compression ignition engine, *Renewable Energy*, Vol. 33, No. 6, pp. 1147–1156.

Agarwal AK, and **Rajamanoharan K**, (2009), Experimental investigations of performance and emissions of karanja oil and its blends in a single cylinder agricultural diesel engine, *Applied Energy*, Vol. 86, No. 1, pp. 106–112.

Agudelo J, Gutiérrez E, and **Benjumea P,** (2009), Experimental combustion analysis of a HSDI diesel engine fuelled with palm oil biodiesel-diesel fuel blends, *Dyna*, Vol. 76, No. 159, pp. 103-113.

Ajav EA, Singh B, and **Bhattacharya TK**, (2000), Thermal balance of a single cylinder diesel engine operating on alternative fuels, *Energy Conversion and Management*, Vol. 41, No. 14, pp. 1533-1541.

Almeida SCAde, Belchior CR, Nascimento MVG, Vieira LSR, and **Fleury G,** (2002), Performance of a diesel generator fuelled with palm oil, *Fuel*, Vol. 81, pp. 2097–2102.

Al-Najem NM, and **Diab JM**, (1992). Energy – exergy analysis of a diesel engine, *Heat Recovery Systems and CHP*, Vol. 12, No. 6, pp. 525–529.

Altin R, Cetinkaya S, and **Yucesu HS,** (2001), The potential of using vegetable oil fuels as fuel for diesel engines, *Energy Conversion and Management*, Vol. 42, No. 5. pp. 529-538.

Armas O, Ballesteros R, **Martos FJ,** and **Agudelo JR**, (2005), Characterization of light duty diesel engine pollutant emissions using water-emulsified fuel, *Fuel*, Vol. 84, No. 7-8, pp. 1011–1018.

Ashok MP, (2012a), Identification of best additive using the selected ratio of ethanol–diesel-based emulsified fuel, *International Journal of Sustainable Energy*, Vol. 31, No. 3, pp. 203-212.

Ashok MP, (2012b), Effect of best emulsified fuel: with and without water addition for the reduction of automobile CO and NO_X emissions in human life, *International Journal of Sustainable Energy*, Vol. 31, No. 5, pp. 1–9.

Ashok MP, and **Saravanan CG**, (2007), Combustion characteristics of compression engine driven by emulsified fuel under various fuel injection angles, *ASME Journal of Energy Resources Technology*, Vol. 129, No. 4, pp. 325-331.

Aziz AA, Said MF, and **Awang MA**, (2005), Performance of palm oil-based biodiesel fuels in a single cylinder direct injection engine, *Palm Oil Developments*, Vol. 42, pp. 15-27.

Aziz AA, Said MF, Awang MA, and **Said M**, (2006), The effects of neutralized palm oil methyl esters (NPOME) on performance and emission of a direct injection diesel engine, Paper No. 3383, Proceedings of the 1st International Conference on Natural Resources Engineering and Technology, July 24-25, Putrajaya, Malaysia.

Banapurmath NR, and **Tewari PG,** (2008) Performance of a low heat rejection engine fuelled with low volatile Honge oil and its methyl ester (HOME), *Proceedings of the Institution of Mechanical Engineers, Part A: Journal of Power and Energy*, Vol. 222, No. A3, pp. 323-330.

Banapurmath NR, and **Tewari PG**, (2009), Comparative performance studies of a 4-stroke CI engine operated on dual fuel mode with producer gas and honge oil and its methyl ester (HOME) with and without carburetor, *Renewable Energy*, Vol. 34, No. 4, p. 1009–1015.

Banapurmath NR, **Tewari PG**, and **Hosmath RS**, (2008), Experimental investigations of a four-stroke single cylinder direct injection diesel engine operated on dual fuel mode with producer gas as inducted fuel and Honge oil and its methyl ester (HOME) as injected fuels, *Renewable Energy*, Vol. 33, No. 9, pp. 2007–2018.

Banapurmath NR, Tewari PG, Yaliwal VS, Kambalimath S, and **Basavarajappa YH**, (2009), Combustion characteristics of a 4-stroke CI engine operated on Honge oil, Neem and Rice Bran oils when directly injected and dual fuelled with producer gas induction, *Renewable Energy*, Vol. 34, No. 7, pp. 1877–1884.

Bari S, Yu CW, and **Lim TH**, (2002) Performance deterioration and durability issues while running a diesel engine with crude palm oil. *Proceedings of the Institution of Mechanical Engineers, Part D: Journal of Automobile Engineering*, Vol. 216, No. D9, pp. 785-792.

Basha SJ, and **Anand RB**, (2011a), An experimental investigation in a diesel engine using carbon nanotubes blended water-diesel emulsion fuel, *Proceedings of the Institution of Mechanical Engineers, Part A: Journal of Power and Energy*, Vol. 225, No. 3, pp. 279-288.

Basha SJ, and **Anand RB**, (2011b), An experimental study in a CI engine using nanoadditive blended water–diesel emulsion fuel, *International Journal of Green Energy*, Vol. 8, No. 3, pp. 332-348.

Becher P, (1965), *Emulsions: Theory and Practice*, Chemical Rubber Co. Scientific Review Press, Cleveland, Ohio, USA.

Benjumea P, **Agudelo J**, and **Agudelo A**, (2009), Effect of altitude and palm oil biodiesel fuelling on the performance and combustion characteristics of a HSDI diesel engine, *Fuel*, Vol. 88, No. 4, pp. 725–731.

Bhatt YC, (1987), *Use of some non-edible oils as a source of energy for CI engines*, PhD thesis, Indian Institute of Technology Kharagpur, India.

Bora BJ, Debnath BK, Gupta N, Sahoo N, and **Saha UK,** (2013), Investigation on the flow behaviour of a venturi type gas mixer designed for dual fuel diesel engines, *International Journal of Emerging Technology and Advanced Engineering*, Vol. 3, No. 3, pp. 202-209.

Born C, and **Peters N**, (1998), Reduction of soot emission at a DI diesel engine by additional injection of hydrogen peroxide, *Society of Automotive Engineers*, Paper No. 982676.

Buyukkaya E, (2010), Effects of biodiesel on a DI diesel engine performance, emission and combustion characteristics, *Fuel*, Vol. 89, No. 10, pp. 3099–3105.

Buehler Ltd., *Buehler Analyst Section*, USA, 1993.

Caliskan H, **Tat ME**, **Hepbasli A**, and **Van Gerpen JH**, (2010), Exergy analysis of engines fuelled with biodiesel from high oleic soybeans based on experimental values, *International Journal of Exergy*, Vol. 7, No. 1, pp. 20–36.

Canakci M, and **Hosoz M**, (2006), Energy and exergy analyses of a diesel engine fuelled with various biodiesels, *Energy Sources, Part B: Economics, Planning, and Policy*, Vol. 1, No. 4, pp. 379–394.

Carter C, Finley W, Fry J, Jackson D, and **Willis L**, (2007), Palm oil markets and future supply, *European Journal of Lipid Science and Technology*, Vol. 109, No. 4, pp. 307–314.

Caton JA, (2000), On the destruction of availability (exergy) due to combustion process – with specific application to internal-combustion engines, *Energy*, Vol. 25, No. 11, pp. 1097–1117.

Caton JA, (2012), The thermodynamic characteristics of high efficiency, internal combustion engines, *Energy Conversion and Management,* Vol. 58, pp. 84–93.

Chavannavar PS, and **Caton JA**, (2006), Destruction of availability (exergy) due to combustion processes: a parametric study, *Proceedings of the Institution of Mechanical Engineers, Part A: Journal of Power and Energy*, Vol. 220, No. 7, pp. 655–668.

Chen K-S, Lin Y-C, Hsieh L-T, Lin L-F, and **Wu C-C**, (2010), Saving energy and reducing pollution by use of emulsified Palm-biodiesel blends with bio-solution additive, *Energy*, Vol. 35, No. 5, pp. 2043–2048.

Chokri B, Ridha E, Rachid S, and **Jamel B,** (2012), Experimental study of a diesel engine performance running on waste vegetable oil biodiesel blend, *ASME Journal of Energy Resources Technology*, Vol. 134, pp. 032202(1-6).

Choo YM, Ong ASH, Cheah KY, and **Bakar A**, (1992), Production of alkyl esters from oils and fats. *Australian Patent*, Patent No. AU 626014.

Chung SH, and **Kim JS**, (1990), An Experiment on vaporization and microexplosion of emulsion fuel droplets on a hot surface, *Twenty-Third Symposium (International) on Combustion*, Vol. 23, No. 1, pp. 1431–1435.

Clean Alternative Fuels: Biodiesel, An article published by United States Environmental Protection Agency, National Biodiesel Board, MO, USA, 2012.

Crookes RJ, **Kiannejad F**, and **Nazha MAA**, (1997), Systematic assessment of combustion characteristics of biofuels and emulsions with water for use as diesel engine fuels, *Energy Conservation and Management*, Vol. 38, No. 15, pp. 1785– 1795.

Crookes RJ, **Nazha MAA**, and **Kiannejad F**, (1992), Single and multi-cylinder diesel-engine tests with vegetable oil emulsions, *Society of Automotive Engineers*, Paper No. 922230.

Curran HJ, **Gaffuri P**, **Pitz WJ**, and **Westbrook CK**, (1998), A comprehensive modeling study of n-heptane oxidation. *Combustion and Flame,* Vol. 114, No. (1–2), pp. 149–177.

Debnath BK, Saha UK, and **Sahoo N**, (2011), Effect of compression ratio on the performance characteristics of a palm oil methyl ester run diesel engine, Proceedings of ASME 2011 International Mechanical Engineering Congress & Exposition Energy and Water Scarcity, Paper No. IMECE2010–65135, November 11-17, Colorado, USA.

Debnath BK, Saha UK, and **Sahoo N**, (2013), Thermodynamic analysis of a variable compression ratio diesel engine running with palm oil methyl ester, *Energy Conversion and Management*, Vol. 65, pp. 147–154.

Devan PK, and **Mahalakshmi NV**, (2009), A study of the performance, emission and combustion characteristics of a compression ignition engine using methyl ester of Paradise oil–Eucalyptus oil blends, *Applied Energy*, Vol. 86, No. 5, pp. 675–680.

Devan PK, and **Mahalakshmi NV**, (2010), Development of bio-diesel from low fatty acid poon oil and evaluation of its performance and emission characteristics in a DI diesel engine, *Journal of the Institution of Engineers (India): Mechanical Engineering Division*, Vol. 91, pp. 10-14.

DOW Surfactants, TRITON™ X-45 Surfactant, Product Information and Technical data sheet, http://www.dow.com/surfactants/products/octyl.htm, Saturday, September 17, 2011 5:35:01 PM.

Dryer FL, (1977), Water addition to practical combustion systems—Concepts and applications, *Symposium (International) on Combustion*, Vol. 16, No. 1, pp. 279-295.

Dual Fuel (Natural Gas/Diesel) Engines: Operation, Applications and Contribution. Published by Group of Experts on Pollution & Energy (GRPE), The European Natural Gas Vehicle Association, Informal document No. 18, May, 2001.

Duarte ARCdeLM, Bezerra UH, Tostes MEdeL, and **Filho GNdaR**, (2007), Alternative energy sources in the amazon: evaluating the energy potential of palm oil for the generation of electricity in isolated communities, *IEEE Power and Energy Magazine*, Vol. 5, No. 1, pp. 51-57.

Duran A, Lapuerta M, and **Rodriuez-Fernandez J**, (2005), Neural networks estimation of diesel particulate matter composition from transesterified waste oils blends, *Fuel*, Vol. 84, No. 16, pp. 2080–2085.

Ebiana AB, Savadekar RT, and **Patel KV**, (2006), Entropy Generation/Availability Energy Loss Analysis Inside MIT Gas Spring and 'Two Space' Test Rigs, Technical report published by National Aeronautics and Space Administration (NASA), Report No. N20060023345, USA.

Ehsan Md, and **Bhuiyan S**, (2010), Dual fuel performance of a small diesel engine for applications with less frequent load variations, *International Journal of Mechanical & Mechatronics Engineering*, Vol. 9, pp.30-39.

Emission Standards. Obtained through the Internet: http://www.dieselnet.com/standards. [accessed 07/07/2012 at 23:30 hrs]

FAO, (2008), The State of Food and Agriculture. Biofuels: Prospects, Risks and Opportunities, Food and Agriculture Organization of the United Nations, Rome.

Flynn PF, Hoag KL, Kamel MM, and **Primus RJ**, (1984), A new perspective on diesel engine evaluation based on second law analysis, *Society of Automotive Engineers*, Paper No. 840032.

Freudenstein F, and **Maki ER**, (1981), Variable displacement piston engine, *US Patent*, Patent No. 4,270,495.

Ganesan S, and **Ramesh A**, (2002), An experimental study of the characteristics of a LPG-based dual-fuel engine using a water/Diesel emulsions as the pilot fuel, *Journal of the Institute of Energy*, Vol. 75, No. 502, pp. 2–10.

Garg P, (2012), Energy scenario and vision 2020 in India, *Journal of Sustainable Energy & Environment*, Vol. 3, pp. 7-17.

Garti N, (1997), Double emulsions -- scope, limitations and new achievements, *Colloids and Surfaces, A: Physicochemical and Engineering Aspects*, Vol. 123-124, pp. 233-246.

Ghannam MT, and **Selim MYE**, (2009), Stability behavior of water-in-diesel fuel emulsion, *Petroleum Science and Technology*, Vol. 27, No. 4, pp. 396-411.

Giakoumis EG, (2007), Cylinder wall insulation effects on the first- and second-law balances of a turbocharged diesel engine operating under transient load conditions, *Energy Conversion and Management*, Vol. 48, No. 11, pp. 2925–2933.

Giakoumis EG, Rakopoulos CD and **Rakopoulos DC, (**2013), An assessment of NO_X emissions during transient diesel engine operation with biodiesel blends. *ASCE Journal of Energy Engineering*; doi:10.1061/(ASCE)EY.1943-7897.0000136, (In Press).

Goering CE, (1998), Engine heat release via spread sheet, *American Society of Agricultural Engineers*, Vol. 98, pp. 1249-1253.

Gokalp B, Buyukkaya E, and **Soyhan HS**, (2011), Performance and emissions of a diesel tractor engine fueled with marine diesel and soybean methyl ester, *Biomass and Bioenergy*, Vol. 35, No. 8, pp. 3575-3583.

Greeves G, **Khan IM**, and **Onion G**, (1976), Effects of water introduction on diesel engine combustion and emissions, *Symposium (International) on Combustion*, Vol. 16, No. 1, pp. 321–336.

Griffin WC, (1949), Classification of surface-active agents by HLB, *Journal of the Society of Cosmetic Chemists*, Vol. 1, pp. 311–320.

Griffin WC, (1954), Calculation of HLB values of non-ionic surfactants, *Journal of the Society of Cosmetic Chemists*, Vol. 5, pp. 235-249.

Grundy JR, Kiley LR, and **Brevick EA,** (1976), AVCR 1360-2 High specific output-variable compression ratio diesel engine, *Society of Automotive Engineers*, Paper No. 760051.

Guo X, Rong Z, and **Ying X,** (2006), Calculation of hydrophile–lipophile balance for polyethoxylated surfactants by group contribution method, *Journal of Colloid and Interface Science*, Vol. 298, pp. 441–450**.**

Guo Z, **Li T, Dong J, Chen R, Xue P**, and **Wei X**, (2011), Combustion and emission characteristics of blends of diesel fuel and methanol-to-diesel, *Fuel*, Vol. 90, pp. 1305–1308.

Hanson AC, (1989), *A Diagnostic Quasi-Dimensional Model of Heat Transfer and Combustion in Compression-Ignition Engines*, Ph.D. thesis, Department of Agricultural Engineering, University of Natal, Pietermaritzburg, South Africa.

Henham A, and **Makkar MK**, (1998), Combustion of simulated biogas in a dual-fuel diesel engine, *Energy Conversion and Management*, Vol. 39, No. 16–18, pp. 2001–2009.

Heywood JB, (1988), *Internal Combustion Engine Fundamentals*, McGraw-Hill Book Company, New York, USA.

Holmberg K, and **Österberg E**, (1986), Structure of a cosurfactant-free microemulsion. *Journal of Dispersion Science and Technology*, Vol. 7, No. 3, pp. 299-306.

Hou W, and **Papadopoulos KD**, (1997), $W_I/O/W_2$ and $O_1/W/O_2$ globules stabilized with Span 80 and Tween 80, *Colloids and Surfaces A: Physicochemical and Engineering Aspects*, Vol. 125, No. 2-3, pp. 181-187.

Huang Y, **Han X, Shang S**, and **Wang L**, (2012), Performance and emissions of a direct injection diesel engine operating on emulsions of corn stalk bio-oil in diesel. *Proceedings of the Institution of Mechanical Engineers, Part D: Journal of Automobile Engineering*, Vol. 226, No. 8, pp. 1119-1129.

Husnawan M, Masjuki HH, Mahlia TMI, and **Saifullah MG**, (2009), Thermal analysis of cylinder head carbon deposits from single cylinder diesel engine fueled by Palm oil–diesel fuel emulsions, *Applied Energy*, Vol. 86, No. 10, pp. 2107–2113.

India Energy Book 2012, *World Energy Council*, Indian Member Committee, Lodhi Road, New Delhi – 110003.

Inventions and Innovations - A Dual Fuel Conversion System For Diesel Engines, Project Fact Sheet published by the Office of the Industrial Technologies, U.S. Department of Energy, DOE/GO-102001-0862, Order number I-OT-649, January 2001.

IS 10000, Part I-XIII, *Indian Standards, Book Supply Bureau*, A-68, South Extension-I, New Delhi-49.

Ishida M, and **Chen ZL**, (1994), An analysis of the added water effect on NO formation in DI diesel engines. *Society of Automotive Engineers*, Paper No. 941691.

Ishida M, **Ueki H**, and **Sakauguo D**, (1997), Prediction of NO_X reduction rate due to port water Injection in a DI diesel engine. *Society of Automotive Engineers*, Paper No. 972961.

Jiang C-q, **Liu T-w**, and **Zhong J**, (1989), A study on compressed biogas and its application to the compression ignition dual-fuel engine, *Biomass*, Vol. 20, No. (1-2), pp. 53–59.

Jindal S, Nandwana BP, and **Rathore NS,** (2010a**),** Comparative evaluation of combustion, performance, and emissions of Jatropha methyl ester and Karanj methyl ester in a direct injection diesel engine, *Energy and Fuels*, Vol. 24, No. 3, pp. 1565-1572

Jindal S, Nandwana BP, Rathore NS, and **Vashistha V**, (2010b), Experimental investigation of the effect of compression ratio and injection pressure in a direct injection diesel engine running on jatropha methyl ester, *Applied Thermal Engineering*, Vol. 30, No. 5, pp. 442–448.

Kadota T, and **Yamasaki H**, (2002), Recent advances in the combustion of water fuel emulsion, *Progress in Energy and Combustion Science*, Vol. 28, No. 5, pp. 385–404.

Kalam MA, and **Masjuki HH**, (2002), Biodiesel from palm oil - an analysis of its properties and potential, *Biomass and Bioenergy*, Vol. 23, No. 6, pp. 471 – 479.

Kannan GR, and **Anand R**, (2011), Experimental Investigation on Diesel Engine with Diestrole-Water Micro Emulsions, *Energy*, 36 , pp. 1680-1687.

Kannan D, **Pachamuthu S, Nabi MdN, Hustad JE**, and **Løvås T**, (2012), Theoretical and experimental investigation of diesel engine performance, combustion and emissions analysis fuelled with the blends of ethanol, diesel and Jatropha methyl ester, *Energy Conversion and Management*, Vol. 53, No. 1, pp. 322–331.

Karthikeyan R, and **Mahalakshmi NV**, (2007), Performance and emission characteristics of turpentine–diesel dual fuel engine and knock suppression using water diluents, *International Journal of Energy Research*; Vol. 31, No. 10, pp. 960–974.

Keçebas A, (2012), Determination of insulation thickness by means of exergy analysis in pipe insulation, *Energy Conversion and Management*, Vol. 58, pp. 76–83.

Kemper JY, (1978), *Variable displacement piston engine*, U.S. Patent, Patent No. 4,100,815.

Kiannejad F, (1993), *Assessment of Vegetable Oil and Emulsions for Use as Fuels in Diesel Engines*, PhD thesis, Queen Mary and Westfield College, University of London, UK.

Kline SJ, and **McClintock FA**, (1953), Describing uncertainties in single-sample experiments, *Mechanical Engineering*, Vol. 75, pp. 3–8.

Korakianitis T, Namasivayam AM, and **Crookes RJ**, (2010), Hydrogen dual-fuelling of compression ignition engines with emulsified biodiesel as pilot fuel, *International Journal of Hydrogen Energy*, Vol. 35, No. 24, pp. 13329-13344.

Kotas TJ, (1985), *The Exergy Method of Thermal Plant Analysis*, London, UK Butterworths.

Kumar MS, Ramesh A, and **Nagalingam B**, (2003), An experimental comparison of methods to use methanol and Jatropha oil in a compression ignition engine, *Biomass and Bioenergy*, Vol. 25, No. 3, pp. 309–318.

Kumar PR, Srinivas PN, Nelson JEB, and **Rao SS**, (2004), Experimental studies on energy appropriation in a single cylinder diesel engine, *Journal of the Institution of Engineers (India), Part MC, Mechanical Engineering Division*, Vol. 85, pp. 45–49.

Kumar SM, Kerihuel A, Bellettre J, and **Tazerout M**, (2005), Effect of water and methanol fractions on the performance of a CI engine using animal fat emulsions as fuel. *Proceedings of the Institution of Mechanical Engineers, Part A: Journal of Power and Energy*, Vol. 219, No. 7, pp. 583-592.

Kumar MS, Ramesh A, and **Nagalingam B**, (2003), Use of hydrogen to enhance the performance of a vegetable oil fuelled compression ignition engine. *International Journal of Hydrogen Energy*, Vol. 28, No. 10, pp. 1143–1154.

Kumar SM, Ramesh A, and **Nagalingam B**, (2010), A comparison of the different methods of using Jatropha oil as fuel in a compression ignition engine, *ASME Journal of Engineering for Gas Turbines and Power*, Vol. 132, No. 3, pp. 032801(1-10).

Kumar SM, Ramesh A, **Nagalingam B**, and **Tazerout MA**, (2011), Comprehensive study on performance, emission, and combustion characteristics of a dual-fuel engine fuelled with orange oil and Jatropha oil, *Proceedings of the Institution of Mechanical Engineers, Part A: Journal of Power and Energy*, Vol. 225, No. 5, pp. 601-613.

Laguitton O, Crua C, Cowell T, Heikal MR, and **Gold MR**, (2007), The effect of compression ratio on exhaust emissions from a PCCI diesel engine, *Energy Conversion and Management*, Vol. 48, No. 11, pp. 2918–2924.

Langer DA, and **Daly DT**, (2000), Future fuels and fuel additives for vehicle emissions control, Proceedings of the 219th American Chemical Society National Meeting, March 26-31, San Francisco, USA.

Lapidus AI, **Krylov IF**, and **Tonkonogov BP**, (2005), Natural gas motor fuel, *Chemistry and Technology of Fuels and Oils*, Vol. 41, No. 3, pp. 165–174.

Likos B, **Callahan TJ**, and **Moses CA**, (1981), Performance and emissions of ethanol and ethanol-diesel blends in direct-injected and pre-chamber diesel engines, *Society of Automotive Engineers*, Paper No. 821039.

Lin C-Y, and **Chen L-W**, (2006a), Emulsification characteristics of three- and two-phase emulsions prepared by the ultrasonic emulsification method, *Fuel Processing Technology*, Vol. 87, No. 4, pp. 309 – 317.

Lin C-Y, and **Chen L-W**, (2006b), Engine performance and emission characteristics of three-phase diesel emulsions prepared by an ultrasonic emulsification method, *Fuel*, Vol. 85, No. 5-6, pp. 593–600.

Lin C-Y, and **Chen L-W**, (2008), Comparison of fuel properties and emission characteristics of two- and three-phase emulsions prepared by ultrasonically vibrating and mechanically homogenizing emulsification methods, *Fuel*, Vol. 87, No. 10-11, pp. 2154–2161.

Lin C-Y, and **Lin S-A**, (2007a), Effects of emulsification variables on fuel properties of two- and three-phase biodiesel emulsions, *Fuel*, Vol. 86, No. 1-2, pp. 210–217.

Lin C-Y, and **Lin S-A**, (2007b), Engine performance and emission characteristics of a three-phase emulsion of biodiesel produced by peroxidation, *Fuel*, Vol. 88, No. 1, pp. 35–41.

Lin Y-C, Lee W-J, and **Hou H-C**, (2006), PAH emissions and energy efficiency of Palm-biodiesel blends fueled on diesel generator, *Atmospheric Environment*, Vol. 40, No. 21, pp. 3930–3940.

Lin C-Y, and **Wang K-H**, (2003), The fuel properties of three-phase emulsions as an alternative fuel for diesel engines, *Fuel*, Vol. 82, No. 11, pp. 1367–1375.

Lin C-Y, and **Wang K-H**, (2004a), Diesel engine performance and emission characteristics using three-phase emulsions as fuel, *Fuel*, Vol. 83, No. 4-5, pp. 537–545.

Lin C-Y, and **Wang K-H**, (2004b), Effects of an oxygenated additive on the emulsification characteristics of two- and three-phase diesel emulsions, *Fuel*, Vol. 83, pp. 4-5, pp. 507–515.

Lyn WT, (1963), Study of burning rate and natural of combustion in diesel engines, *Symposium (International) on combustion*. Vol. 9, No. 1, pp. 1069–1082.

Mahanta P, Mishra S C, and **Kushwah YS**, (2006), An experimental study of Pongamia pinnata L. oil as a diesel substitute, *Proceedings of the Institution of Mechanical Engineers, Part A: Journal of Power and Energy*, Vol. 220, No. A7, pp. 803-808.

Masjuki H, Abdulmuin MZ, and **Sii SH**, (1997), Indirect injection diesel engine operation on palm oil methyl esters and its emulsions, *Proceedings of the Institution of Mechanical Engineers*, November, *Part D: Journal of Automobile Engineering*, Vol. 211, No. D4, pp. 291-299.

Masjuki H, Abdulmuin MZ, and **Sii SH**, (1996), Investigations on preheated Palm oil methyl esters in the diesel engine, *Proceedings of the Institution of Mechanical Engineers, Part A: Journal of Power and Energy*, Vol. 210, No. A2, pp. 131-138.

Masjuki H, Zaki AM, and **Sapuan SM**, (1993), A rapid test to measure performance, emission and wear of a diesel engine fueled with palm oil diesel, *Journal of American Oil Chemists*, Vol. 70, No. 10, pp. 1021-1025.

Modi A, (2012) Diesel consumption grows 11.9% in FY12, Article published in Business Standard, April 13, 2012, (http://www.business-standard.com/india/news/diesel-onsumption-grows-119-in-fy12/471189/), [accessed 28/04/2013 at 16:40 hrs].

Moffat RJ, (1982), Contributions to the theory of single-sample uncertainty analysis, *ASME Journal of Fluids Engineering*, Vol. 104, No. 2, pp. 250–260.

Moran MJ, and **Shapiro HN**, (1995), *Fundamentals of Engineering Thermodynamics*, John Wiley and Sons Inc., USA.

Muralidharan K, Vasudevan D, and **Sheeba KN**, (2011), Performance, emission and combustion characteristics of biodiesel fuelled variable compression ratio engine, *Energy*, Vol. 36, No. 8, pp. 5385-5393.

Murayama T, **Tsukahara M**, **Morishima Y**, and **Miyamoto N**, (1978), Experimental reduction in NO_X, smoke and BSFC in a diesel engine using uniquely produced water (0–80%) to fuel emulsion, *Society of Automotive Engineers*, Paper No. 780224.

Nadeem M, Rangkuti C, Anuar K, Haq MRU, Tan IB, and **Shah SS**, (2006), Diesel engine performance and emission evaluation using emulsified fuels stabilized by conventional and gemini surfactants, *Fuel*, Vol. 85, No. 14-15, pp. 2111–2119.

Nagi J, Ahmed SK, and **Nagi F,** (2008), Palm biodiesel an alternative green renewable energy for the energy demands of the future, International Conference on Construction and Building Technology, Kuala Lumpur, Malaysia, Vol. F, No. 07, pp. 79-94.

Namasivayam AM, Korakianitis T, Crookes RJ, Bob-Manuel KDH, and **Olsen J**, (2010), Biodiesel, emulsified biodiesel and dimethyl ether as pilot fuels for natural gas fuelled engines, *Applied Energy*, Vol. 87, No. 3, pp. 769–778.

Owen K, and **Coley T**, (1995), *Automotive Fuels Reference Book*, Society of Automotive Engineers Inc., USA.

Ozcan H, and **Yamin JAA**, (2008), Performance and emission characteristics of LPG powered four stroke SI engine under variable stroke length and compression ratio, *Energy Conversion and Management*, Vol. 49, No. 5, pp. 1193–1201.

Ozsezen AN, and **Canakci M**, (2010), Determination of performance and combustion characteristics of a diesel engine fueled with canola and waste palm oil methyl esters. *Energy Conversion and Management*, Vol. 52, No. 1, pp. 108–116.

Panwar NL, Shrirame HY, Rathore NS, Jindal S, and **Kurchania AK,** (2010), Performance evaluation of a diesel engine fueled with methyl ester of castor seed oil, *Applied Thermal Engineering*, Vol. 30, No. 2-3, pp. 245-249.

Papagiannakis RG, Hountalas DT, and **Rakopoulos CD**, (2007), Theoretical study of the effects of pilot fuel quantity and its injection timing on the performance and emissions of a dual fuel diesel engine, *Energy Conversion and Management*, Vol. 48, No. 11, pp. 2951–2961.

Park JW, Huh KY, and **Lee JH**, (2001), Reduction of NO_X, smoke and brake specific fuel consumption with optimal injection timing and emulsion ratio of water-emulsified diesel, *Proceedings of the Institution of Mechanical Engineers, Part D: Journal of Automobile Engineering*, Vol. 215, No. D1, pp. 83-93.

Park JW, Huh KY, and **Park KH**, (2000), Experimental study on the combustion characteristics of emulsified diesel in a rapid compression and expansion machine, *Proceedings of the Institution of Mechanical Engineers, Part D: Journal of Automobile Engineering*; Vol. 214, No. D5, pp. 579–586.

Park SH, **Youn IM**, and **Lee CS**, (2011), Influence of ethanol blends on the combustion performance and exhaust emission characteristics of a four-cylinder diesel engine at various engine loads and injection timings, *Fuel*, Vol. 90, No. 2, pp. 748–755.

Parlak A. (2005), The effect of heat transfer on performance of the diesel cycle and exergy of the exhaust gas stream in a LHR diesel engine at the optimum injection timing, *Energy Conversion and Management*, Vol. 46, No. 2, pp. 167–179.

Parlak A, Yasar H, and **Eldogan O**, (2005), The effect of thermal barrier coating on a turbocharged diesel engine performance and exergy potential of the exhaust gas, *Energy Conversion and Management*, Vol. 46, No. 3, pp. 489–499.

Parlak A, Yasar H, and **Sahin B**, (2003), Performance and exhaust emission characteristics of a lower compression ratio LHR diesel engine, *Energy Conversion and Management*, Vol. 44, No. 1, pp. 163–175.

Pirouzpanah V, and **Mohammadi AB**, (1996), Dual-fuelling of an industrial indirect injection diesel engine by diesel and liquid petroleum gas, *International Journal of Energy Research*, Vol. 20, No. 10, pp. 903-912.

Puhan S, Nagarajan G, Vedaramana N, and **Ramabramhmam BV,** (2007), Mahua oil (madhuca indica oil) derivatives as a renewable fuel for diesel engine systems in India: A performance and emissions comparative study, *International Journal of Green Energy*, Vol. 4, No. 1, pp. 89-104

Puhan S, Vedaramana N, Sankaranarayanana G, and **Bharat Rama BV**, (2005), Performance and emission study of Mahua oil (madhuca indica oil) ethyl ester in a 4-stroke natural aspirated direct injection diesel engine, *Renewable Energy*, Vol. 30, No. 8, pp. 1269–1278.

Pundir BP, (2010), *IC Engines Combustion and Emissions*, Narosa Publishing House Private Limited, New Delhi, India.

Raheman H, and **Phadatare AG**, (2004), Diesel engine emissions and performance from blends of Karanja methyl ester and diesel, *Biomass and Bioenergy*, Vol. 27, No. 4, pp. 393 – 397.

Raheman H and **Ghade SV**, (2008), Performance of diesel engine with biodiesel at varying compression ratio and ignition timing, *Fuel*, Vol. 87, No. 12, pp. 2659–2666.

Rakopoulos CD, Andritsakis EC, Rakopoulos DC, Hountalas DT, and **Giakoumis EG**, (2006), Comparative performance and emissions study of a direct injection diesel engine using blends of diesel fuel with vegetable oils or bio-diesels of various origins, *Energy Conversion and Management*, Vol. 47, No. 18-19, pp. 3272–3287.

Rakopoulos CD, and **Andritsakis EC**, (1993), DI and IDI diesel engines combustion irreversibility analysis. Article published in *ASME-WA Meeting*, Vol. 30. pp. 17–32.

Rakopoulos CD, and **Giakoumis EG**, (2004), Parametric study of transient turbocharged diesel engine operation from the second-law perspective, *Society of Automotive Engineers*, Paper No. 2004-01-1679.

Rakopoulos CD, and **Giakoumis EG**, (2005), The influence of cylinder wall temperature profile on the second-law diesel engine transient response, *Applied Thermal Engineering*, Vol. 25, No. 11-12, pp. 1779–1795.

Rakopoulos CD, and **Giakoumis EG**, (2006), Comparative first- and second-law parametric study of transient diesel engine operation, *Energy*, Vol. 31, No. 12, No. 1927–1942.

Rakopoulos CD, Hountalas DT, Zannis TC, and **Levendis YA**. (2004), Operational and environmental evaluation of diesel engines burning oxygen-enriched intake air or oxygen-enriched fuels: a review. SAE paper 2004-01-2924.

Rakopoulos CD, and **Kyritsis DC**, (2001), Comparative second-law analysis of internal combustion engine operation for methane, methanol and dodecane fuels, *Energy*, Vol. 26, No. 7, pp. 705–722.

Rakopoulos CD, Rakopoulos DC, Hountalas DT, Giakoumis EG, and **Andritsakis EC**, (2008), Performance and emissions of bus engine using blends of diesel fuel with bio-diesel of Sunflower or Cottonseed oils derived from Greek feedstock, *Fuel*, Vol. 87, No. 2, pp. 147–157.

Rakopoulos CD, Rakopoulos DC, Giakoumis EG, and **Dimaratos AM**, (2010), Investigation of the combustion of neat cottonseed oil or its neat bio-diesel in a HSDI diesel engine by experimental heat release and statistical analyses, *Fuel*, Vol. 89, No. 12, pp. 3814-3826.

Rakopoulos DC, Rakopoulos CD, Giakoumis EG, Dimaratos AM, and **Kakaras EC**, (2013b), Comparative evaluation of two straight vegetable oils and their methyl ester bio-diesels as fuel extenders in HDDI diesel engine: performance and emissions. *ASCE Journal of Energy Engineering*; doi:10.1061/(ASCE)EY.1943-7897.0000137, (In Press).

Rakopoulos DC, **Rakopoulos CD**, **Giakoumis EG**, and **Dimaratos AM**, (2013), Studying combustion and cyclic irregularity of diethyl ether as supplement fuel in diesel engine. *Fuel*, Vol. 109, pp. 325-335.

Ravikkumar TS, **Basar PD**, and **Attffield MJ**, (2001), Emulsified diesel – an immediate and effective solution for diesel exhaust emission reduction, *Society of Automotive Engineers*, Paper No. 2001–28–0037.

Reding TJ, **Naraghi M**, **Bosco S**, **Rodriguez SA**, **Miranda AW**, and **Basinger M**, (2009), Effects of waste vegetable oil/water emulsions on the emissions of a listeroid diesel engine, Proceedings of ASME 2009 International Mechanical Engineering Congress and Exposition, IMECE2009-11774; November 13–19, 2009, Lake Buena Vista, Florida, USA.

Rieger MM, and **Rhein LD**, (1997), Surfactants in Cosmetics. 2nd ed.; Dekker, New York; USA.

Rodríguez RP, Sierens R, and **Verhelst S,** (2011), Ignition delay in a Palm oil and Rapeseed oil biodiesel fuelled engine and predictive correlations for the ignition delay period, *Fuel*, Vol. 90, No. 2, pp. 766–772.

Rosen MJ, (2004), *Surfactants and Interfacial Phenomena*, Wiley Interscience, John Wiley and Sons Inc., Hoboken, New Jersey.

Roy MM, (2009), Effect of fuel injection timing and injection pressure on combustion and odorous emissions in DI diesel engines, *ASME Journal of Energy Resources Technology*, Vol. 131, No. 3, pp. 032201(1-8).

Sahoo BB, (2010), *Clean Development Mechanism Potential of Compression Ignition Diesel Engines Using Gaseous Fuels in Dual Fuel Mode*, Ph.D. thesis, Centre for Energy, Indian Institute of Technology Guwahati, Guwahati, India.

Sahoo BB, Saha UK, and **Sahoo N**, (2011), Theoretical performance limits of a syngas-diesel fueled compression ignition engine from second law analysis, *Energy*, Vol. 36, No. 2, pp.760–769.

Sahoo BB, Saha UK, **Sahoo N**, and **Prusty P**, (2009), Analysis of throttle opening variation impact on a diesel engine performance using second law of thermodynamics, Proceedings of the ASME 2009 Internal Combustion Engine Division Spring Technical Conference, WI, USA.

Sahoo BB, Sahoo N, and **Saha UK,** (2012a)**,** Effect of H_2:CO ratio in syngas for a dual fuel engine operation**,** *Applied Thermal Engineering***,** Vol. 49, pp. 139–146**.**

Sahoo BB, Sahoo N, and **Saha UK,** (2012b), Dual fuel performance studies of a small diesel engine using green fuels**,** *Applied Mechanics and Materials*, Vol. 110-116, pp. 2101-2108.

Sajith V, **Sobhan CB**, and **Peterson GP**, (2010), Experimental investigations on the effects of cerium oxide nanoparticle fuel additives on biodiesel, *Advances in Mechanical Engineering*, doi:10.1155/2010/581407, Article ID 581407.

Samec N, **Dibble RW**, **Chen JY**, and **Pagon A**, (2000), Reduction of NO_X and soot emission by water injection during combustion in a diesel engine, Paper No. F2000A075, Seoul 2000 FISITA World Automotive Congress, June 12-15, 2000, Seoul, Korea.

Samec N, Kegl B, and **Dibble RW**, (2002), Numerical and experimental study of water/oil emulsified fuel combustion in a diesel engine, Fuel, Vol. 81, No. 16, pp. 2035–2044.

Sawa N, and **Kajitani S**, (1992), Physical properties of emulsion fuel (water-oil-type) and its effect on engine performance under transient operation. *Society of Automotive Engineers*, Paper No. 920198.

Sayin C, Ilhan M, Canakci M, and **Gumus M**, (2009), Effect of injection timing on the exhaust emissions of a diesel engine using diesel–methanol blends, *Renewable Energy*, Vol. 34, No. 5, pp. 1261–1269.

Sayin C, Ozsezen AN, and **Canakci M**, (2010), The influence of operating parameters on the performance and emissions of a DI diesel engine using methanol-blended-diesel fuel, *Fuel*, Vol. 89, No. 7, pp. 1407–1414.

Sayin C, Uslu K, and **Canakci M**, (2008), Influence of injection timing on the exhaust emissions of a dual-fuel CI engine, *Renewable Energy*, Vol. 33, No. 6, pp. 1314–1323.

Schmidt K, and **Van Gerpen JH**, (1996), The effect of biodiesel fuel composition on diesel combustion and emission, *Society of Automotive Engineers*, Paper No. 961086.

Schwartz M, **Perry JW**, and **Berch J**, (1977), *Surface Active Agents and Detergents*, Vol. II, Reprint, Krieger RE.; Huntington, New York, USA.

Selim MYE, (2004), Sensitivity of dual fuel engine combustion and knocking limits to gaseous fuel composition, *Energy Conversion and Management*, Vol. 45, No. 3, pp. 411–425.

Selim MYE, Radwan MS, and **Saleh HE**, (2008), Improving the performance of dual fuel engines running on natural gas/LPG by using pilot fuel derived from Jojoba seeds, *Renewable Energy*, Vol. 33, No. 6, pp. 1173–1185.

Sequera AJ, Parthasarathy RN, and **Gollahalli SR**, (2011), Effects of fuel injection timing in the combustion of biofuels in a diesel engine at partial loads, *ASME Journal of Energy Resources Technology*, Vol. 133, No. 2, pp. 022203 (1-6).

Sheng HZ, **Chen L**, and **Wu CK**, (1995), The droplet group micro-explosions in W/O diesel fuel emulsion spray, *Society of Automotive Engineers*, Paper No. 950855.

Singh RN, **Singh SP**, and **Pathak BS**, (2007), Extent of replacement of methyl ester of rice bran oil by producer gas in CI engine, *International Journal of Energy Research*; Vol. 31, No. 15, pp. 1545–1555.

Sinha S, and **Agarwal AK**, (2010), Experimental investigation of the effect of biodiesel utilization on lubricating oil degradation and wear of a transportation CIDI engine, *ASME Journal of Engineering for Gas Turbines and Power*, Vol. 132, No. 4, pp. 042801 (1-9).

Sobotowski RA, **Porter BC**, and **Pilley AD**, (1991), The development of a novel variable compression ratio, direct injection diesel engine, *Society of Automotive Engineers*, Paper No. 910484.

Song KH, **Lee YL**, and **Litzinger TA**, (2000), Effects of emulsified fuels on soot evolution in an optically-accessible DI diesel engine, *Society of Automotive Engineers*, Paper No. 2000-01-2794.

Stepanov VS, (1995), Chemical energies and exergies of fuels, *Energy*, Vol. 2, No. 3, pp. 235–242.

Stone R, (1997), *Introduction to Internal Combustion Engines*, Society of Automotive Engineers Inc., Warrendale, USA.

Subramanian KA, (2011), A comparison of water–diesel emulsion and timed injection of water into the intake manifold of a diesel engine for simultaneous control of NO and smoke emissions, *Energy Conversion and Management*, Vol. 52, No. 2, pp. 849–857.

Subramanian KA, and **Ramesh A**, (2001), Experimental investigation on the use of water diesel emulsion with oxygen enriched air in a DI diesel engine, *Society of Automotive Engineers*, Paper No. 2001-01-0205.

Sumathi S, Chai SP, and **Mohamed AR**, (2008), Utilization of oil Palm as a source of renewable energy in Malaysia, *Renewable and Sustainable Energy Reviews*, Vol. 12, No. 9, pp. 2404–2421.

Swami Nathan S, **Mallikarjuna JM,** and **Ramesh A**, (2010), An experimental study of the biogas–diesel HCCI mode of engine operation, *Energy Conversion and Management*, Vol. 51, No. 7, pp. 1347–1353.

Thipse SS, (2011), *Alternative Fuels – Concepts, Technologies and Developments*, Jaico Publishing House, Mumbai.

Tsukahara M, **Murayama T**, and **Yoshimoto Y**, (1982a), Influence of fuel properties on the combustion in diesel engine driven by the emulsified fuel, *Japan Society of Mechanical Engineers*, Vol. 25, No. 202, pp. 612-619.

Tsukahara M, **Murayama T**, and **Yoshimoto Y**, (1982b), Influence of combustion chamber configurations on the combustion in diesel engine driven by the emulsified fuel, *Japan Society of Mechanical Engineers*, Vol. 25, No. 208, pp. 1567-1573.

Tsukahara M, and **Yoshimoto Y**, (1992), Reduction of NO_X, smoke, BSFC, and maximum combustion pressure by low compression ratios in a diesel engine fuelled by emulsified fuel, *Society of Automotive Engineers*, Paper No. 920464.

Van-Gerpen JH, and **Shapiro HN**, (1990), Second-law analysis of diesel engine combustion, *ASME Journal of Engineering for Gas Turbines and Power*, Vol. 112, No. 1, pp. 129–137.

Vedaramana N, Puhan S, Nagarajan G, Ramabramhmam BV, and **Velappan KC**, (2012a), Methyl ester of Sal oil (Shorea robusta) as a substitute to diesel fuel-A study on its preparation, performance and emissions in direct injection diesel engine, *Industrial Crops and Products*, Vol. 36, No. 1, pp. 282-288.

Vedaramana N, Puhan S, and **Velappan KC**, (2012b), Liquid biofuels from tree borne seed oils for automotive diesel engines, *International Journal of Automotive Technology and Management*, Vol. 12, No. 3, pp. 223 -231.

Von-Mitzlaff K, (1988), *Engines for Biogas - Theory, Modification, Economic Operation*, A publication of Deutsches Zentrum fur Entwicklungstecknologien, GTZ-Gate.

Warnatz J, Mass U, and **Dibble RW**, (1996), *Combustion: Physical and Chemical Fundamentals, Modelling and Simulation, Experiments, Pollutant Formation*, Springer, Berlin, Germany.

Winter J, (2011), Power window- crunch time, *The ASME Magazine- Mechanical Engineering*, Vol. 133, Vol. 4, pp. 1-72.

Wu Y, Huang R, Lee CF, and **Huang C**, (2011), Effects of the exhaust gas recirculation rate and ambient gas temperature on the spray and combustion characteristics of soybean biodiesel and diesel, *Proceedings of the Institute of Mechanical Engineers, Part D: Journal of Automobile Engineering*, Vol. 226, No. D3, pp. 372-384.

Yadav A, and **Singh OA,** (2010), Comparative evaluation of compression ignition engine performance using preheated jatropha, karanja, and neem oils, *Proceedings of the Institute of Mechanical Engineers, Part D: Journal of Power and Energy*, Vol. 224, No. A1, pp. 47-57.

Yang WM, An H, Chou SK, Vedharaji S, Vallinagam R, Balaji M, Mohammad FEA, and **Chua KJE**, (2013), Emulsion fuel with novel nano-organic additives for diesel engine application, *Fuel*, Vol. 104, pp. 726–731.

Zhu L, **Cheung CS, Zhang WG,** and **Huang Z**, (2011), Combustion, performance and emission characteristics of a DI diesel engine fueled with ethanol–biodiesel blends, *Fuel*, Vol. 90, No. 5, pp. 1743–50.

APPENDIX-A

Equations for Performance and Combustion Analysis

I. Performance Analysis:

(i) Brake power (BP):

$$\mathrm{BP} = \frac{2 \times \pi \times N \times W \times r}{60000}, \text{ kW} \quad \text{(A1)}$$

where N, W and r are the speed of the engine (rpm), engine load (kg-m/s^2) and dynamometer arm radius (m), respectively.

(ii) Brake thermal efficiency (BTHE):

For neat diesel/ neat POME/ neat WIP mode, $\eta_{bthe} = \frac{BP}{\dot{m}_{lf} \times LHV_{lf}} \times 100,\%$ (A2)

For dual fuel mode, $\eta_{bthe} = \frac{BP}{\dot{m}_{plf} \times LHV_{lf} + \dot{m}_{gf} \times LHV_{gf}} \times 100,\%$ (A3)

where $\dot{m}_{lf}$ (kg/s), $\dot{m}_{plf}$ (kg/s) and $\dot{m}_{gf}$ (kg/s) are the liquid, pilot liquid and gaseous fuel mass flow rate respectively, and LHV_{lf} (kJ/kg) and LHV_{gf} (kJ/kg) are the lower heating values of liquid and gaseous fuel respectively.

Pilot fuel replacement (Z) in dual fuel mode, $Z = \frac{\dot{m}_{lf} - \dot{m}_{plf}}{\dot{m}_{lf}}, 100\%$

(iii) Brake specific fuel consumption (BSFC):

$$BSFC = \left[\frac{\sum\left(\dot{m}_f \times 3600\right)}{BP}\right] \frac{\left(kg/h\right)_f}{kW_{output}} \quad \text{(A4)}$$

Brake specific energy consumption (BSEC):

$$BSEC = \left[\frac{\sum\left(\dot{m}_f \times LHV_f\right)}{BP}\right] \frac{\left(kJ/s\right)_f}{kW_{output}} \quad \text{(A5)}$$

where $\dot{m}_f$ and LHV_f are the mass flow rate(s) and the lower heating vale(s) of the fuel(s) used in either uni-fuel or dual fuel modes.

(iv) Volumetric efficiency (VE)

Air flow rate, $\dot{m}_{air} = C_d \times (\pi/4) \times d^2 \times \sqrt{\frac{2gh \times W_{den}}{A_{den}}} \times 3600 \times A_{den}, kg/hr$

where C_d, d, h, W_{den}, and A_{den} are coefficient of discharge, diameter of the orifice of air flow (m), manometer reading across orifice (m), water density (kg/m^3) and the density of ambient air (kg/m^3), respectively.

$$\text{Volumetric efficiency, } VE = \frac{\dot{m}_{air}}{(\pi/4)\times D^2 \times L \times (N/n) \times 60 \times K \times A_{den}} \times 100,\% \quad \text{(A6)}$$

where D, L, n, and K are engine cylinder diameter (m), engine stroke length (m), number of revolution per cycle (2 for four stroke engine), number of cylinders.

(v) Stoichiometric air-fuel ratio of POME (λ):

The complete combustion of POME with air generates following equation

$$C_{18.07}H_{34.93}O_2 + 25.8025\ [O_2 + 3.76\ N_2] = 18.07\ [CO_2] + 17.465\ [H_2O] + 97.0174\ [N_2] \quad \text{(A7)}$$

The complete combustion of 5% WIP, 6 HLB and 3% surfactant with air can be shown by following equation

$$0.92\times C_{18.07}H_{34.93}O_2 + 24.5115\ [O_2 + 3.76\ N_2] = 17.1665\ [CO_2] + 16.59\ [H_2O] + 93.8\ [N_2] \quad \text{(A8)}$$

(vi) Lower heating value of POME:

The measured higher heating value (HHV) of POME and 5% WIP, 6 HLB and 3% surfactant are 42.333 MJ/kg and 40.46 MJ/kg. The quantity of water generated (mole) are obtained from Eq. (A7) and (A8).

Therefore,

$$\text{LHV}_{\text{POME}} = \text{HHV} - \left[\text{Heat of vaporisation of air} \times \frac{\text{Mass of water formed}}{\text{Mass of fuel used}}\right] \quad \text{(A9)}$$

$$= 39.83 \text{ MJ/kg}$$

Similarly, LHV_{WIP} = 37.88 MJ/kg

(vii) The molecular weight of POME ($C_{18.07}H_{34.93}O_2$) is 284.12.

Therefore, stoichiometric air-fuel ratio of POME (λ)

$$= \frac{\text{Mole of air}}{\text{Mole of fuel}} \times \frac{\text{Molecular weight of air}}{\text{Molecular weight of fuel}} = 12.52 \quad \text{(A10)}$$

Similarly, stoichiometric air-fuel ratio of 5% WIP (λ) is 12.93.

(viii) Energy density:

To study the energy consumption in the engine, a very important parameter is energy density or energy content. The energy density is calculated by using the calorific value of fuel used and the stoichiometric air requirement for its combustion. Taking POME as a fuel in a diesel engine, its energy density the energy density can be calculated as follows.

Stoichiometric A/F for POME= 12.52

Now, considering 20% of excess air, used to be inhaled in the engine, the actual air fuel ratio of POME = 15.02

Density of air = 1.2 kg/m^3, and density of POME= 870 kg/m^3

The specific volume of charge = volume of air + volume of fuel

$$= (15.02 /1.2) + (1/ 870) = 12.52 \text{ m}^3$$

Lower heating value of POME = 39.84 MJ/kg

Hence, the energy density of cylinder for POME at the nominal rating of the engine mixture

$$\text{Energy density} = \frac{\text{Lower heating value}}{(\text{Specific volume of air} + \text{Specific volume of fuel})} \quad \text{(A11)}$$

$$= (39.84 /12.52) = 3.18 \text{ MJ /m}^3.$$

II. Combustion Analysis:

(i) Pressure smoothing:

The DAC can record cylinder pressure variation with each degree of crank angle change. Differentiating the raw pressure data shows a noisy trend between successive values. Therefore after treatment of these pressure data in the form of smoothing becomes necessary (Stone 1997). For this the smoothing algorithm for (2b+1) value is used as follows:

$$P_n = \frac{1}{b^2}\left[P_{n-(b-1)} + 2P_{n-(b-2)} + 3P_{n-(b-3)} + \ldots + bP_n + \ldots + 3P_{n+(b-3)} + 2P_{n+(b-2)} + P_{n+(b-1)}\right] \quad \textbf{(A12)}$$

The terms in Eq. (A9) are only evaluated when the part of the subscript in bracket is not negative. This is illustrated by simplest case when *b = 2*

$$P_n = \frac{(P_{n-1}) + 2(P_n) + (P_{n+1})}{4} \quad \text{(A13)}$$

where, '*p'* is the instantaneous pressure data. The above equation is used for smoothing the instantaneous pressure data.

(ii) Rate of pressure rise:

The rate of pressure rise calculated from the smoothened pressure data by using first order finite difference equation with fourth order accuracy (Stone 1997).

$$\frac{dP}{d\theta} = \frac{(P_{n-2}) - 8(P_{n-1}) + 8(P_{n+1}) - (P_{n+2})}{12(\Delta\theta)} \tag{A14}$$

where 'p' is the instantaneous pressure data and '$\Delta\theta$' is successive change of crank angle.

(iii) Net heat release rate:

The crank angle encoder, connected to the engine shaft, detects each degree rotation of the crank for each cycle. Hence, for a particular cycle, a total of 720 data for both cylinder pressure and volume are recorded at each load and CR-IT combination. Therefore, to avoid annoying calculations of huge data, at least three cycles are considered for the purpose of heat release calculations at each load and each CR-IT combination. The equation used for net heat release rate is obtained from the first law analysis by implementing rate of pressure rise and rate of volume change, which is given below.

$$\frac{dQ_n}{d\theta} = \left(\frac{\gamma}{\gamma - 1} \times P \times \frac{dV}{d\theta}\right) + \left(\frac{1}{\gamma - 1} \times V \times \frac{dP}{d\theta}\right) \tag{A15}$$

where, $\frac{dQ_n}{d\theta}$ is the net heat release rate, γ is the ratio of specific heats, P the cylinder pressure, V the instantaneous volume of the cylinder. The ranges of γ varies from 1.3 to 1.35 (Heywood, 1988; Pundir, 2010). However, in this study the value of γ is considered as 1.35. In order to select the constant value of γ a short analysis has been performed as follows.

Although combustion in a CI, DI engine is quite heterogeneous, the contents of the combustion chamber are assumed to be homogeneous in the heat release calculations. Some investigators (Hanson, 1989) have developed more complex, quasi-dimensional models, but these are only slightly more accurate than these model. The value of γ varies with temperature and the gas temperature is also needed in calculating heat transfer to the wall. The ideal gas law is used to calculate the spatially averaged temperature in the combustion chamber, i.e.:

$$T_j = \frac{P_j V_j}{M R_g} \tag{A16}$$

where, T_j is bulk gas temperature at point j (°K), R_g is idea gas constant, M is mass of charge, g is (1 + AF)m_f, AF is air/fuel ratio of engine, m_f is mass of fuel injected into each engine cycle (g). It can be shown that the value of γ can be calculated from the following equation

$$\gamma = \left(1 - \frac{R_g}{C_P}\right)^{-1} \tag{A17}$$

According to Goering (1998), the value of C_p/R_g can be calculated from:

$$\frac{C_P}{R_g} = a_0 + a_1 T_j + a_2 T_j^{\,2} + a_3 T_j^{\,3} + a_4 T_j^{\,4} \tag{A18}$$

where a_0 =3.04473, a_1 =1.33805e-3, a_2 =-4.88256e-7, a_3 =8.55475e-11 and a_5 =-5.70132e-15

The values of gamma for temperature variation and NHRR obtained using this variable gamma are plotted in Figs. A1 and A2. The NHRR values for variable gamma showed in Fig. A2 are also compared with the NHRR values obtained by putting γ = 1.35. The results indicate that, there is vary negligible difference between the NHRR values obtained for constant and variable γ. Hence throughout the result analysis γ is maintained as 1.35.

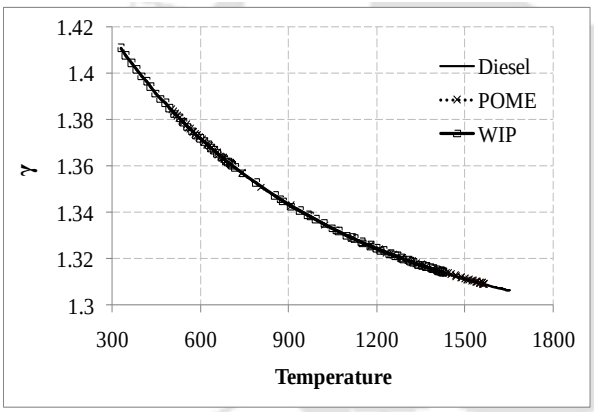

Figure A1: Variation of gamma with respect to temperature

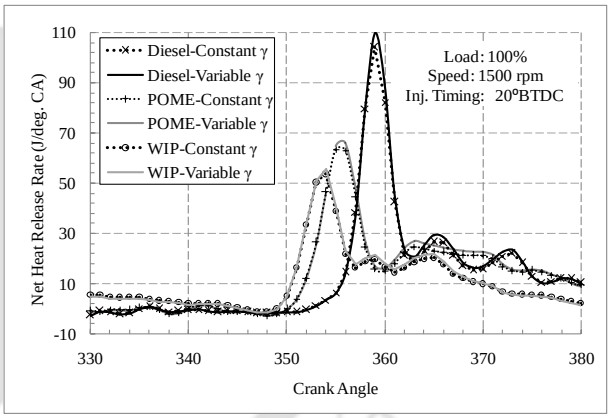

Figure A2: NHRR for diesel, POME and WIP with constant and variable gamma

(iv) Ignition delay:

Ignition delay can be defined as the duration between the fuel IT (θ_{IN}) and the crank angle at which combustion starts (θ_{IG}). Therefore,

$$\theta_R = \theta_{IG} - \theta_{IN},\ ^oCA \tag{A19}$$

The standard fuel IT is obtained from the manufacturer specifications, 23ºBTDC. The ITs, other than the standard one are obtained from the fuel pressure data stored during data acquisition. The crank angle at which combustion starts is obtained from the $\frac{dP}{d\theta}$ diagram as it changes its concavity when combustion starts.

APPENDIX-B

Experimental Uncertainties

The uncertainties of the parameters are calculated by using the universally known theory of sequential perturbation technique brought by Kline and McClintok (1953) and Moffat (1982). The method is described as follows. If N is a dependant measuring parameter which is a function of the independent variables x_1, x_2 , x_3 , x_4,…., x_n. Therefore,

$$N = N(x_1, x_2, ..., x_n) \tag{B1}$$

If ΔN is the uncertainty created due to the individual uncertainties of the independent parameters termed as ΔN_1, ΔN_2, ΔN_3, ΔN_4,…..,ΔN_n. Then the uncertainty of the dependent variable can be written as,

$$\Delta N = \left[\left(\frac{\partial N}{\partial x_1} \Delta N_1 \right)^2 + \left(\frac{\partial N}{\partial x_2} \Delta N_2 \right)^2 + ... + \left(\frac{\partial N}{\partial x_n} \Delta N_n \right)^2 \right]^{\frac{1}{2}} \tag{B2}$$

The calculated uncertainties of each of the measured independent parameter are shown in Table B1. The uncertainties of the dependent performance parameters are included in Table B2. A sample calculation provided here for measurement of uncertainty.

The BP of the engine is given by (A1)

$$BP = \frac{2 \times 3.142 \times N \times W \times R}{60 \times 1000}, kW$$

In the above equation N and W are independent variable, because R has a constant value. The uncertainties of N and W are 1.3% and 0.1% respectively. Therefore uncertainty of BP is

$$\Delta BP = \left(0.013^2 + 0.001^2\right)^{1/2} = 0.01304 \approx 1.3\%$$

Similarly, uncertainties of other dependent parameters are calculated.

Table B1: Uncertainties of independent variables

SL No	Independent variable	Relative error (%)
1	Engine speed	1.2
2	Engine load	0.2
3	Liquid fuel flow rate	0.3
4	Water flow rate	1.1
5	LHV of liquid fuel	1.1
6	Temperature	0.9
7	Cylinder pressure	1.6
8	Cylinder volume	0.1
9	Specific heat of exhaust gas	0.6
10	Ratio of specific heat	0.7
11	CO, CO_2, NO_X, HC emissions	3.3

Table B2: Uncertainties of performance parameters

SL No	Performance parameters	Neat POME mode error	WIP mode error
1	Air flow rate	1.1	1.2
2	Air fuel ratio	1.1	1.0
3	Brake power	1.3	1.5
4	Brake thermal efficiency	1.6	2.0
5	Brake specific fuel consumption	1.3	1.8
6	Net heat release rate	1.6	1.2
7	Volumetric efficiency	1.7	1.5
8	Ignition delay	0.2	0.3

APPENDIX-C

Equations for Thermodynamic Potential Study

I. Energy Analysis

In compression ignition (CI) engine, the fuel energy supplied per unit time (Q_{in}) is transferred in its different processes, namely, shaft power (Q_s), energy in cooling water per unit time (Q_w), energy in exhaust gas per unit time (Q_e) and uncounted energy losses per unit time (Q_u) in the form of friction, radiation, heat transfer to the surrounding, operating auxiliary equipments, etc. These different forms of energies are calculated according to the following analytical expressions (Heywood 1988; Al-Najem and Diab, 1992; Sahoo, 2010).

- Fuel energy supplied per unit time (Q_{in}):

$$Q_{in} = \left[\dot{m}_{fuel} \times LHV_{fuel}\right], kW \quad \text{(C1)}$$

- Shaft power (Q_s):

$$Q_s = \text{Brake power of the engine, } kW \quad \text{(C2)}$$

- Energy in cooling water per unit time (Q_w):

$$Q_w = \left[\dot{m}_{we} \times C_{pw} \times \left(T_{woe} - T_{wie}\right)\right], kW \quad \text{(C3)}$$

where $\dot{m}_{we}$ is the mass flow rate of cooling water in kg/s passing through engine jacket, C_{pw} is the specific heat of water in kJ/kg-K and T_{wie} and T_{woe} are the inlet and outlet temperature of cooling water passing through engine jacket.

- Energy in exhaust gas per unit time (Q_e):

$$Q_e = \left[\left(\dot{m}_f + \dot{m}_a\right) \times C_{pe} \times \left(T_{eic} - T_{amb}\right)\right], kW \quad \text{(C4)}$$

where $\dot{m}_a$ is the mass flow rate of air in kg/s, specific heat of exhaust gas (C_{pe}) is obtained from the energy balance of the flows passing through the calorimeter, as follows:

$$C_{pe} = \left[\dot{m}_{wc} \times C_{pw} \times \left(T_{woc} - T_{wic}\right)\right] / \left[\left(\dot{m}_f + \dot{m}_a\right) \times \left(T_{eic} - T_{eoc}\right)\right] \ , kJ/kg\text{-}K \quad \text{(C5)}$$

where $\dot{m}_{wc}$, T_{wic} and T_{woc} are the mass flow rate, inlet and outlet temperature of the cooling water passing through the calorimeter and T_{eic} and T_{eic} are the inlet and outlet temperatures of exhaust gas passing through calorimeter.

- Uncounted energy losses per unit time (Q_u):

$$Q_u = \left[Q_{in} - \left(Q_s + Q_w + Q_e\right)\right], kW \quad \text{(C6)}$$

II. Exergy Analysis

The availability can be described as the ability to perform useful amount of work by the supplied energy (Heywood, 1988). In the CI engine the availability of fuel (A_{in}) supplied is converted into different types of exergy, namely, shaft availability (A_s), cooling water availability (A_w), exhaust gas availability (A_e) and destructed availability (A_d) in the form of friction, radiation, heat transfer to the surrounding, operating auxiliary equipments, etc. These forms of energies are calculated according to the following analytical expressions as described in the literature (Flynn *et al.*, 1984; Kotas, 1985; Van Gerpen and Shapiro, 1990; Stepanov, 1995).

- Input availability of fuel (A_{in}):

$$A_{in} = \dot{m}_f \times LHV_f \times \left[1.0401 + 0.1728\left(H/C\right) + 0.0432\left(O/C\right) + 0.2169\left(S/C\right)\left\{1 - 2.0628\left(H/C\right)\right\}\right], kW \quad \text{(C7)}$$

where, *H*, *C*, *O* and *S* are the mass fractions of hydrogen, carbon, oxygen and sulfur contents (Lyn, 1963).

- Shaft availability (A_s)

$$A_s = \text{Brake power of the engine, } kW \quad \text{(C8)}$$

- Cooling water availability (A_w):

$$A_w = Q_w - \left[\dot{m}_{we} \times C_{pw} \times T_{amb} \times ln\left(T_{woe}/T_{wie}\right)\right], kW \quad \text{(C9)}$$

- Exhaust gas availability (A_e):

$$A_e = Q_e + \left[\left(\dot{m}_f + \dot{m}_a\right) \times T_{amb} \times \left\{C_{pe}\, ln\left(T_{amb}/T_{eic}\right) - R_e\, ln\left(p_{amb}/p_e\right)\right\}\right], kW \quad \text{(C10)}$$

where, R_e is the specific gas constant of the exhaust gas in kJ/kg-K. It is calculated from the thermodynamic relation R_e= (R_U/molecular weight). R_U is the universal gas constant in kJ/kmol-K and the molecular weight (kg/kmol) of combustion products is calculated taking into account complete combustion.

- Destructed availability (A_d):

A_s, A_w and A_e are the enxrgies which can be recovered. Destructed availability

$$A_d = \left[A_{in} - \left(A_s + A_w + A_e\right)\right], kW \quad \text{(C11)}$$

- Exergy efficiency (η_{II}) :

$$\eta_{II} = \left[1 - \left(A_d / A_{in}\right)\right], \% \quad \text{(C12)}$$

- Entropy Generation rate:

The method of entropy generation is fairly a novel way to decide perfectly, the losses in various components in an energy system and to identify the scopes of enhancement of overall system performance (Ebiana *et al.*, 2006). The entropy generation can be expressed as,

$$\dot{S} = \left[A_d / T_{amb}\right], kW/K \quad \text{(C13)}$$

List of Publications

Journals:

1. **Debnath BK**, Saha UK, and Sahoo N, (2014), An experimental way of assessing the application potential of emulsified palm biodiesel towards alternative diesel, ***ASME Journal of Engineering for Gas Turbines and Power***, Vol. 136, pp. 021401(1-12).
2. **Debnath BK**, Saha UK, and Sahoo N, (2013), Theoretical route towards the estimation of second law potential of an emulsified palm biodiesel run diesel engine, ***ASCE Journal of Energy Engineering*** (doi: 10.1061/(ASCE)EY.1943-7897.0000134).
3. **Debnath BK**, Saha UK, and Sahoo N, (2013), Influence of emulsified palm biodiesel as pilot fuel in a biogas run dual fuel diesel engine, ***ASCE Journal of Energy Engineering,*** (10.1061/(ASCE)EY.1943-7897.0000163)**.**
4. **Debnath BK**, Saha UK, and Sahoo N, (2013), Effect of compression ratio and injection timing on the performance characteristics of a diesel engine run on palm oil methyl ester, ***Proc. of IMechE, Part-A, Journal of Power and Energy***, Vol. 227, pp. 368 – 382.
5. **Debnath BK**, Sahoo N, and Saha UK, (2013), Adjusting the operating characteristics to improve the performance of an emulsified palm oil methyl ester run diesel engine, ***Energy Conversion and Management,*** Vol. 69, pp. 191–198.
6. **Debnath BK**, Sahoo N, and Saha UK, (2013), Thermodynamic analysis of a variable compression ratio diesel engine running with palm oil methyl ester**,** ***Energy Conversion and Management***, Vol. 65, pp. 147-154.
7. Bora BJ, **Debnath BK,** Gupta N, Sahoo N, and Saha UK, (2013), Investigation on the flow behaviour of a venturi type gas mixer designed for dual fuel diesel engines, ***International Journal of Emerging Technology and Advanced Engineering***, Vol. 3, pp. 202-209.
8. **Debnath BK,** Saha UK, and Sahoo N, (2012), Effect of hydrogen-diesel quantity variation on brake thermal efficiency of a dual fuelled diesel engine, ***Journal of Power Technologies,*** Vol. 92, pp. 55–67**.**

Conferences:

9. **Debnath BK**, Sahoo N, and Saha UK, (2012), Experimental analysis of emulsified palm oil methyl ester towards alternative diesel fuel, **Paper No.** ESDA2012-82033, ***ASME 11th Biennial Conference on Engineering Systems Design and Analysis***, July 2–4, Nantes, France.
10. **Debnath BK**, Saha UK, and Sahoo N, (2011), Effect of compression ratio on the performance characteristics of a palm oil methyl ester run diesel engine, Paper No. IMECE2010–65135, ***ASME International Mechanical Engineering Congress & Exposition***, November 11 – 17, Colorado, USA.
11. **Debnath BK**, Sahoo BB, Saha UK, and Sahoo N, (2011), Simulation of combustion and emission characteristics in a dual fuelled diesel engine, Paper No. ICEF2010- 35095, ***ASME Internal Combustion Engine Division Fall Technical Conference***, September 12 – 15, Texas, USA.
12. **Debnath BK**, Saha UK, and Sahoo N, 2012, Application of emulsified biofuel for emission reductions in diesel engines, ***National Seminar on New and Renewable Sources of Energy***, March 21–22**,** Guwahati-781039, Assam, India.

Under Review:

13. **Debnath BK**, Bora BJ, Sahoo N, and Saha UK, (2013), A comprehensive review on the application of emulsion as an alternative fuel for diesel engine, ***Renewable & Sustainable Energy Reviews.***